

**NASA
Technical
Paper
2569**

1986

Investigation of Solid
Plume Simulation Criteria
To Produce Flight Plume
Effects on Multibody
Configuration in
Wind Tunnel Tests

Alonzo L. Frost
and Charlie C. Dill

*George C. Marshall Space Flight Center
Marshall Space Flight Center, Alabama*



National Aeronautics
and Space Administration

Scientific and Technical
Information Branch

TABLE OF CONTENTS

	Page
INTRODUCTION.....	1
FACILITY DESCRIPTION.....	1
MODEL DESCRIPTION.....	2
INSTRUMENTATION AND DATA REDUCTION.....	2
TEST PROCEDURE.....	4
ANALYSIS AND RESULTS.....	4
Base Pressure Effects.....	5
Orbiter.....	5
External Tank.....	5
Solid Rocket Boosters.....	5
Body Force and Moment Effects.....	6
Wing and Elevon Effects.....	6
Effects of Change in Angle-of-Attack.....	7
CONCLUSIONS.....	7
APPENDICES.....	17

PRECEDING PAGE BLANK NOT FILMED

LIST OF ILLUSTRATIONS

Figure	Title	Page
1.	SSLV model with solid plumes	8
2.	Plume parameters	9
3.	Base pressure tap locations	9
4.	Aerodynamic body-axis reference system	10
5.	Wing coordinate axes.	11
6.	Elevon coordinate axes	11
7.	SSLV element base pressure	12
8.	Orbiter base pressure coefficient	13

LIST OF TABLES

Table	Title	Page
1.	Plume Configurations Tested.	14
2.	Reference Dimensions and Constants	15
3.	Tunnel Operating Conditions	16

DEFINITION OF SYMBOLS

A_{ORB}	Orbiter base area
A_{ET}	External tank base area
A_{SRB}	SRB base area (one SRB)
A_{BF}	Body flap planform area
C_{AT}	Total axial force coefficient
C_N	Normal force coefficient (uncorrected)
C_M	Pitching moment coefficient (uncorrected)
C_{AF}	Forebody axial force coefficient
C_{NF}	Forebody normal force coefficient
C_{MF}	Forebody pitching moment coefficient
C_{NW}	Wing normal force coefficient
C_{BW}	Wing bending moment coefficient
C_{TW}	Wing torsion moment coefficient
$C_{H\ eo}$	Outboard elevon hinge moment coefficient
$C_{H\ ei}$	Inboard elevon hinge moment coefficient
$C_{NB\ ORB}$	Orbiter base normal force coefficient correction
$C_{N\ BF}$	Body flap normal force coefficient correction
$C_{MB\ ORB}$	Orbiter base pitching moment coefficient correction
$C_{M\ BF}$	Body flap pitching moment coefficient correction
$C_{AB\ ORB}$	Orbiter base axial force coefficient correction
$C_{AB\ ET}$	External tank base axial force coefficient correction
$C_{AB\ SRB}$	SRB base axial force coefficient correction

$C_{P_{B \text{ ORB, ET, SRB}}}$	Element base pressure coefficient
\bar{C}	Mean aerodynamic chord
\bar{C}_e	Elevon reference length
D	Solid plume cone base diameter
D_{ORB}	Orbiter fuselage width
D_{SRB}	SRB aft skirt base diameter
F_A	Total axial force
F_N	Total normal force
F_{N_W}	Wing normal force
HM_{ei}	Inboard elevon hinge moment
HM_{eo}	Outboard elevon hinge moment
L_{REF}	Reference length
q	Tunnel freestream dynamic pressure
S_{REF}	Reference area
$S_{e\text{REF}}$	Elevon reference area
X_1	Horizontal distance from centroid of orbiter base to MRP
X_{TO}	Horizontal distance from balance center to MRP
Z_1	Vertical distance from centroid of orbiter base to MRP
Z_{TO}	Vertical distance from balance center to MRP
α	Angle of attack
θ	Solid plume cone angle
X	Distance from SRB/ORB base to SRB/SSME cone base
M_{B_W}	Wing bending moment
M_{T_W}	Wing torsion moment

TECHNICAL PAPER

INVESTIGATION OF SOLID PLUME SIMULATION CRITERIA TO PRODUCE FLIGHT PLUME EFFECTS ON MULTIBODY CONFIGURATION IN WIND TUNNEL TESTS

INTRODUCTION

The Space Shuttle flight test program revealed that the propulsion system exhaust plume effect on vehicle base pressure had been considerably underestimated by ground testing. Flight base pressures were much higher on all of the vehicle elements than was predicted. The results of the ascent aerodynamic extraction process seemed to indicate that forebody forces, most significantly normal force and pitching moment, were also inconsistent with experimental results. One hypothesis was that the differences between flight and predicted forebody aerodynamics was a direct result of the higher base pressures feeding forward on the vehicle. To test this hypothesis, a wind tunnel test was conducted by MSFC to determine propulsion system plume effects on Space Shuttle Launch Vehicle (SSLV) aerodynamic force and moment coefficients when test model element base pressure coefficients were made equivalent to flight values. The test, designated TWT 675, was conducted in May 1982 in the Marshall Space Flight Center 14-in. Trisonic Wind Tunnel with a 0.004-scale model. Several solid body sting attachments simulating Space Shuttle Main Engine (SSME) and Solid Rocket Booster (SRB) plumes were used to produce the orbiter, SRB, and External Tank (ET) base pressures and orbiter elevon hinge moments observed in flight data. The test data yielded base pressures on the orbiter, ET, and SRBs that were within the flight data band for all Mach numbers. The best match of base pressures and inboard elevon hinge moments with flight data yielded forebody normal force changes of approximately 50 to 80 percent of flight deltas for both mated vehicle and orbiter. From these results, two important conclusions were drawn. Solid body plume simulation can be used to produce observed flight base pressures, and the flight extracted-preflight predicted differences may be attributed to plume effects. Solid plume simulators may therefore be an inexpensive, quick method of approximating the effect of engine exhaust plumes on the base and forebody aerodynamics of future, complex multibody launch vehicles.

The objective of this present investigation was to determine the sensitivity of the Shuttle base and forebody aerodynamics to the size and shape of various solid plume simulators. To support this task, a parametric evaluation of solid plume simulators was made in the MSFC 14-in. TWT using the 0.004-scale model of the SSLV. Families of cones of varying angle and base diameter at various axial positions behind the SSLV model were studied during this test, designated TWT 700.

FACILITY DESCRIPTION

The MSFC 14 x 14-in. Trisonic Wind Tunnel is an intermittent blowdown tunnel which operates by high pressure air flowing from storage to either vacuum or atmospheric conditions. The transonic section used for this test provides a Mach number range from 0.2 to 2.5. Mach numbers between 0.2 and 0.9 are obtained by using a controllable diffuser. The range from 0.95 to 1.3 is achieved through the use of plenum suction and perforated walls. A hydraulically controlled pitch sector located downstream of the test section provides the capability of testing up to 20 angles of attack from -10 to +10 deg during each run. On-line data is reduced to coefficient form by a solid-state data acquisition and computing system.

MODEL DESCRIPTION

The 0.004-scale model is a replica of the Space Shuttle launch vehicle consisting of the Orbiter (ORB), ET, and two SRBs. The total SSLV model was supported by a single sting and six-component balance in the orbiter. Two SRB dummy stings were also mounted in proximity to each SRB base. These stings in no way contacted the model, but served only to support the SRB plume simulators.

A typical plume simulation configuration is shown with the model in Figure 1. Plume geometry and position parameters are defined by Figure 2, and the test configuration geometries are given in Table 1. The SSME plume effects were simulated by mounting one of the cones with the CS designation to the main supporting sting, which was specially constructed so that the segment just aft of the orbiter is angled 16 deg from horizontal to simulate engine cant. Each CS cone was accompanied by a cylindrical extension of the same diameter to accommodate plume interference effects. The SRB plume effects were produced by mounting C designated cones to the dummy SRB stings, yet the SRB cones did not have extensions. The distances of the cones from the base of the respective vehicle element were variable as desired.

INSTRUMENTATION AND DATA REDUCTION

The SSLV model was mounted on a six-component balance which measured total mated-vehicle forces and moments. Model base pressures were measured using external tubes placed next to the base of each element as shown in Figure 3 and were sampled by transducers mounted outside the test section. The right-hand wing was supported on a single-beam, three-component balance in all degrees of freedom. The left-hand elevons were instrumented to measure hinge moment directly via gaged beams which supported each individual control surface.

Six-component force and moment coefficients were computed for the main balance using the axis system and reference point in Figure 4. Elevon hinge moments and wing forces and moments were computed in coefficient form about the reference locations given in Figures 5 and 6. Angles of attack were calculated from the sector reading, taking into account the sting and balance deflections as determined by pretest calibrations. The reference dimensions and constants used in data reduction are given in Table 2.

The following equations were used to reduce the force and moment data for wing, elevon, and mated vehicle coefficients.

For the mated vehicle total forces and moment:

$$C_N = \frac{F_N}{q S_{REF}} \quad (1)$$

$$C_M = \frac{M_Y}{q S_{REF} L_{REF}} + \frac{F_N * X_{T_0}}{q S_{REF} L_{REF}} - \frac{F_A * Z_{T_0}}{q S_{REF} L_{REF}} \quad (2)$$

$$C_{AT} = \frac{F_A}{q S_{REF}} \quad (3)$$

Base force and moment coefficients were calculated as follows:

$$C_{N_{BORB}} = \frac{C_{P_{BORB}} A_{ORB} \tan(14.75^\circ)}{S_{REF}} \quad (4)$$

$$C_{N_{BF}} = - \frac{C_{P_{BF}} A_{BF}}{S_{REF}} \quad (5)$$

$$C_{M_{BORB}} = C_{N_{BORB}} (X_1/L_{REF}) - C_{A_{BORB}} (Z_1/L_{REF}) \quad (6)$$

$$C_{M_{BF}} = C_{N_{BF}} (X_2/L_{REF}) \quad (7)$$

$$C_{A_{BORB}} = - \frac{C_{P_{BORB}} A_{ORB}}{S_{REF}} \quad (8)$$

$$C_{A_{BET}} = - \frac{C_{P_{BET}} A_{ET}}{S_{REF}}$$

$$C_{A_{BSRB}} = - \frac{C_{P_{BSRB}} A_{SRB}}{S_{REF}}$$

Now, adjusting for base coefficients, forebody coefficients are:

$$C_{N_F} = C_N - C_{N_{BORB}} - C_{N_{BF}} \quad (9)$$

$$C_{M_F} = C_M - C_{M_{BORB}} - C_{M_{BF}} \quad (10)$$

$$C_{AF} = C_A - C_{ABORB} - C_{ABET} - 2C_{ABSRB} \quad (11)$$

Wing-normal force-bending and torsion moments and elevon hinge moments are calculated as follows:

$$C_{NW} = \frac{F_{NW}}{q S_{REF}} \quad (12)$$

$$C_{BW} = \frac{M_{BW}}{q S_{REF} L_{REF}} \quad (13)$$

$$C_{TW} = \frac{M_{TW}}{q S_{REF} \bar{c}} \quad (14)$$

$$C_{heo} = \frac{HM_{eo}}{q S_{eREF} \bar{c}_e} \quad (15)$$

$$C_{Hei} = \frac{HM_{ei}}{q S_{eREF} \bar{c}_e} \quad (16)$$

TEST PROCEDURE

The test schedule followed a systematic variation of the solid plume parameters previously defined. The SRB plumes were varied with two different fixed SSME plume configurations. This procedure was then followed for the SSME plume variation, using two different fixed SRB plume configurations. After completing a set of baseline plume-off runs, one run was made for each configuration at four Mach numbers, $M = 0.8, 0.95, 1.10, \text{ and } 1.25$. During each run, the sector was stepped through five angles of attack: $-6, -4, -2, 0, \text{ and } +2$ deg. For all runs, the angle of sideslip remained at 0 deg. Complete test conditions are given in Table 3.

ANALYSIS AND RESULTS

The test run schedule was successful in providing a parametric matrix of data. As shown in Figure 7, the resultant test base pressures encompassed the measured flight pressure data band observed during Space Shuttle flights STS 1-5. The complete data matrix indicates that any data point within this flight band can be achieved with the hardware used in this test. Since matching base pressures is one of

the most important criteria for plume simulation design, this could be considered the most significant result of this study.

Now, given that a particular data point could be obtained during testing, trying to match a set of desired data points including the various pressure and force coefficients becomes the challenge. Understanding the effects of solid plume geometry on these pressures and forces is necessary to solving the problem. Therefore, the data are presented in such a way that parametric effects become more obvious. An example plot is shown in Figure 8 and includes one orbiter base pressure data point for each of nine different parametric plume configurations at one Mach number. This data is plotted versus two different plume geometry parameters. The larger scale represents the dimensionless position (X/D_{SRB}) of the SRB cone behind the model as defined earlier. D_{SRB} is defined as the diameter of the base of the model SRB aft skirt. For SSME plume variations, the "diameter" of the orbiter, taken to be the width of the fuselage, will determine SSME cone position as X/D_{ORB} . The smaller scale represents the dimensionless diameters of the cones and applies to all three different positions. Complete data from the test for one sector reading ($\alpha = 0$ deg) are included in the appendices. The data are not interpolated to constant values of angle of attack. Therefore, there are slight variations of α versus Mach number. But the deflections are less than 1 deg for all Mach numbers and the spread is only 0.25 deg. An analysis for angle of attack effects appears later in this section.

Base Pressure Effects

Orbiter

Orbiter base pressure coefficient data are given in Appendix A. In general, for SRB plume variations (Figs. A-1 through A-6) the data are more sensitive to diameter than position. As would be expected, the closer the plumes are to the vehicle model, the steeper the slope of $C_{PB\ ORB}$ versus D/D_{SRB} becomes. The greatest data spread and sensitivity occur in the near Mach number equal to one range. Overall, the resulting trends are fairly predictable. For SSME plume variations (Figs. A-7 through A-10) the data display less sensitivity to variation in both position and diameter. However, very distinguishable trends do exist.

External Tank

External tank base pressures presented in Appendix B also displayed predictable behavior in that the effect of SRB cone diameter decreases somewhat proportionately with increase in X/D_{SRB} . The SRB plume variation (Figs. B-1 through B-6) resulted in very few "irregular" data points and shows the high sensitivity of ET base pressure to SRB plumes. Both the orbiter and ET data showed more sensitivity to parametric variation for $M = 0.95$ and 1.10 . It appears that ET base pressures are as sensitive to SSME plume variations (Figs. B-7 through B-10) as the orbiter, and even more sensitive in some cases with larger diameters.

Solid Rocket Boosters

The SRB base pressure data are given in Appendix C. For SRB plume variations (Figs. C-1 through C-6), at the subsonic Mach numbers, the SRB base pressure data responds as expected, but

supersonically the sensitivity of $C_{p_{B_{SRB}}}$ to diameter is not diminished, as it was for the orbiter and ET, by increasing X/D_{SRB} . SSME plume variations (Figs. C-7 through C-10) caused very little effect on SRB base pressure at $M = 0.8$ and only diameter effects can be observed at other Mach numbers. As with the orbiter and ET, the effect of diameter did not taper off until X/D_{ORB} was greater than 4.

Overall, several general observations can be made. The orbiter base pressure is very sensitive to both SSME and SRB plume variation. The ET is very sensitive to the SRB plumes and less sensitive to the SSME plume changes. The SRB base is highly affected by variation in SRB plume geometry, but shows little effect due to SSME plume variation. Finally, flight base pressure values can be obtained in scale model wind tunnel testing utilizing solid plumes.

Body Force and Moment Effects

Forebody axial force (CAF) coefficient data can be found in Appendix D. For both SRB and SSME plume variations, the data reveals very little or no change at $M = 0.8$. There occurred a slight reduction in C_{AF} at all other Mach numbers. This was probably due to reduced interference drag through the aft attach structures. The almost negligible parametric effects of SSME variation were somewhat enhanced by the addition of the larger fixed SRB plume 2.

The observed trends for forebody normal force (CNF) given in Appendix E were similar to those displayed by ET base pressure. This cause and effect is obvious because the pressure distribution on the lower orbiter wing and fuselage surfaces are greatly affected by pressure in the ET base area. Also, as for ET base pressure, the orbiter normal force shows more sensitivity to SRB plume than orbiter plumes. The forebody pitching moment (CMF) trends, shown in Appendix F, are primarily the result of the changes in C_{NF} . By observing the C_{NF} and C_{MF} trends with plume changes, it is obvious that the plume effects are occurring on the aft region of the vehicle.

Wing and Elevon Effects

The wing normal force data in Appendix G indicates that only a small part of the increment in C_{NF} is due to wing load change. These data, along with the wing bending and torsion coefficients in Appendices H and I, display some interesting trends.

The effect of varying plume configurations on the total wing aerodynamics is relatively small. Changes that did occur were primarily due to SRB plumes with changes due to SSME plume changes essentially indistinguishable from data scatter. The wing coefficient trends indicate that plume changes affect both upper and lower surfaces and tend to move aft as the Mach number increases.

The inboard and outboard elevon hinge moment data in Appendices J and K provide an indication of how parametric plume effects vary span-wise along the wing. The inboard elevon proved to be more sensitive at all Mach numbers except $M = 0.95$, and much more sensitive for $M > 1.0$, as the effects become more confined to the vehicle base regions. As might be expected for observing the mated vehicle and wing data, the inboard elevon is more sensitive to changes in SRB plumes than to SSME plumes. Note also, that changes in either SSME and/or SRB plumes results in trailing edge up (negative) moment changes. The effects of plume changes on outboard elevon hinge moments are much smaller than for the

inboard elevon. This is expected as the outboard elevons are further from the plumes. However, as for the inboard elevon, the outboard elevon is more sensitive to SRB plume changes than SSME changes.

Effects of Change in Angle-of-Attack

For both SRB and SSME plume variations the effects of angle-of-attack change appear fairly small. Appendix L presents comparisons of coefficient plots between two angles-of-attack at $M = 0.8$ and $M = 1.25$ for SRB 28 deg cone variations and Appendix M shows the same comparison for SSME 35 deg cone variations. The figures in Appendices L and M show that the various coefficient plots change very little for both SRB and SSME plume variation at both $M = 0.8$ and $M = 1.25$. In general though, significant shifts of baseline numbers occur with change in α for some coefficients, the changes in plume-on minus plume-off deltas remain relatively small. It is obvious that the basic trends with plume size and position are the same for a wide range of angle-of-attack and, therefore, it would be possible for a single plume configuration to cover an entire angle-of-attack range.

CONCLUSIONS

The results of this study show the sensitivity of the aerodynamic characteristics of a complex vehicle (Space Shuttle) to wind tunnel plume simulation consisting of simple, inexpensive solid bodies. These results indicate fairly linear aerodynamic trends for parametric plume geometry changes and that a wide range of plume effects are possible with simple plume designs. The data are very useful for determining the parametric effects of each plume shape and will aid the aerodynamicist in the configuration of a set of solid plume simulators to produce a known desired effect on future vehicle wind tunnel models during testing. Though Space Shuttle launch vehicle flight base pressures were produced on the model, along with considerable variations about the flight values, this study was not intended to derive any method of predicting flight base pressures beforehand, but to evaluate a method of producing predicted or known flight values during wind tunnel testing.

ORIGINAL PAGE IS
OF POOR QUALITY

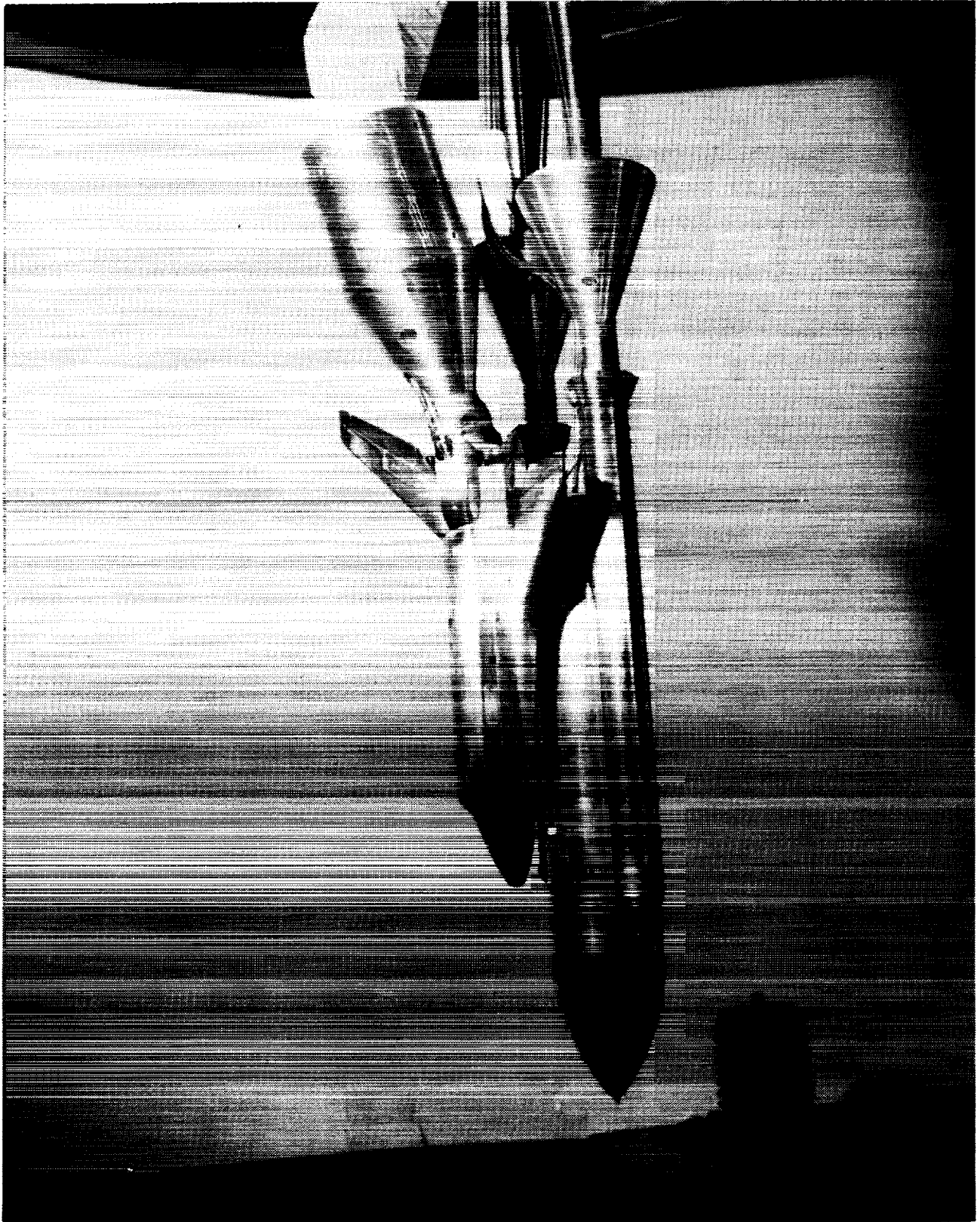


Figure 1. SSLV model with solid plumes.

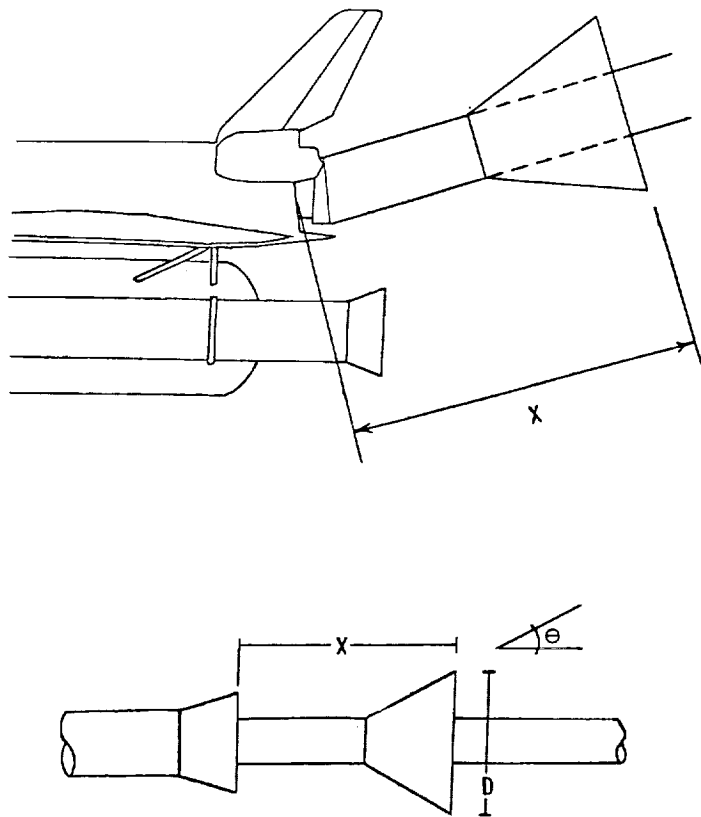


Figure 2. Plume parameters.

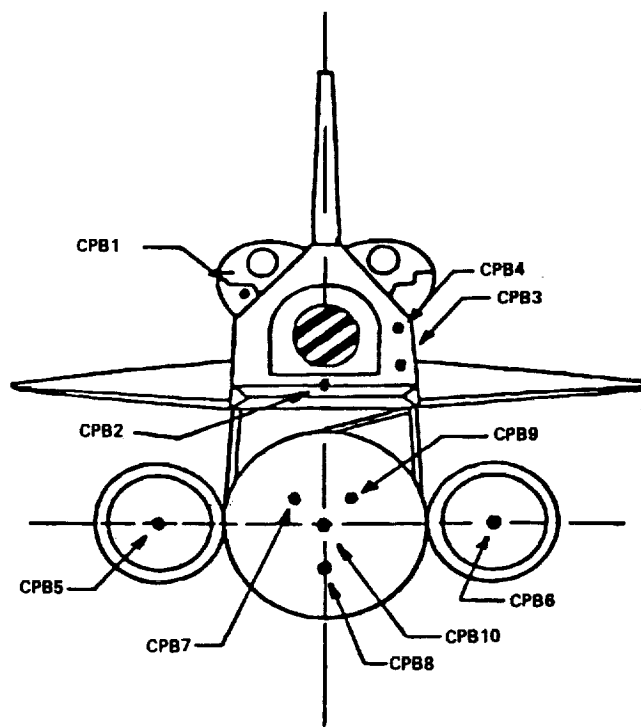


Figure 3. Base pressure tap locations.

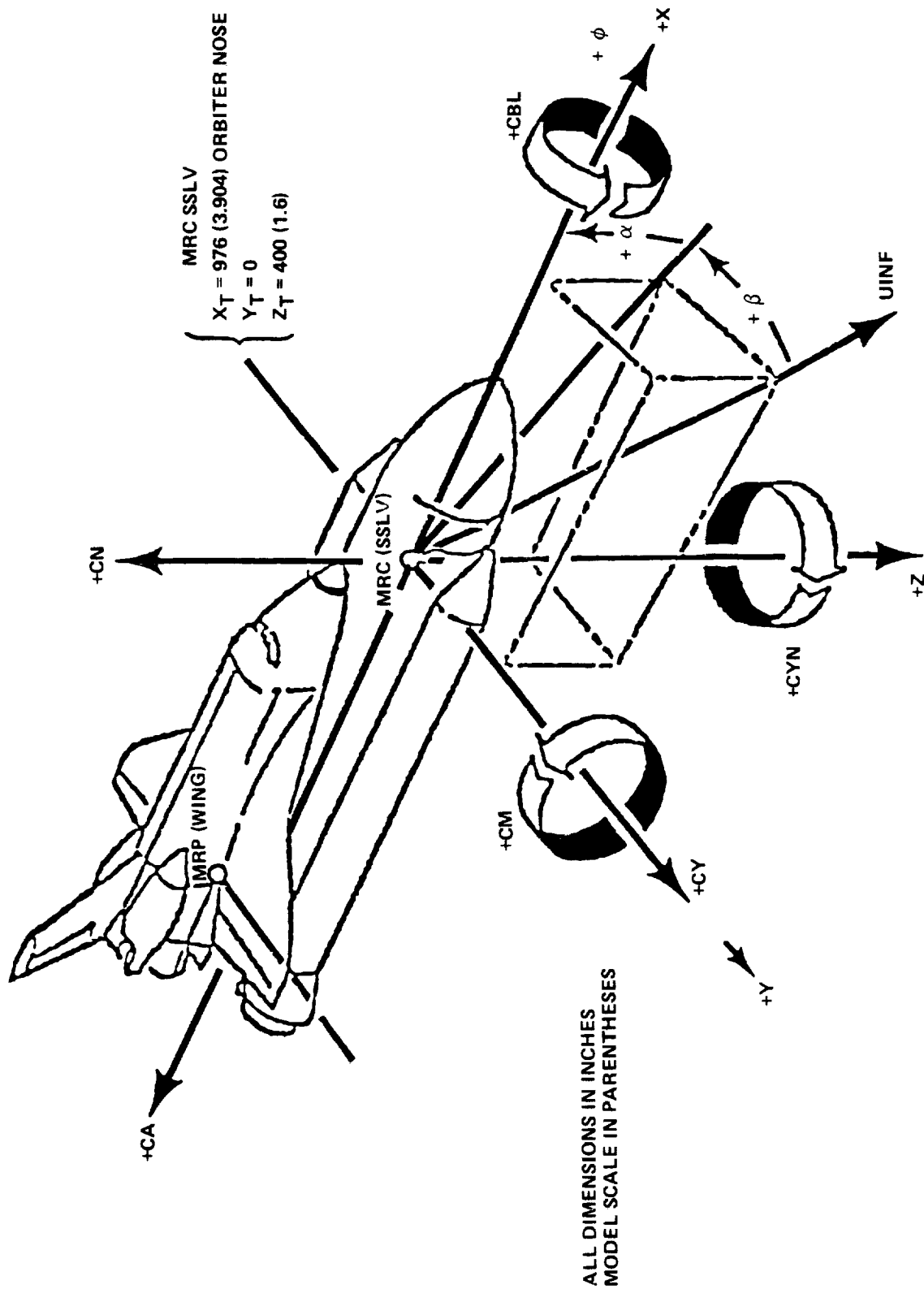
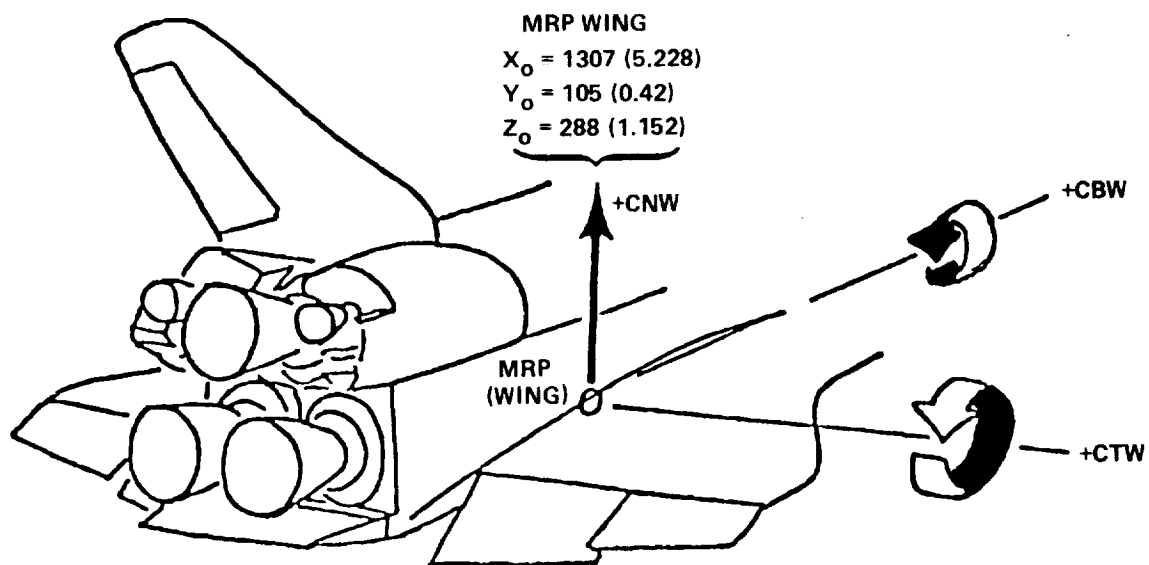
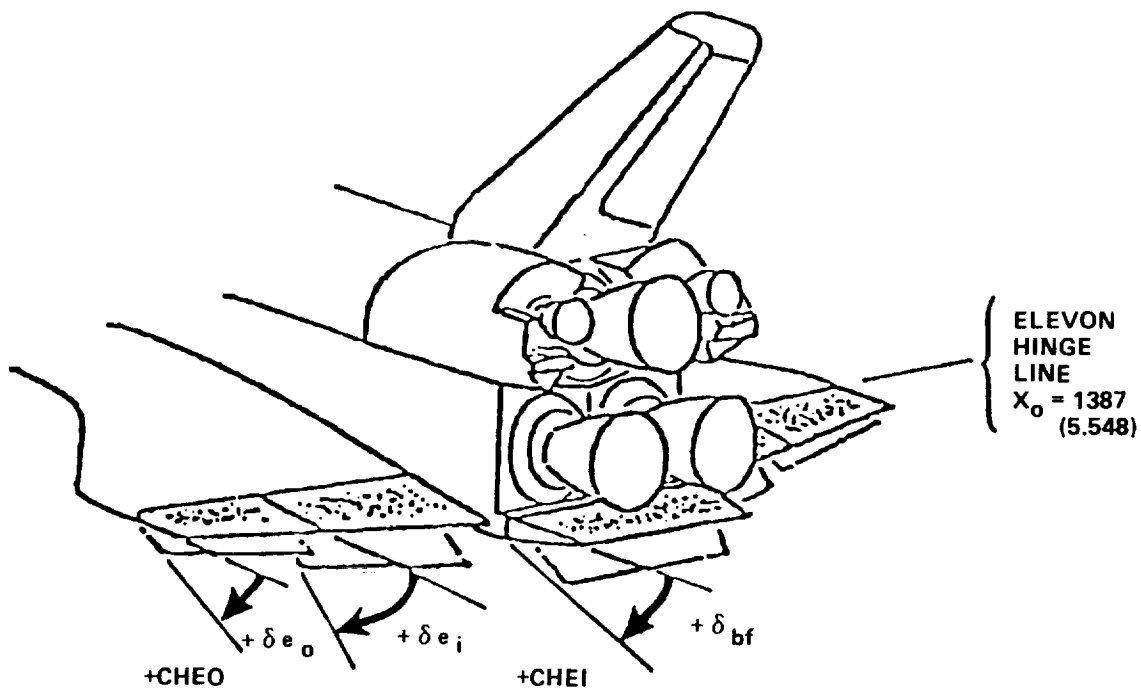


Figure 4. Aerodynamic body-axis reference system.



ALL DIMENSIONS IN INCHES
 MODEL SCALE IN PARENTHESES

Figure 5. Wing coordinate axes.



ALL DIMENSIONS IN INCHES
 MODEL SCALE IN PARENTHESES

Figure 6. Elevon coordinate axes.

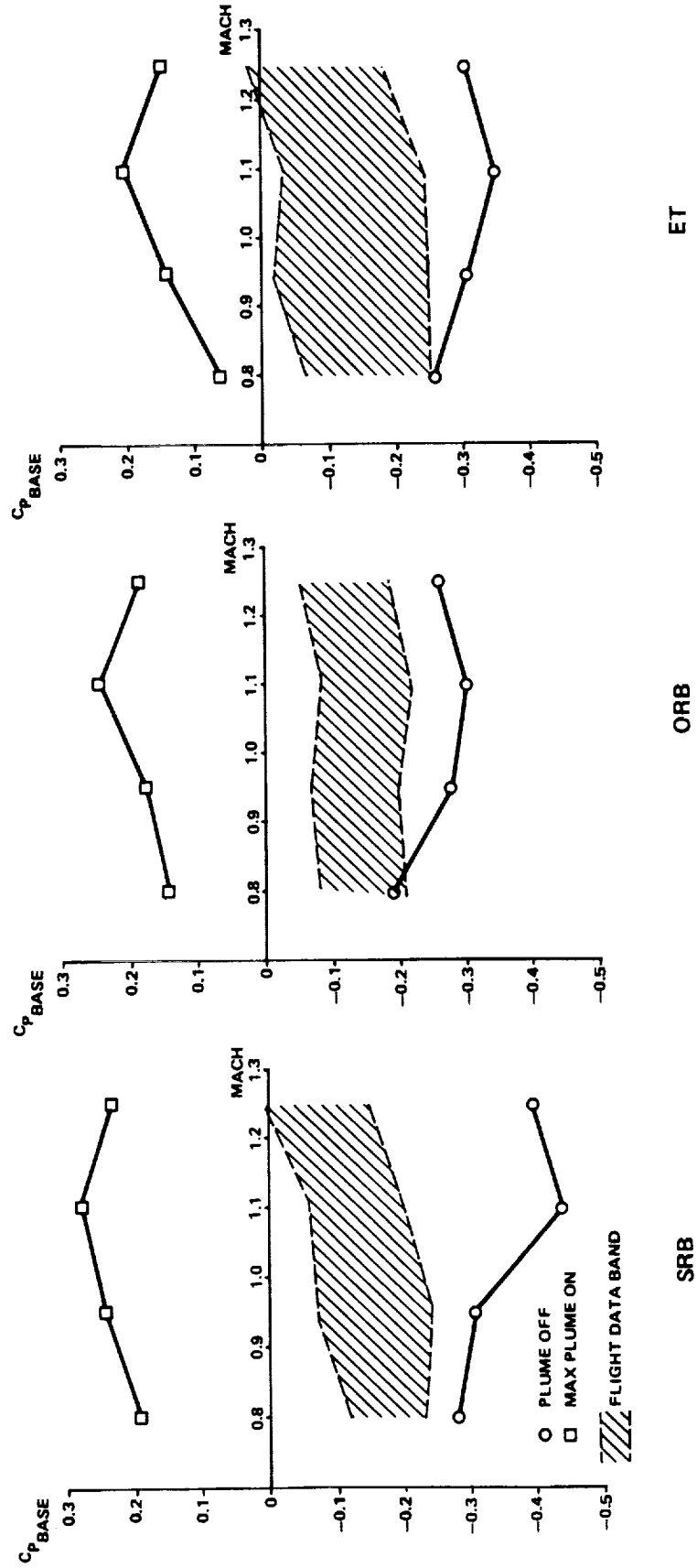


Figure 7. SSLV element base pressure.

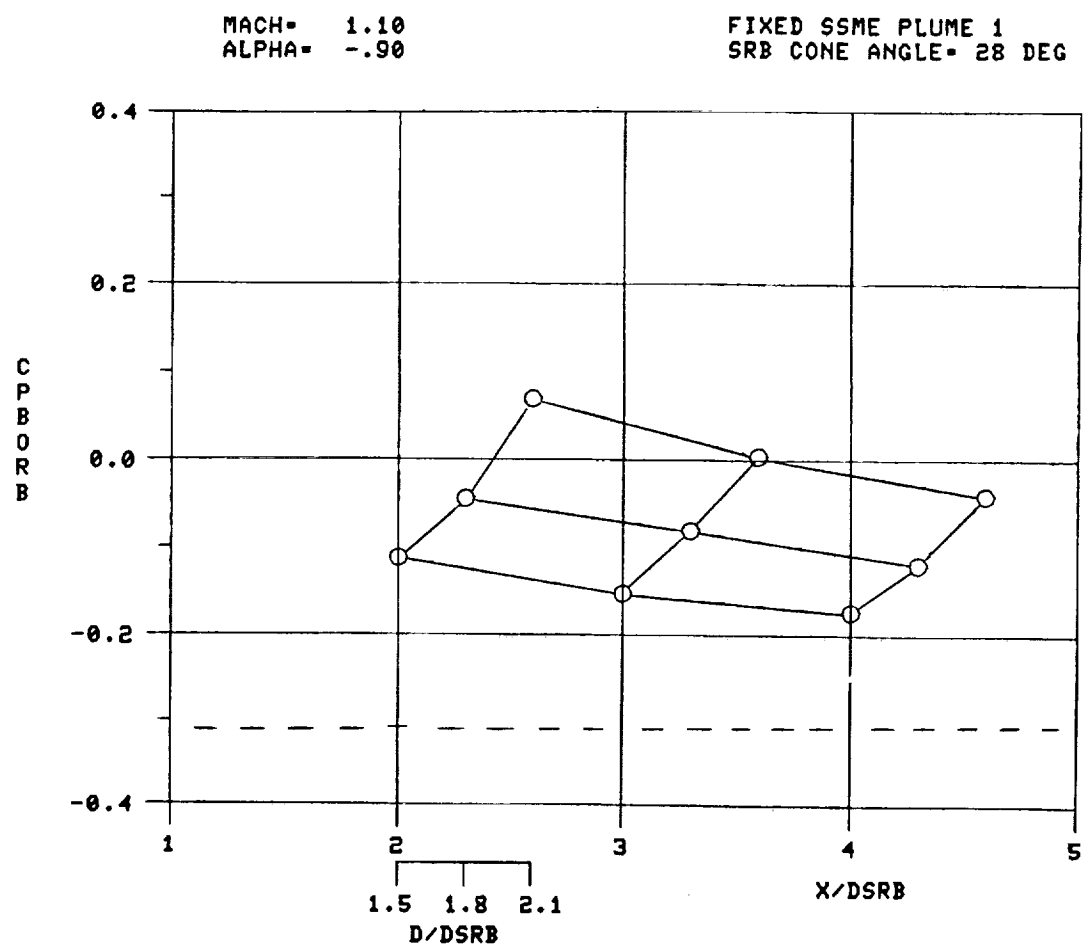


Figure 8. Orbiter base pressure coefficient.

TABLE 1. PLUME CONFIGURATIONS TESTED

Designation	Angle (θ) (deg)	Diameter(s) (in.)	Position(s) (in.)
Variable SRB Plumes			
C1	20	1.25, 1.50, 1.75	1.67, 2.50, 3.33
C2	28	1.25, 1.50, 1.75	1.67, 2.50, 3.33
C3	45	1.25, 1.50, 1.75	1.67, 2.50, 3.33
Variable SSME Plumes			
CS1	20	1.25, 1.50, 1.75	2.57, 3.42, 4.28
CS2	35	1.25, 1.50, 1.75	2.57, 3.42, 4.28
Fixed SRB Plumes			
1	20	1.25	2.50
2	20	1.75	2.50
Fixed SSME Plumes			
1	20	1.25	2.57
1	20	1.75	2.57

TABLE 2. REFERENCE DIMENSIONS AND CONSTANTS

Symbol	Description	Model Scale
A_{ORB}	Orbiter Base Area	6.878 cm ² (1.066 in. ²)
A_{ET}	External Tank Base Area	8.885 cm ² (1.377 in. ²)
A_{SRB}	SRB Base Area (one SRB)	3.510 cm ² (0.544 in. ²)
A_{BF}	Body Flap Planform Area	2.123 cm ² (0.329 in. ²)
\bar{C}	Mean Aerodynamic Chord	4.8240 cm (1.8992 in.)
\bar{C}_e	Elevon Reference Length	0.9215 cm (0.3628 in.)
D_{ORB}	Orbiter Fuselage Width	2.172 cm (0.855 in.)
D_{SRB}	SRB Aft Skirt Base	2.116 cm (0.833 in.)
L_{REF}	Reference Length	13.106 cm (5.160 in.)
S_{REF}	Reference Area	39.987 cm ² (6.198 in. ²)
S_{eREF}	Elevon Reference Area	3.122 cm ² (0.4838 in. ²)
X_1	Horizontal Distance from Centroid of Orbiter Base to MRP	-12.832 cm (-5.052 in.)
X_{TO}	Horizontal Distance from Balance Center to MRP	-9.253 cm (-3.643 in.)
Z_1	Vertical Distance from Centroid	-3.380 cm (-1.306 in.)
Z_{TO}	Vertical Distance from Balance Center to MRP	-3.470 cm (-1.366 in.)

TABLE 3. TUNNEL OPERATING CONDITIONS

Mach Number	Reynolds Number (per ft)	Dynamic Pressure (psig)	Stagnation Temperature (°F)	Stagnation Pressure (psia)
0.80	6.0×10^6	6.45	120	22
0.95	6.4×10^6	7.74	120	22
1.10	6.6×10^6	9.29	120	22
1.25	6.8×10^6	11.38	120	22

APPENDIX A

ORIGINAL PAGE IS
OF POOR QUALITY

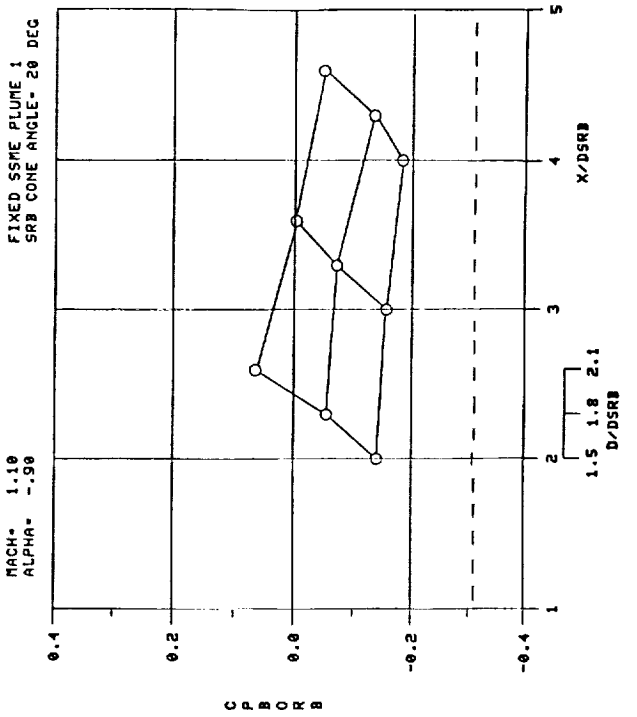
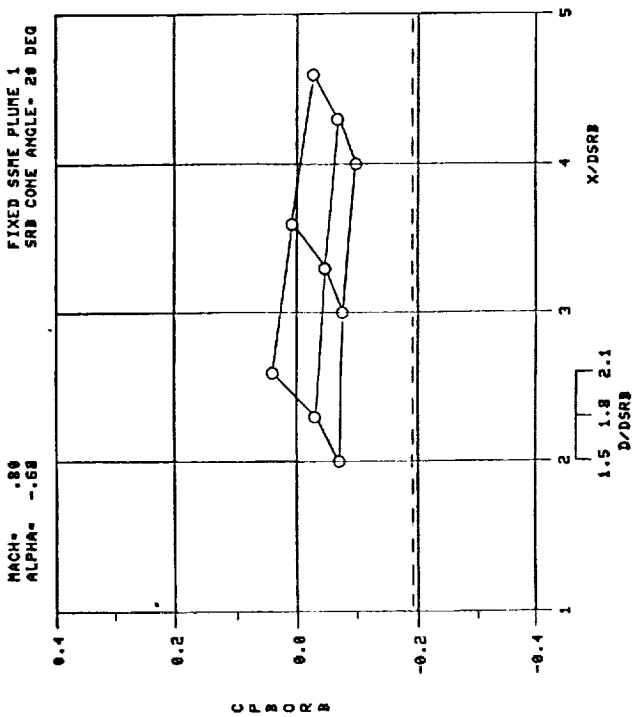
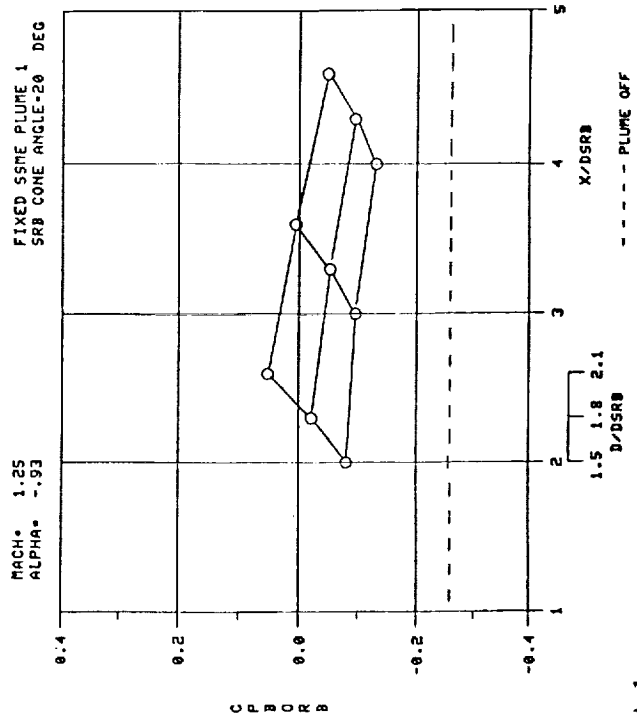
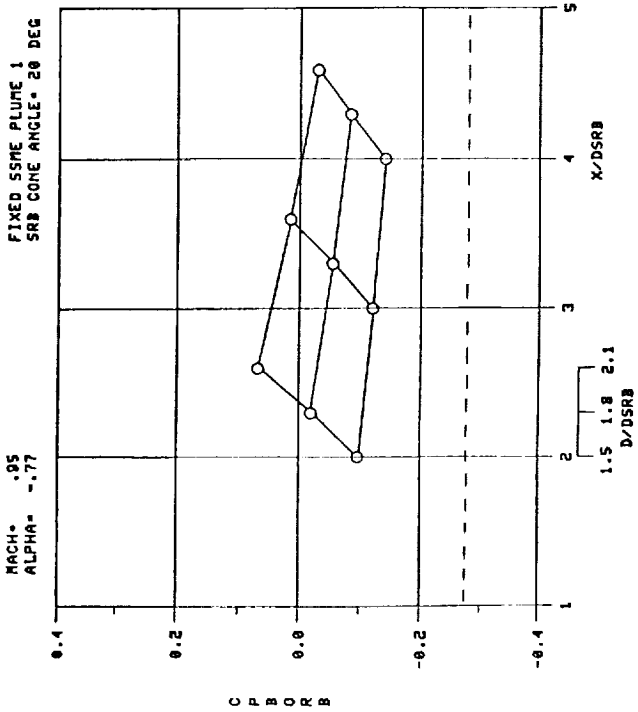


Figure A-1.

PRECEDING PAGE BLANK NOT FILMED

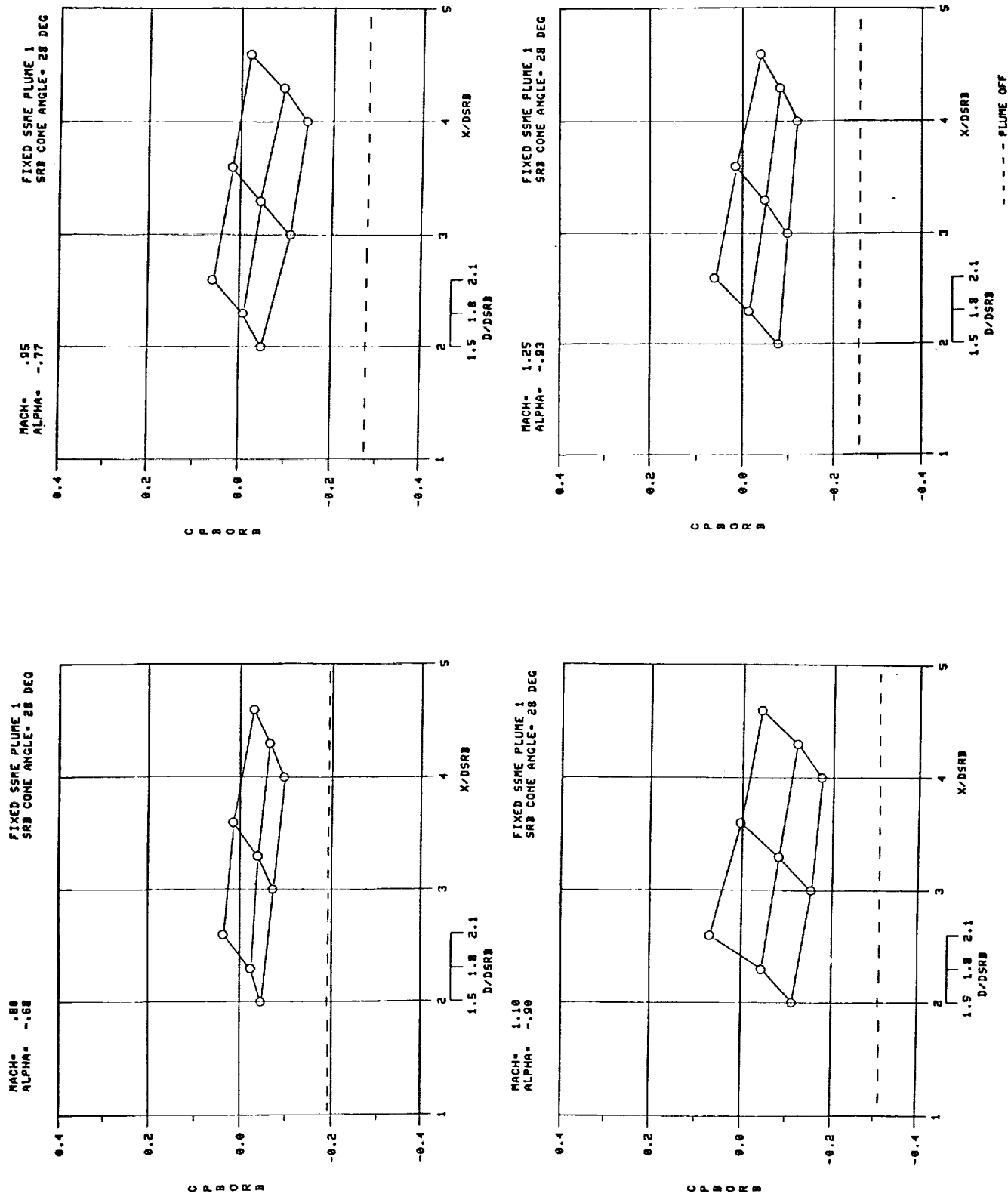


Figure A-2.

ORIGINAL PAGE IS
OF POOR QUALITY

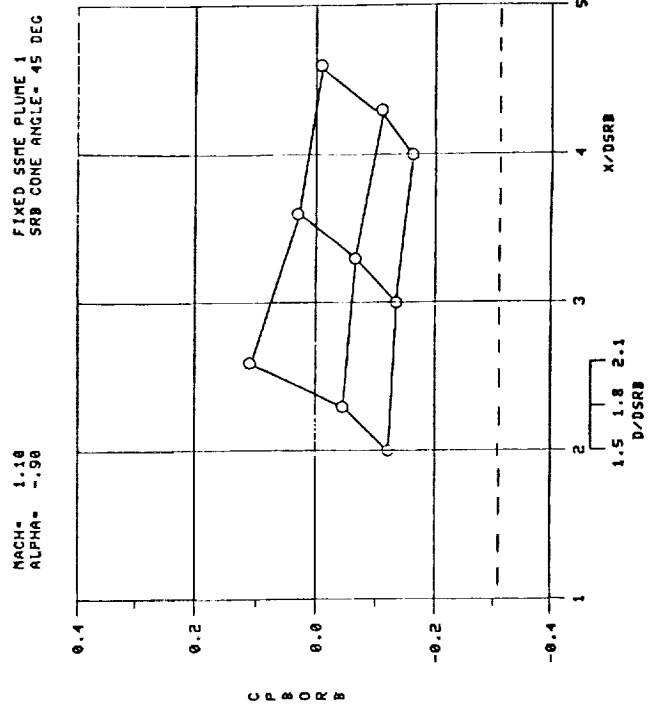
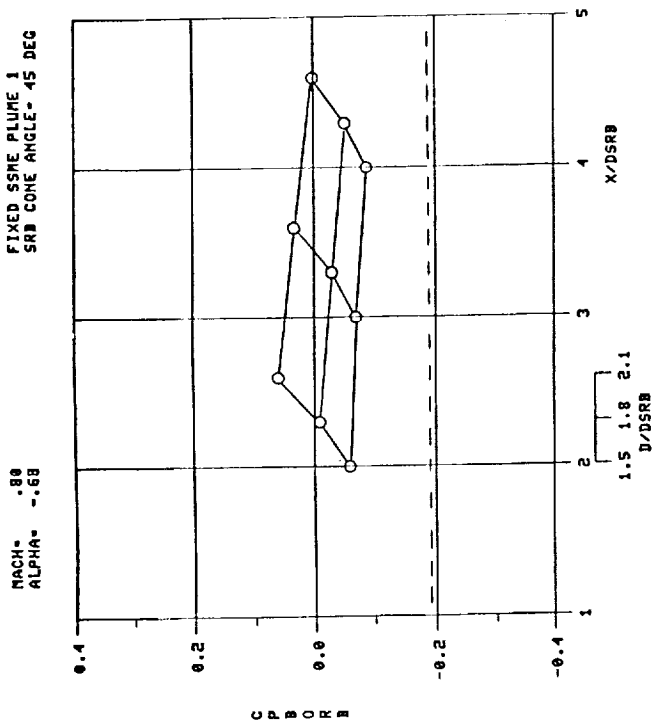
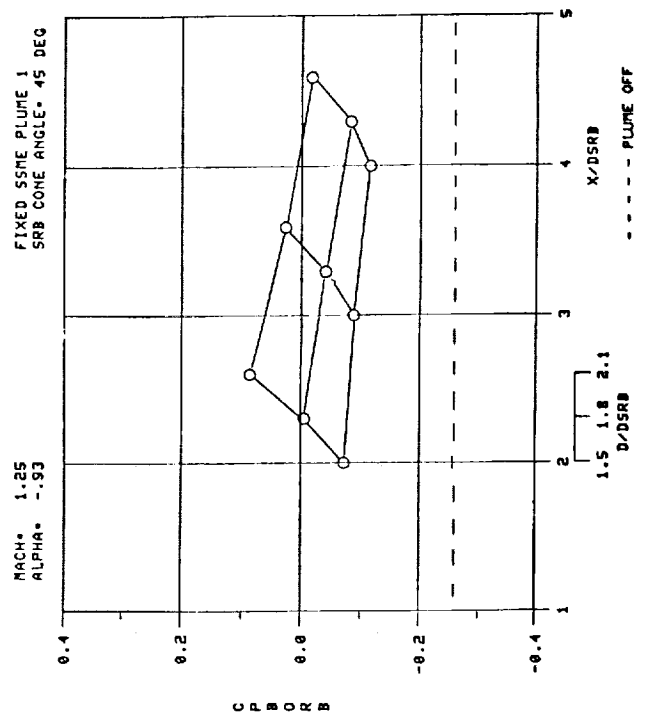
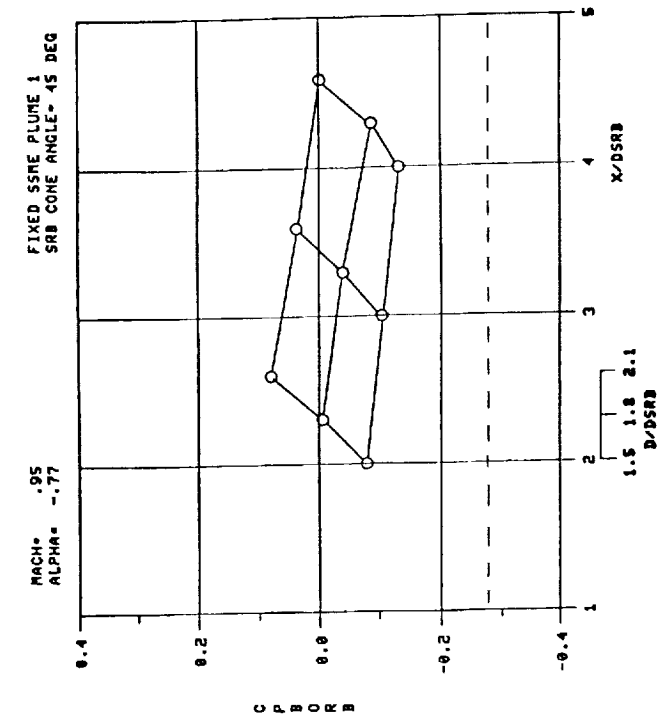


Figure A-3.

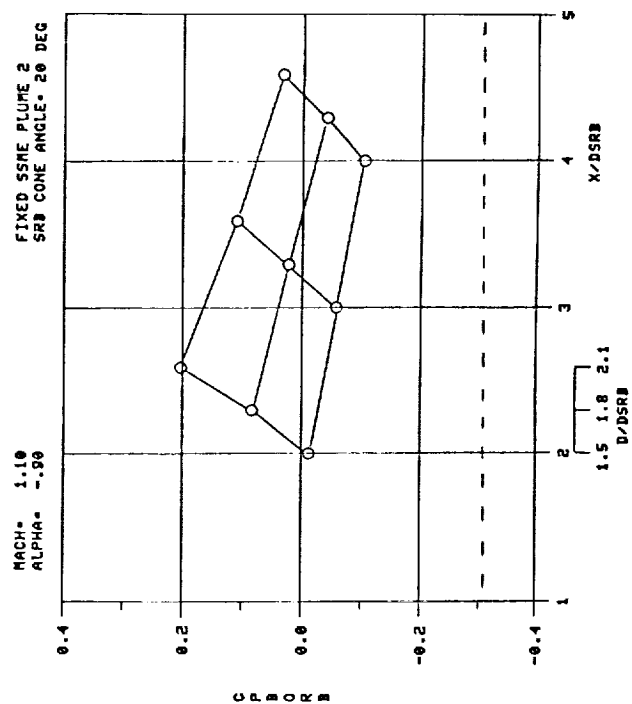
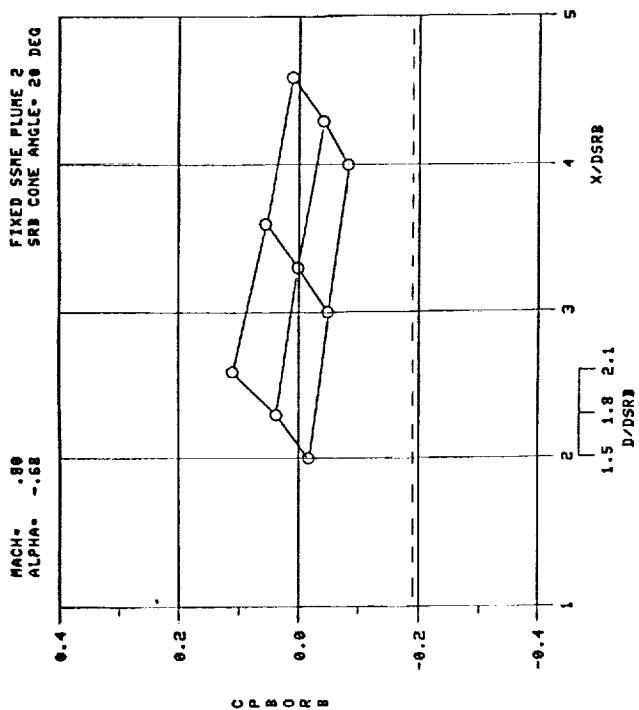
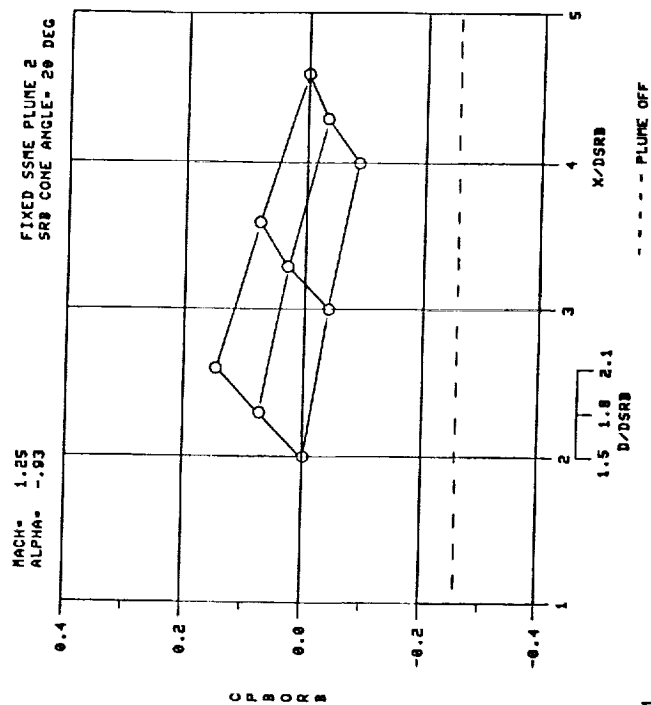
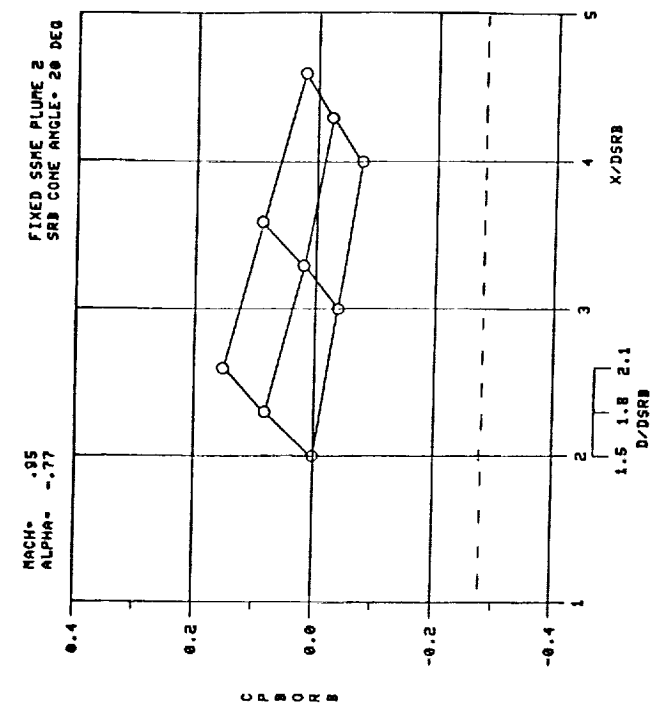


Figure A4.

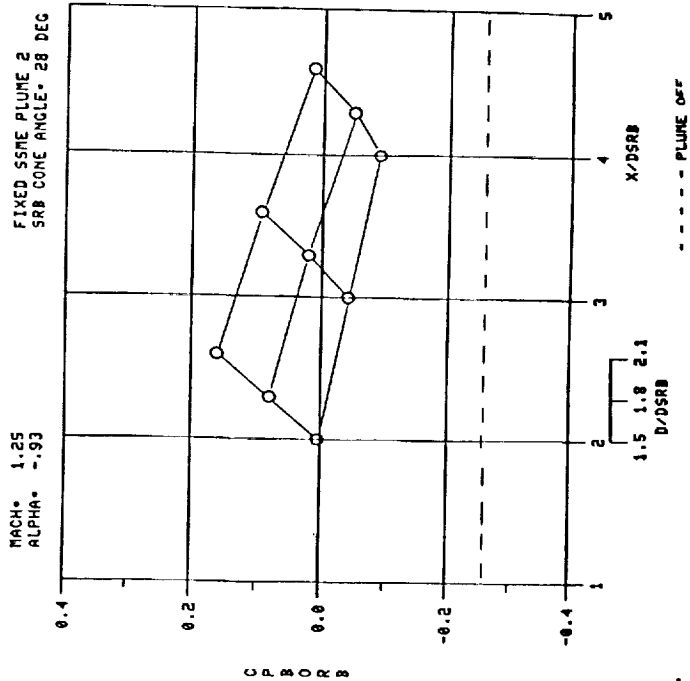
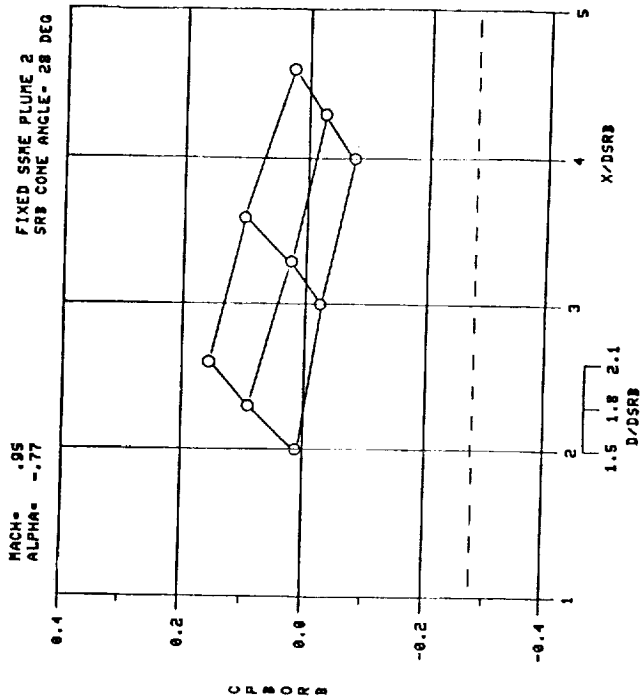
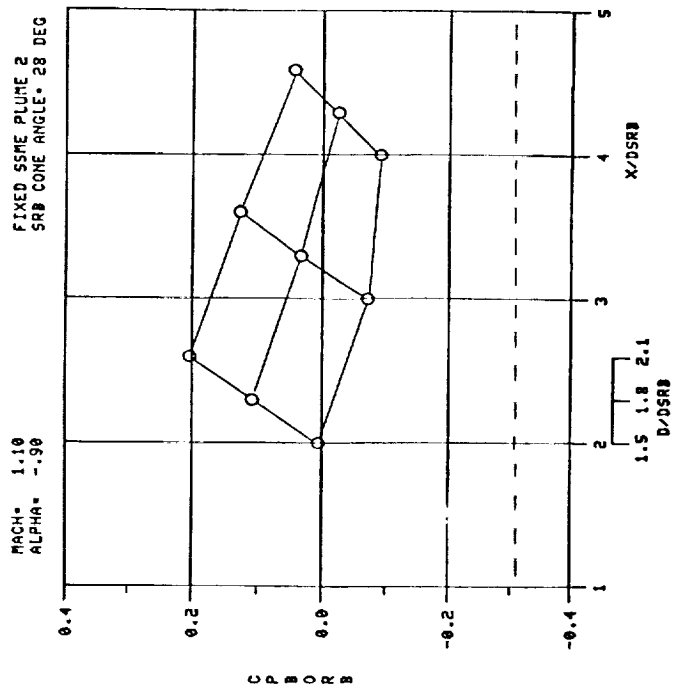
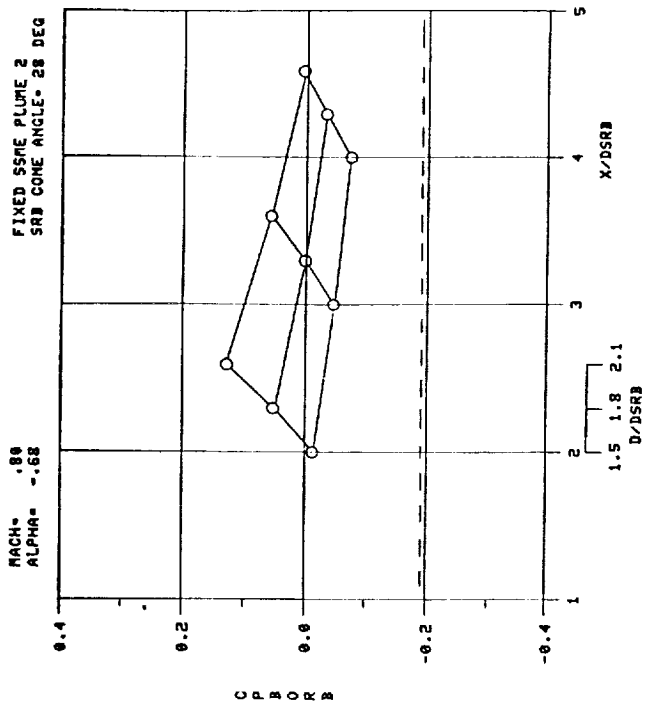


Figure A-5.

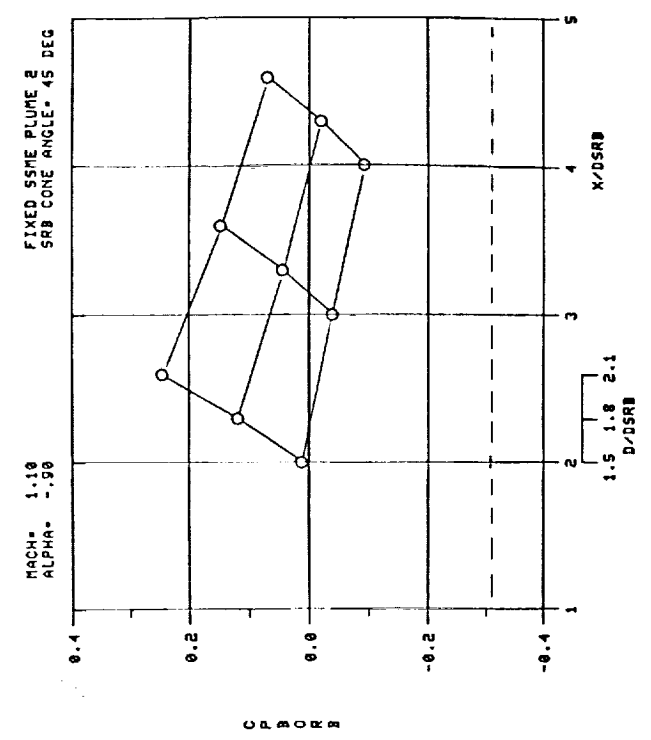
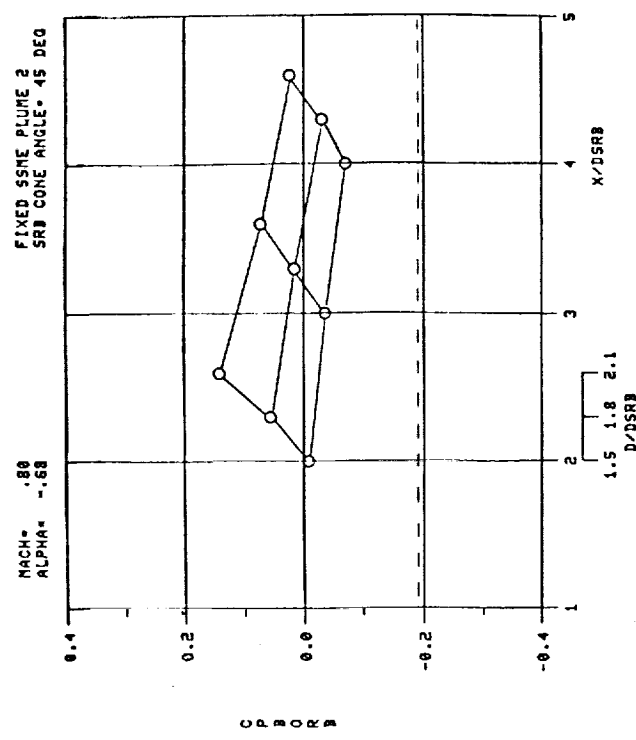
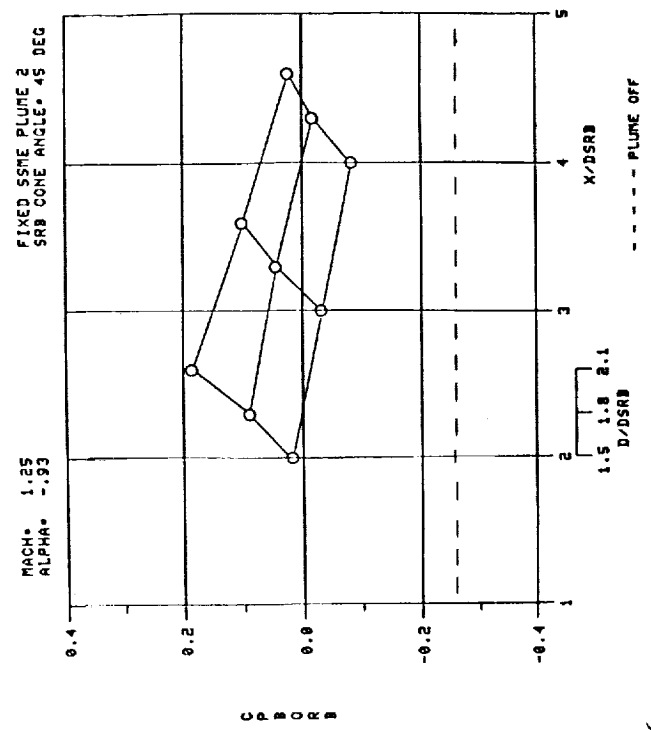
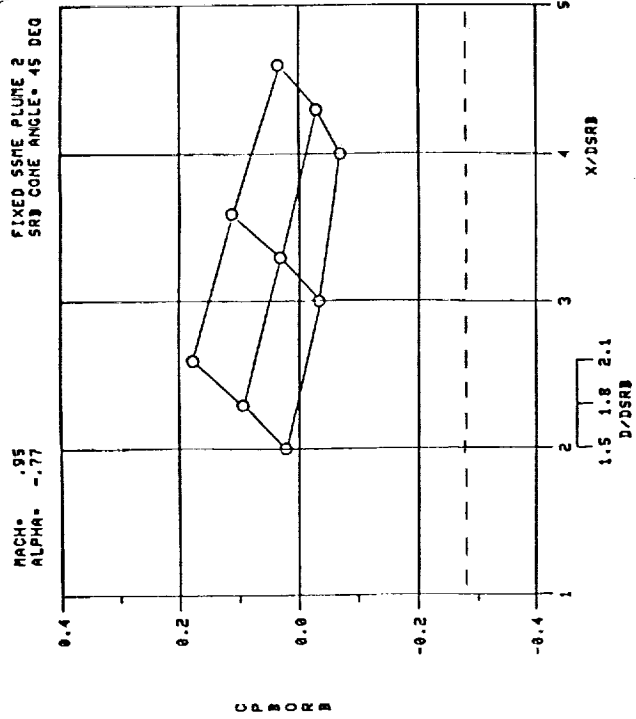


Figure A-6.

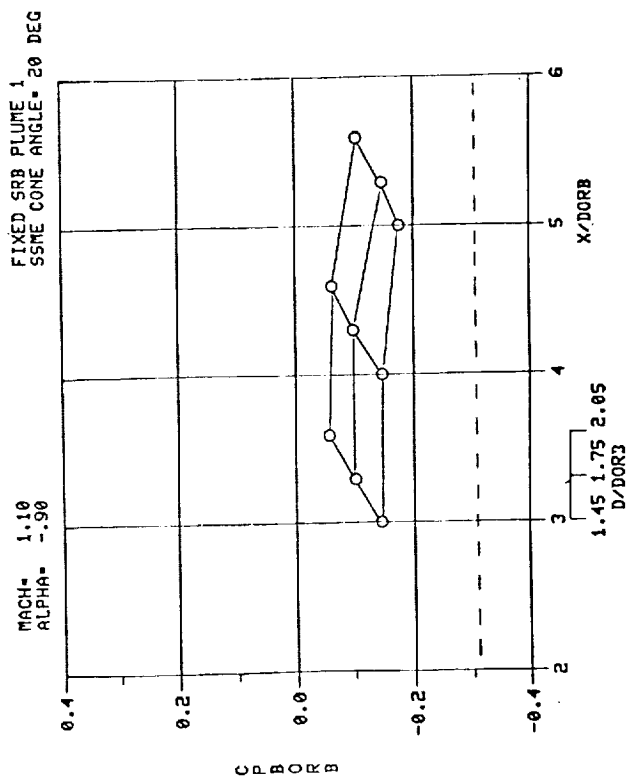
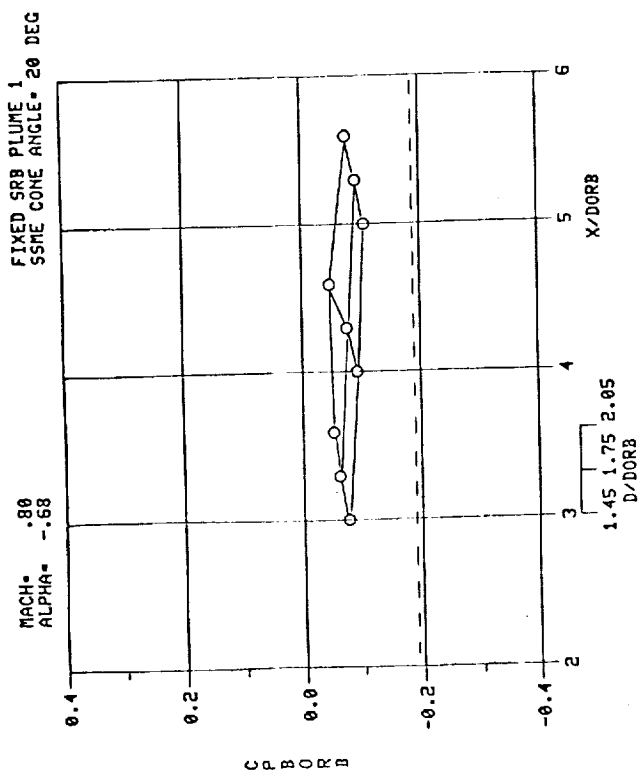
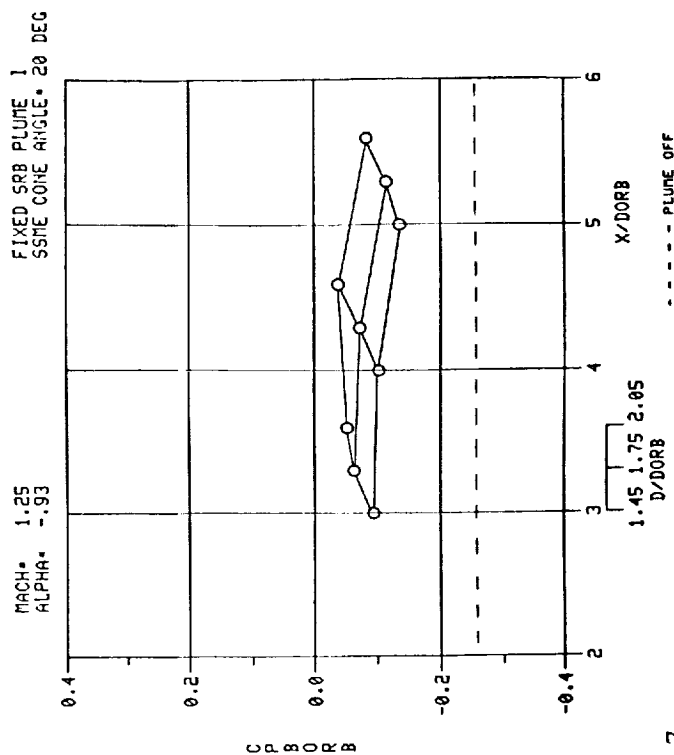
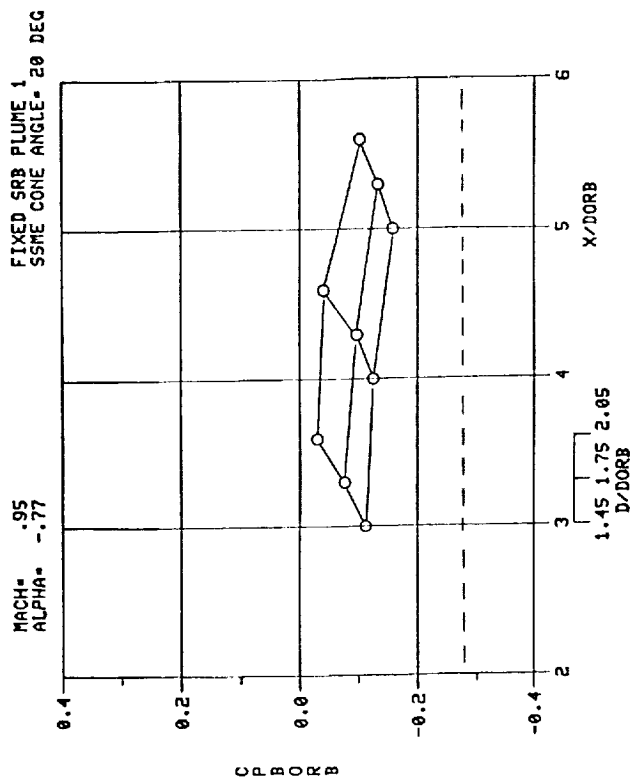


Figure A-7.

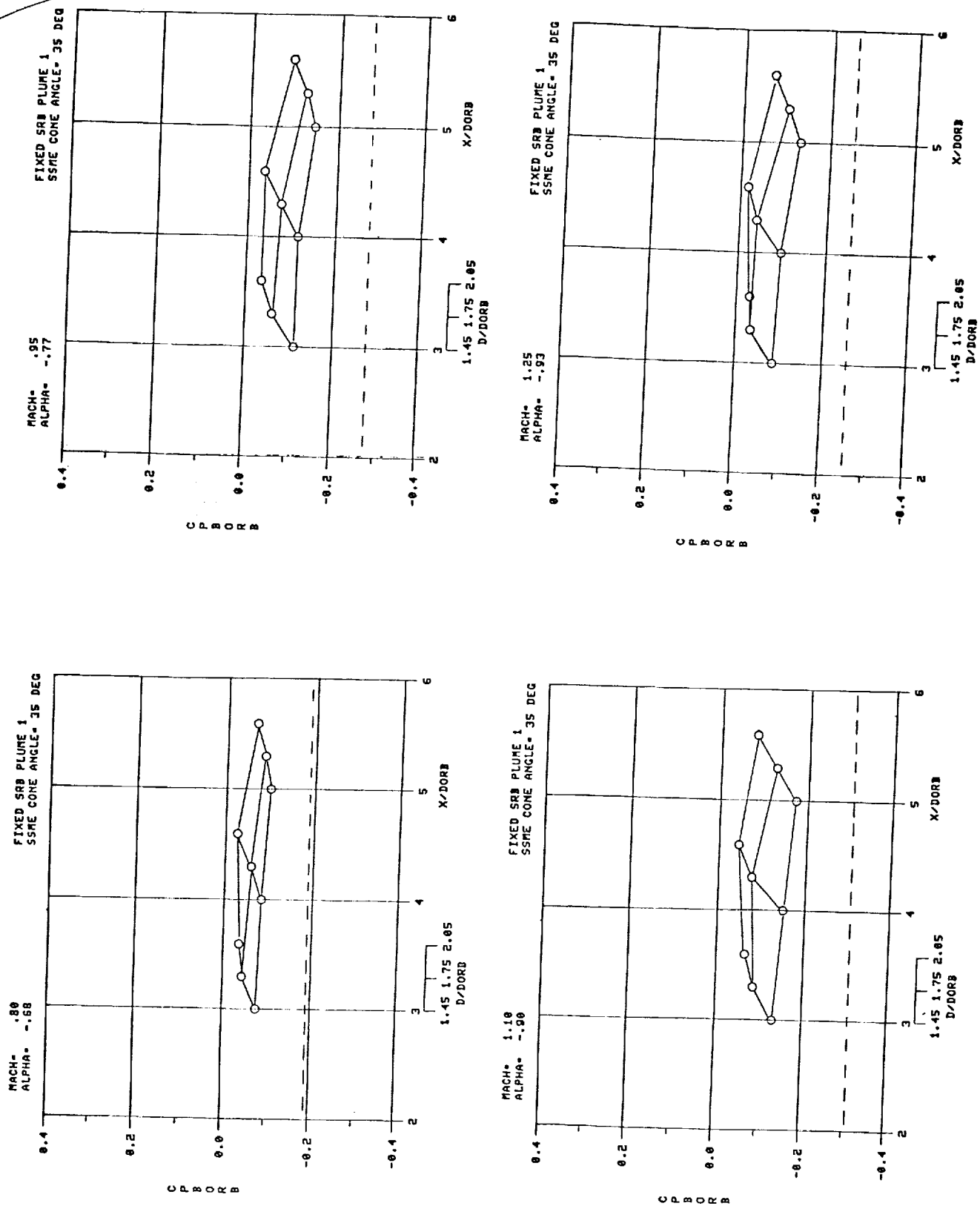


Figure A-8.

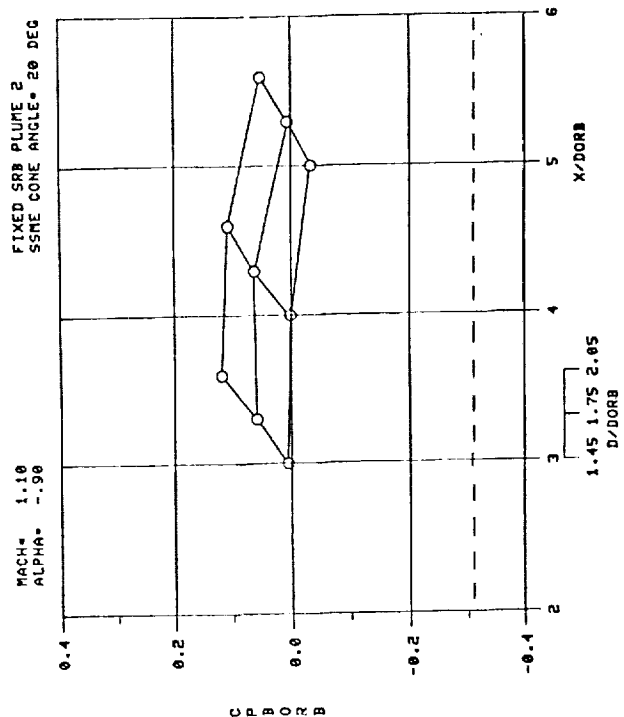
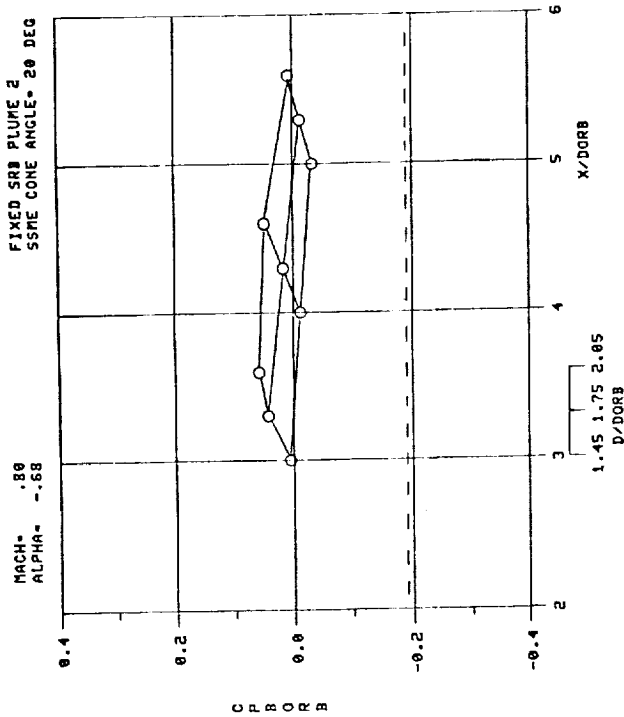
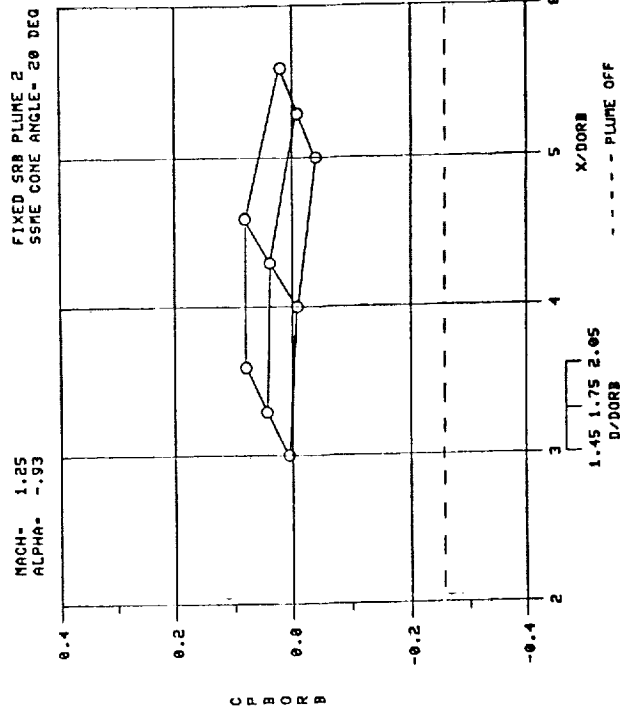
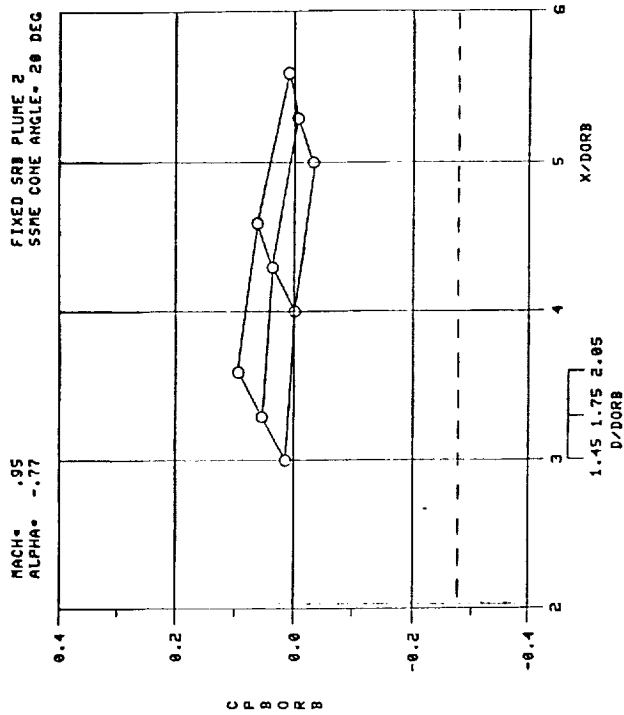


Figure A-9.

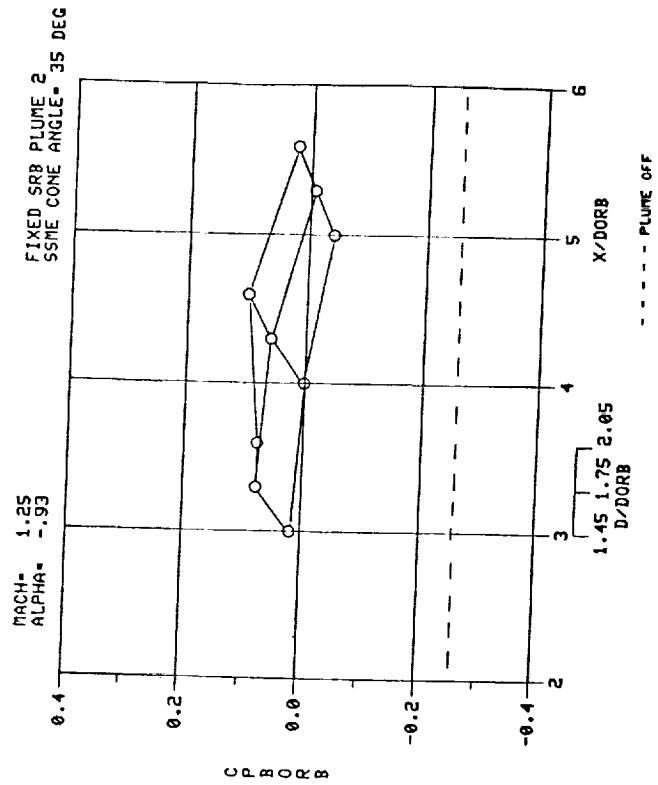
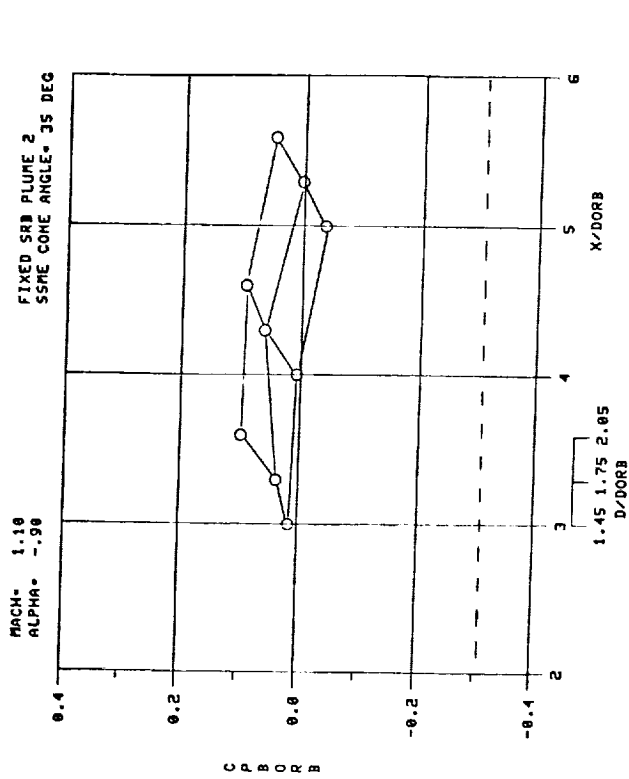
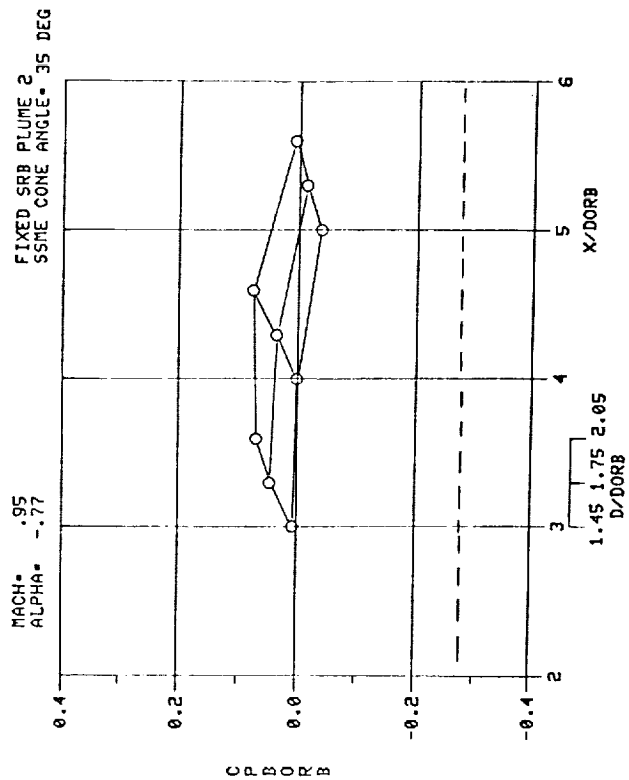
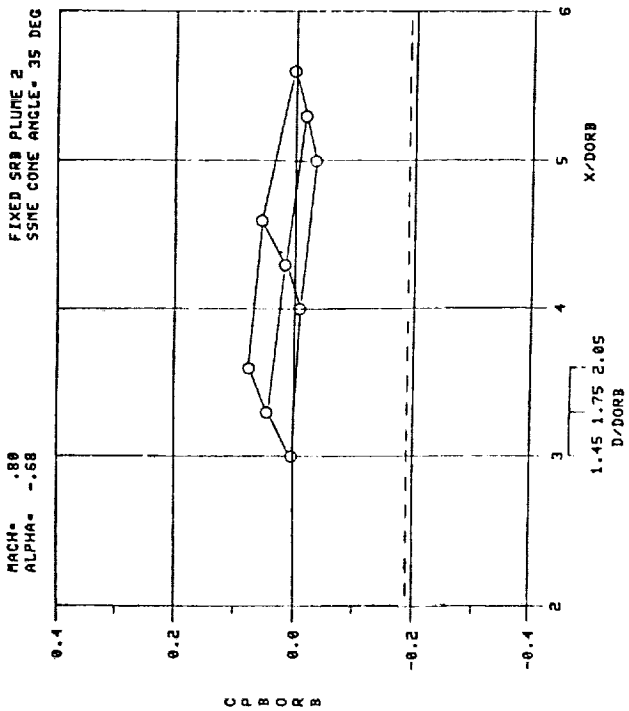


Figure A-10.

APPENDIX B



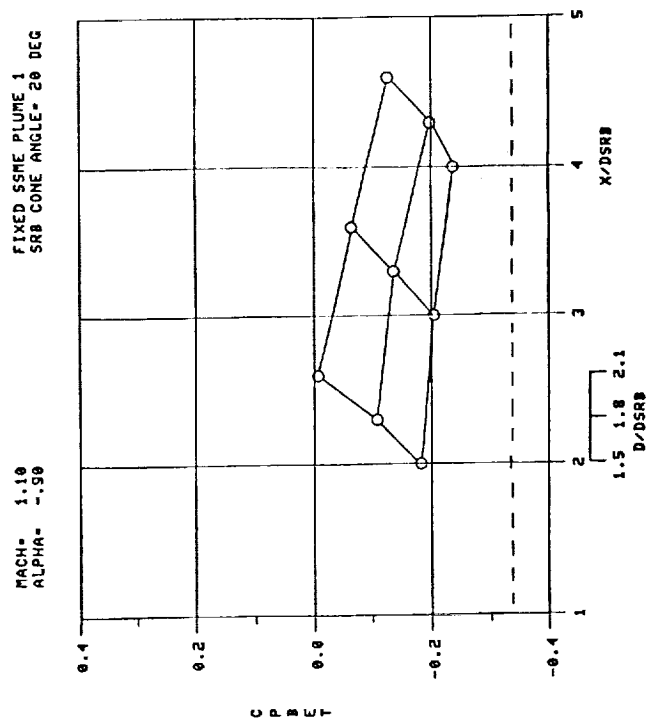
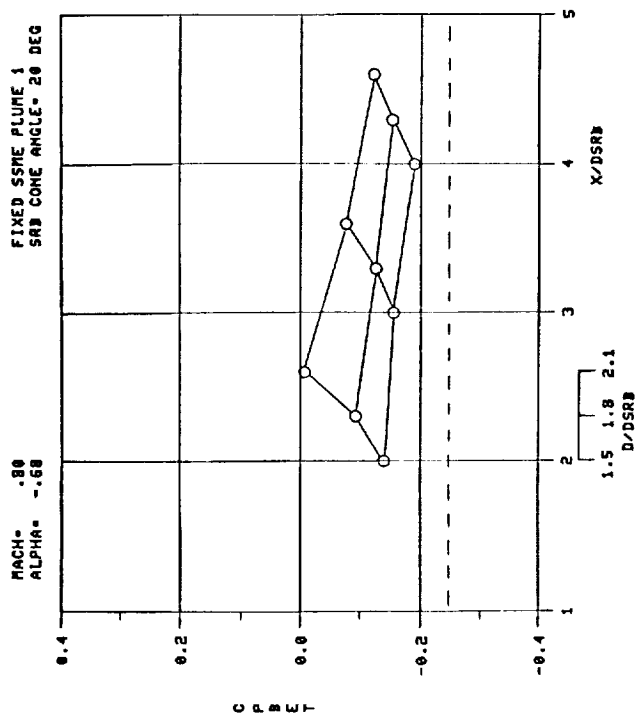
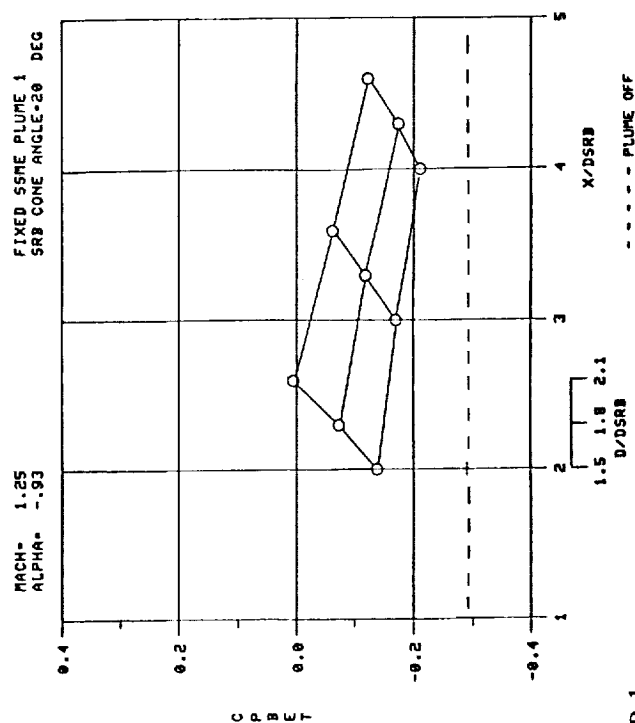
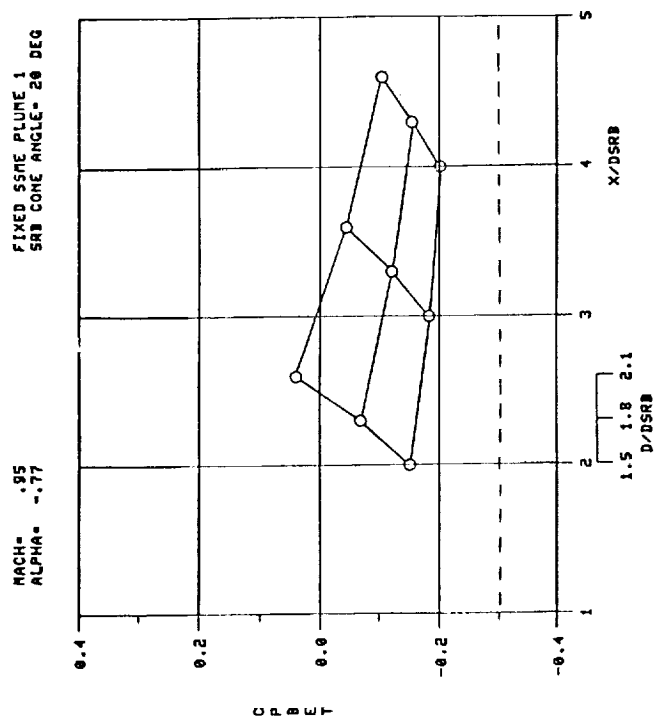


Figure B-1.

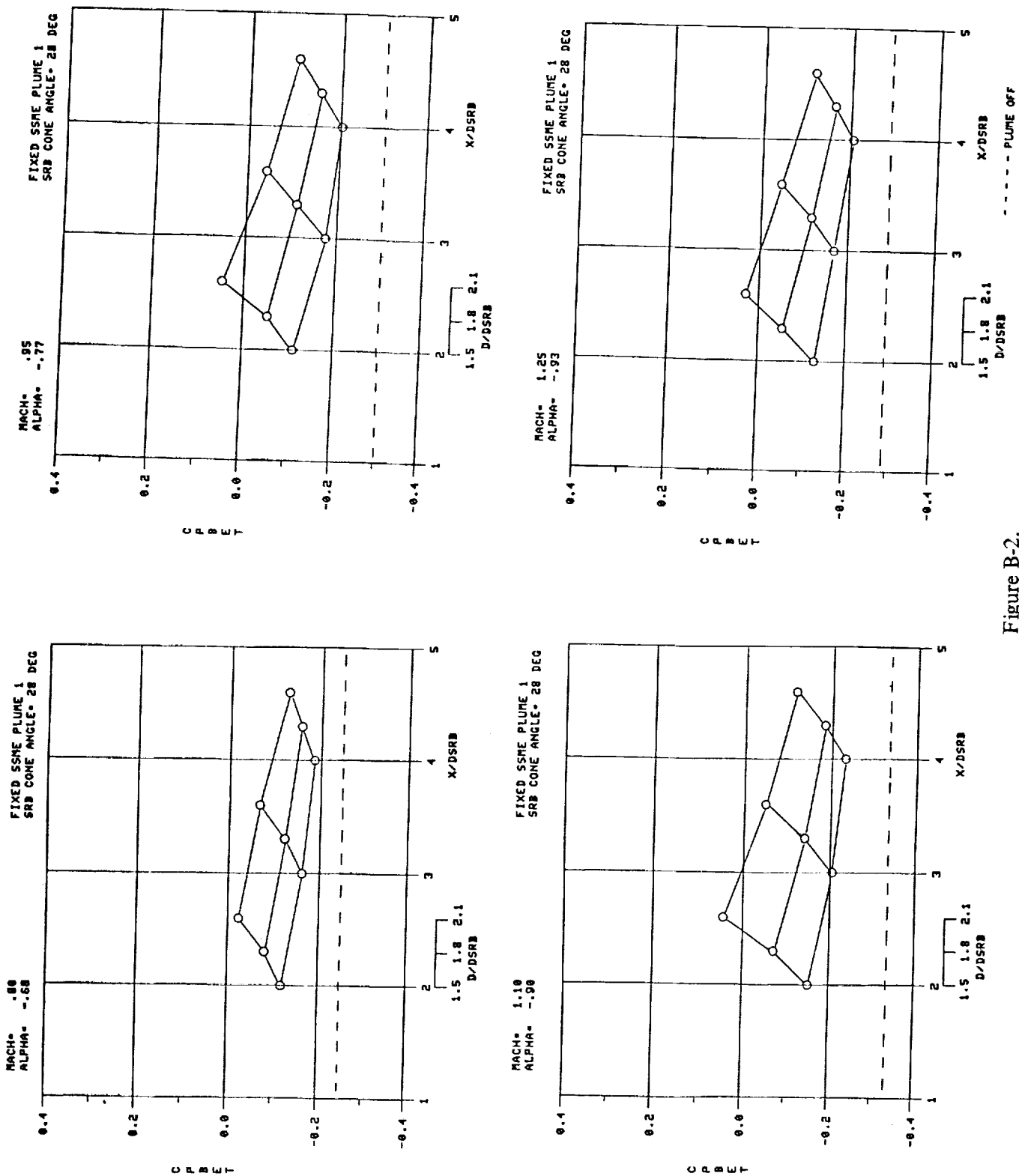


Figure B-2.

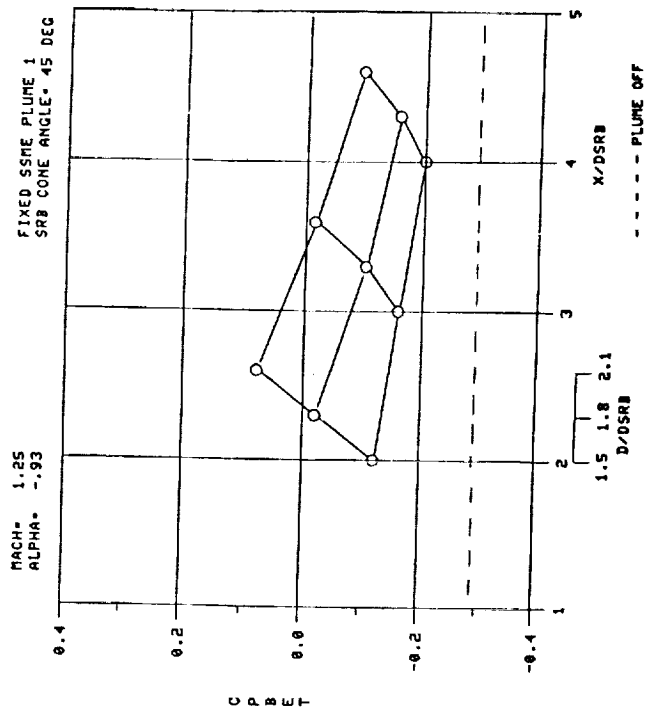
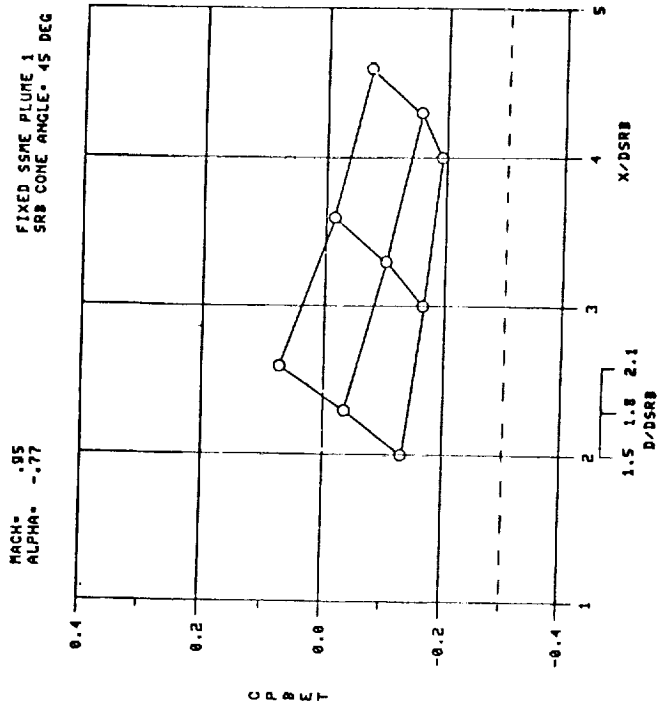
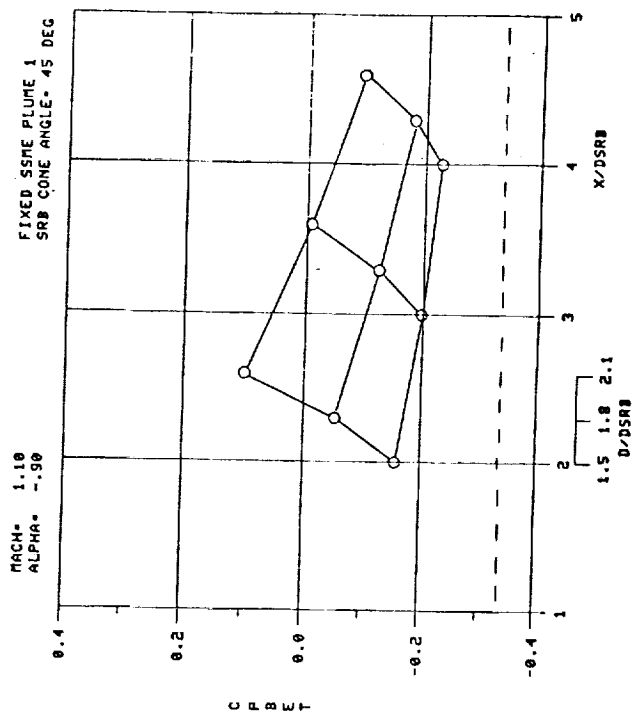
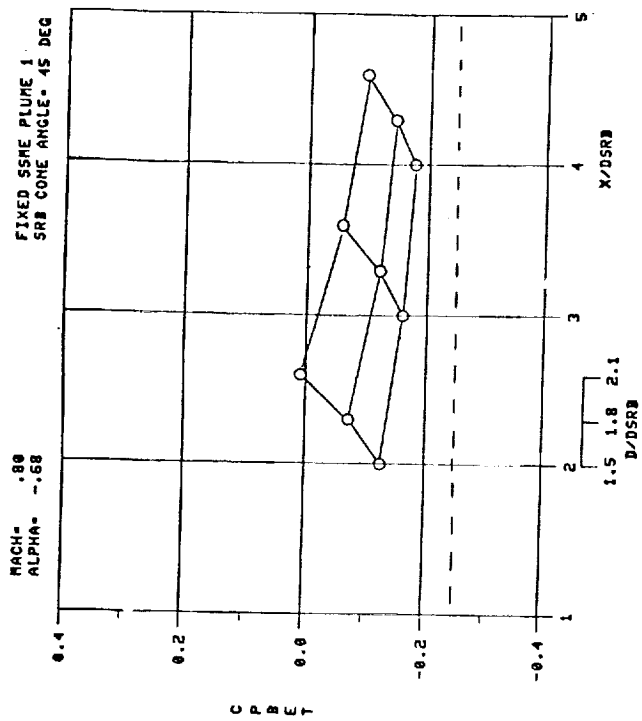


Figure B-3.

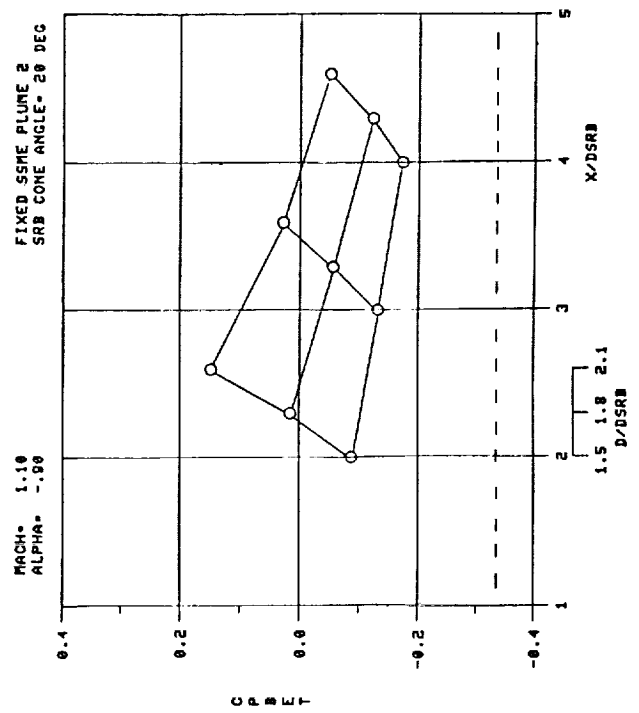
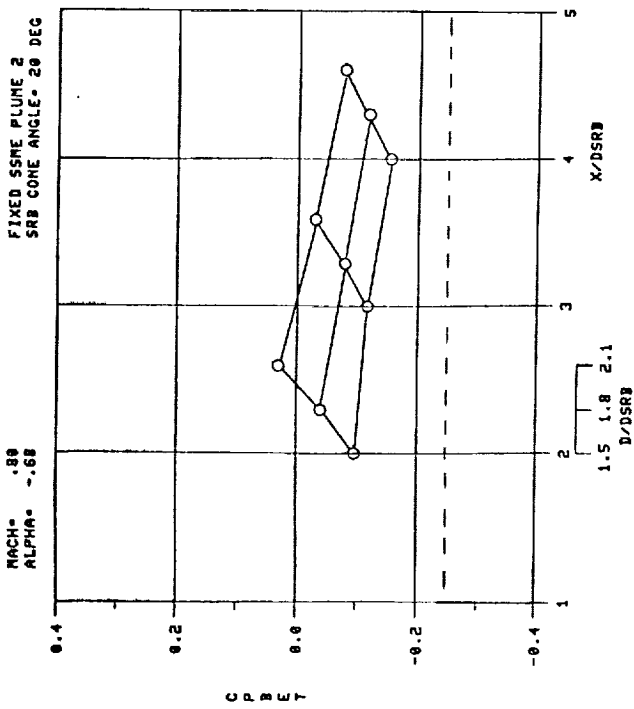
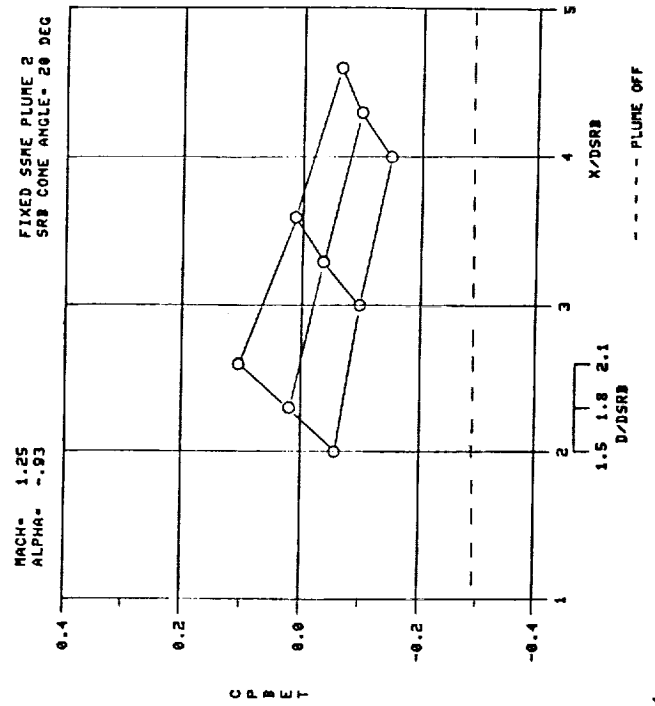
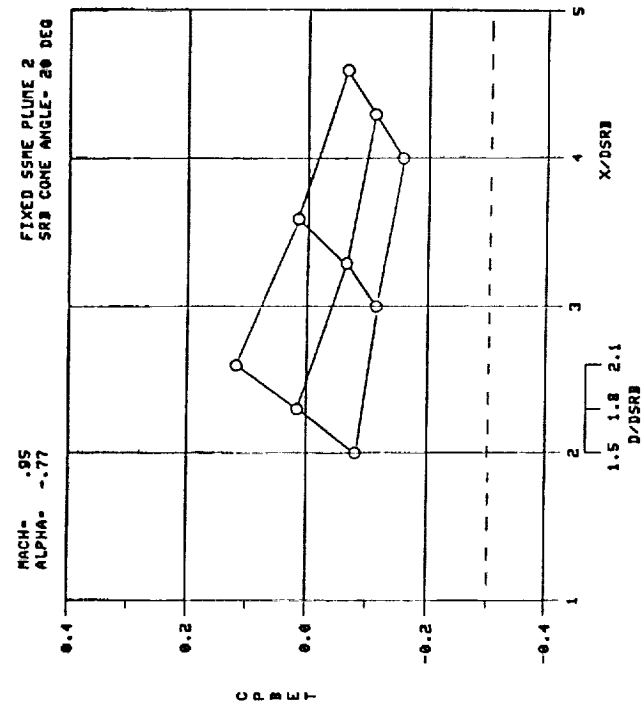


Figure B-4.

ORIGINAL PAGE IS
OF POOR QUALITY

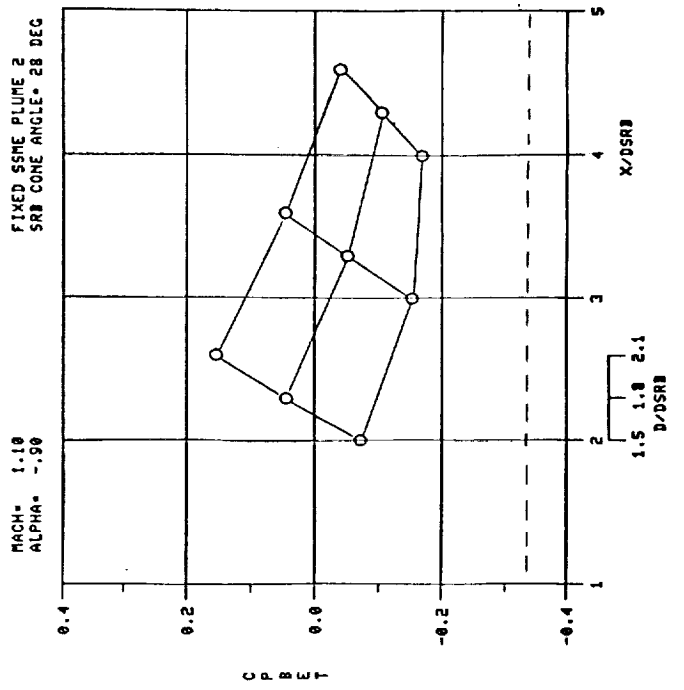
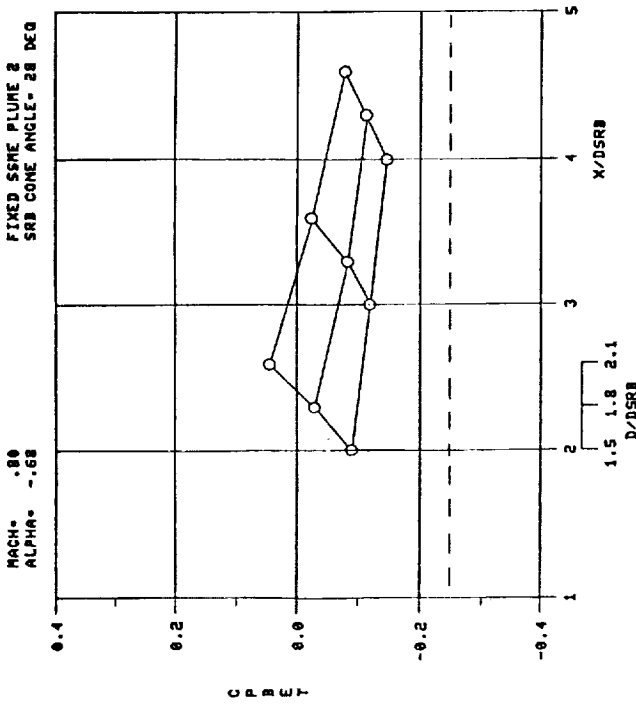
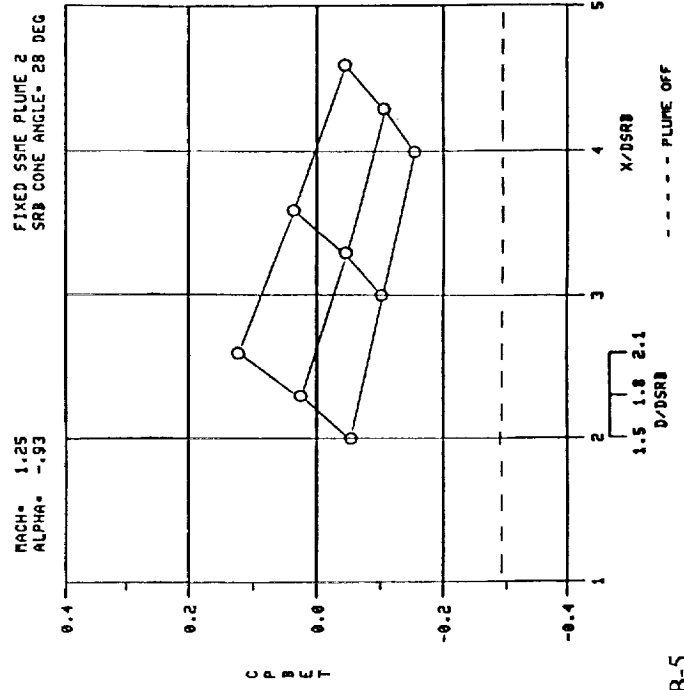
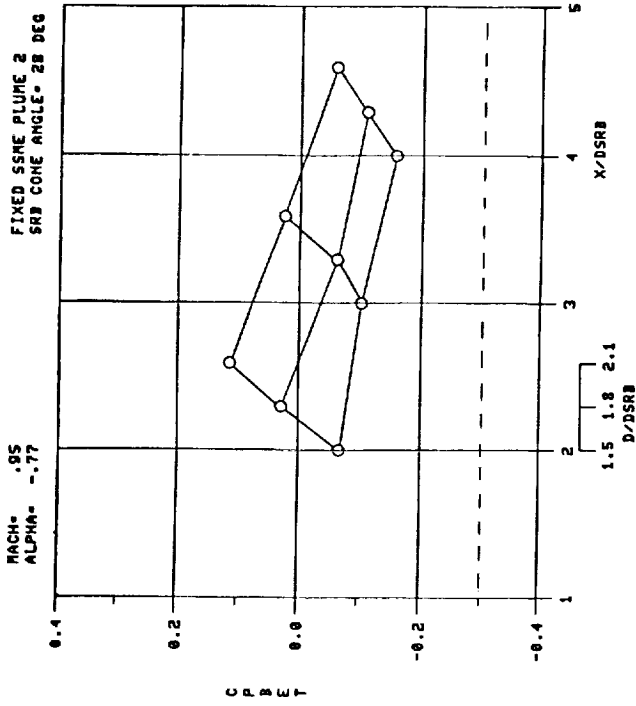


Figure B-5.

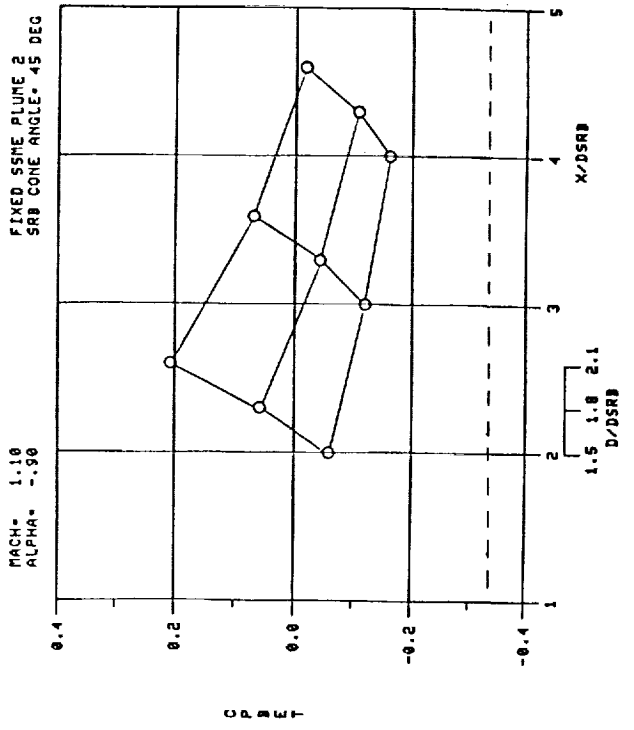
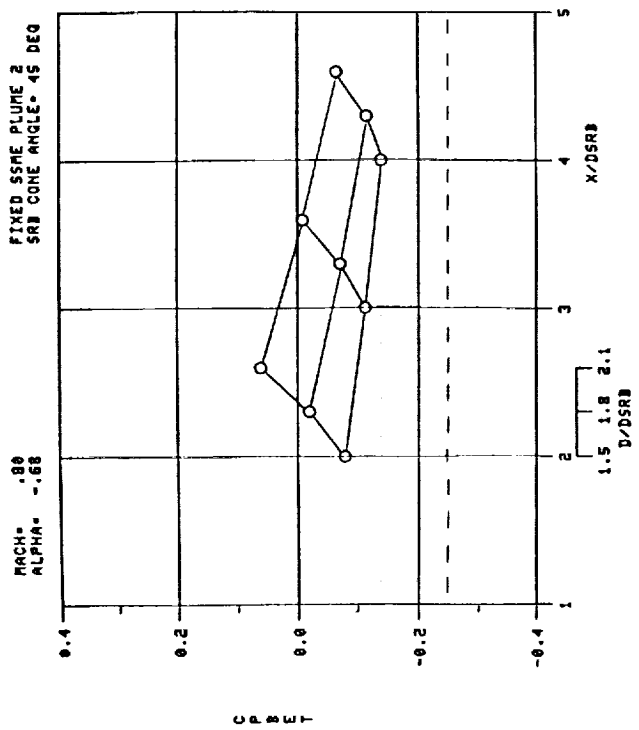
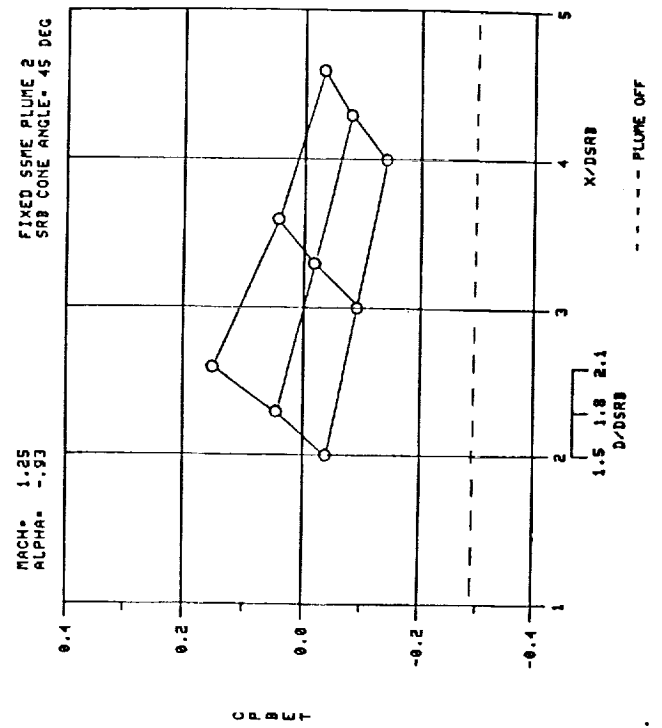
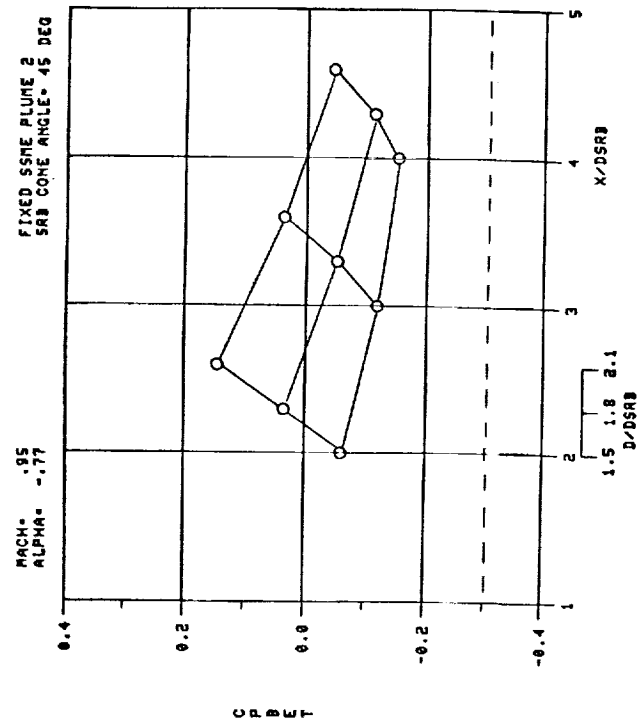


Figure B-6.

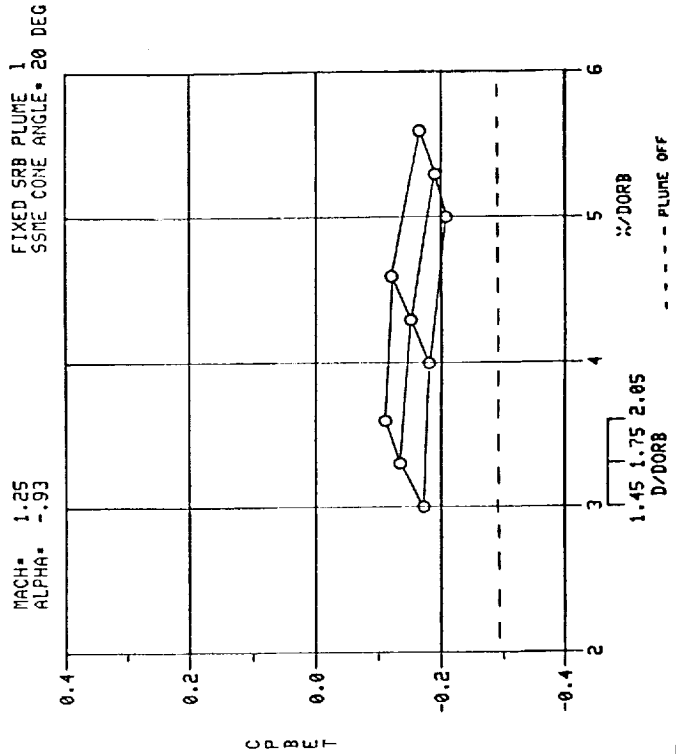
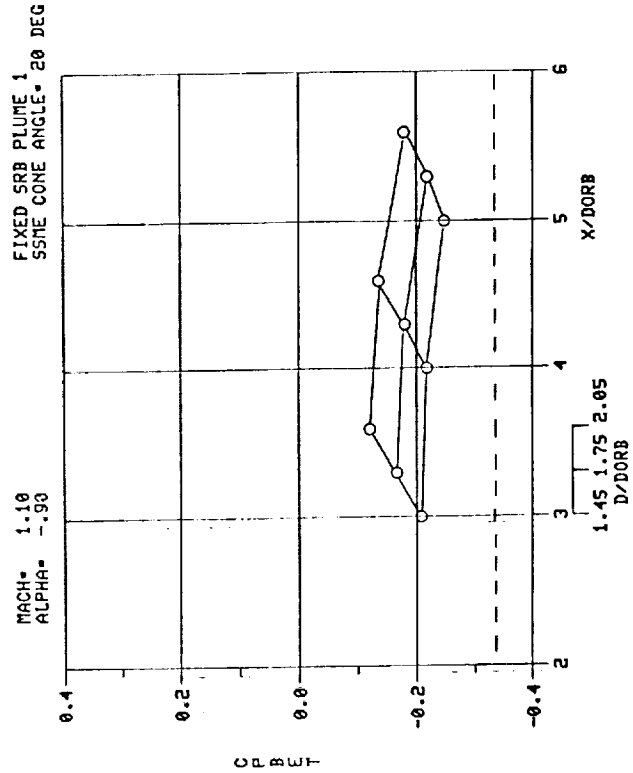
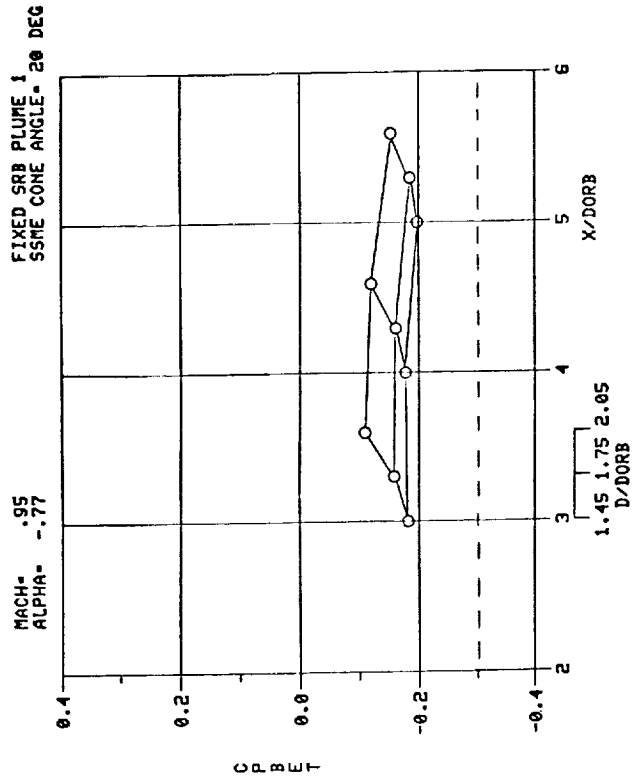
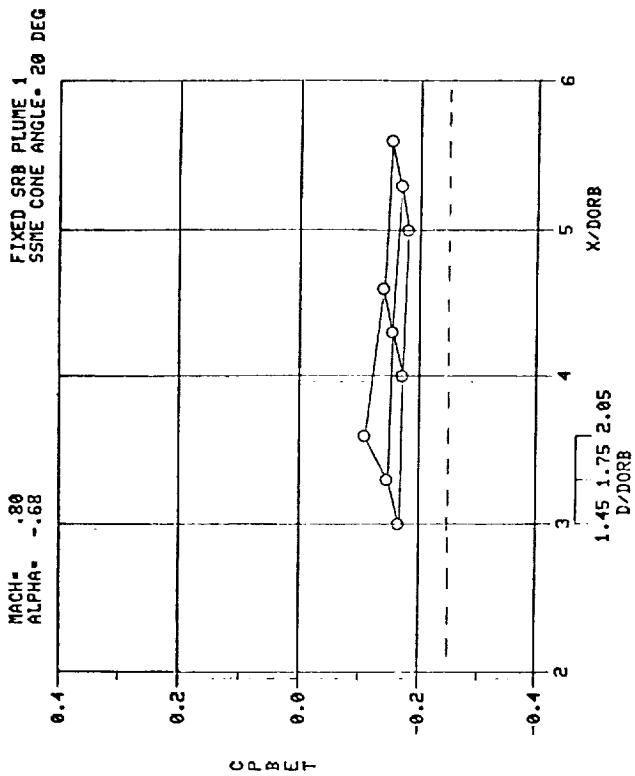


Figure B-7.

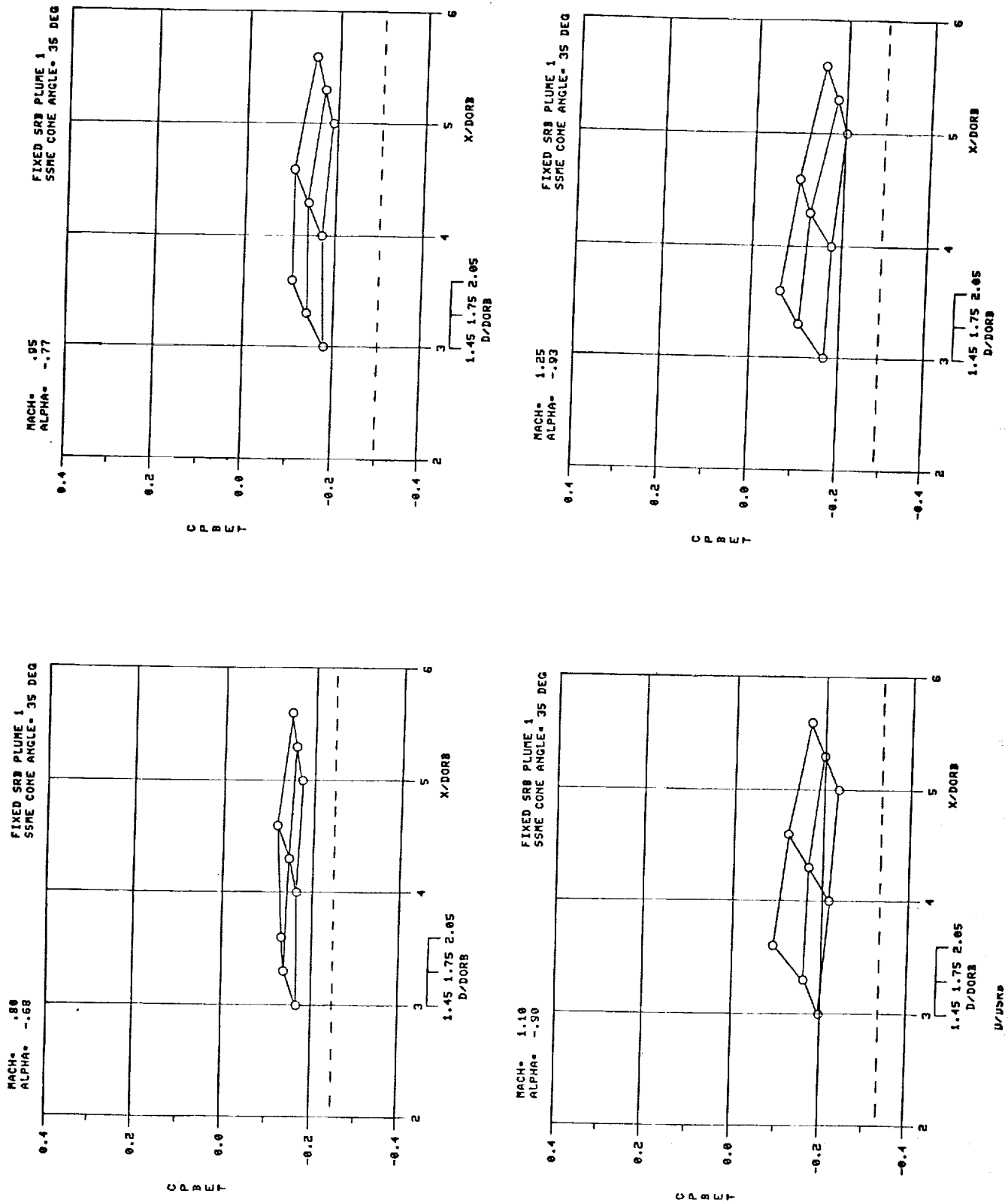


Figure B-8.

ORIGINAL PAGE IS
OF POOR QUALITY

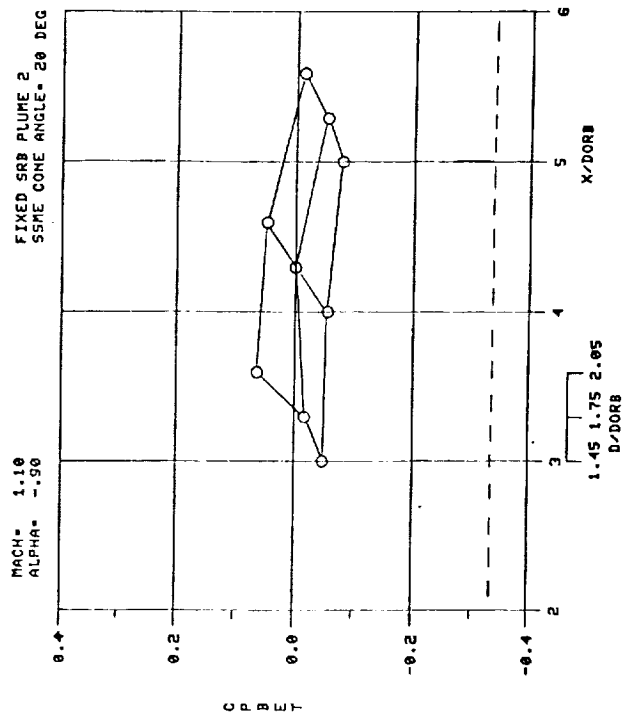
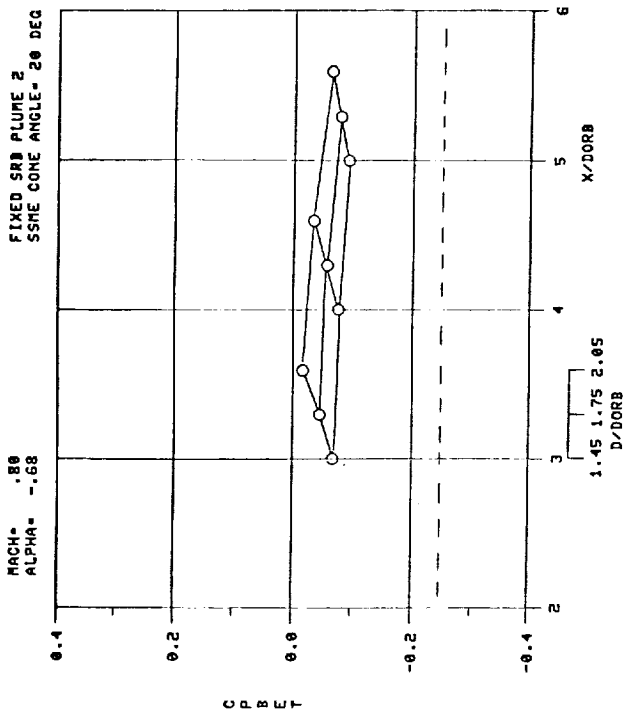
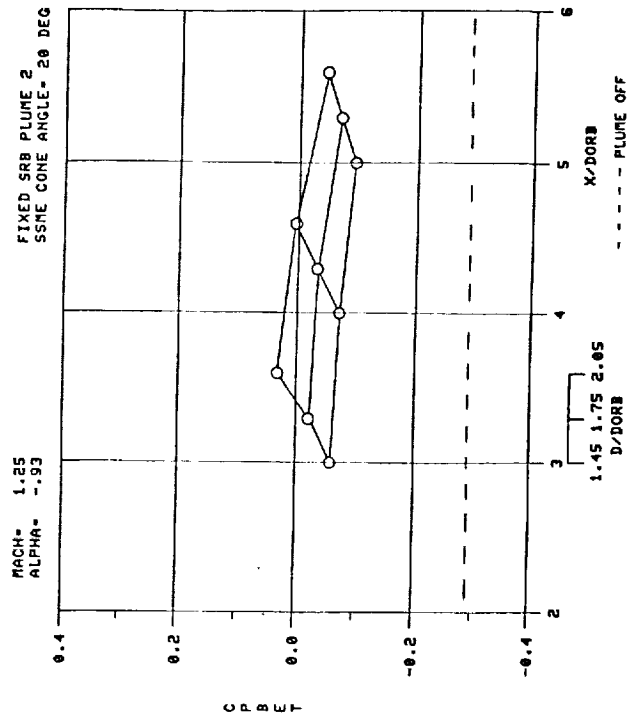
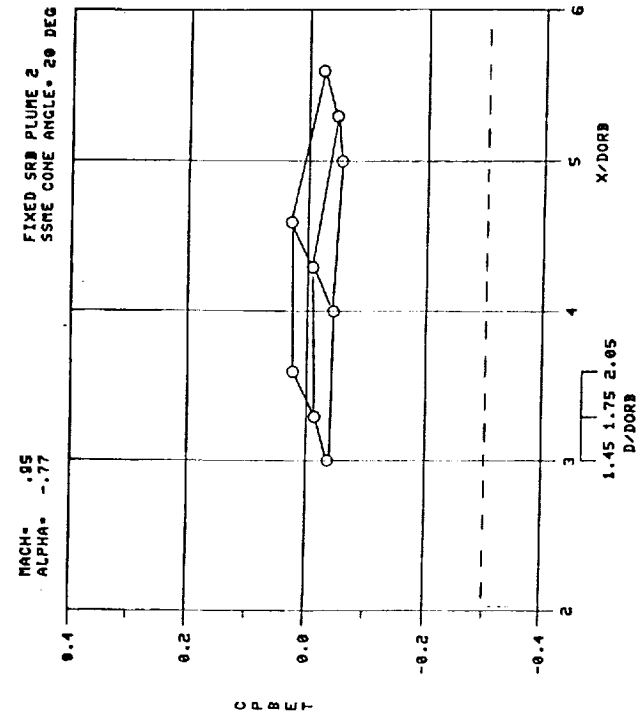


Figure B-9.

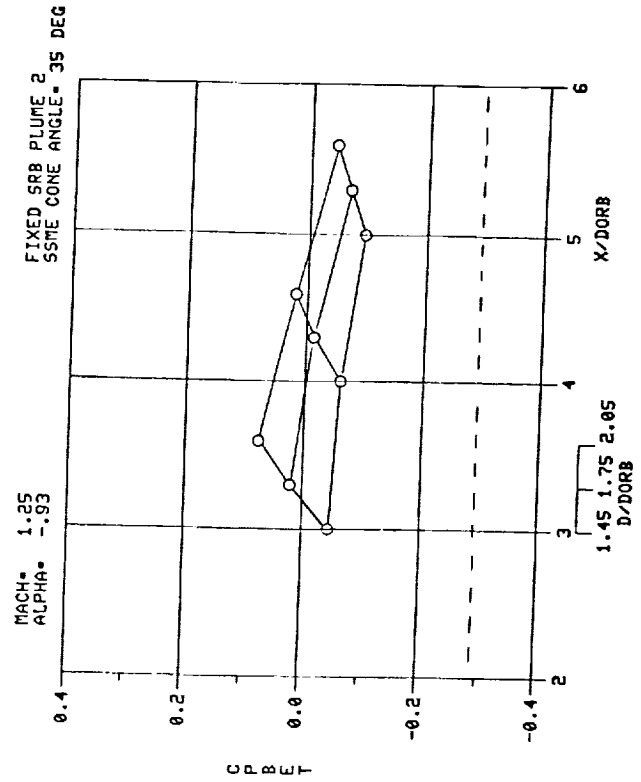
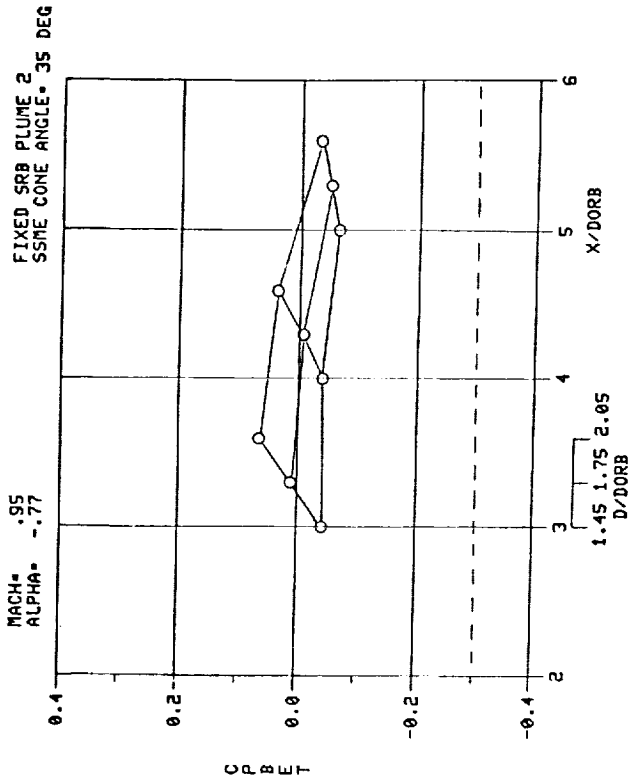
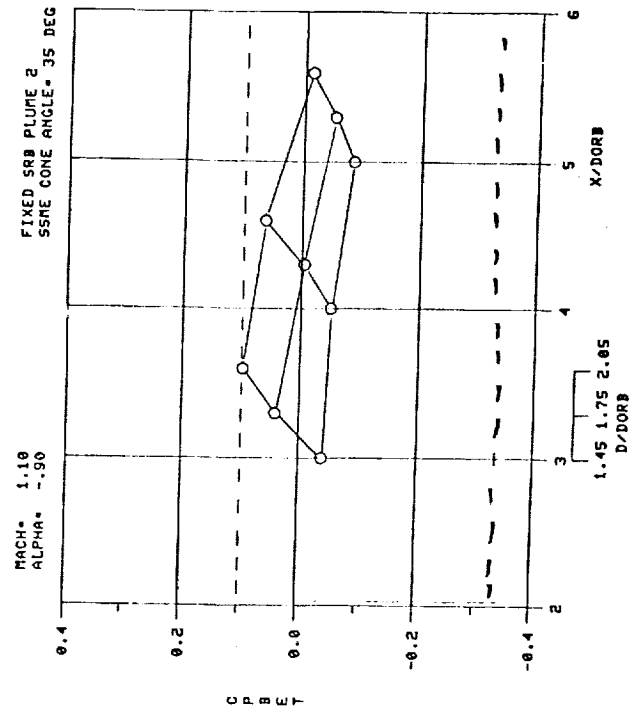
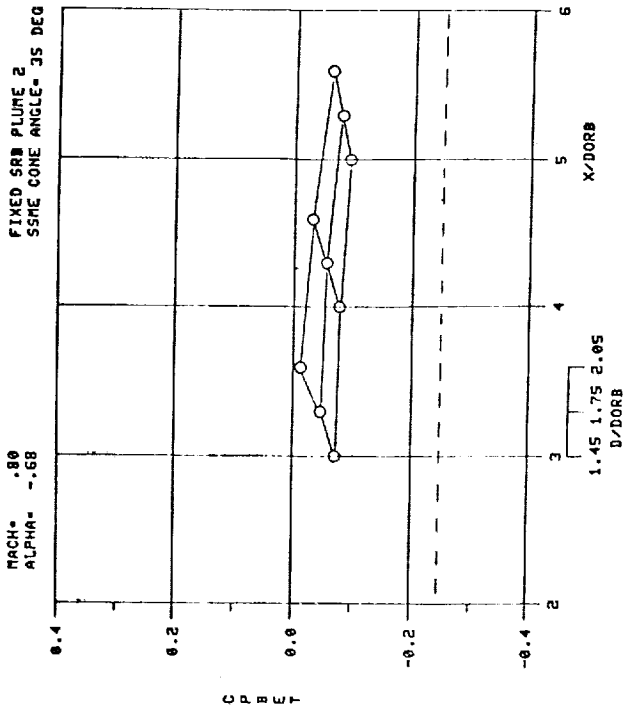


Figure B-10.

APPENDIX C

1
2
3
4
5
6
7
8
9
10
11
12
13
14
15
16
17
18
19
20
21
22
23
24
25
26
27
28
29
30
31
32
33
34
35
36
37
38
39
40
41
42
43
44
45
46
47
48
49
50
51
52
53
54
55
56
57
58
59
60
61
62
63
64
65
66
67
68
69
70
71
72
73
74
75
76
77
78
79
80
81
82
83
84
85
86
87
88
89
90
91
92
93
94
95
96
97
98
99
100
101
102
103
104
105
106
107
108
109
110
111
112
113
114
115
116
117
118
119
120
121
122
123
124
125
126
127
128
129
130
131
132
133
134
135
136
137
138
139
140
141
142
143
144
145
146
147
148
149
150
151
152
153
154
155
156
157
158
159
160
161
162
163
164
165
166
167
168
169
170
171
172
173
174
175
176
177
178
179
180
181
182
183
184
185
186
187
188
189
190
191
192
193
194
195
196
197
198
199
200
201
202
203
204
205
206
207
208
209
210
211
212
213
214
215
216
217
218
219
220
221
222
223
224
225
226
227
228
229
230
231
232
233
234
235
236
237
238
239
240
241
242
243
244
245
246
247
248
249
250
251
252
253
254
255
256
257
258
259
260
261
262
263
264
265
266
267
268
269
270
271
272
273
274
275
276
277
278
279
280
281
282
283
284
285
286
287
288
289
290
291
292
293
294
295
296
297
298
299
300
301
302
303
304
305
306
307
308
309
310
311
312
313
314
315
316
317
318
319
320
321
322
323
324
325
326
327
328
329
330
331
332
333
334
335
336
337
338
339
340
341
342
343
344
345
346
347
348
349
350
351
352
353
354
355
356
357
358
359
360
361
362
363
364
365
366
367
368
369
370
371
372
373
374
375
376
377
378
379
380
381
382
383
384
385
386
387
388
389
390
391
392
393
394
395
396
397
398
399
400
401
402
403
404
405
406
407
408
409
410
411
412
413
414
415
416
417
418
419
420
421
422
423
424
425
426
427
428
429
430
431
432
433
434
435
436
437
438
439
440
441
442
443
444
445
446
447
448
449
450
451
452
453
454
455
456
457
458
459
460
461
462
463
464
465
466
467
468
469
470
471
472
473
474
475
476
477
478
479
480
481
482
483
484
485
486
487
488
489
490
491
492
493
494
495
496
497
498
499
500
501
502
503
504
505
506
507
508
509
510
511
512
513
514
515
516
517
518
519
520
521
522
523
524
525
526
527
528
529
530
531
532
533
534
535
536
537
538
539
540
541
542
543
544
545
546
547
548
549
550
551
552
553
554
555
556
557
558
559
560
561
562
563
564
565
566
567
568
569
570
571
572
573
574
575
576
577
578
579
580
581
582
583
584
585
586
587
588
589
590
591
592
593
594
595
596
597
598
599
600
601
602
603
604
605
606
607
608
609
610
611
612
613
614
615
616
617
618
619
620
621
622
623
624
625
626
627
628
629
630
631
632
633
634
635
636
637
638
639
640
641
642
643
644
645
646
647
648
649
650
651
652
653
654
655
656
657
658
659
660
661
662
663
664
665
666
667
668
669
670
671
672
673
674
675
676
677
678
679
680
681
682
683
684
685
686
687
688
689
690
691
692
693
694
695
696
697
698
699
700
701
702
703
704
705
706
707
708
709
710
711
712
713
714
715
716
717
718
719
720
721
722
723
724
725
726
727
728
729
730
731
732
733
734
735
736
737
738
739
740
741
742
743
744
745
746
747
748
749
750
751
752
753
754
755
756
757
758
759
760
761
762
763
764
765
766
767
768
769
770
771
772
773
774
775
776
777
778
779
780
781
782
783
784
785
786
787
788
789
790
791
792
793
794
795
796
797
798
799
800
801
802
803
804
805
806
807
808
809
810
811
812
813
814
815
816
817
818
819
820
821
822
823
824
825
826
827
828
829
830
831
832
833
834
835
836
837
838
839
840
841
842
843
844
845
846
847
848
849
850
851
852
853
854
855
856
857
858
859
860
861
862
863
864
865
866
867
868
869
870
871
872
873
874
875
876
877
878
879
880
881
882
883
884
885
886
887
888
889
890
891
892
893
894
895
896
897
898
899
900
901
902
903
904
905
906
907
908
909
910
911
912
913
914
915
916
917
918
919
920
921
922
923
924
925
926
927
928
929
930
931
932
933
934
935
936
937
938
939
940
941
942
943
944
945
946
947
948
949
950
951
952
953
954
955
956
957
958
959
960
961
962
963
964
965
966
967
968
969
970
971
972
973
974
975
976
977
978
979
980
981
982
983
984
985
986
987
988
989
990
991
992
993
994
995
996
997
998
999
1000



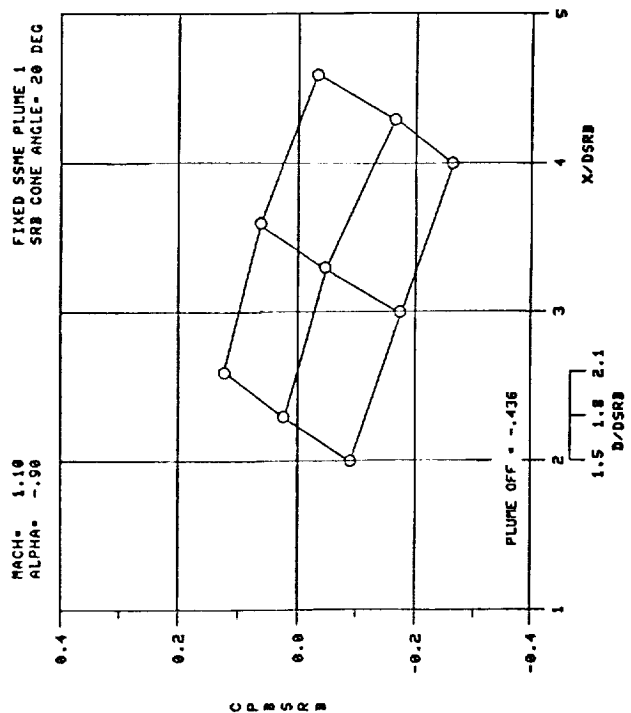
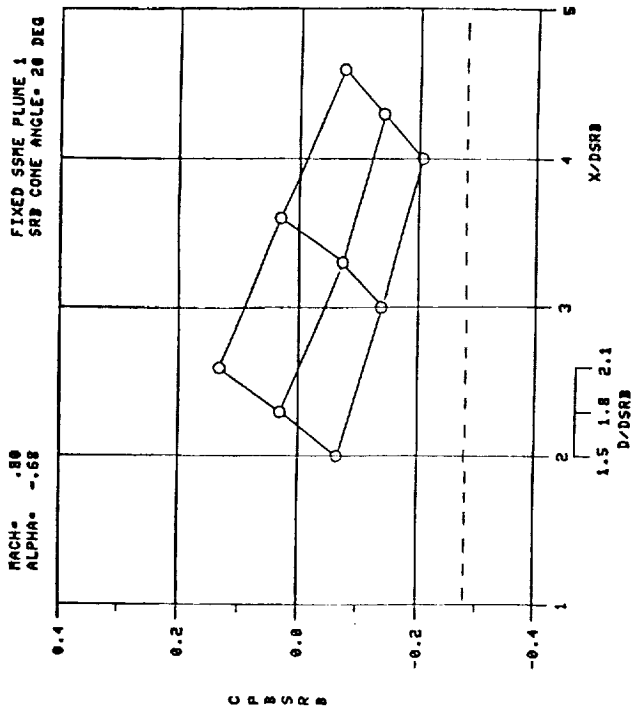
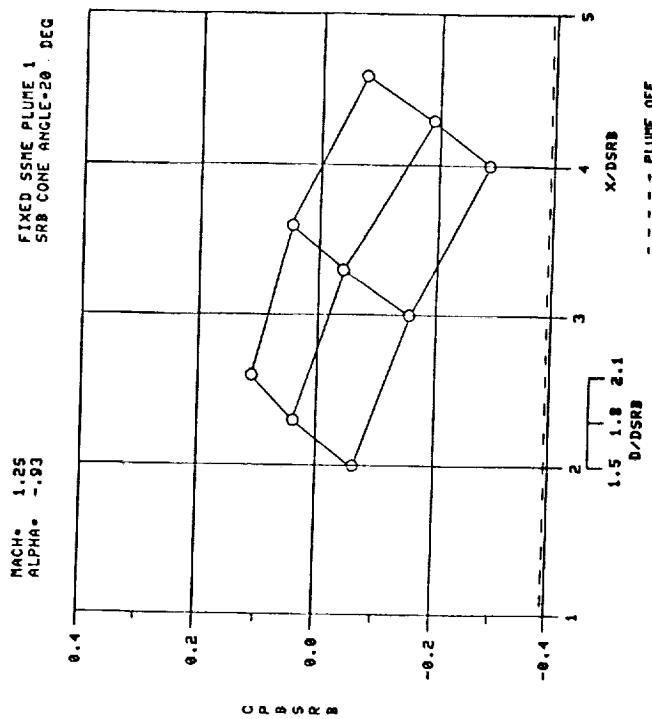
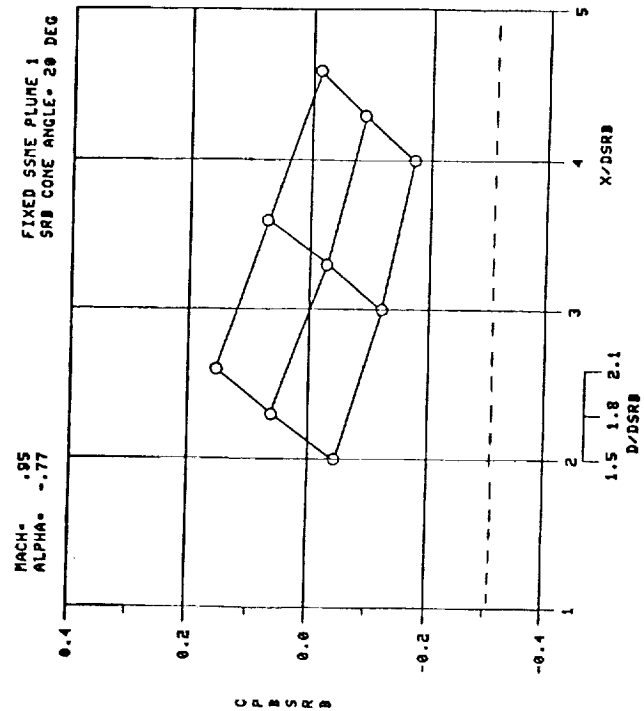


Figure C-1.

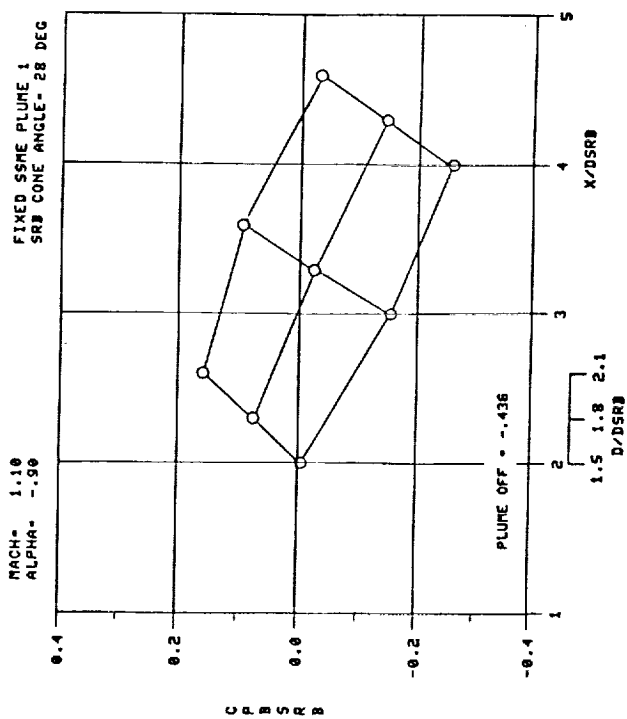
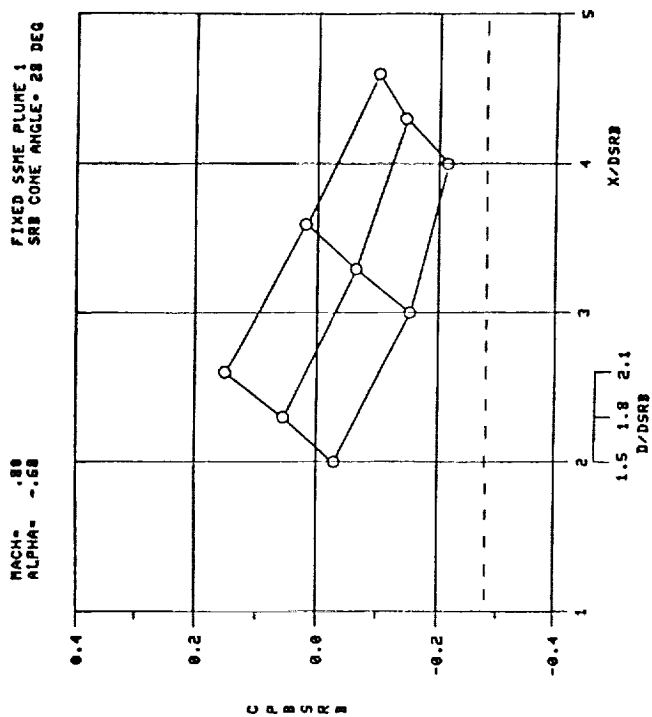
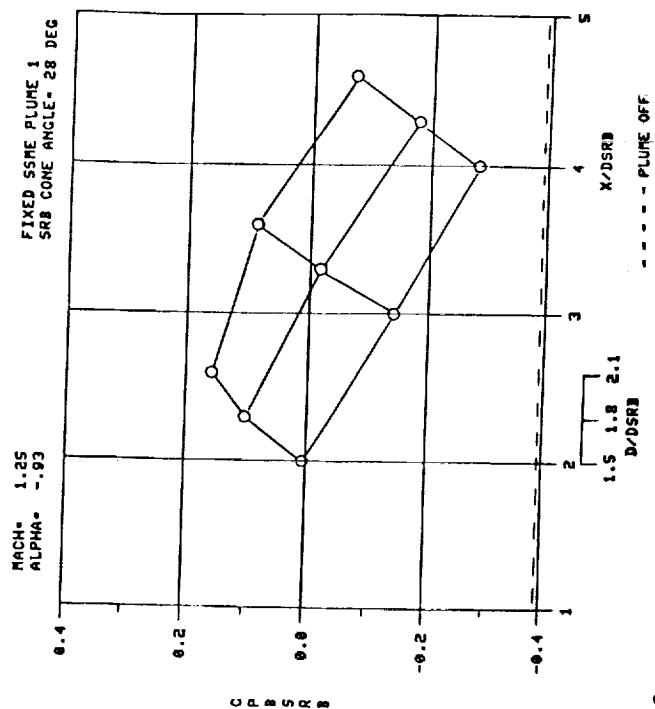
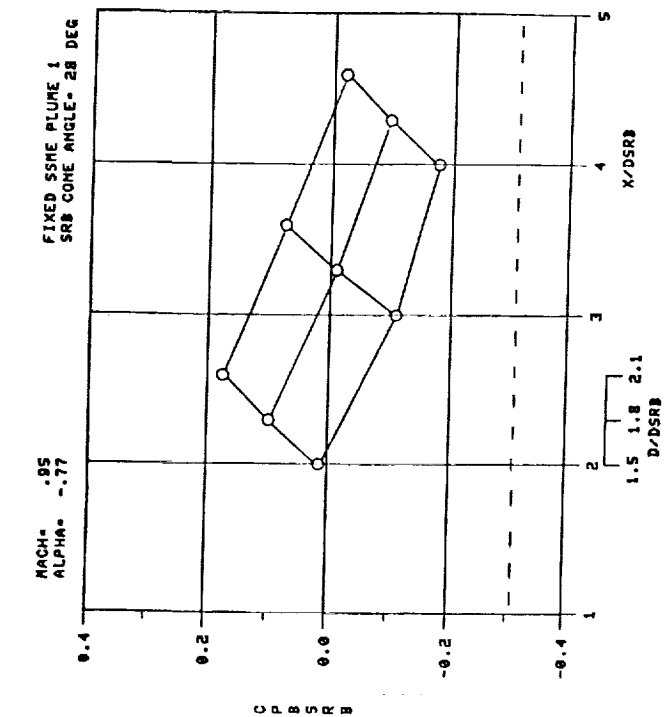
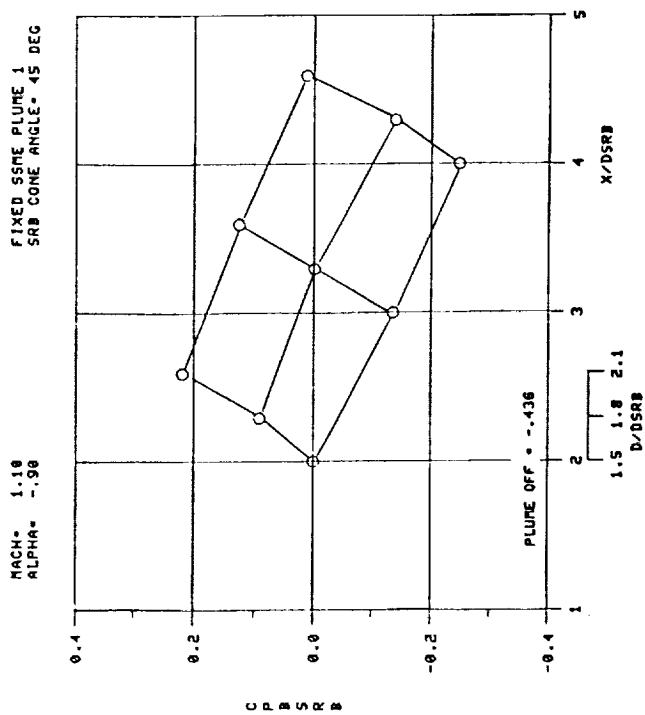
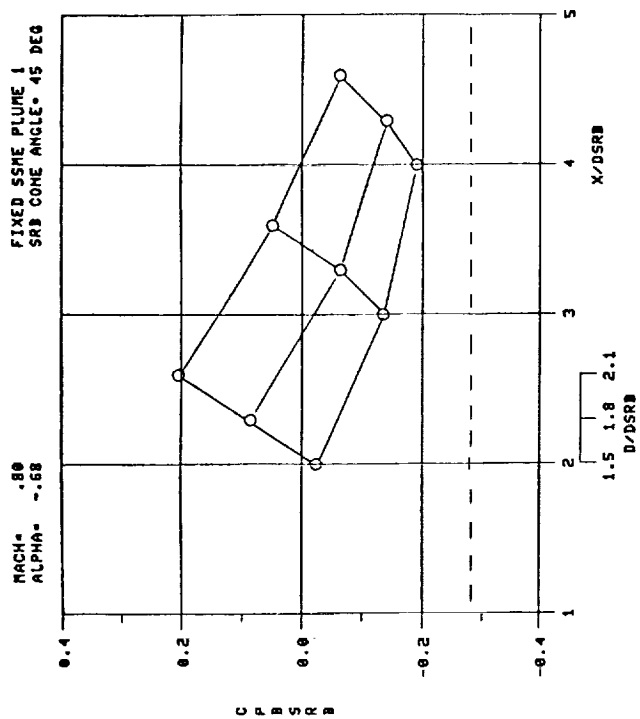
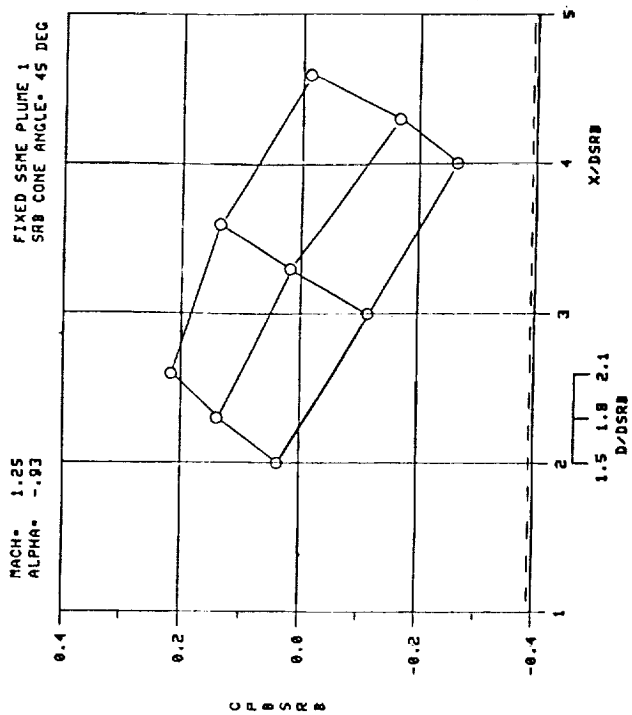
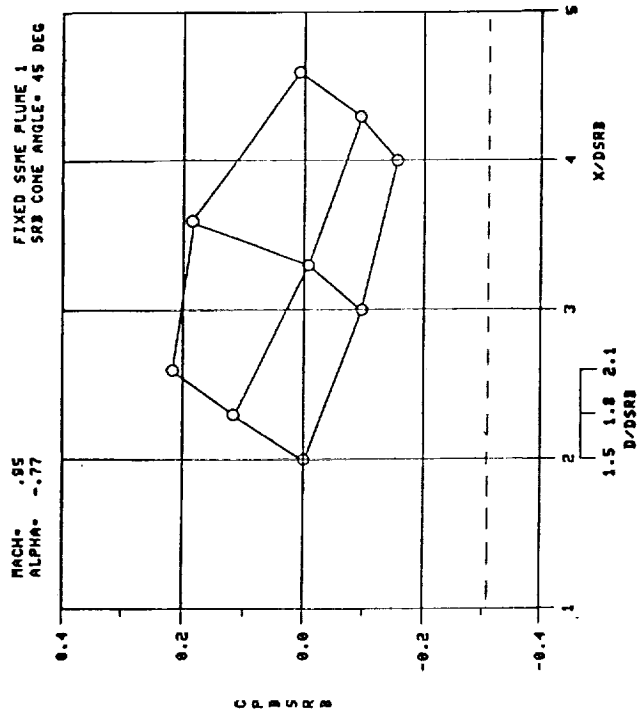


Figure C-2.



----- PLUME OFF

Figure C-3.

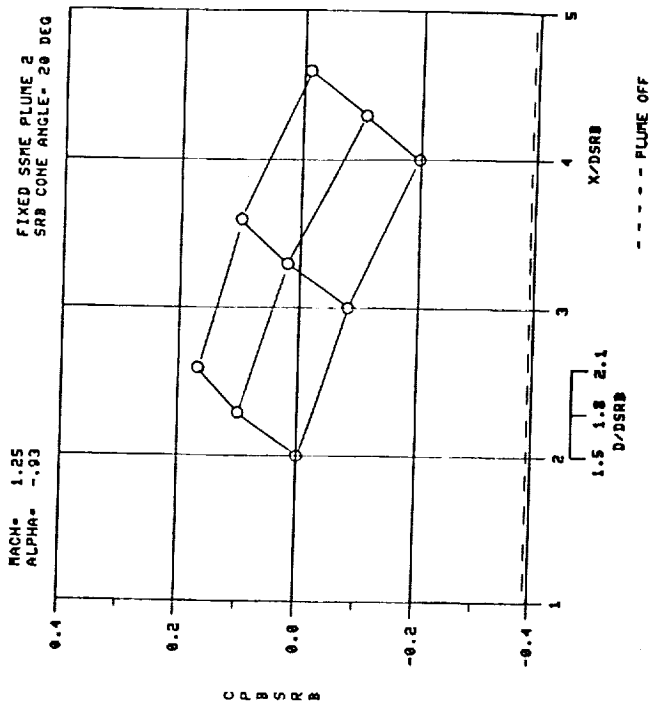
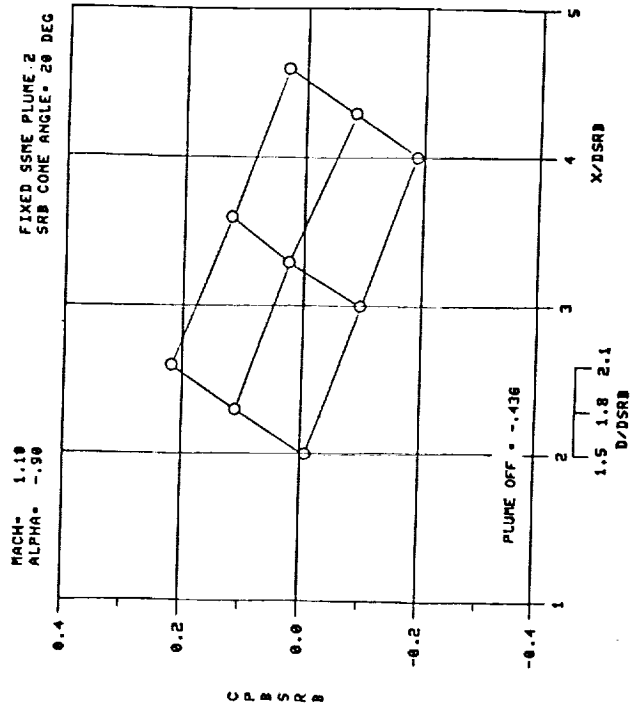
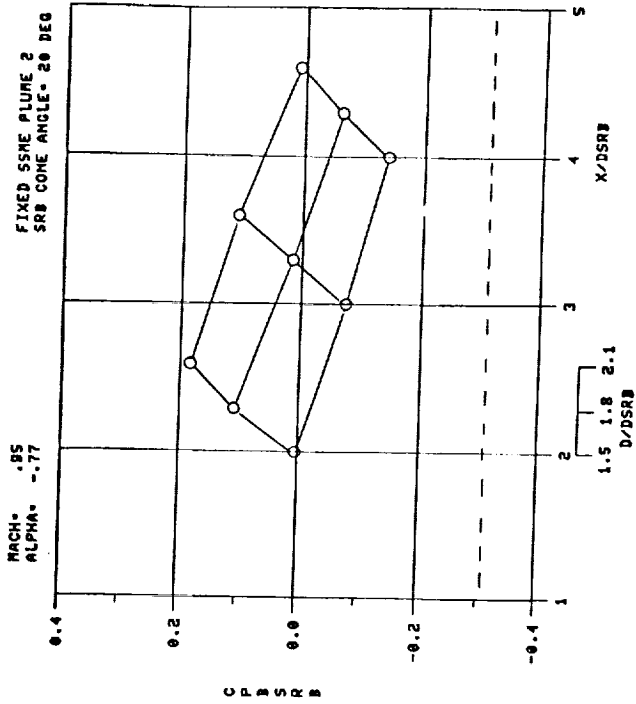
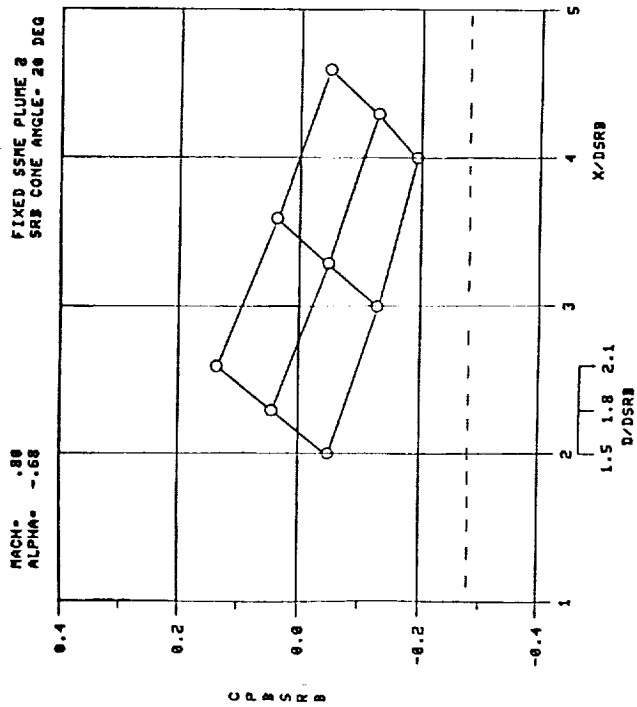


Figure C-4.

ORIGINAL PAGE IS
OF POOR QUALITY

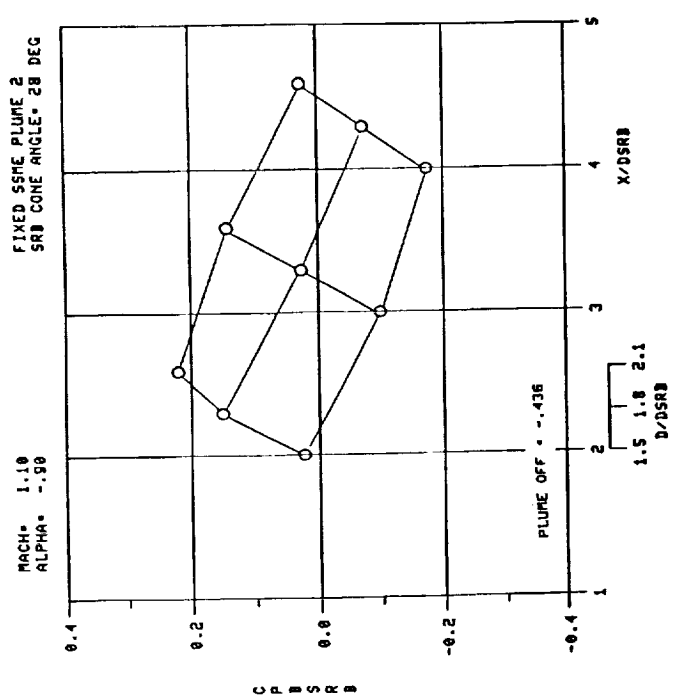
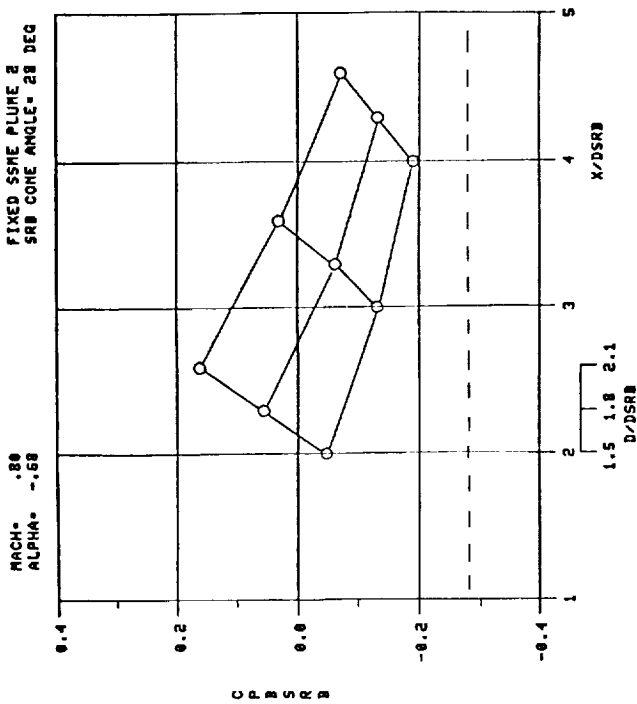
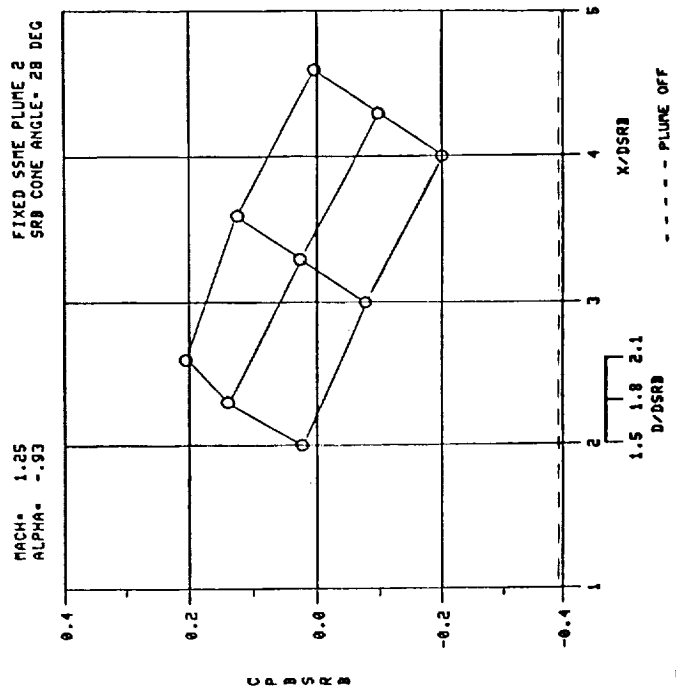
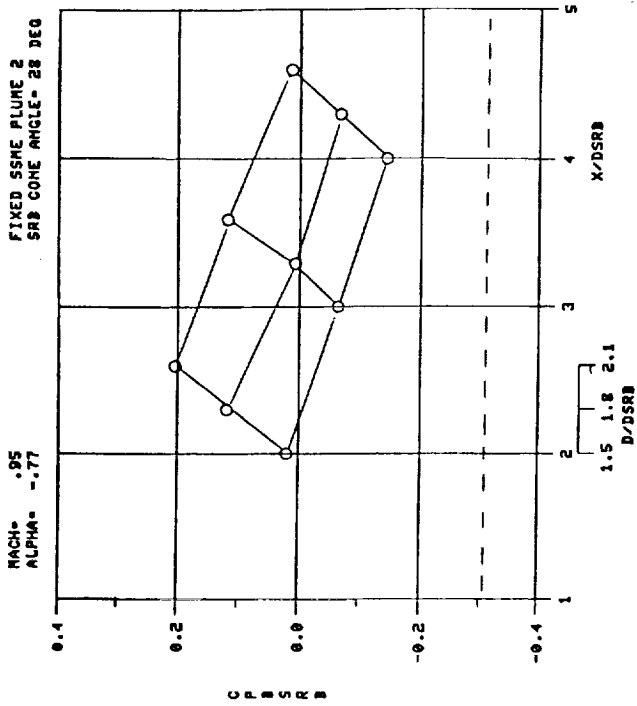


Figure C-5.

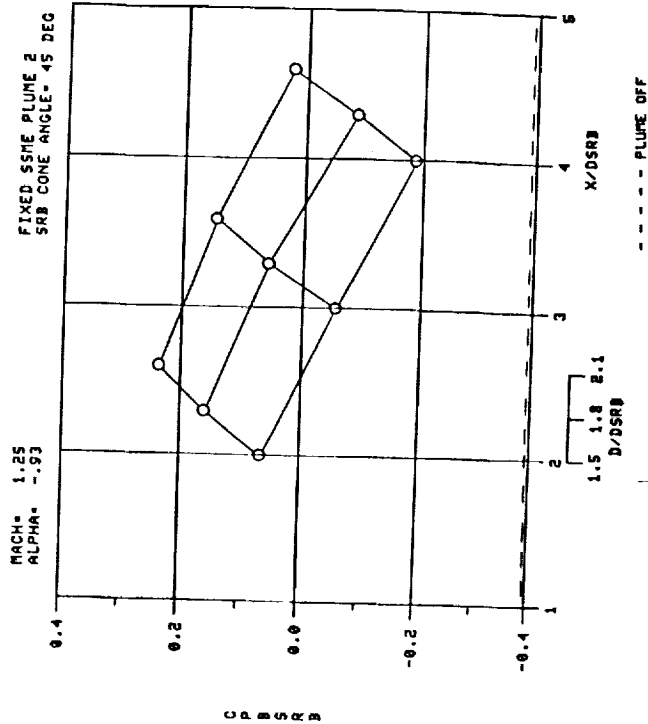
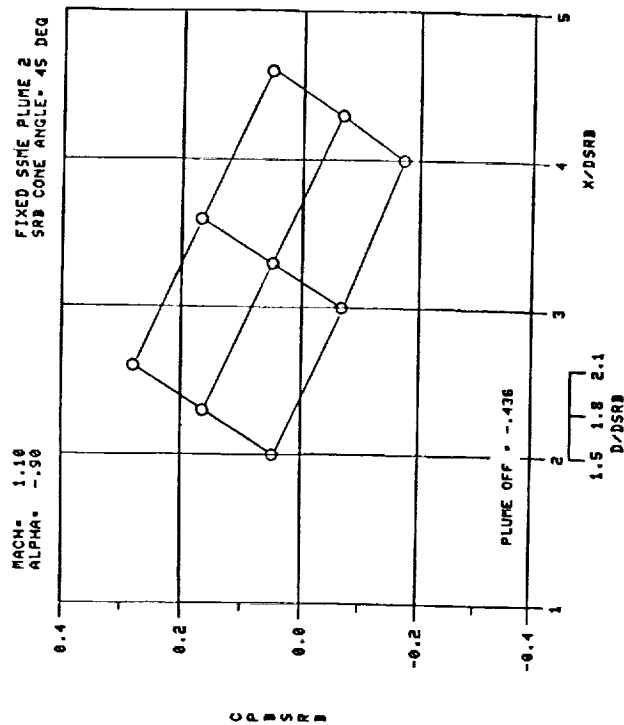
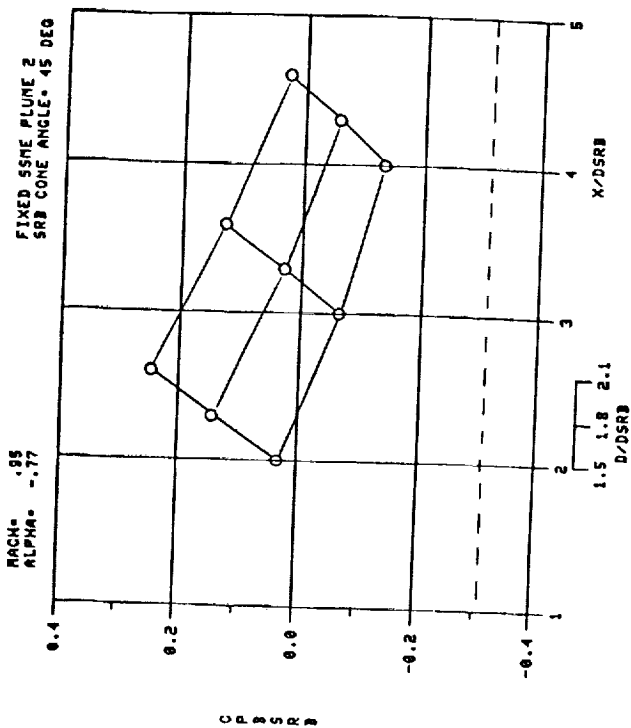
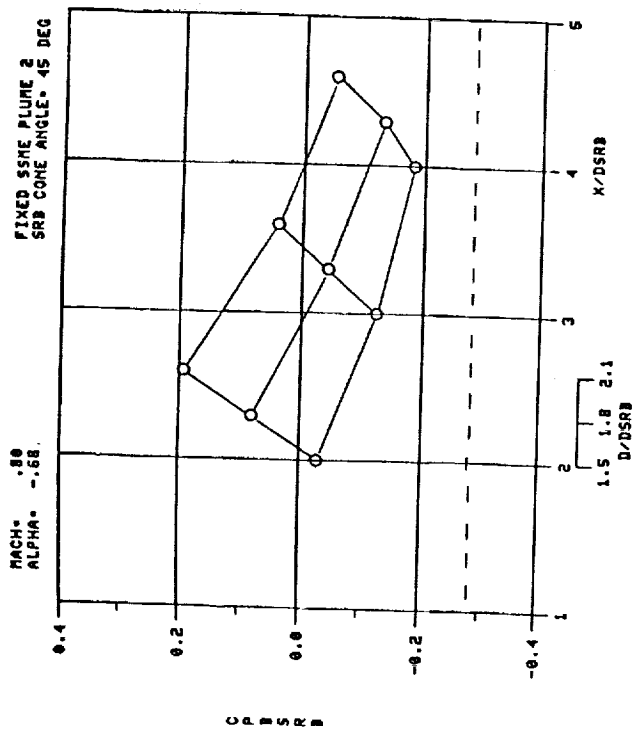


Figure C-6.

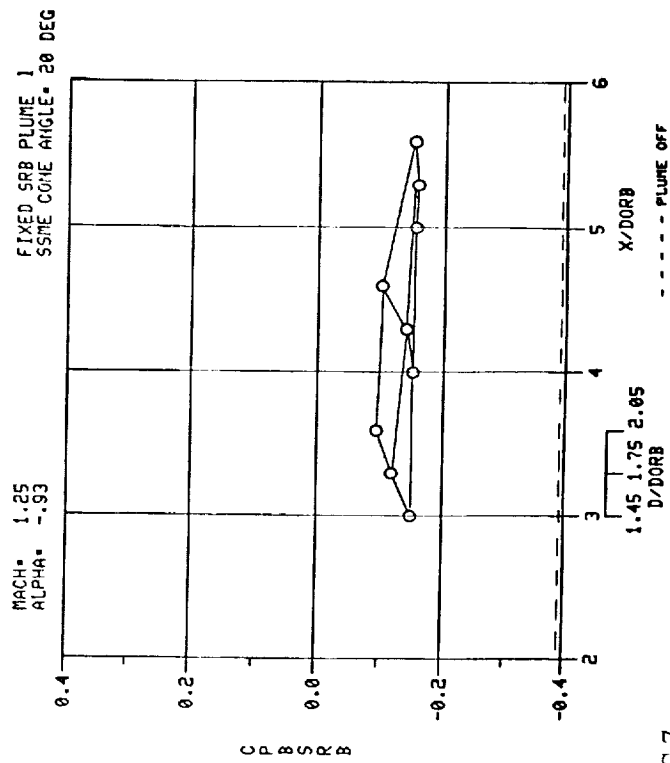
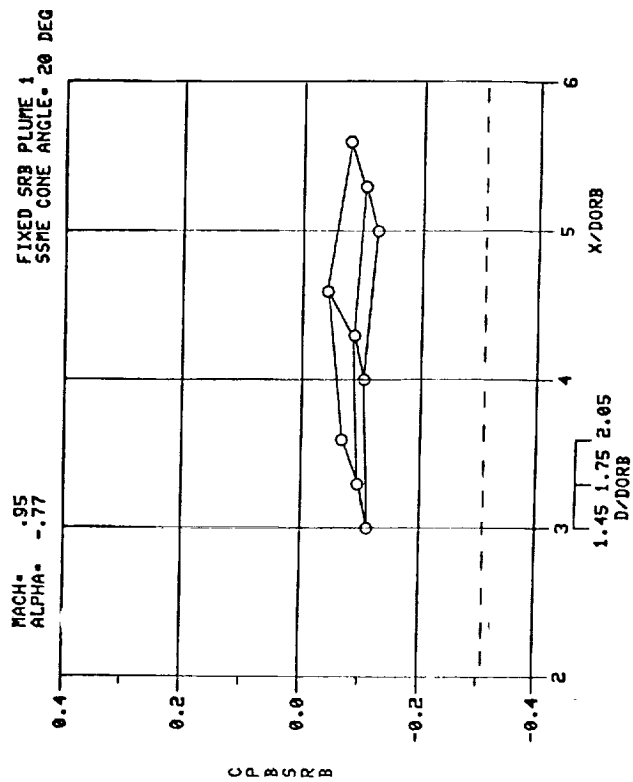
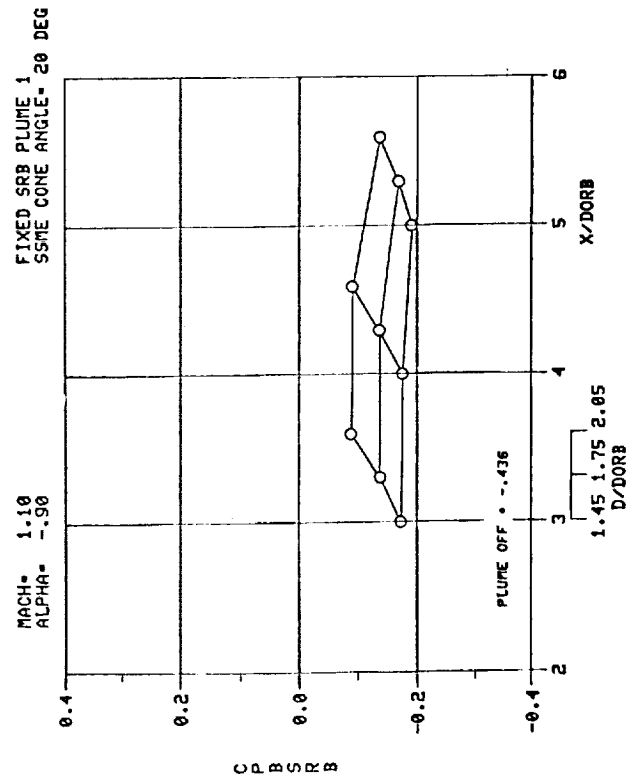
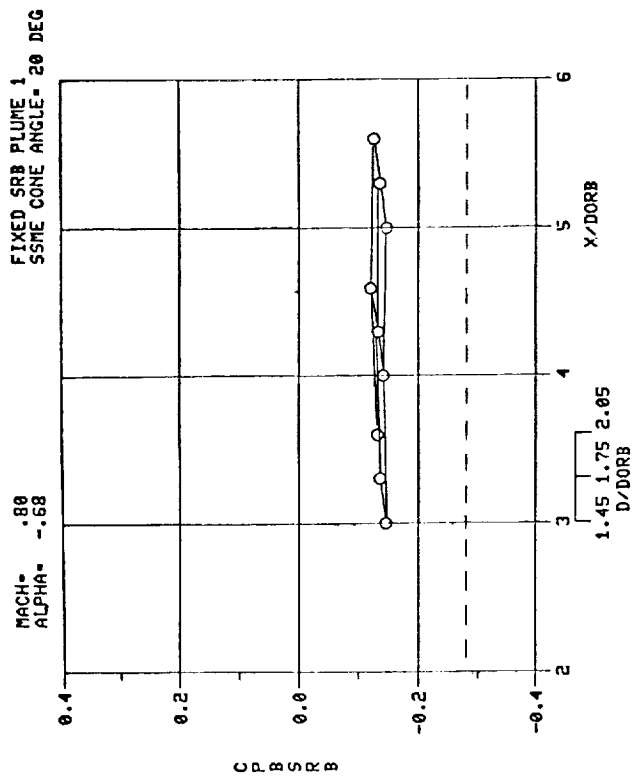


Figure C-7.

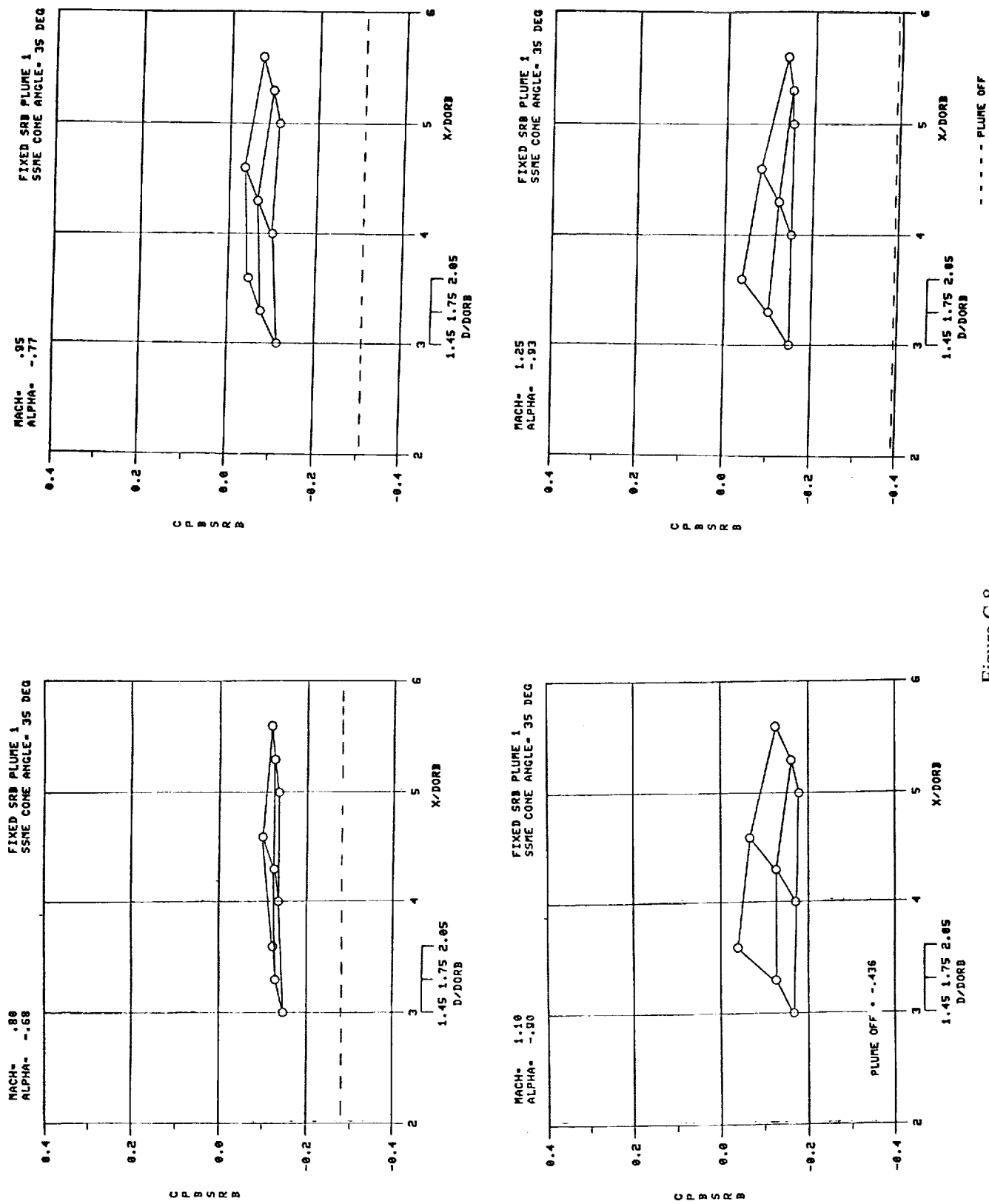


Figure C-8.

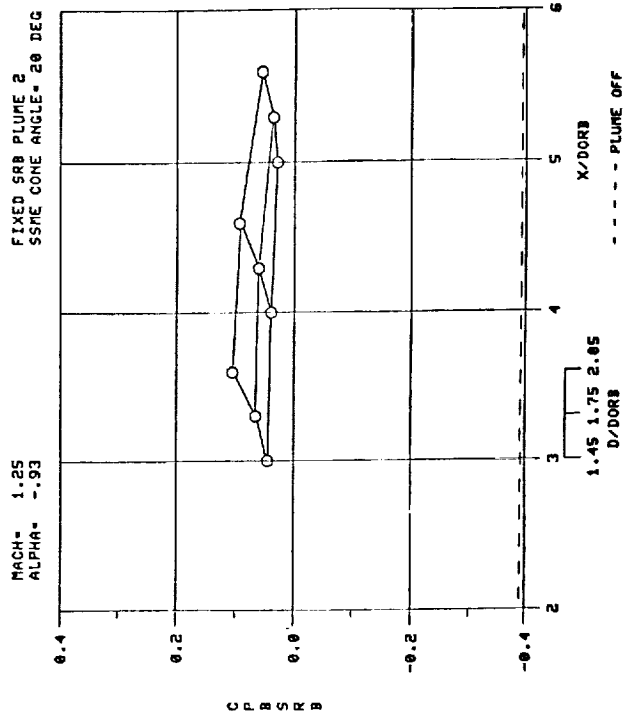
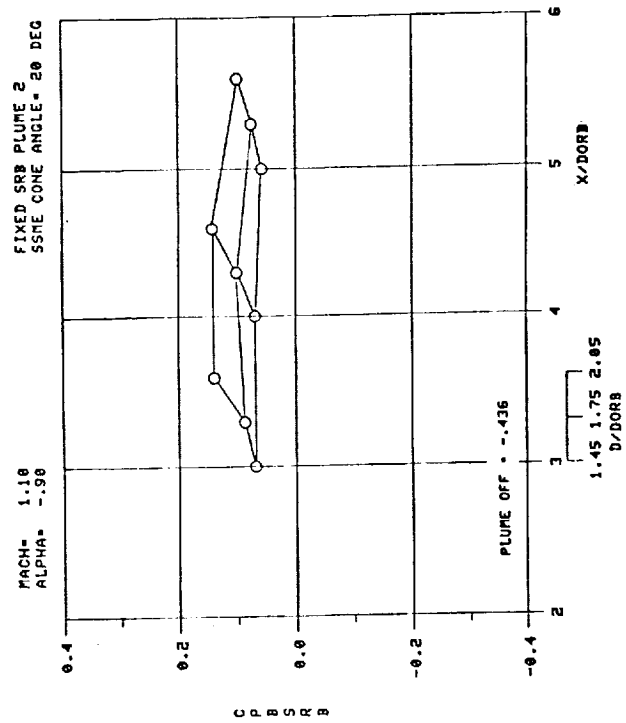
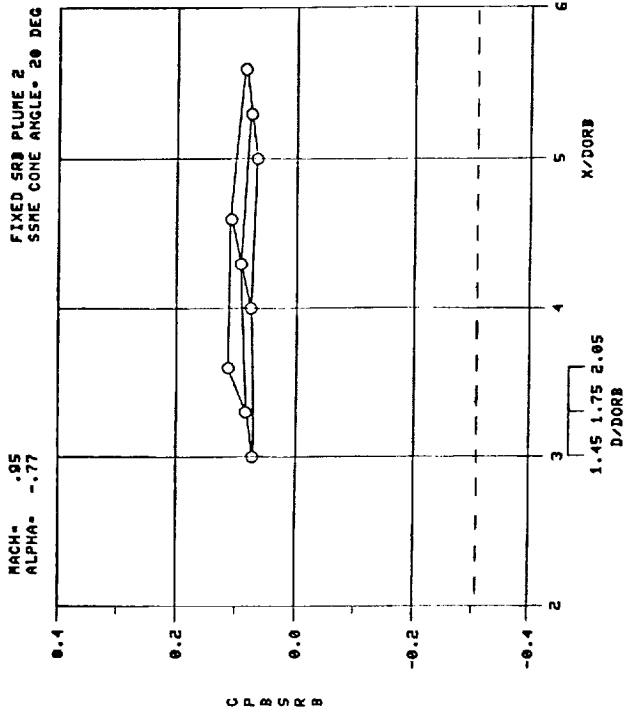
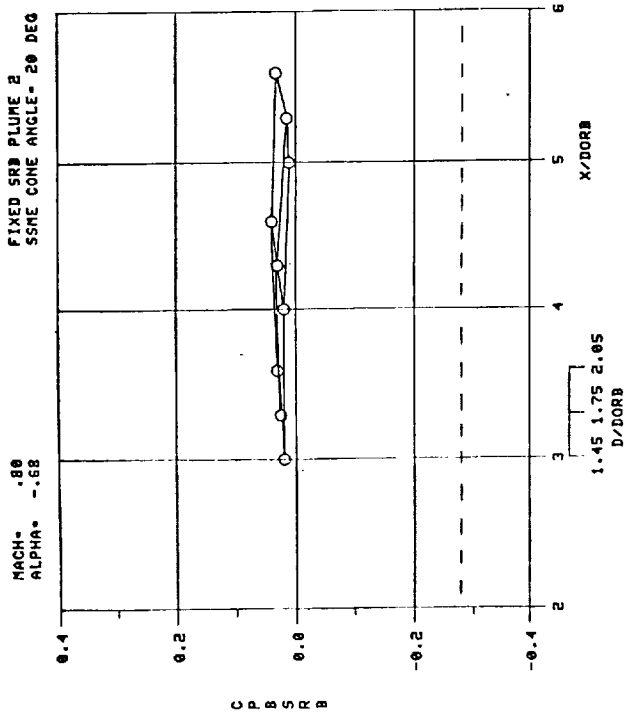


Figure C-9.

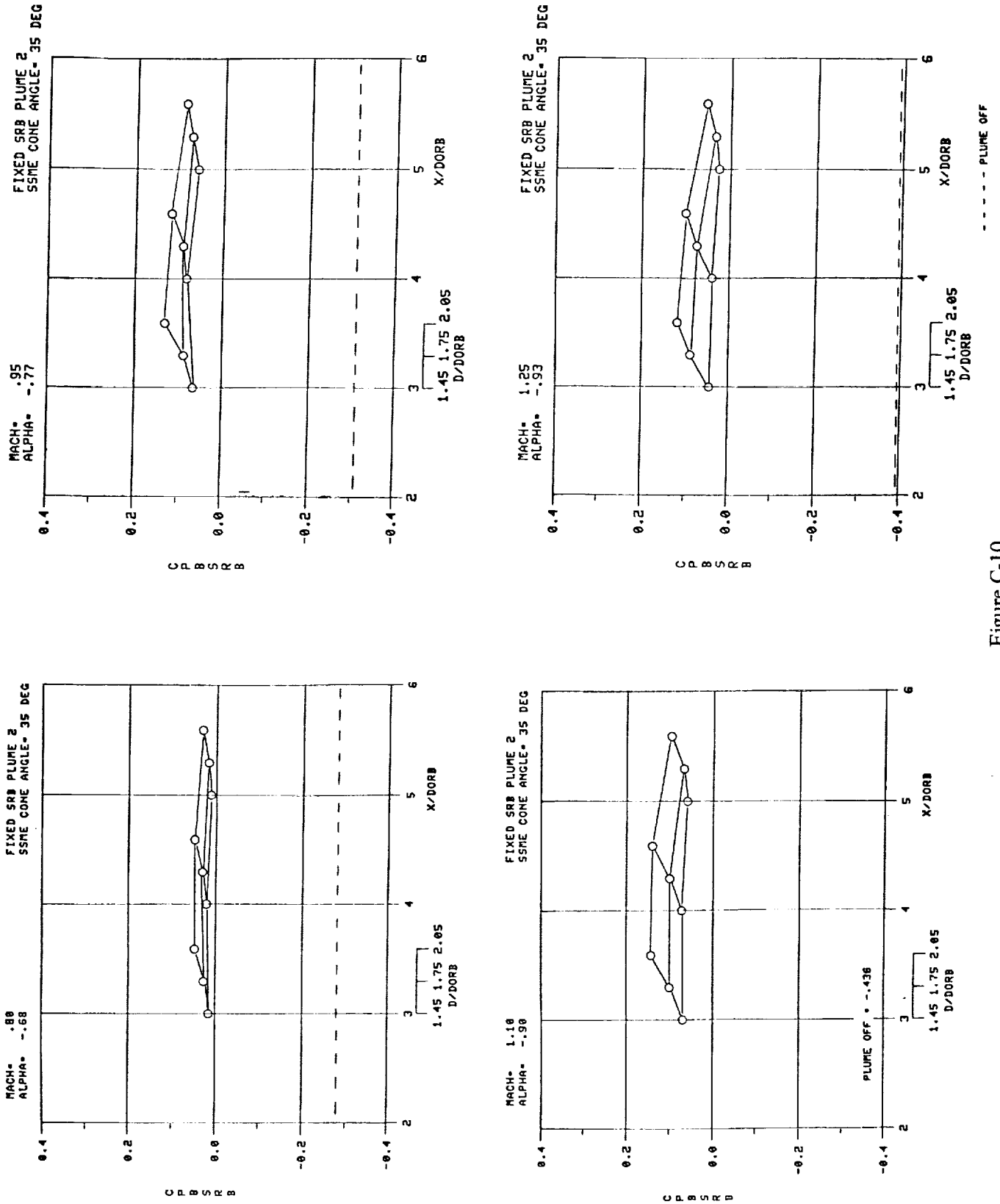


Figure C-10.

APPENDIX D



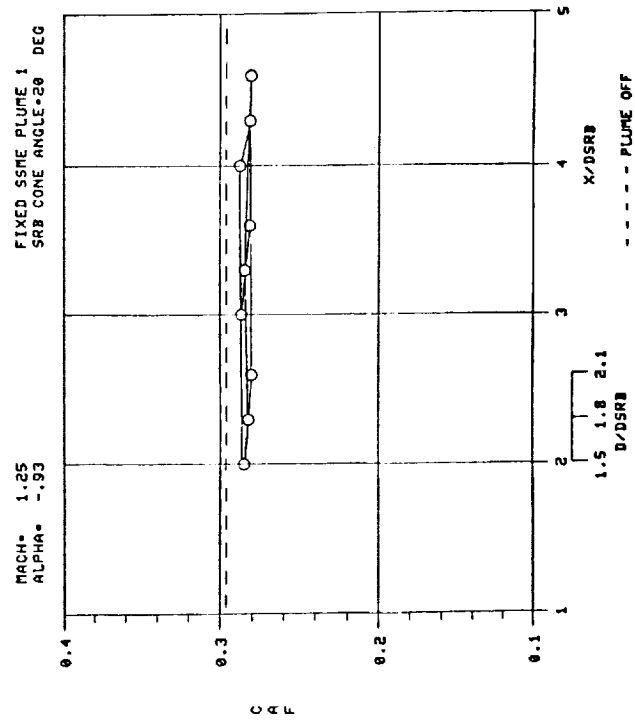
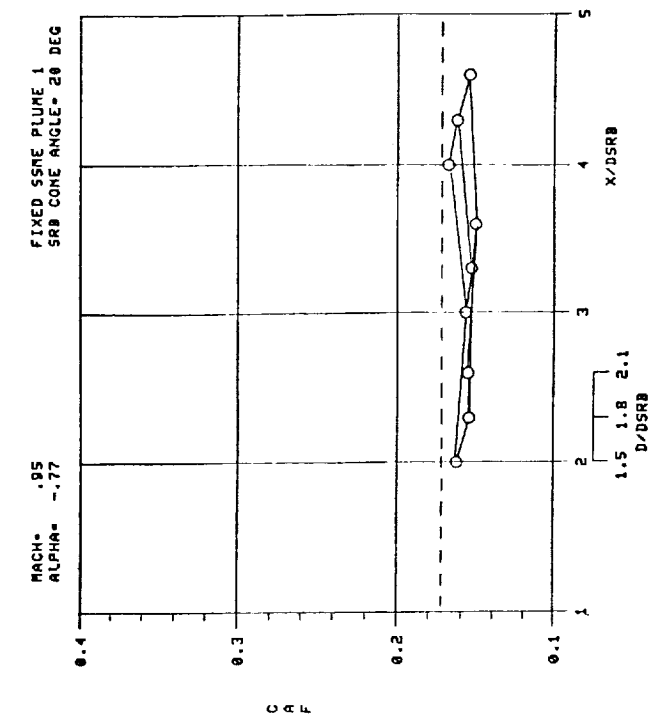
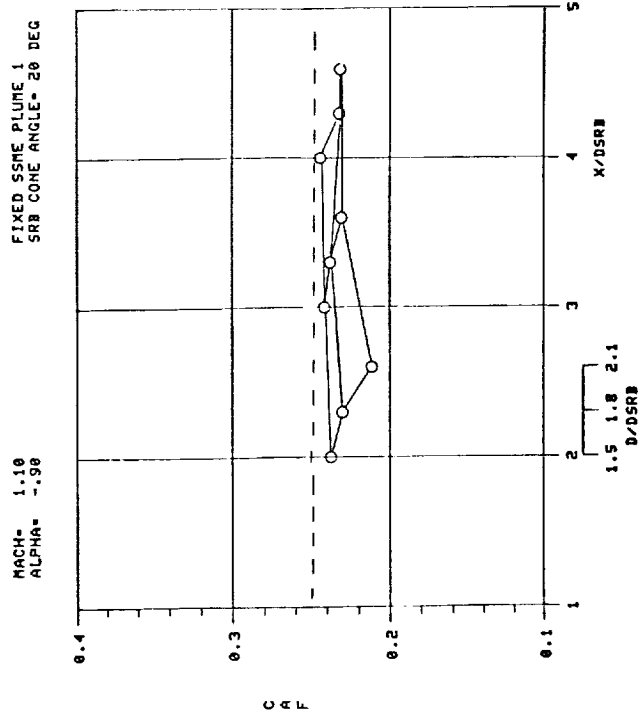
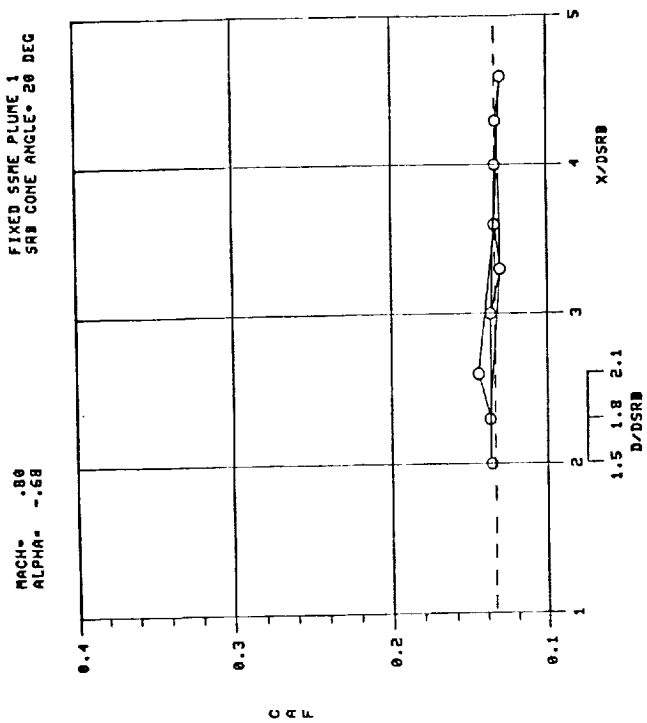


Figure D-1.



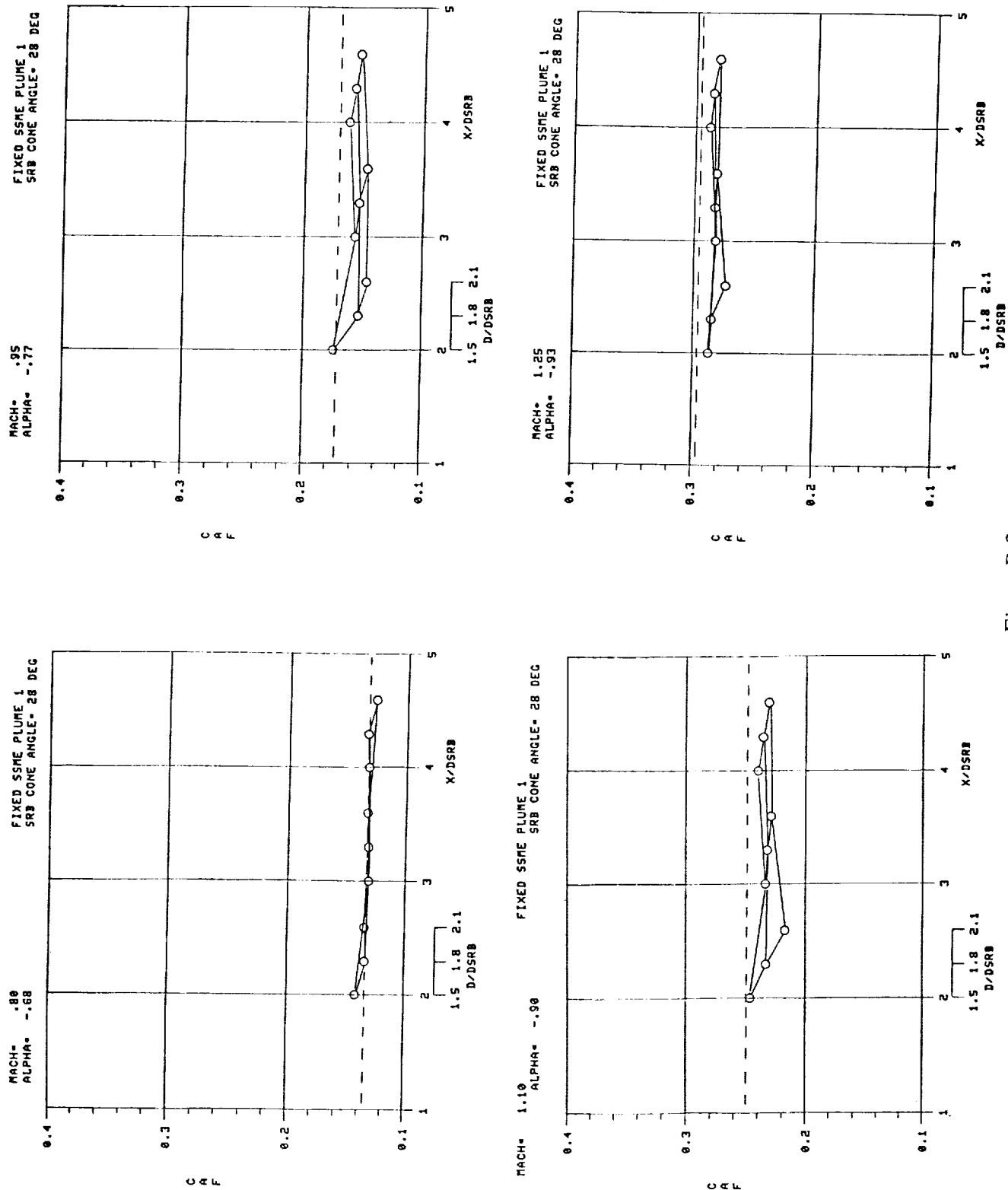


Figure D-2.

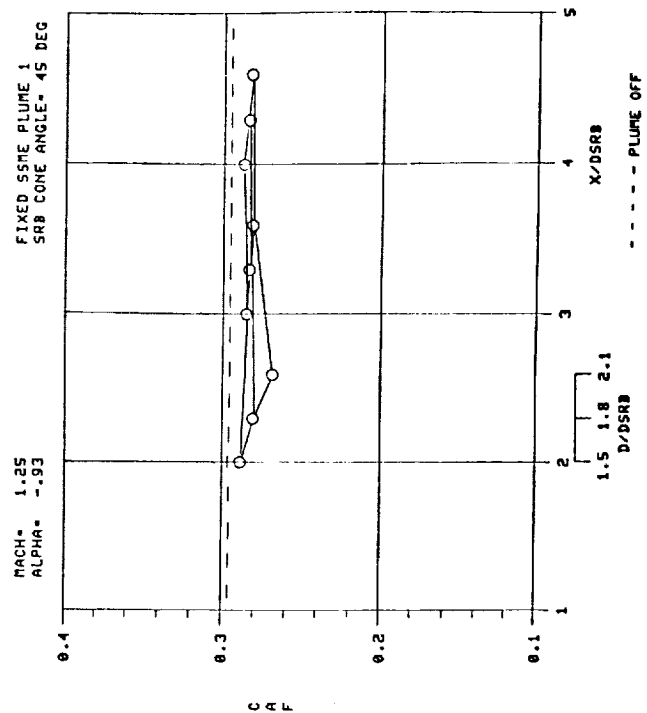
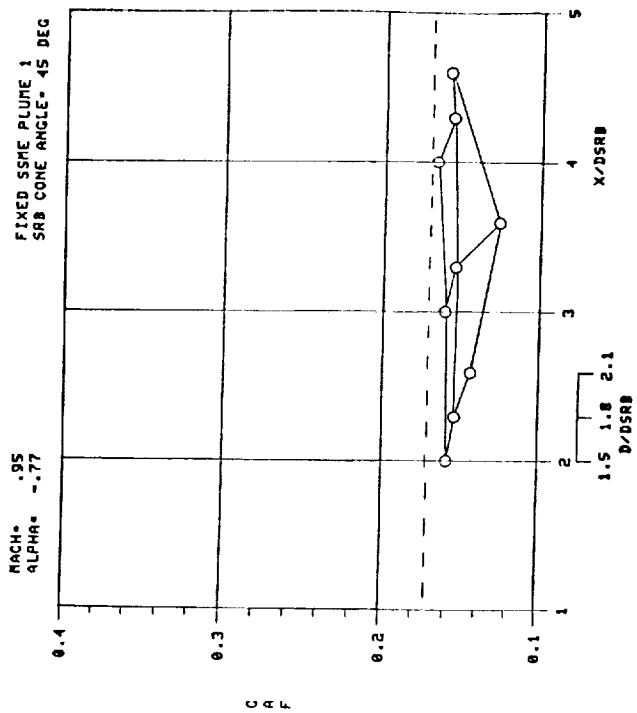
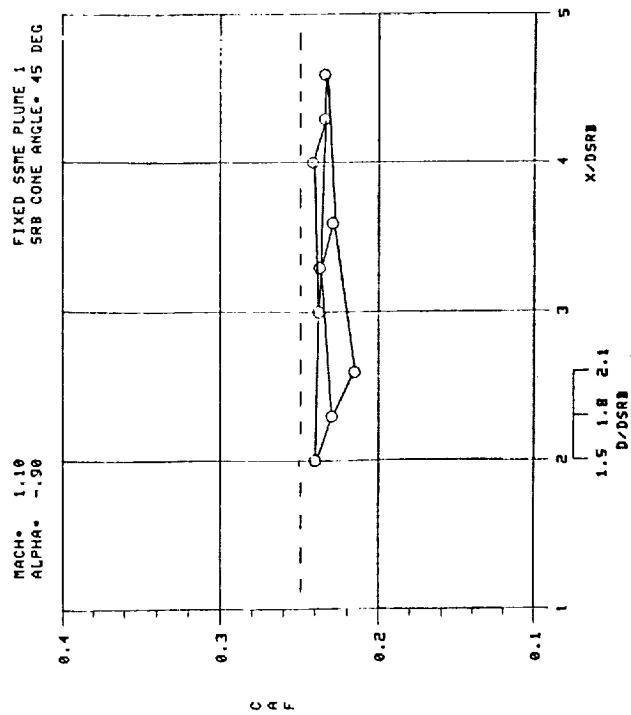
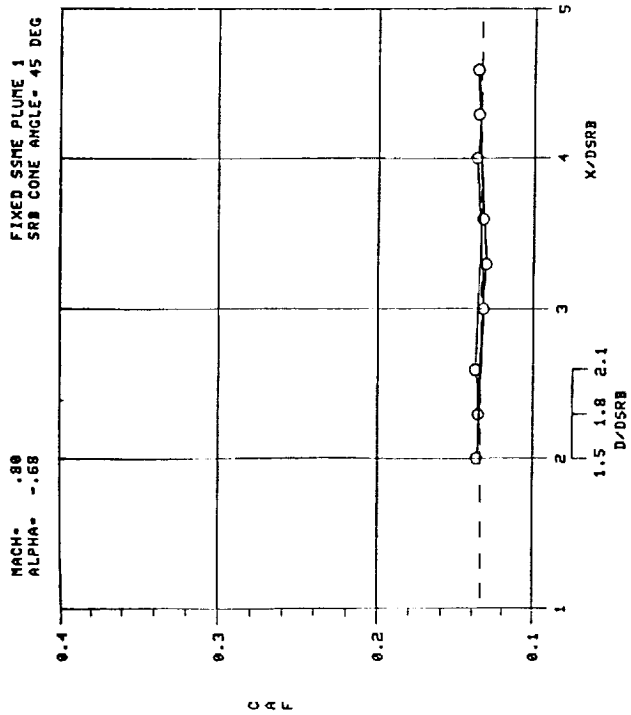


Figure D-3.

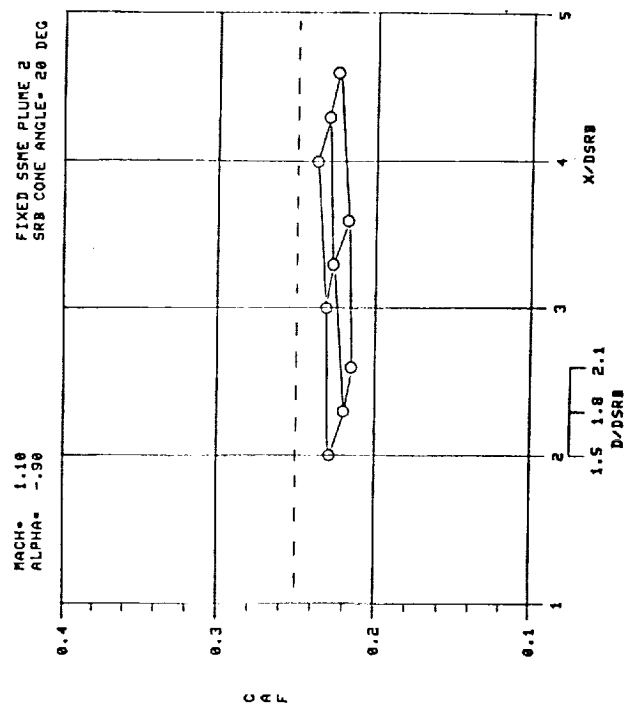
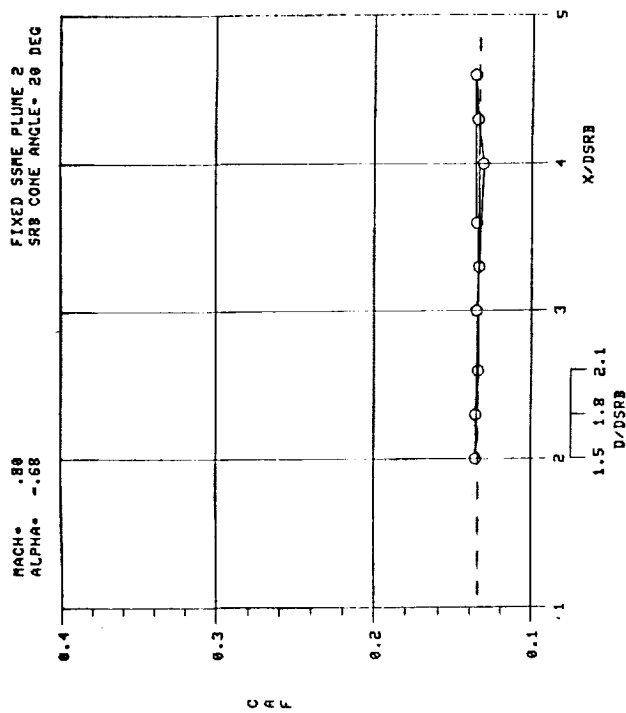
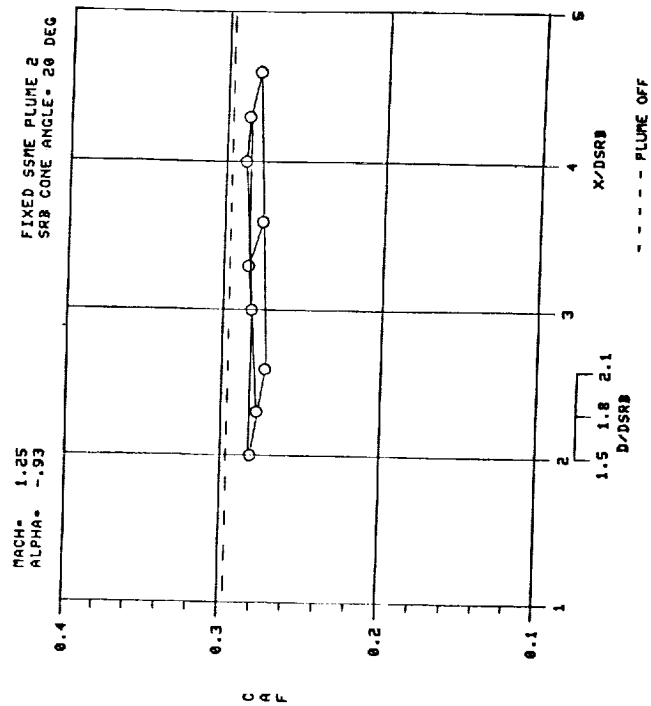
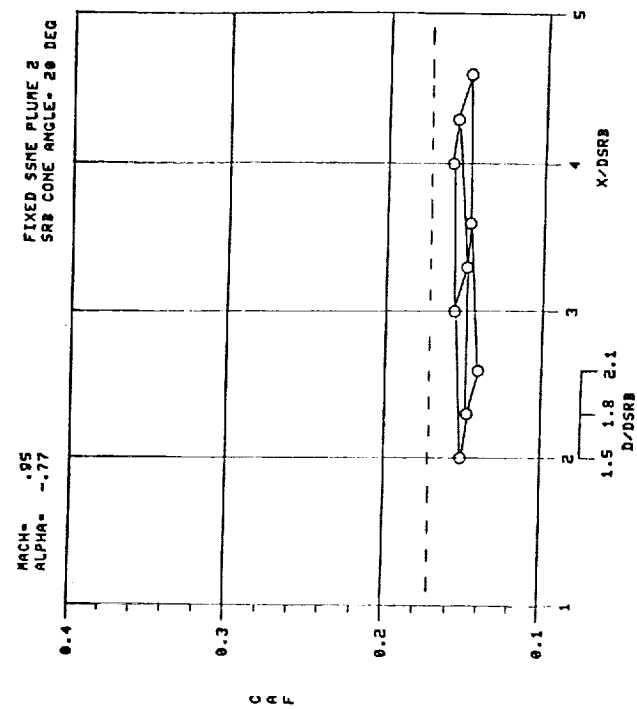


Figure D-4.

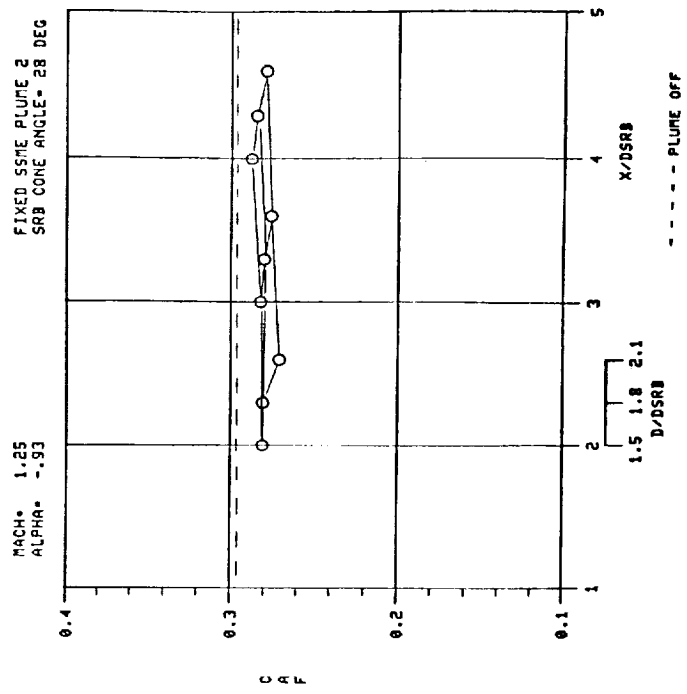
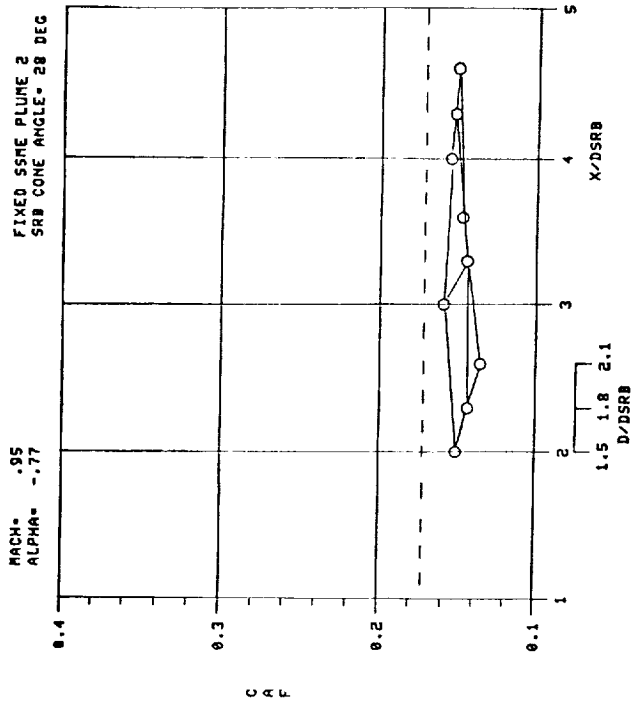
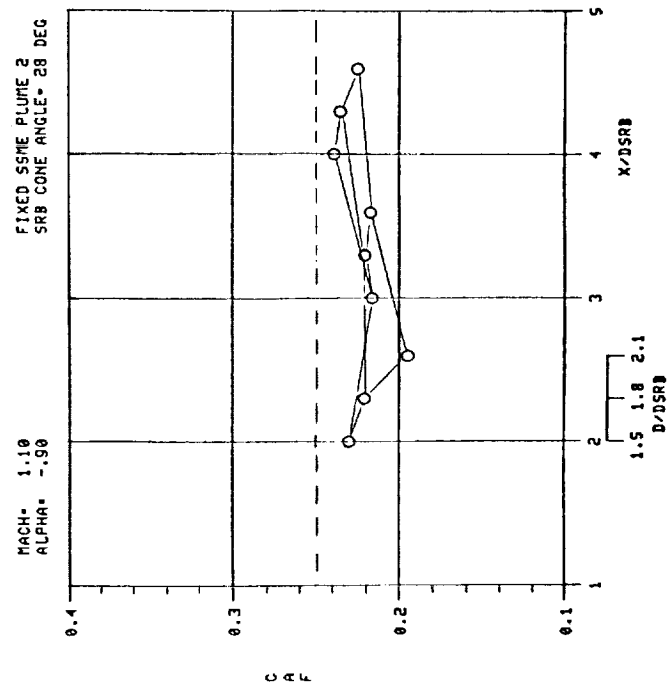
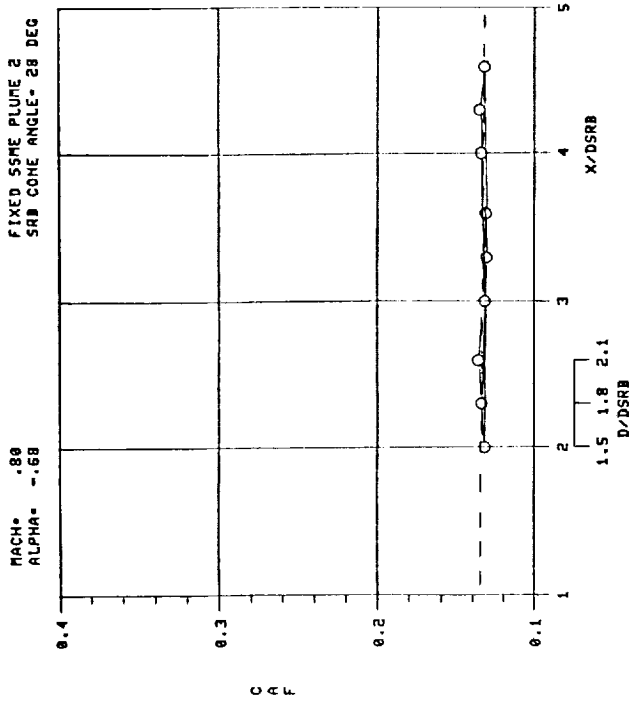


Figure D-5.

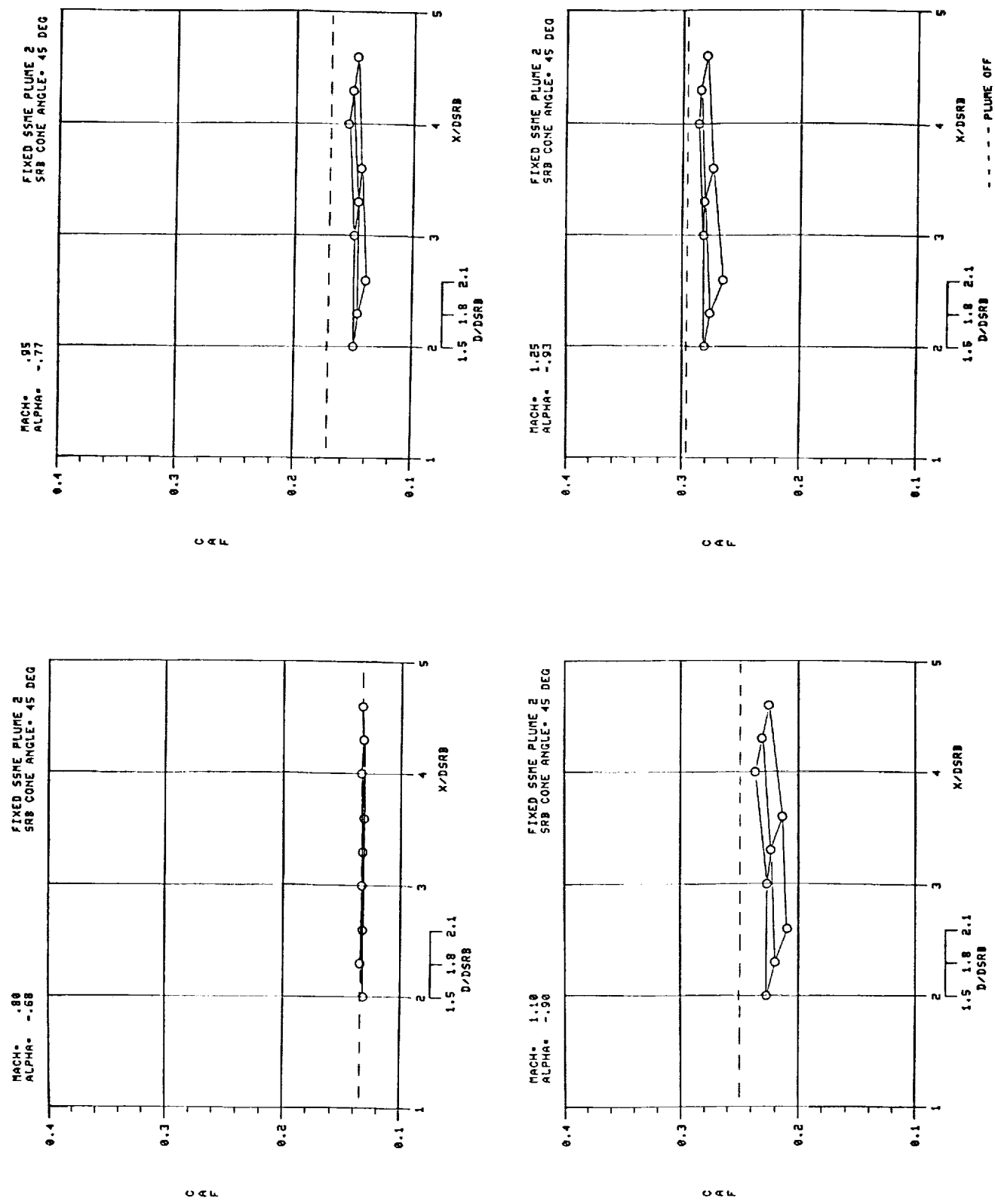


Figure D-6.

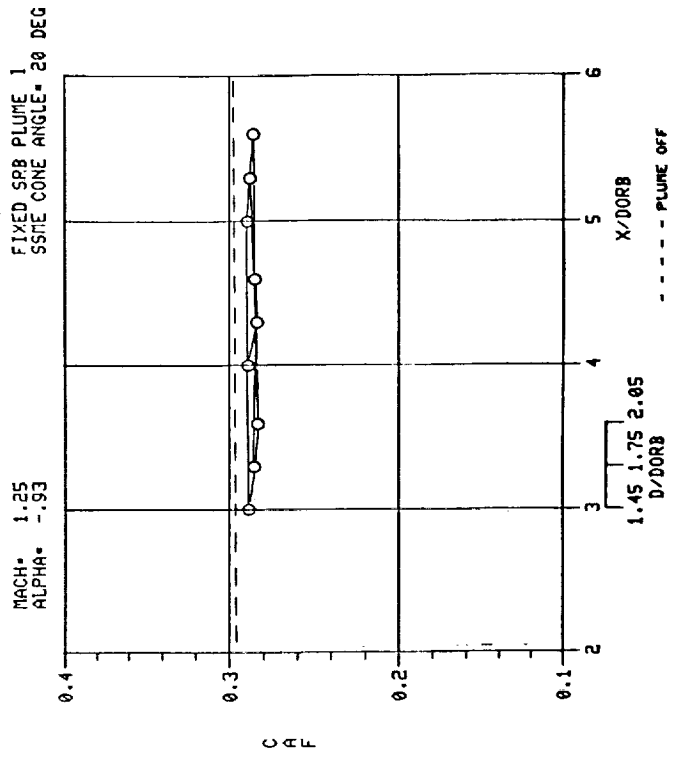
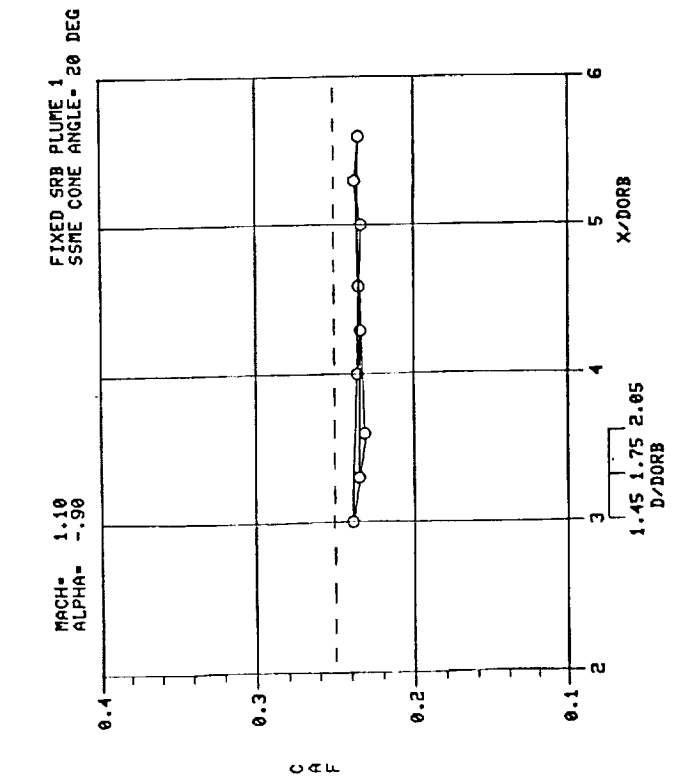
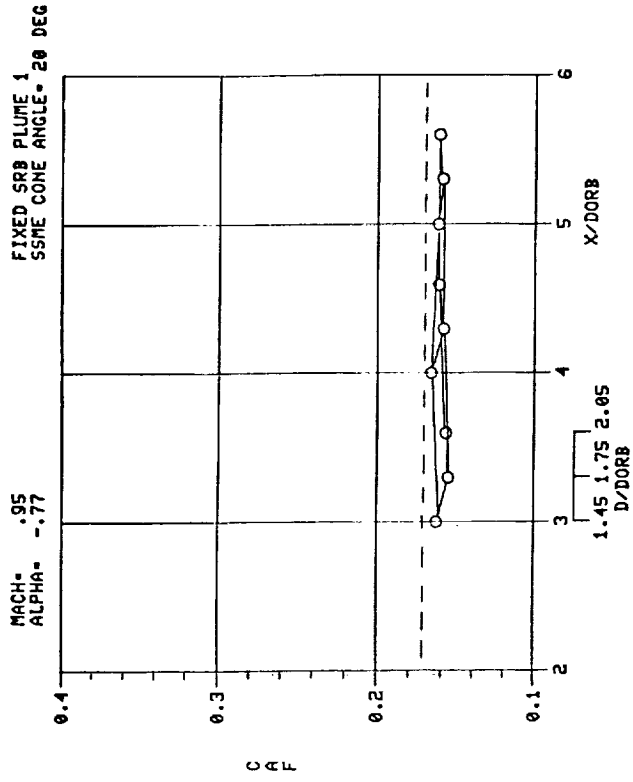
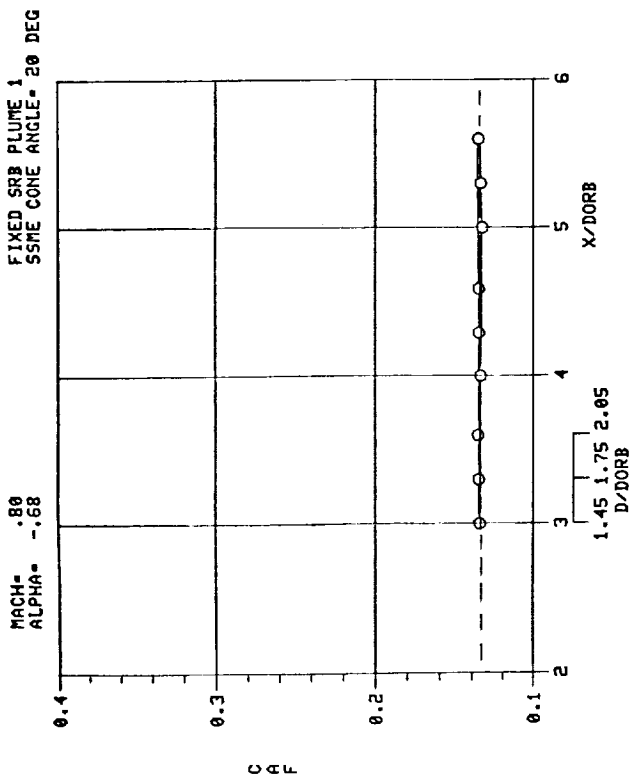


Figure D-7.

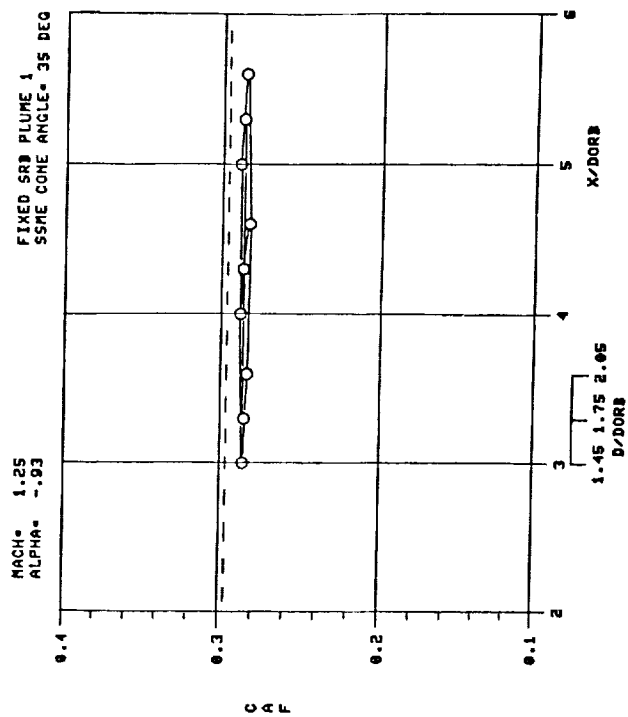
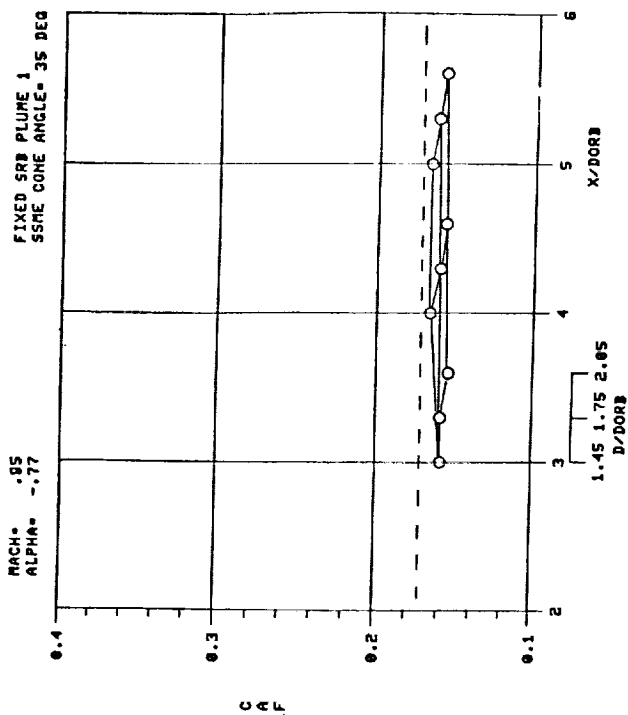
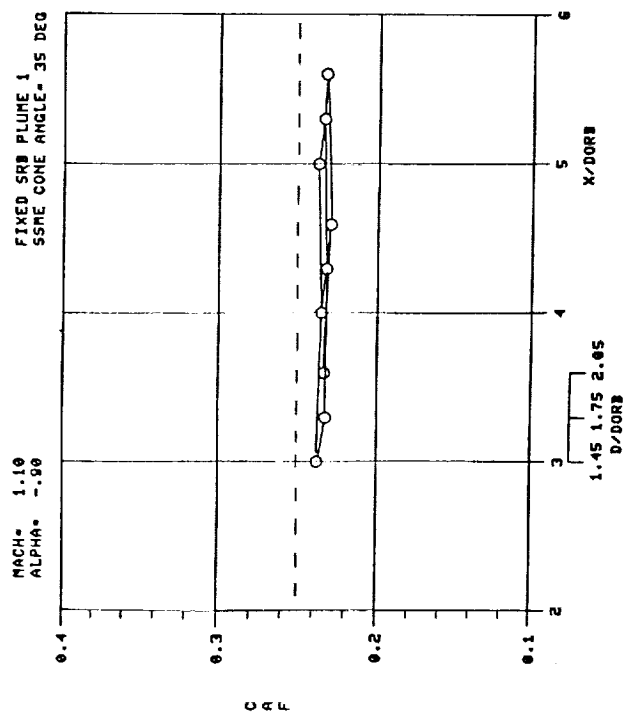
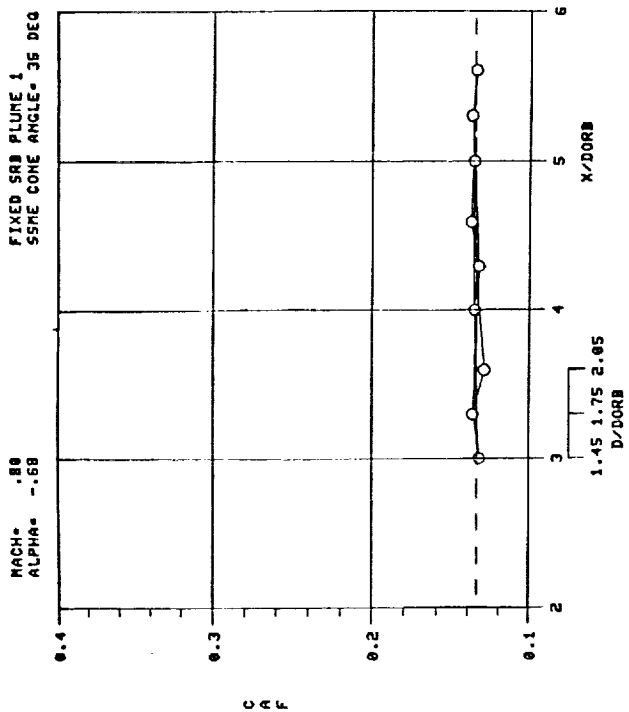


Figure D-8.

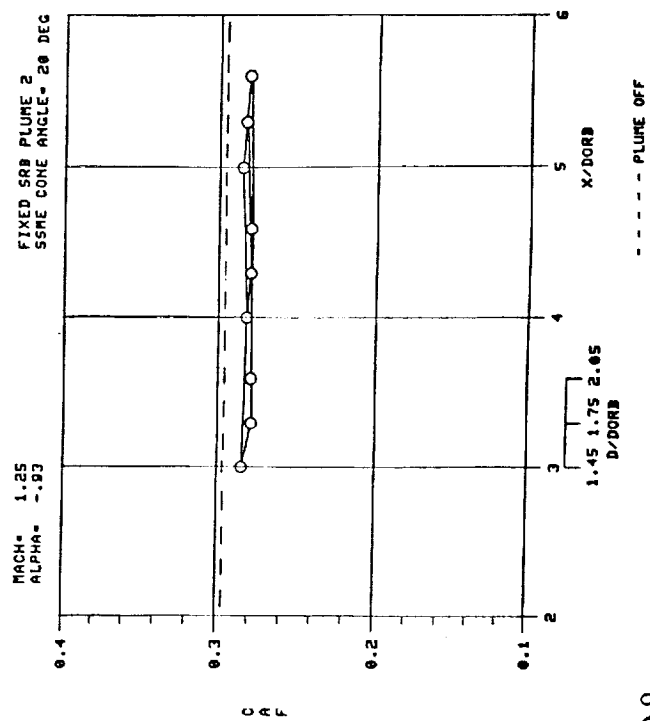
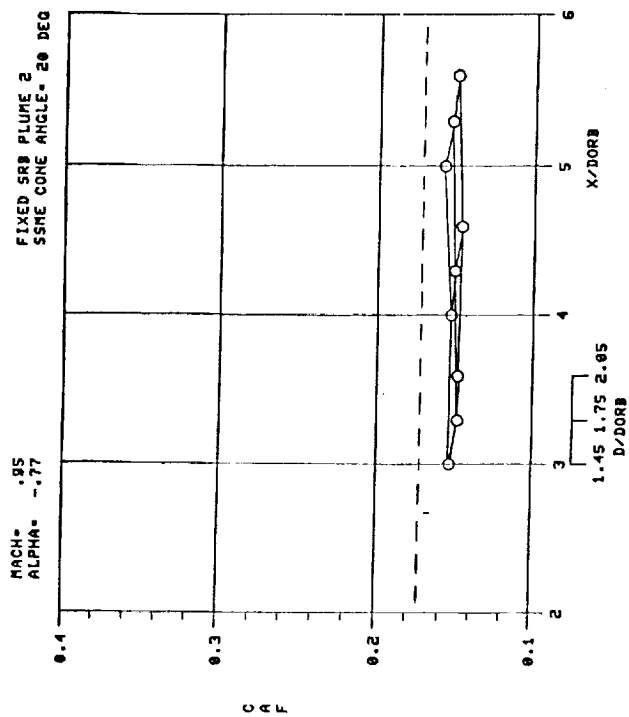
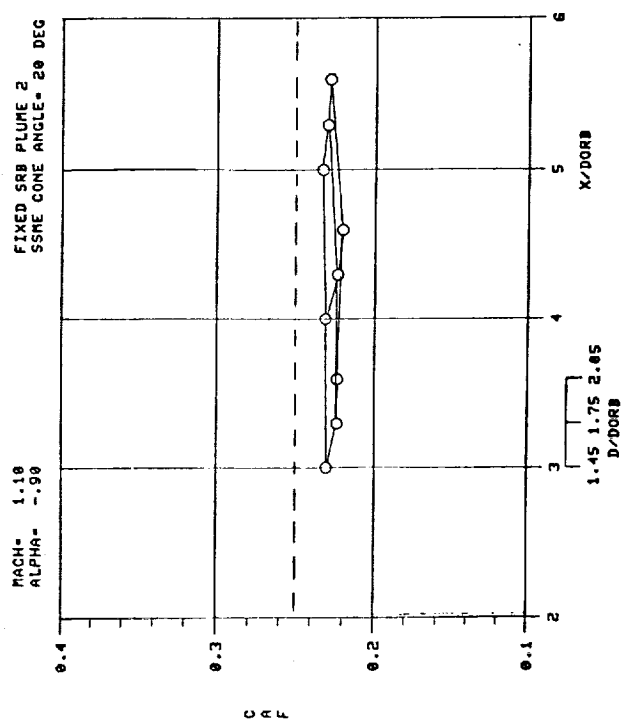
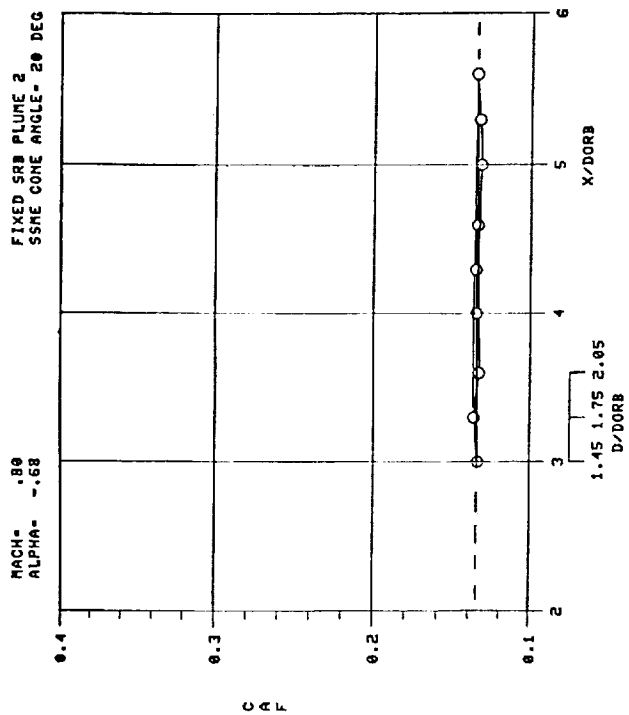
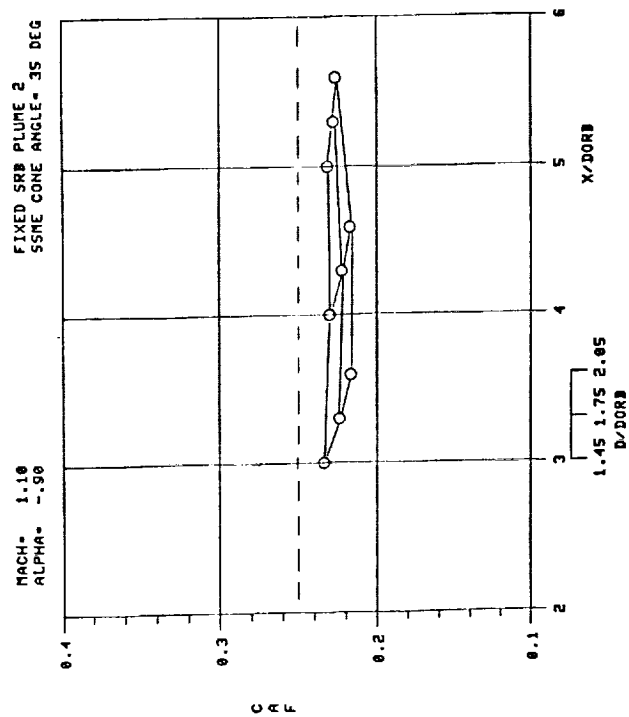
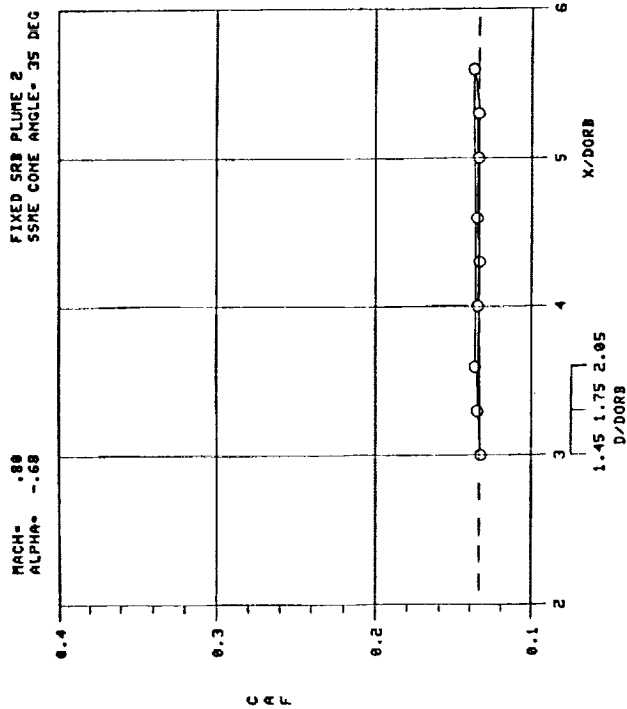
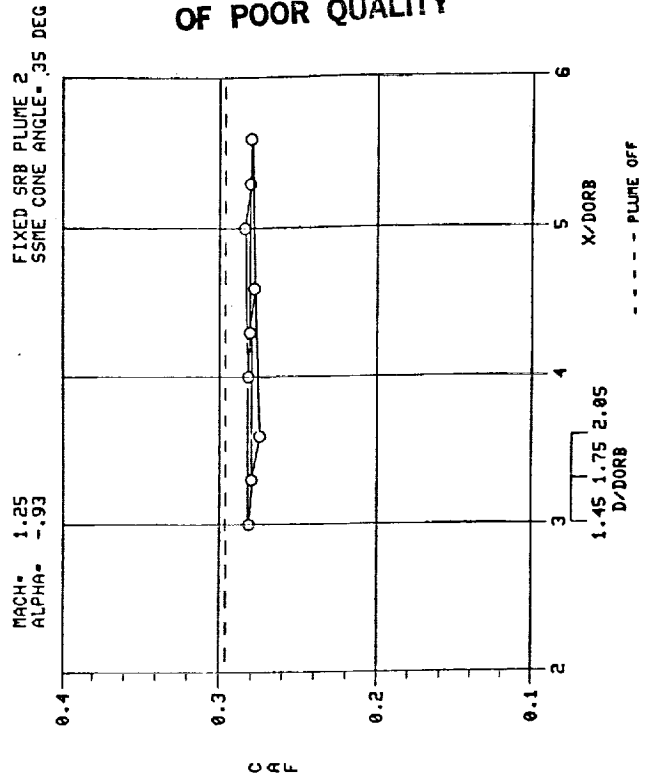
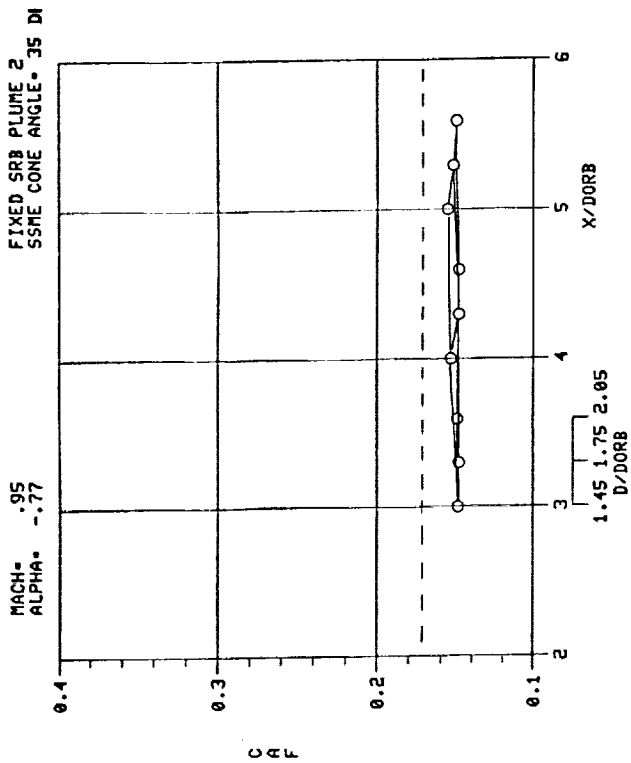


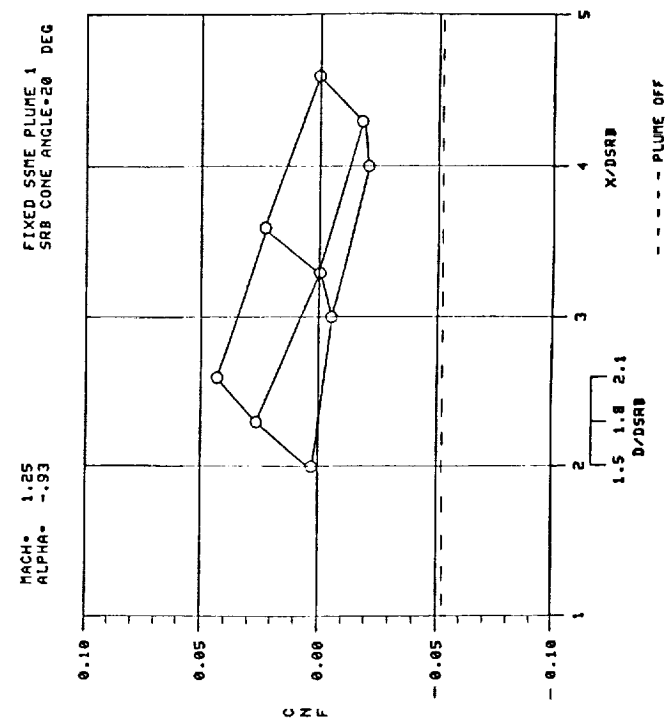
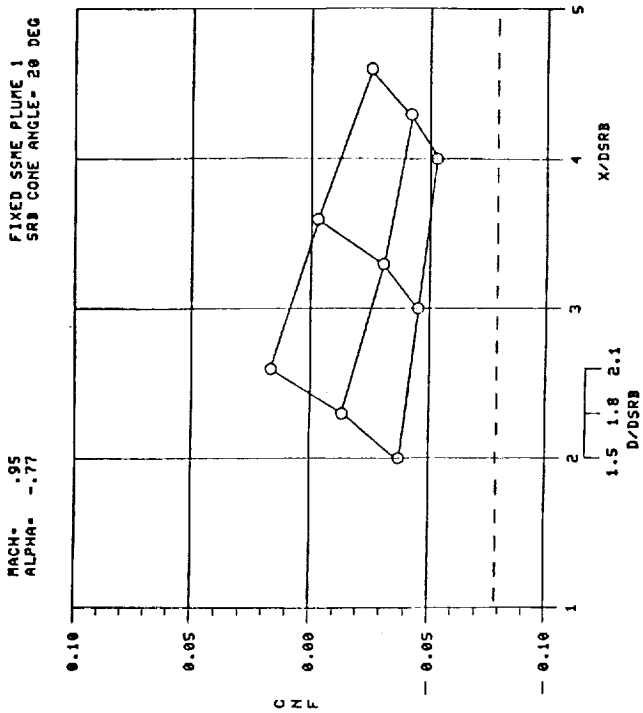
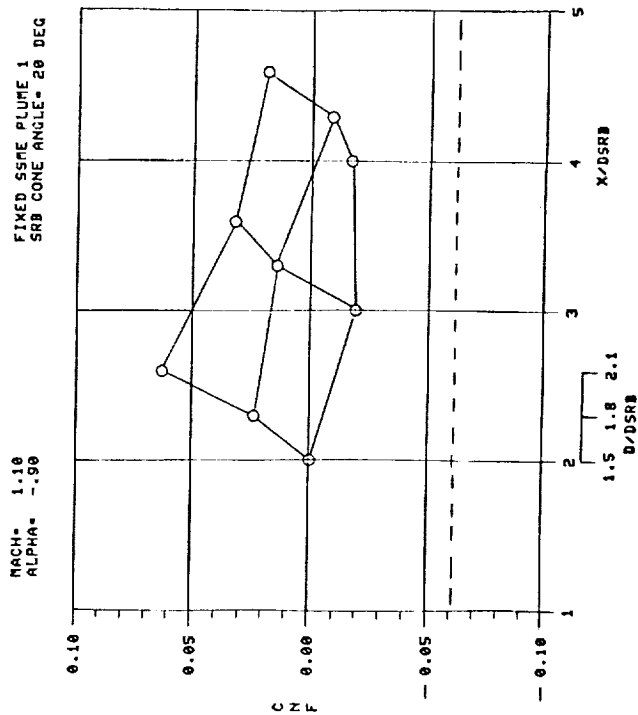
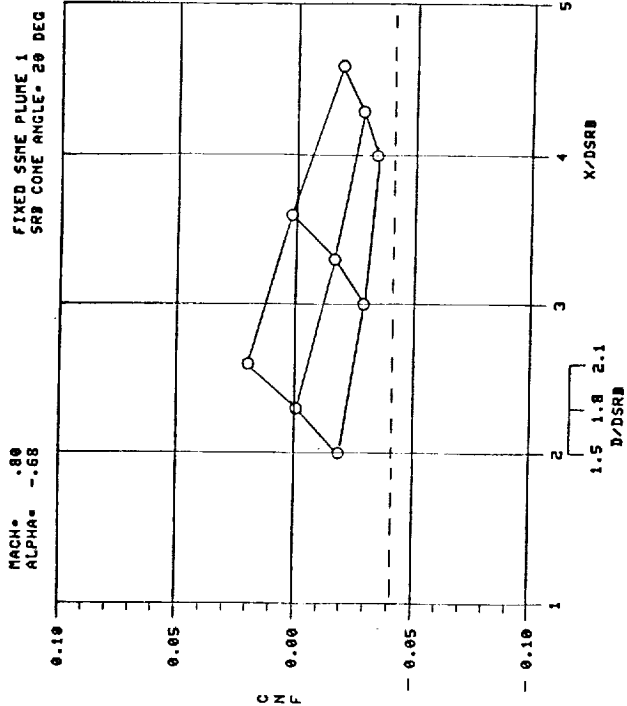
Figure D-9.



ORIGINAL PAGE IS
OF POOR QUALITY

Figure D-10.

APPENDIX E



ORIGINAL PAGE IS
 OF POOR QUALITY

Figure E-1.

PRECEDING PAGE BLANK NOT FILMED

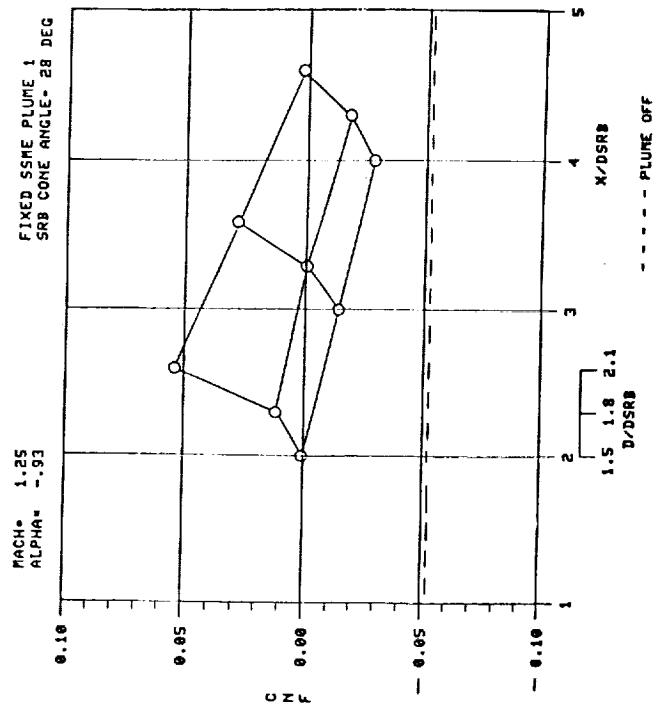
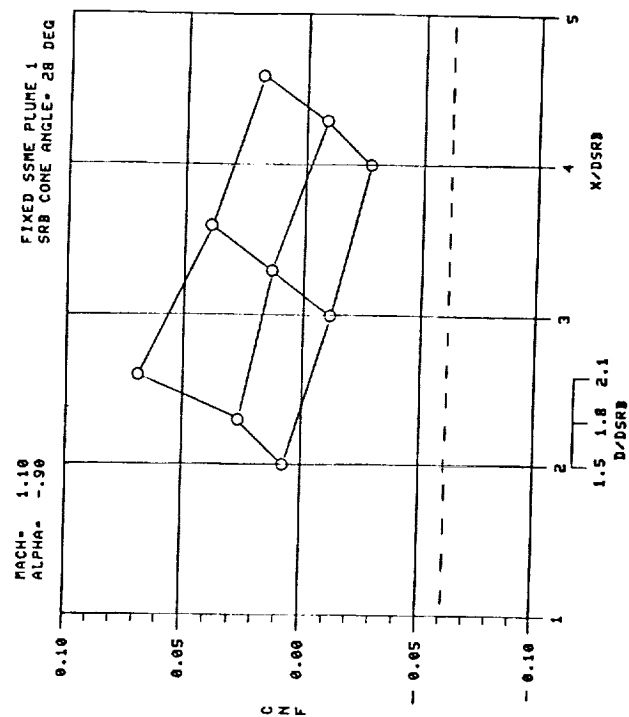
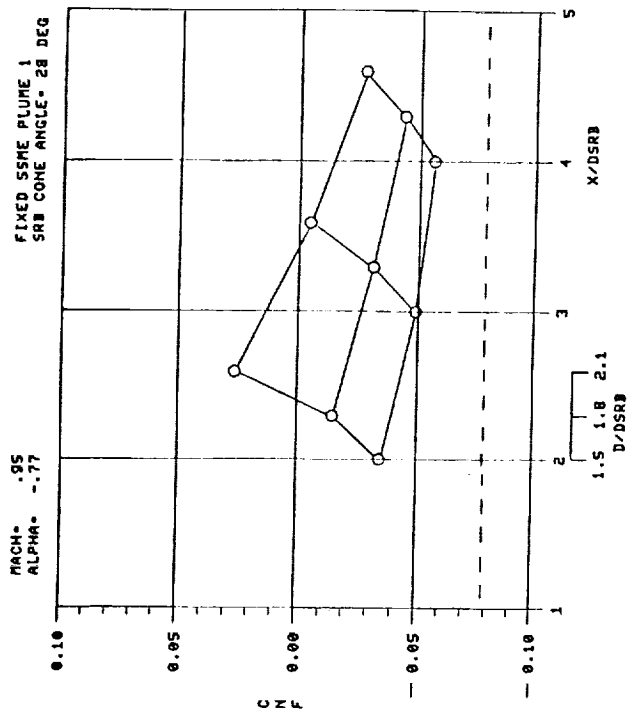
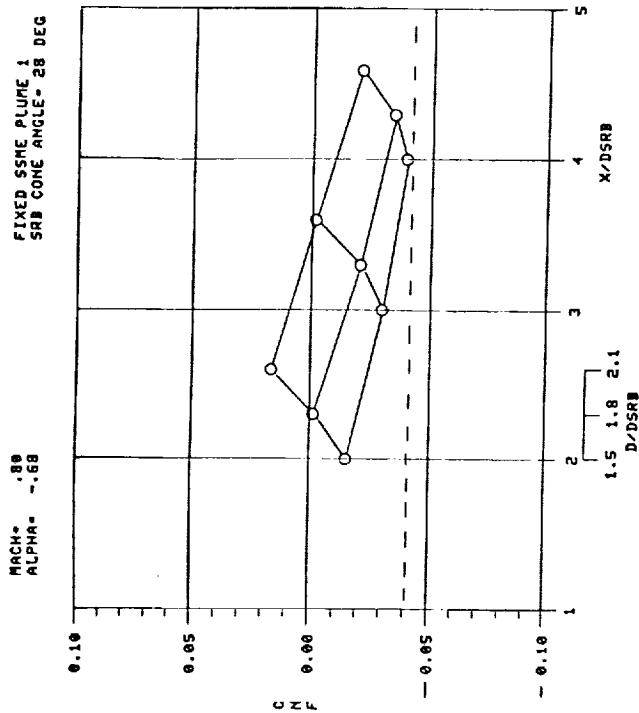


Figure E-2.

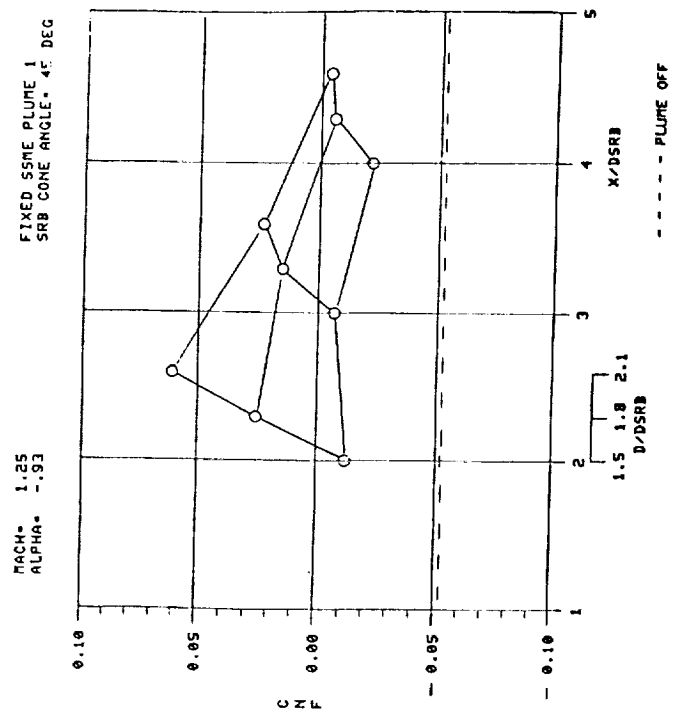
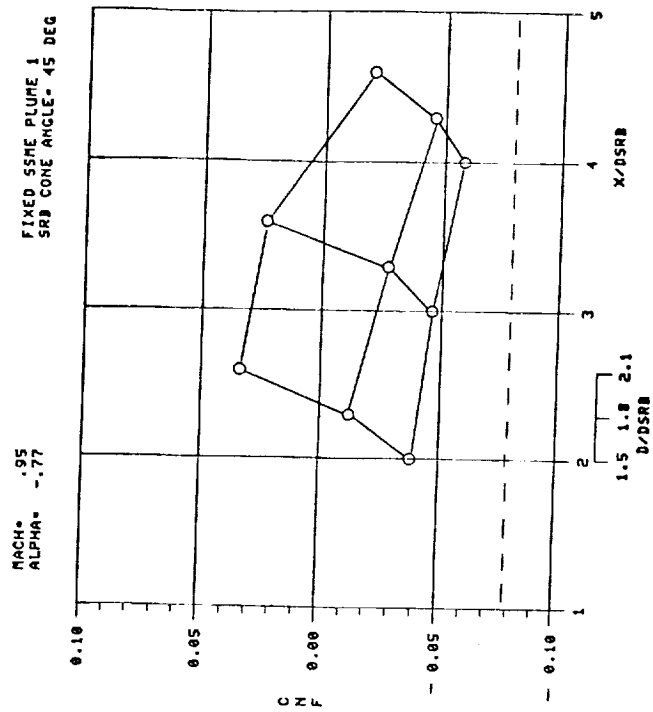
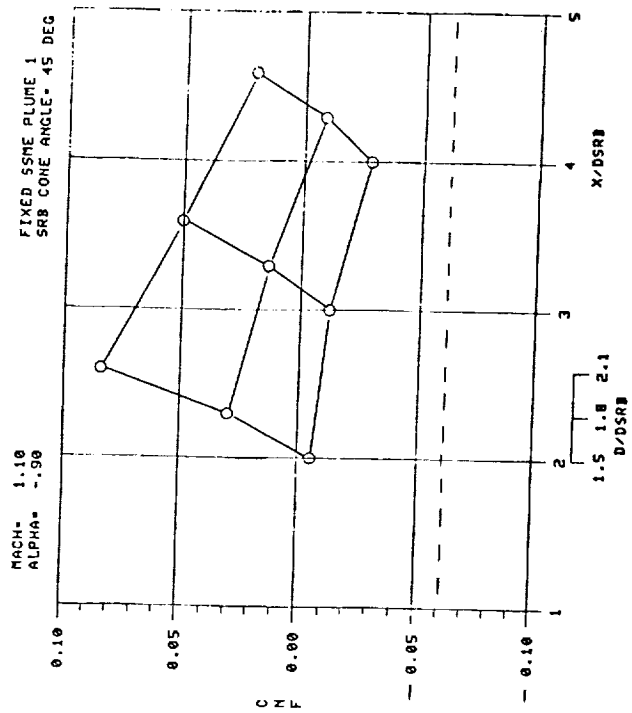
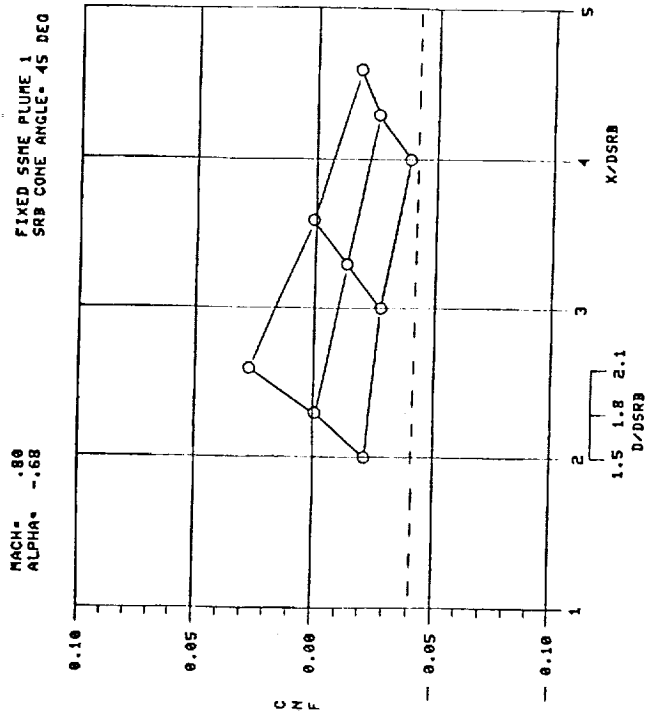


Figure E-3.

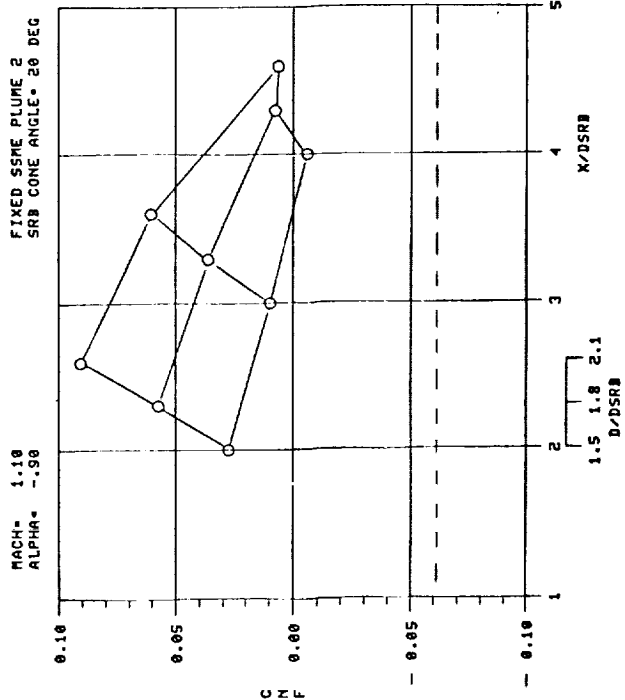
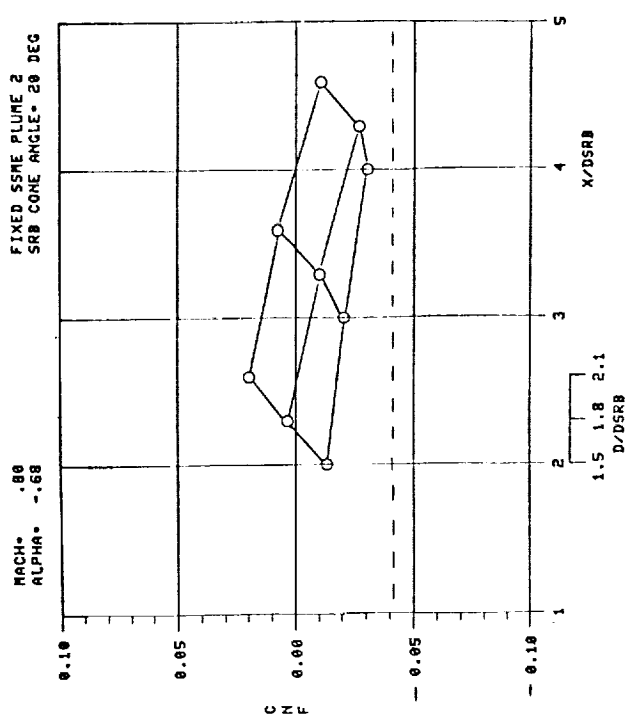
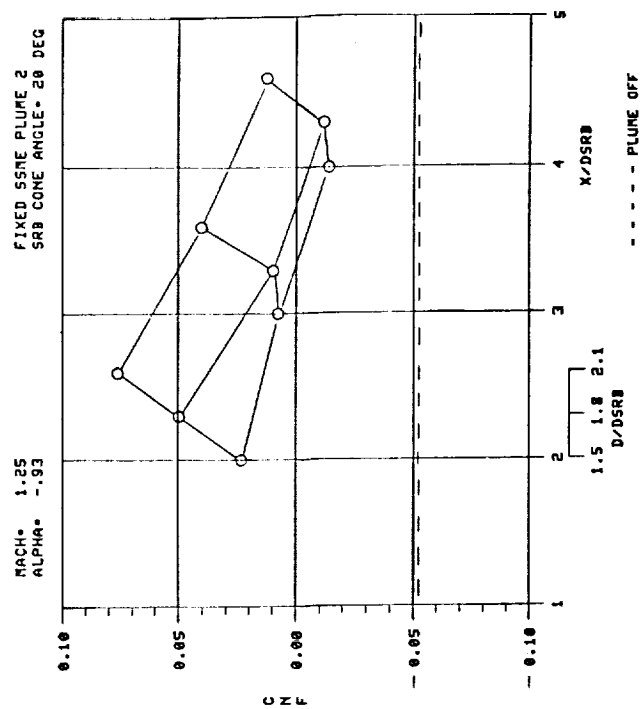
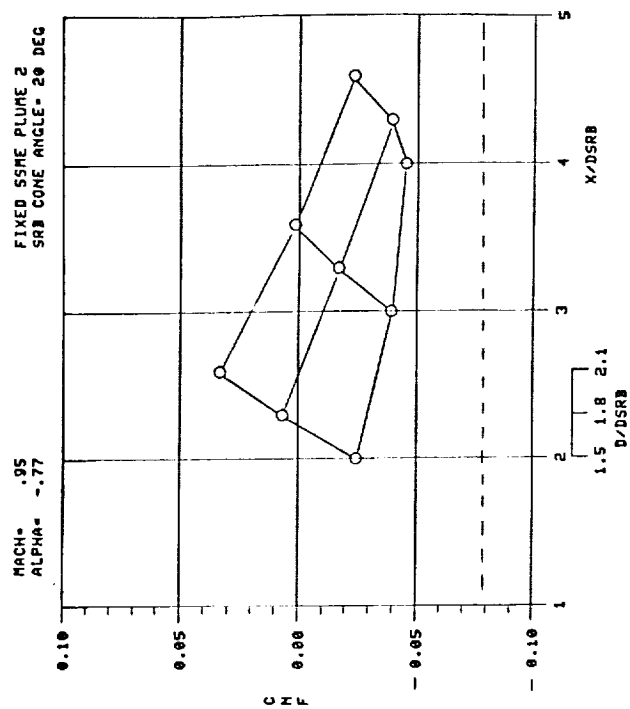


Figure E-4.

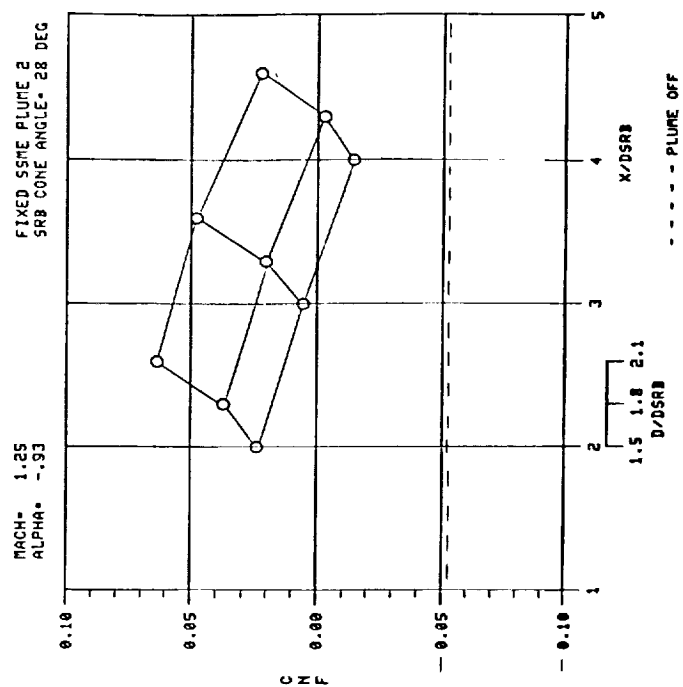
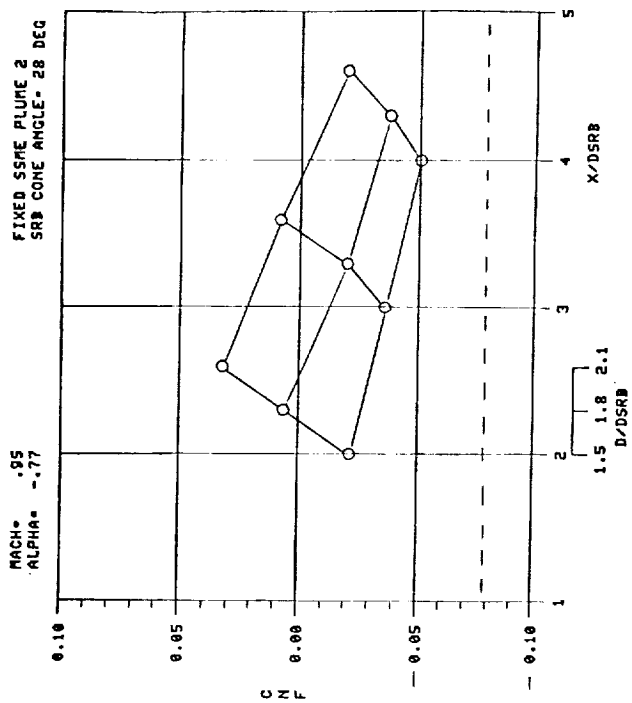
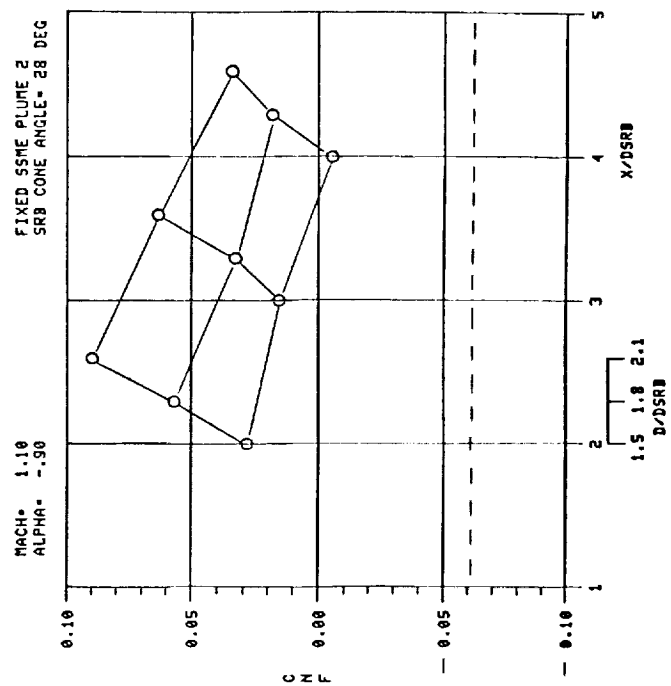
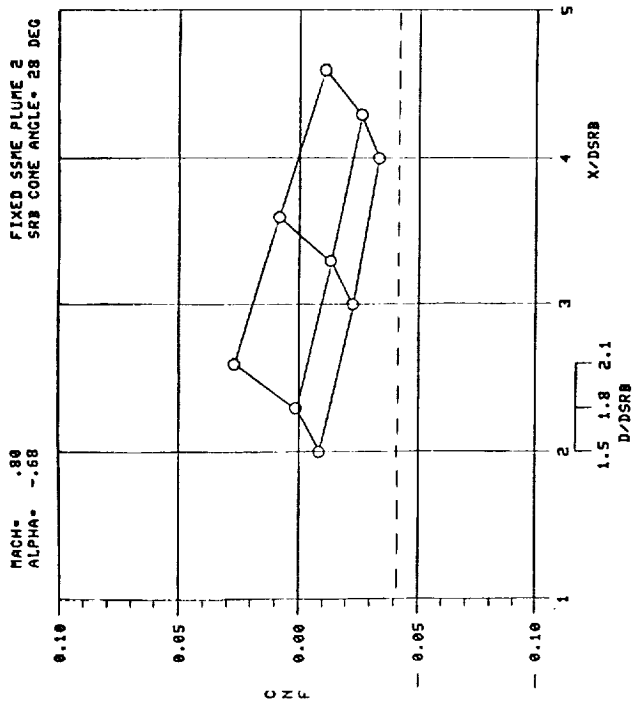


Figure E-5.

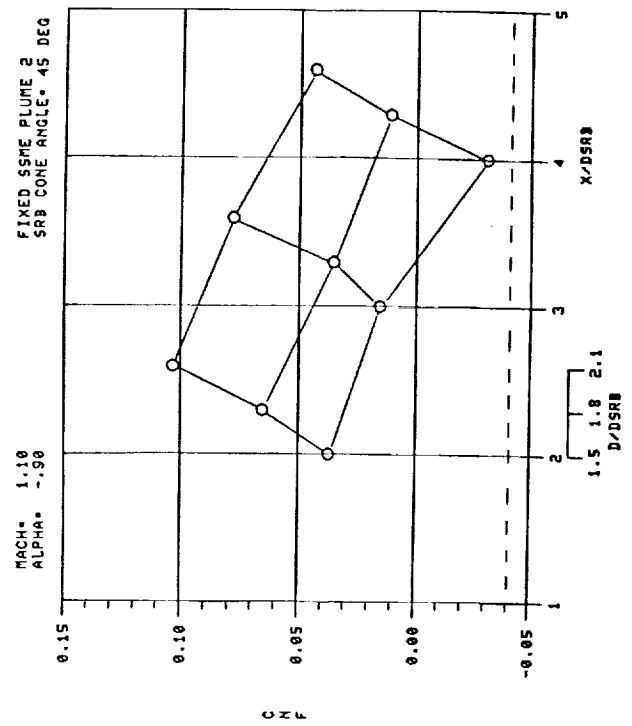
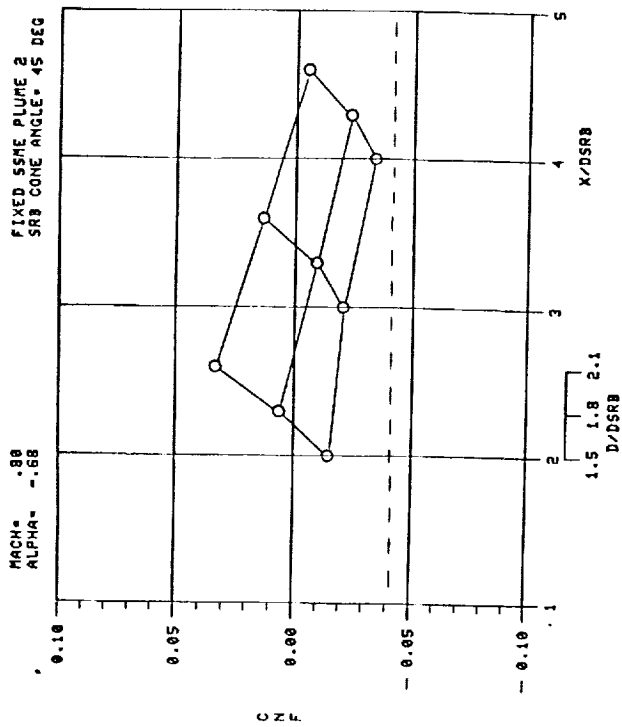
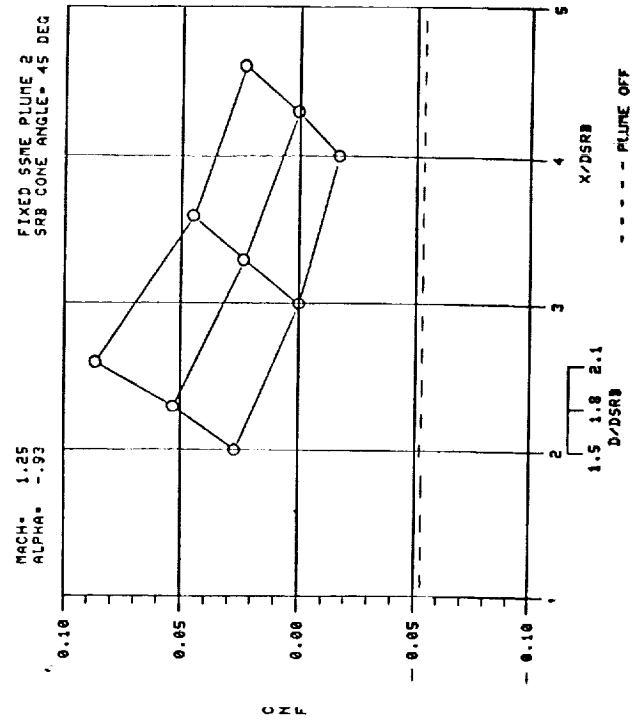
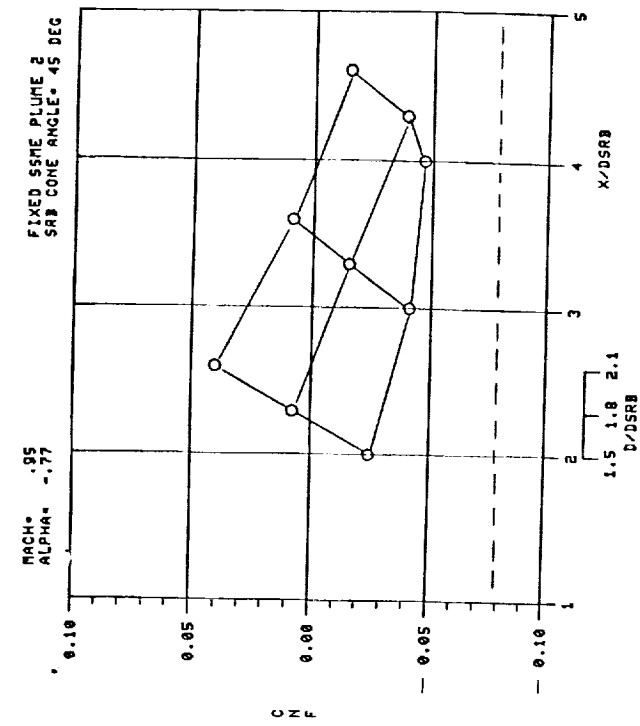
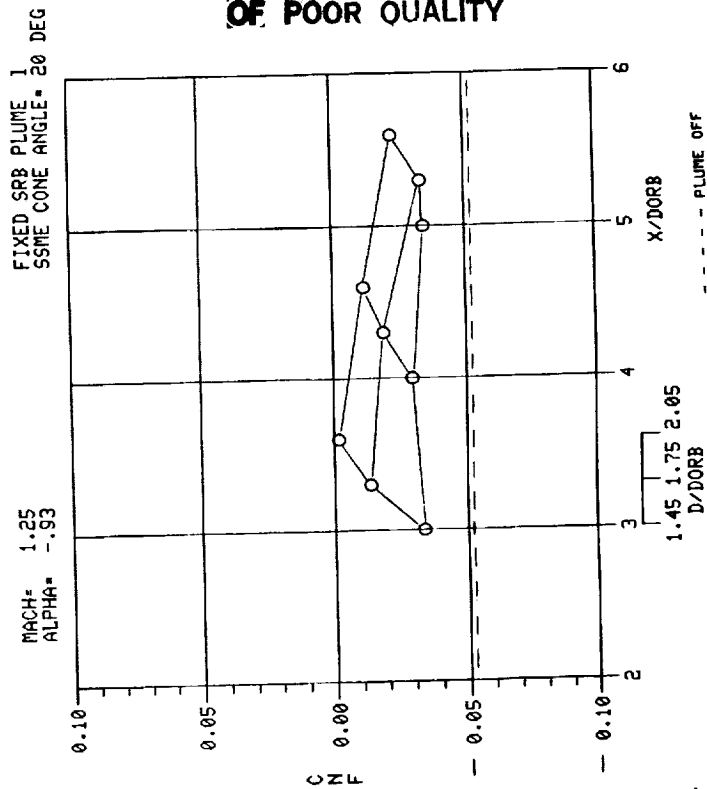
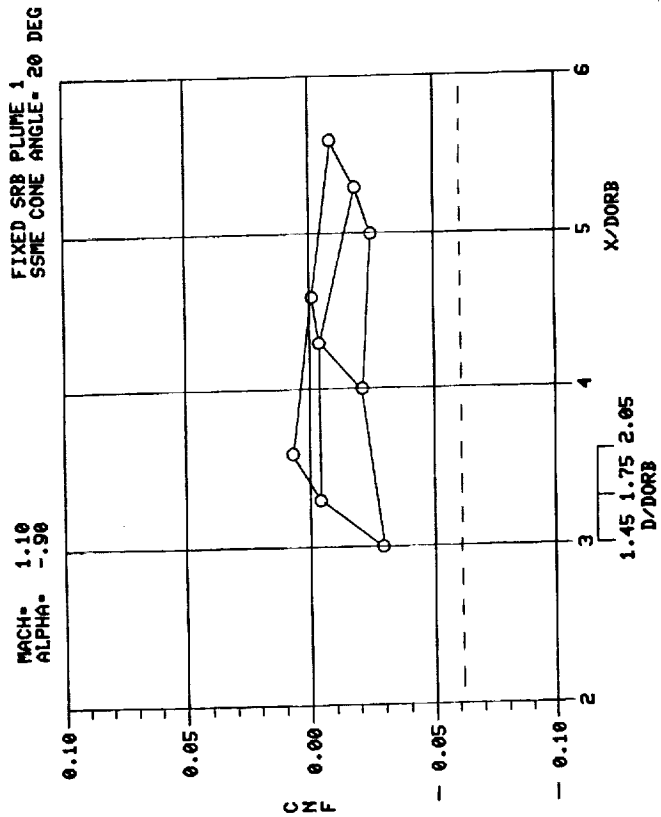
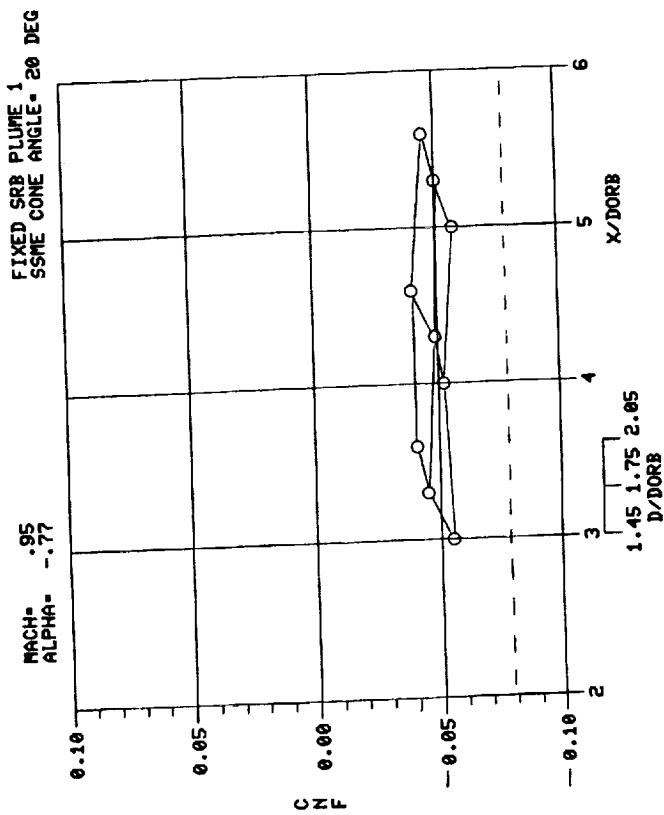
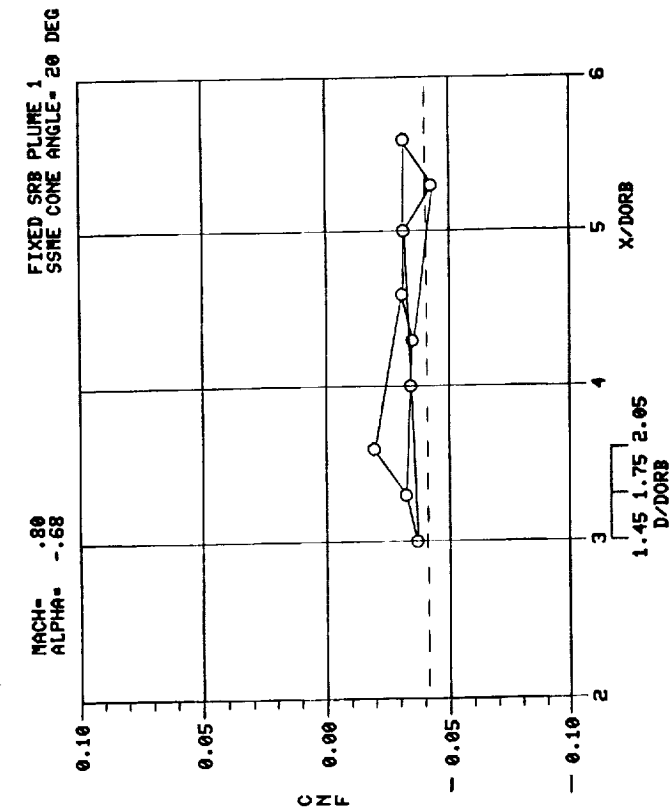


Figure E-6.



ORIGINAL PAGE IS
OF POOR QUALITY

Figure E-7.

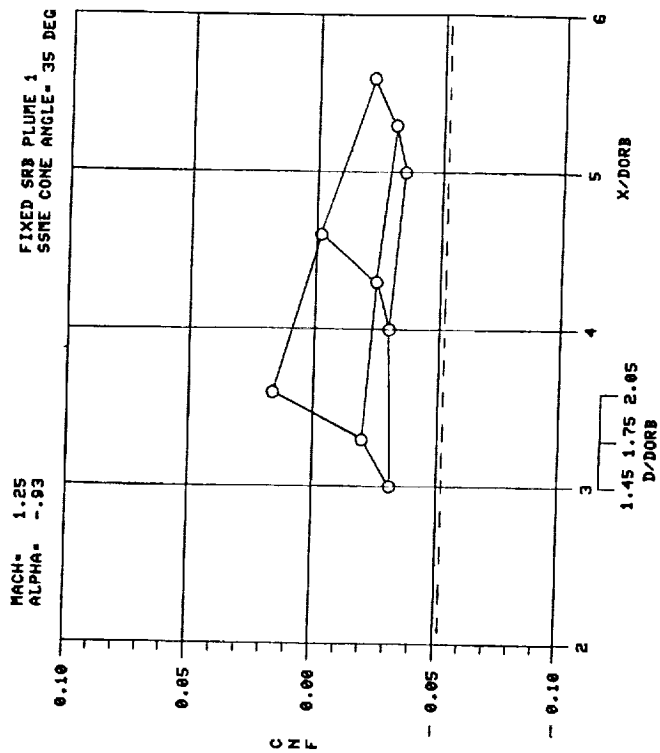
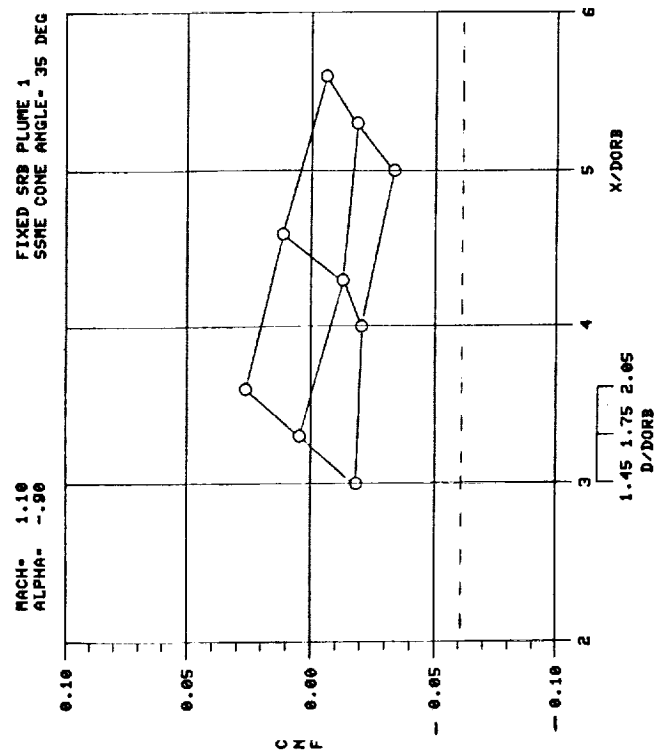
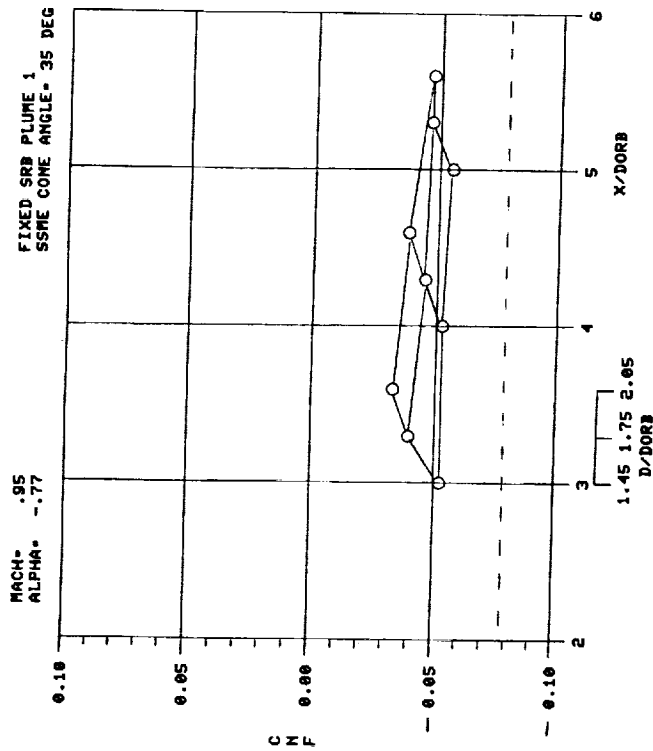
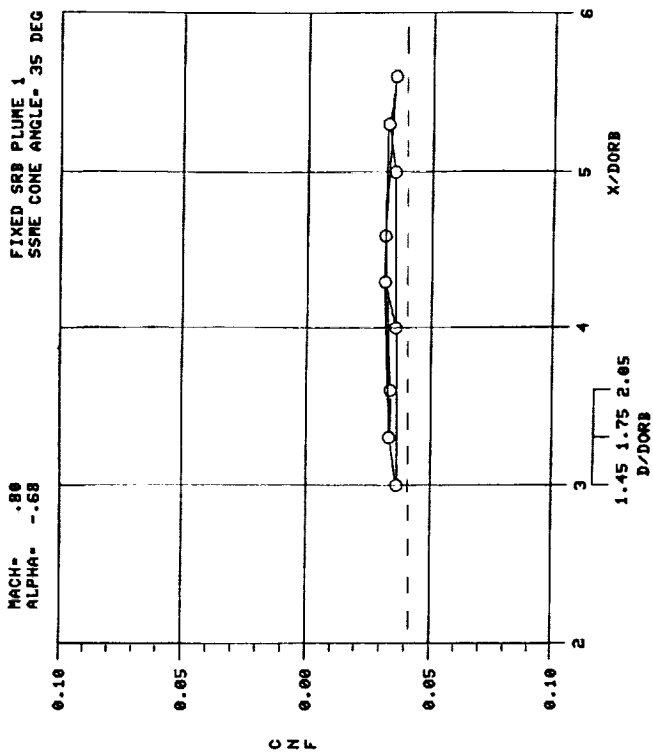


Figure E-8.

----- PLUME OFF

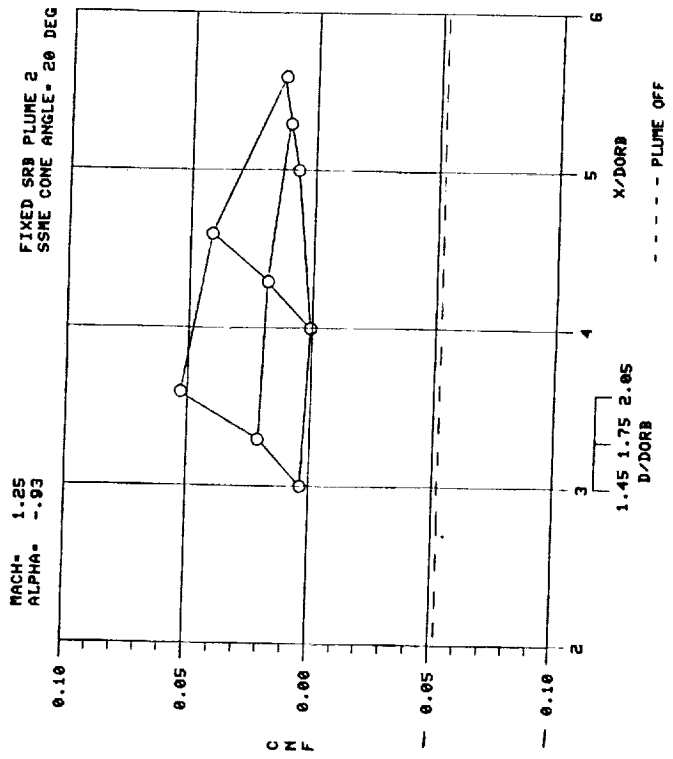
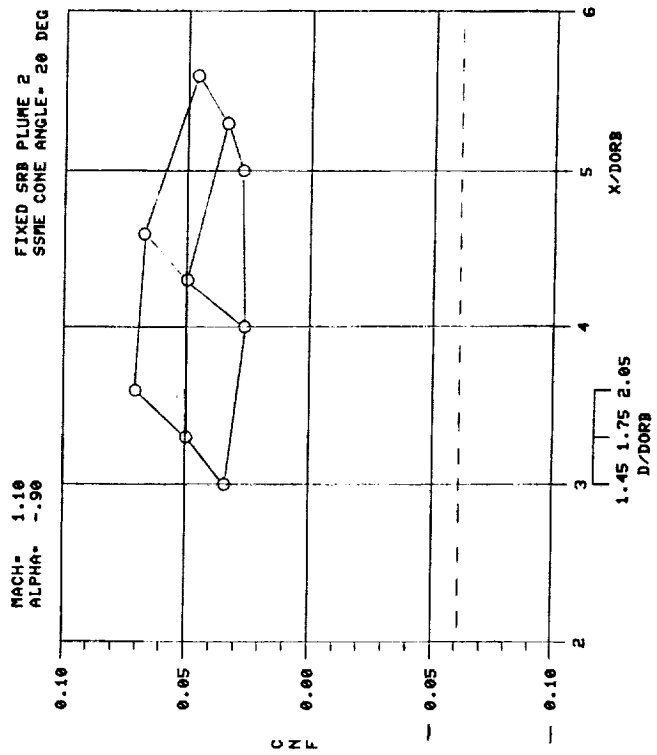
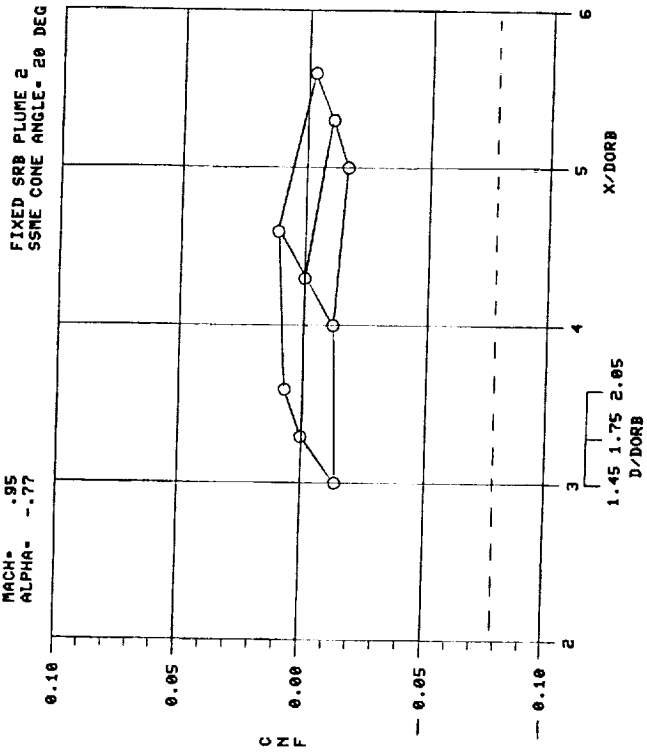
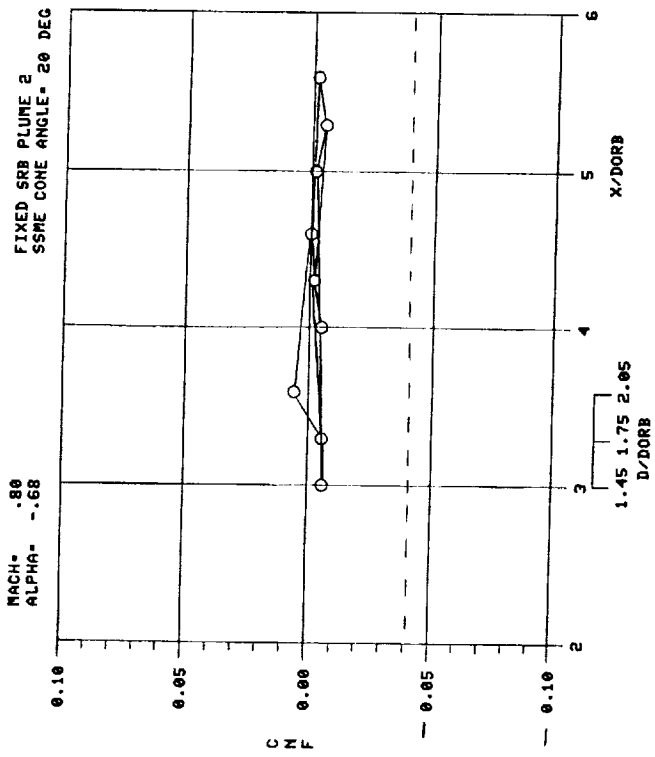


Figure E-9.

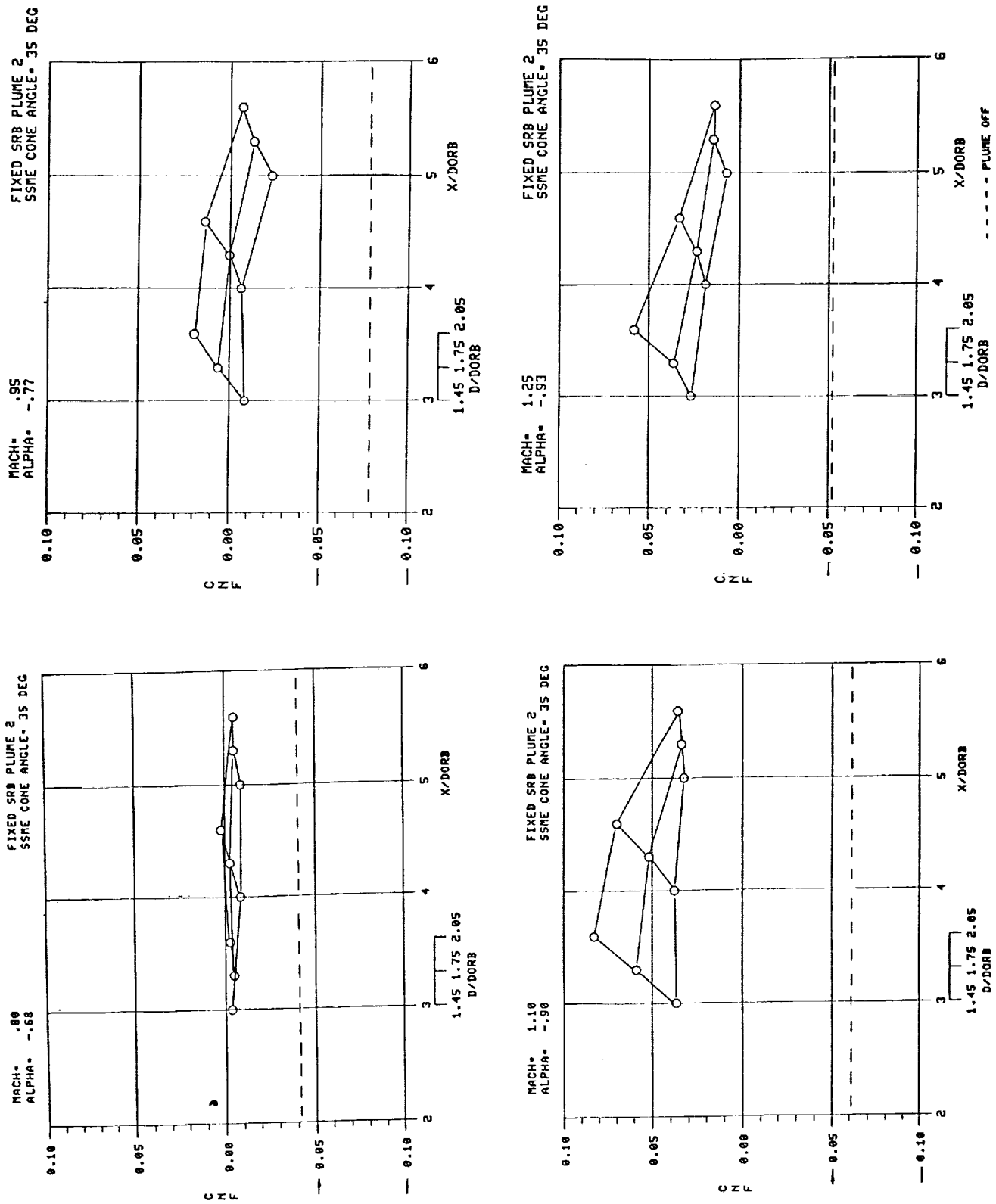


Figure E-10.

APPENDIX F



ORIGINAL PAGE IS
OF POOR QUALITY

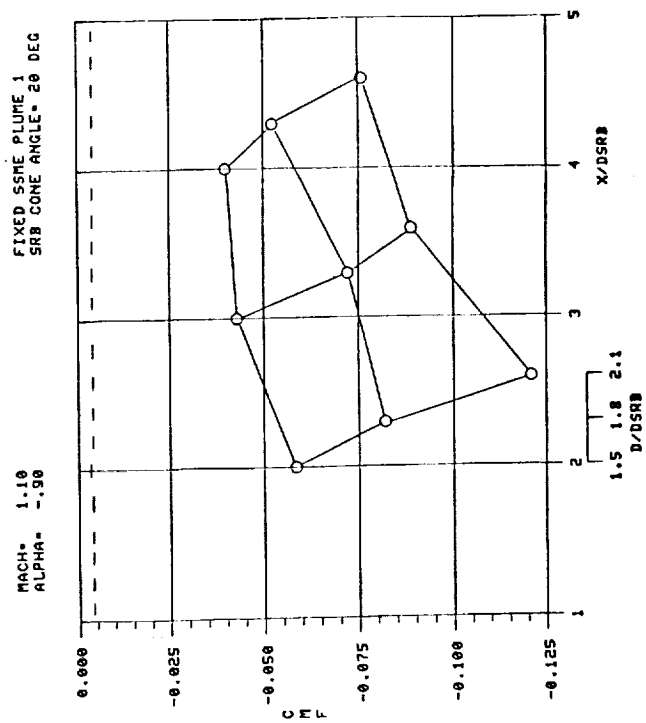
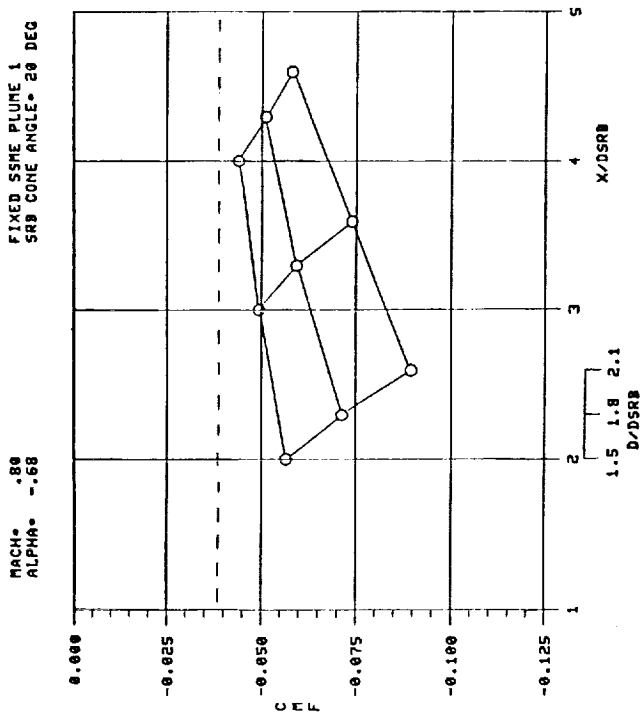
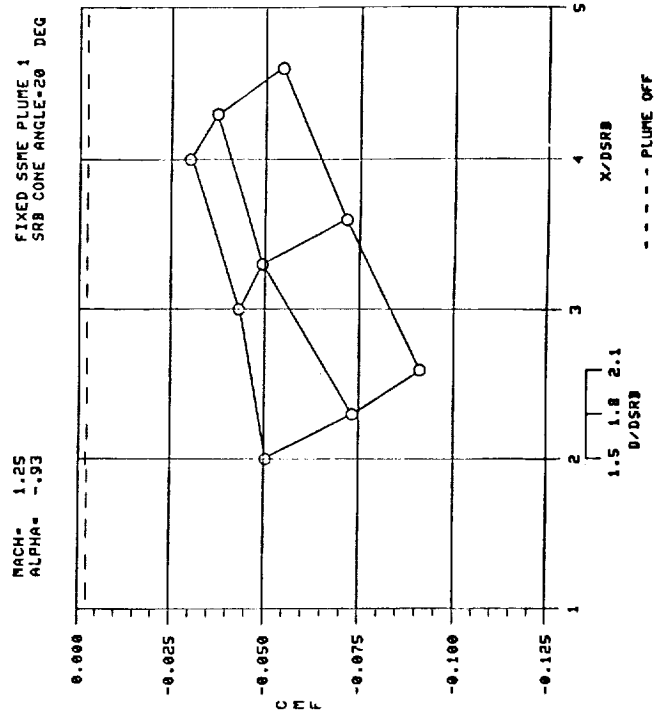
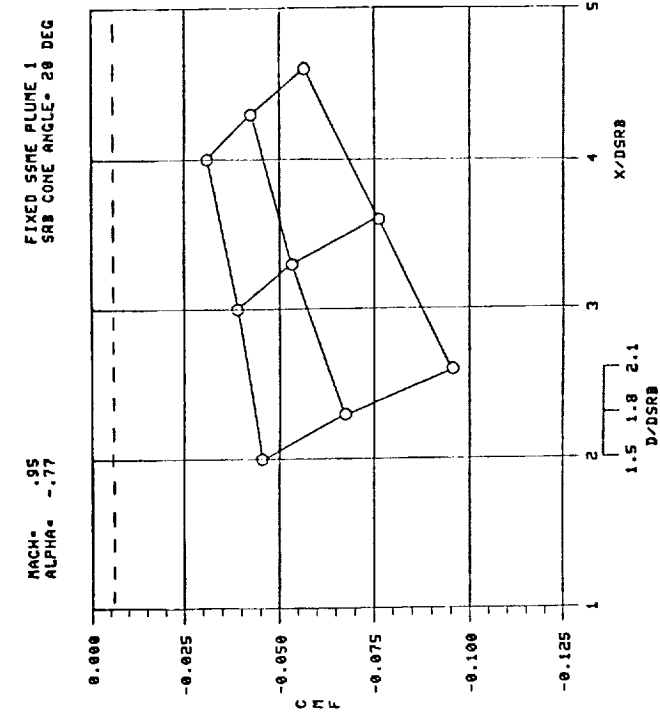


Figure F-1.

PRECEDING PAGE BLANK NOT FILMED

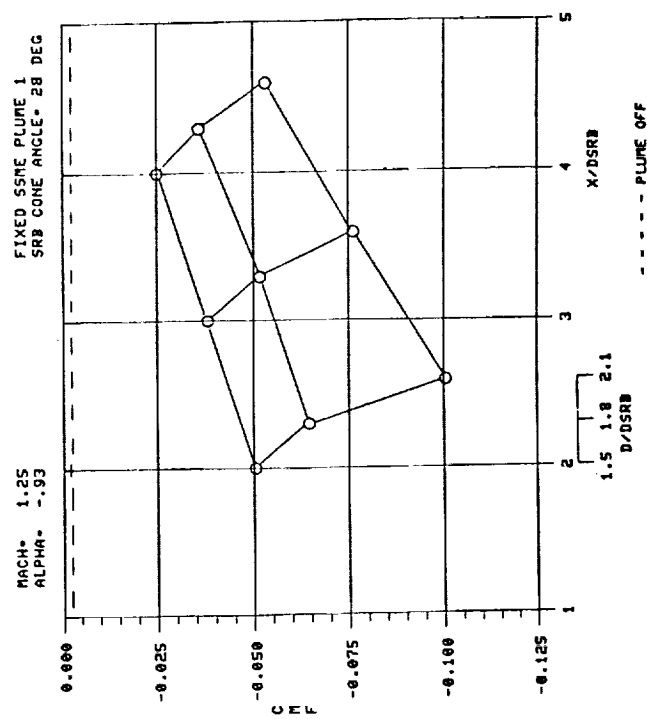
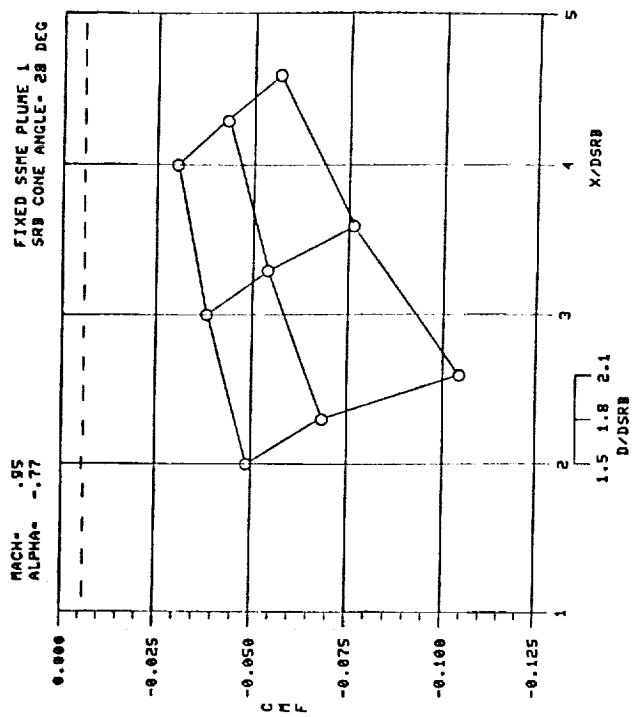
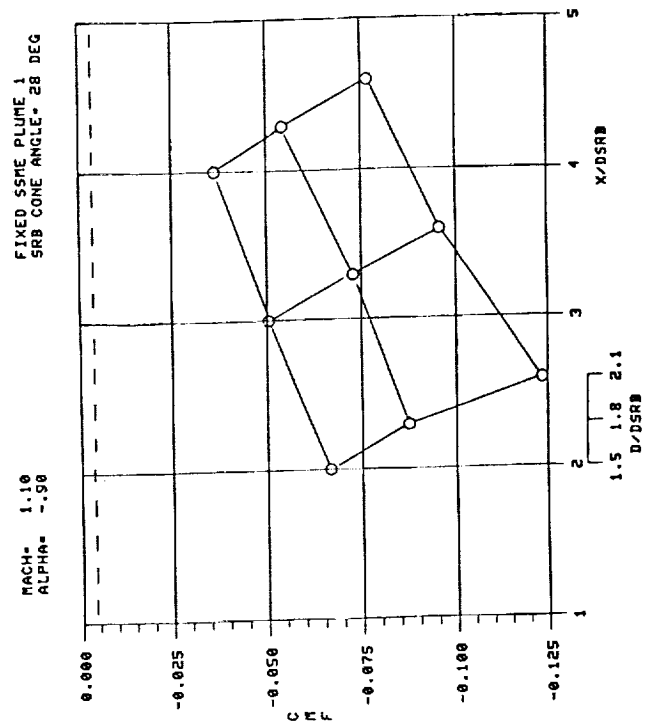
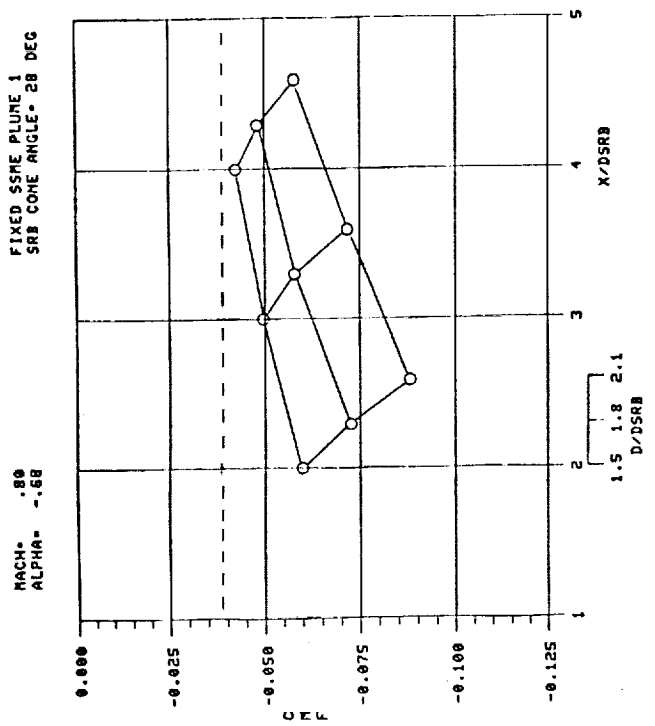


Figure F-2.

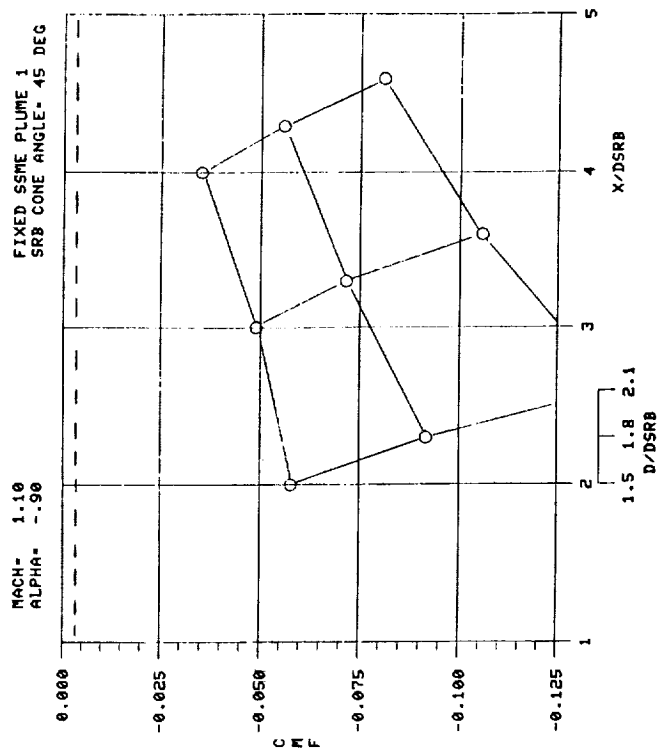
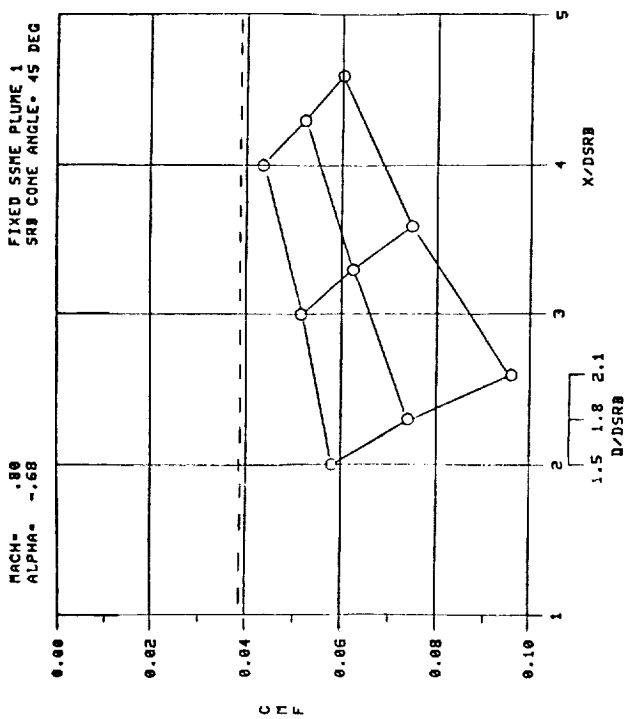
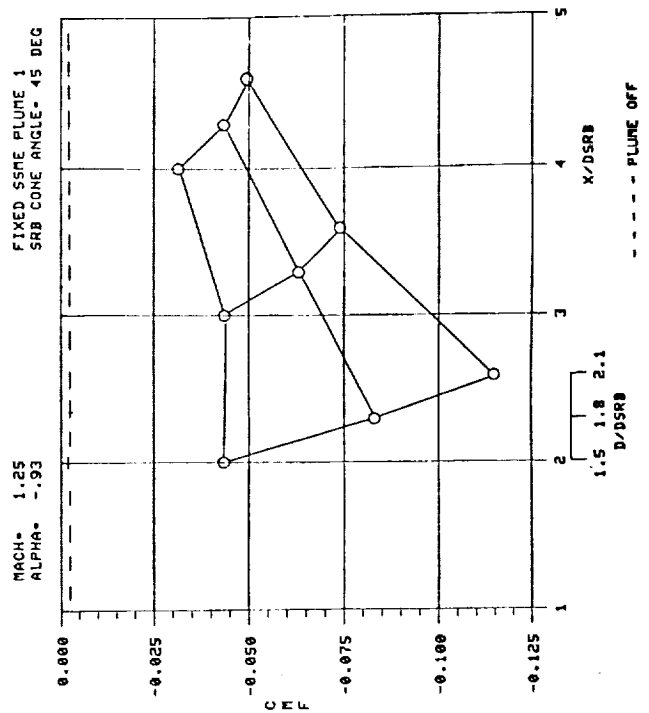
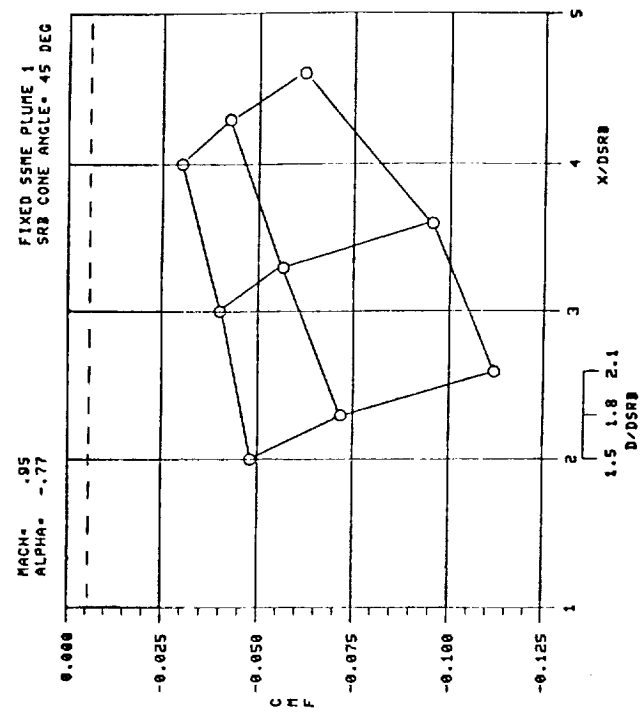


Figure F-3.

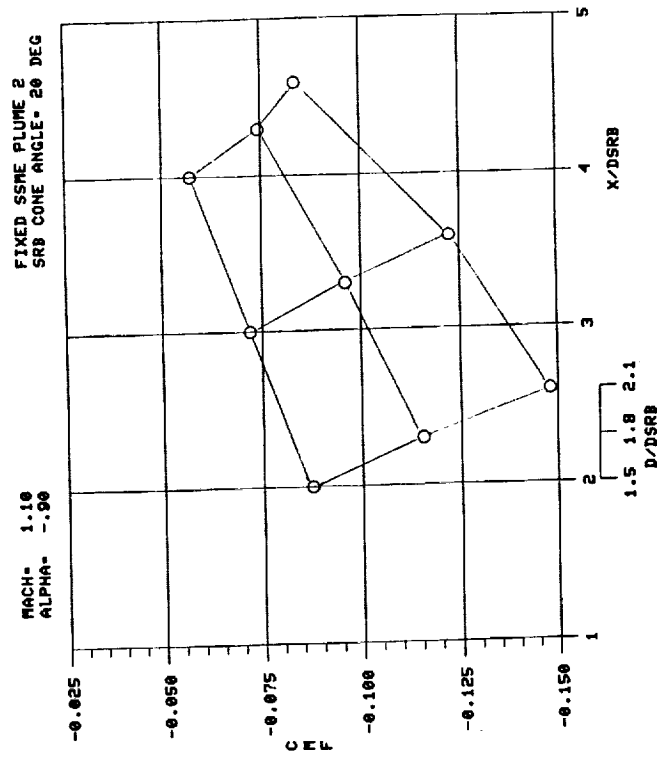
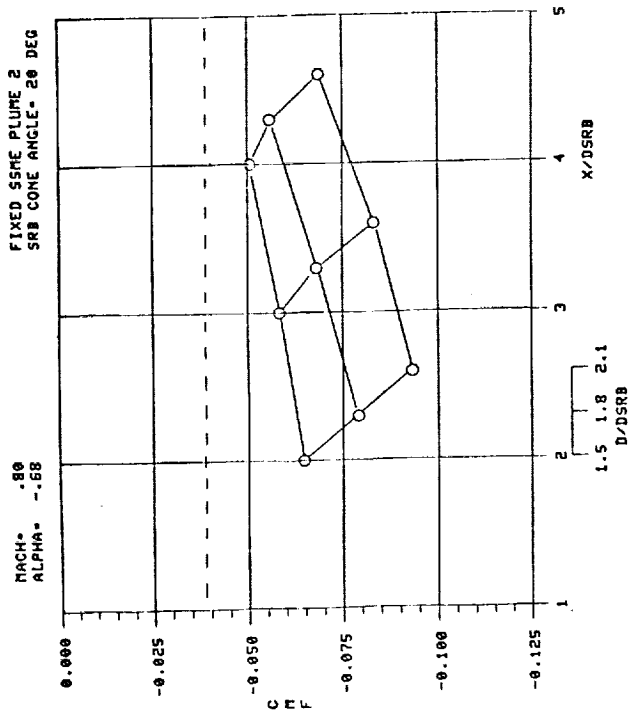
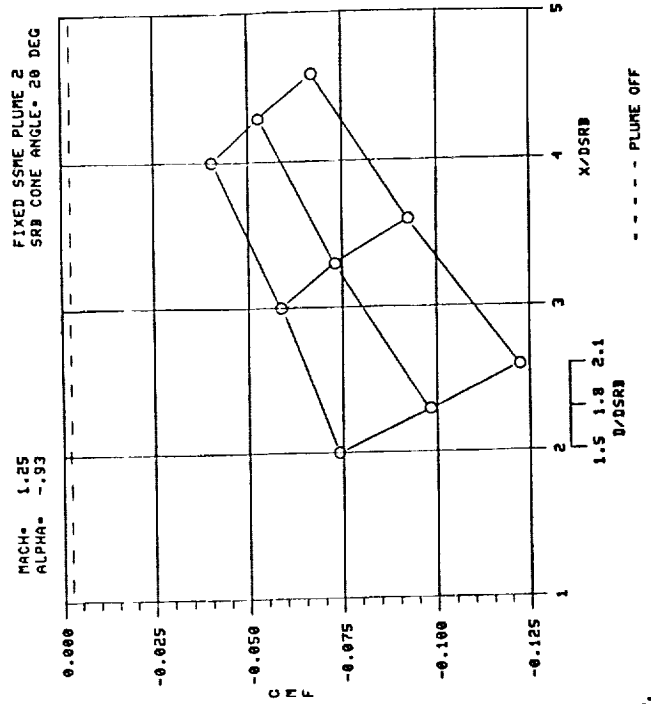
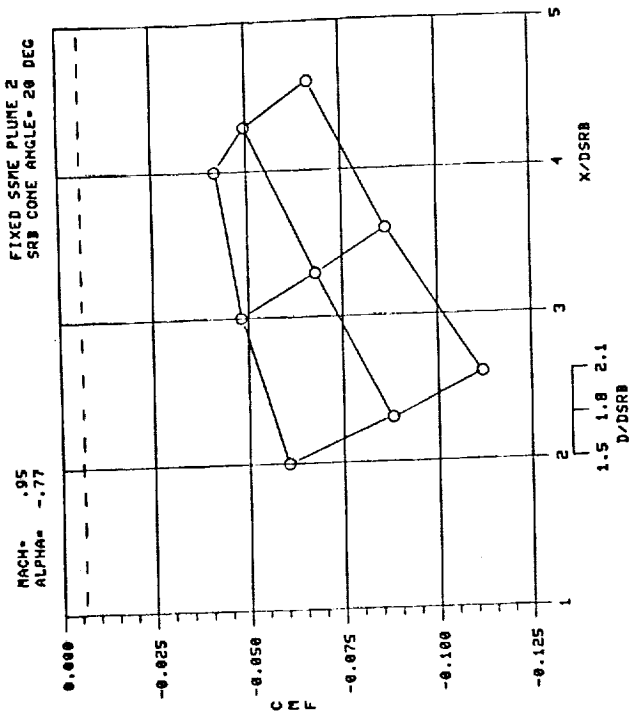


Figure F-4.

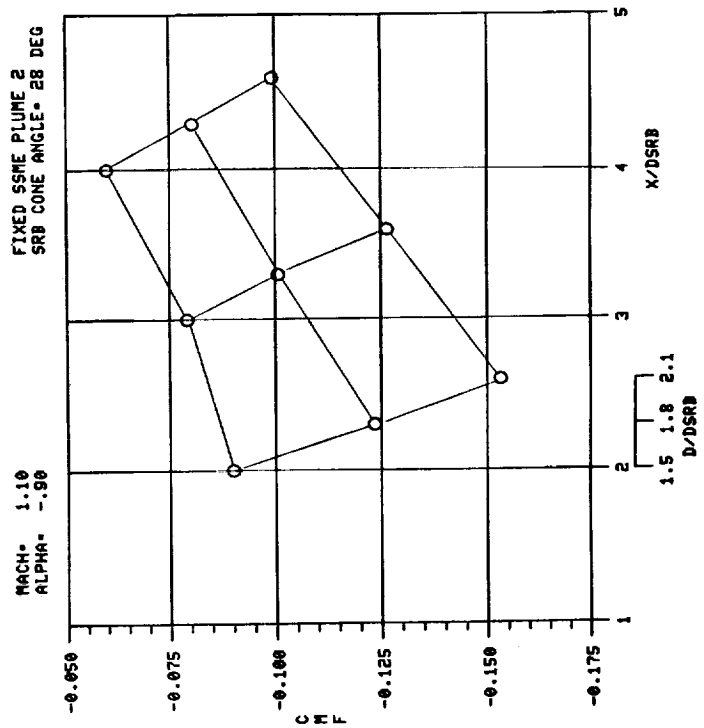
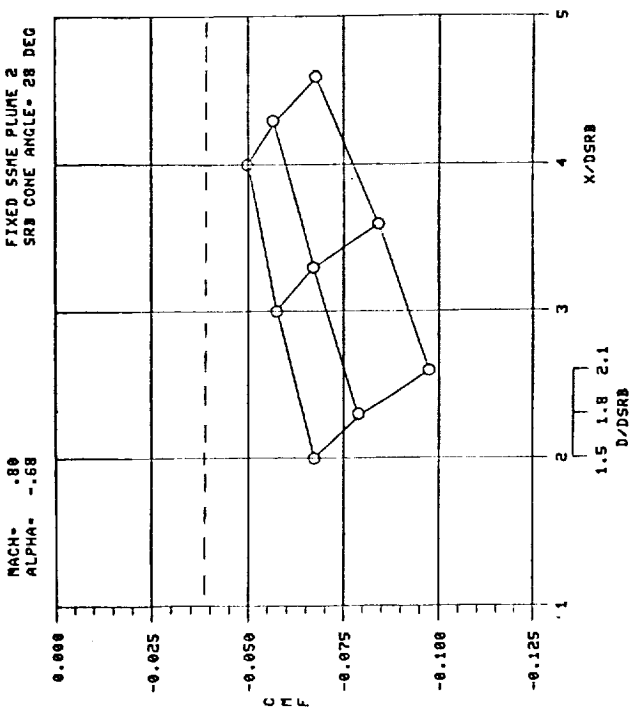
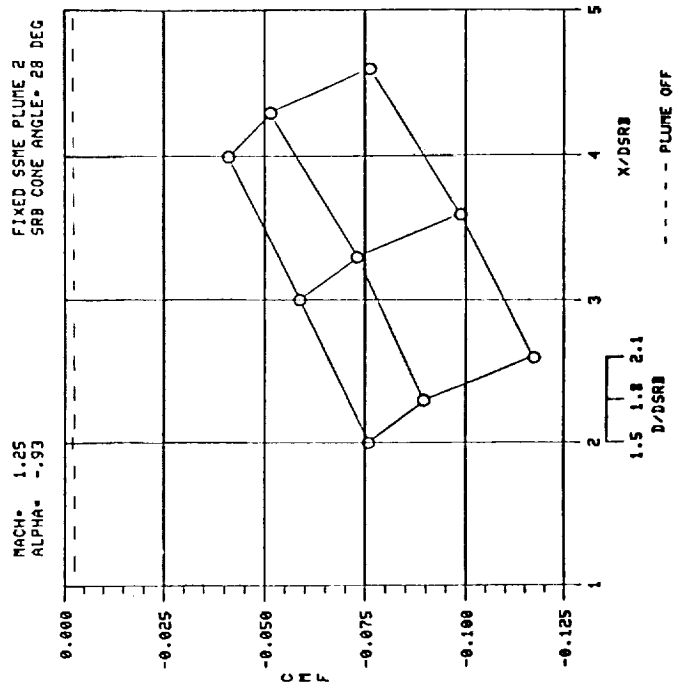
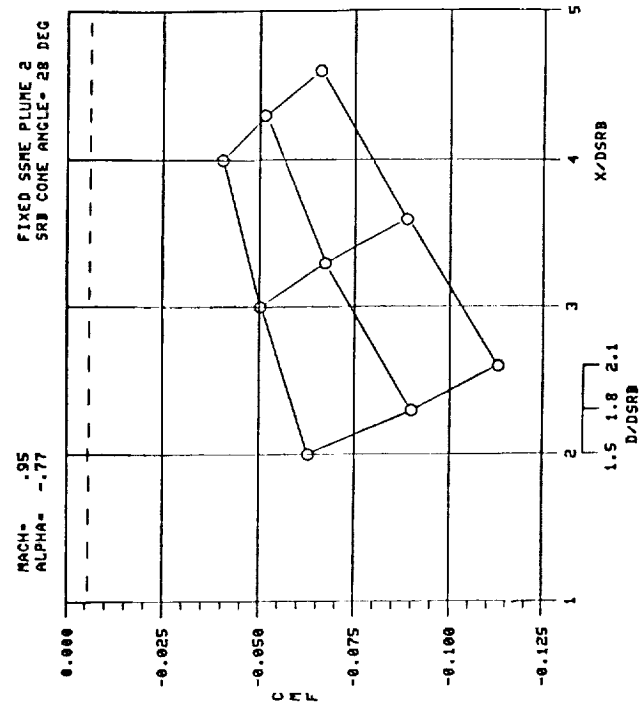


Figure F-5.

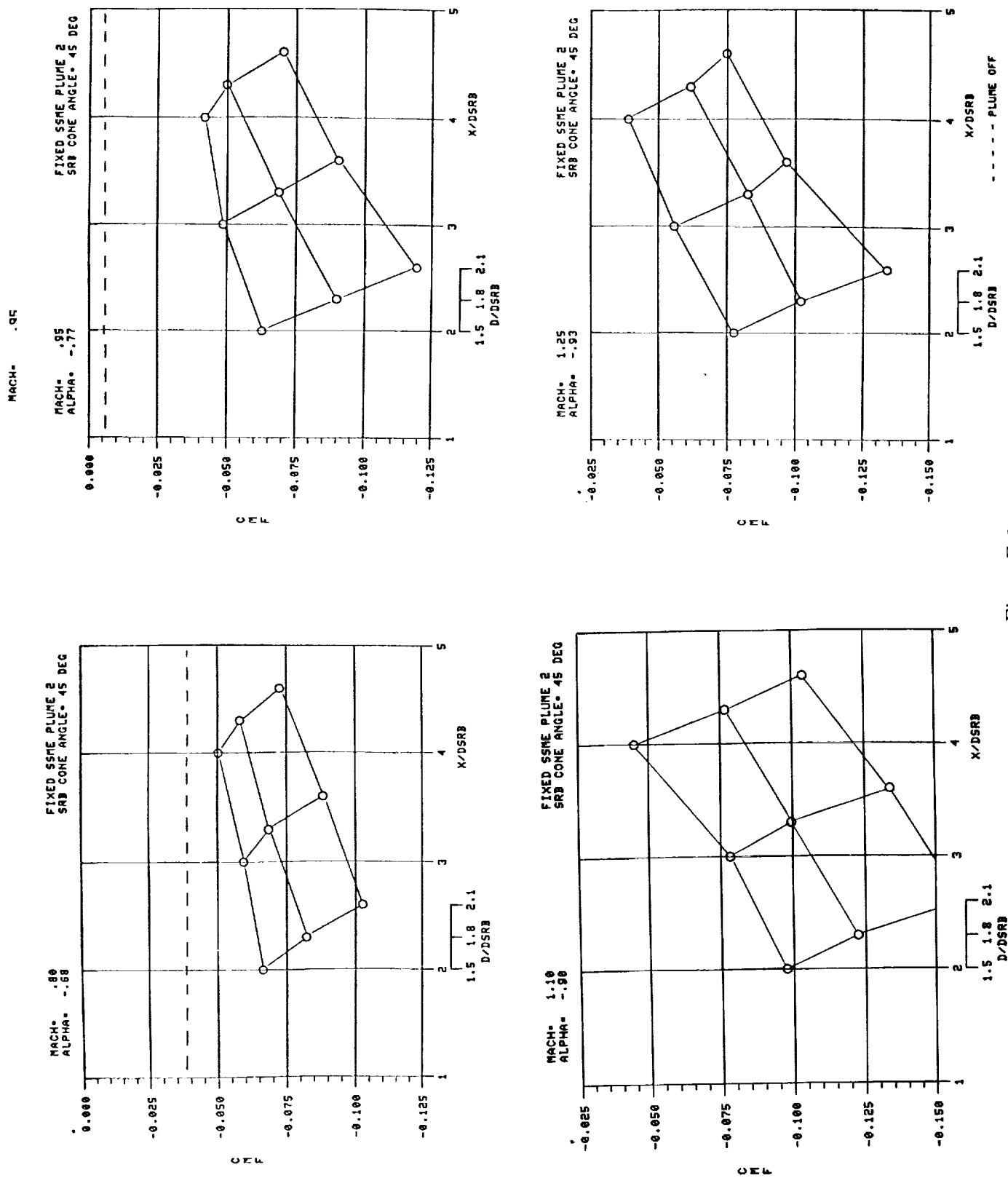


Figure F-6.

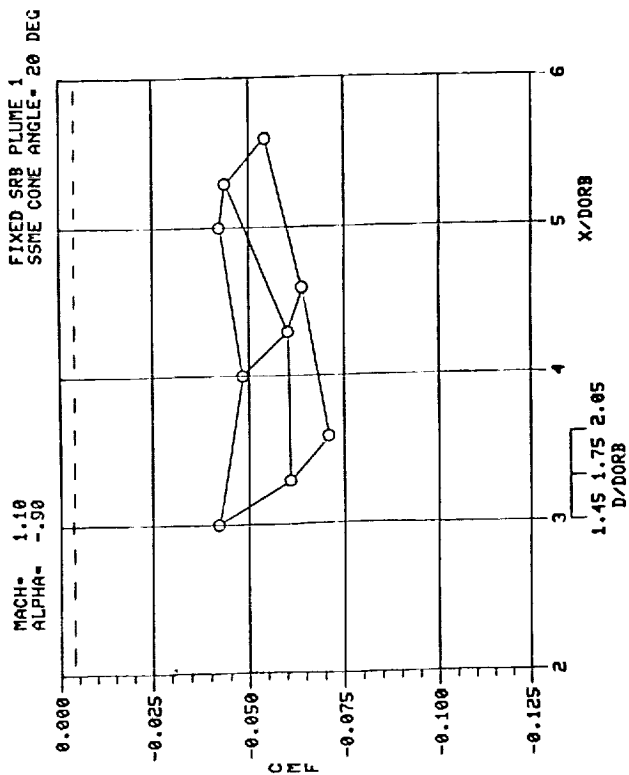
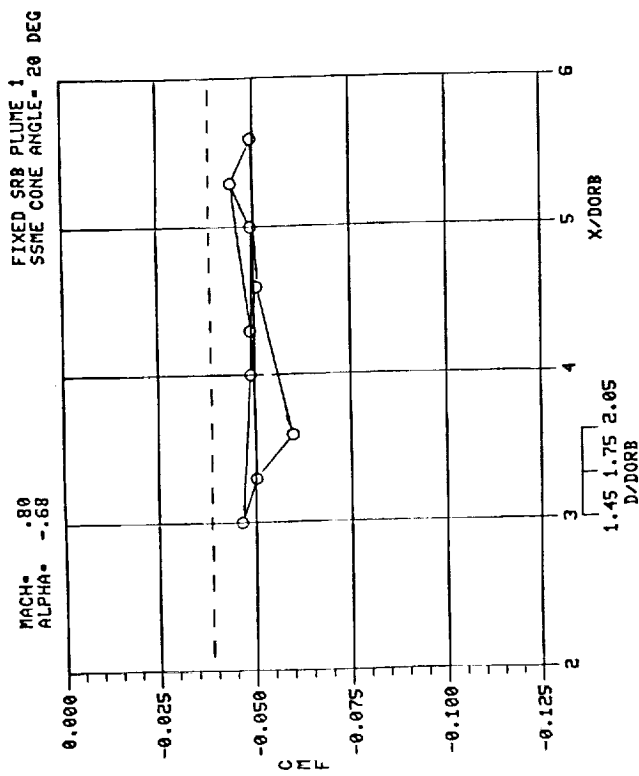
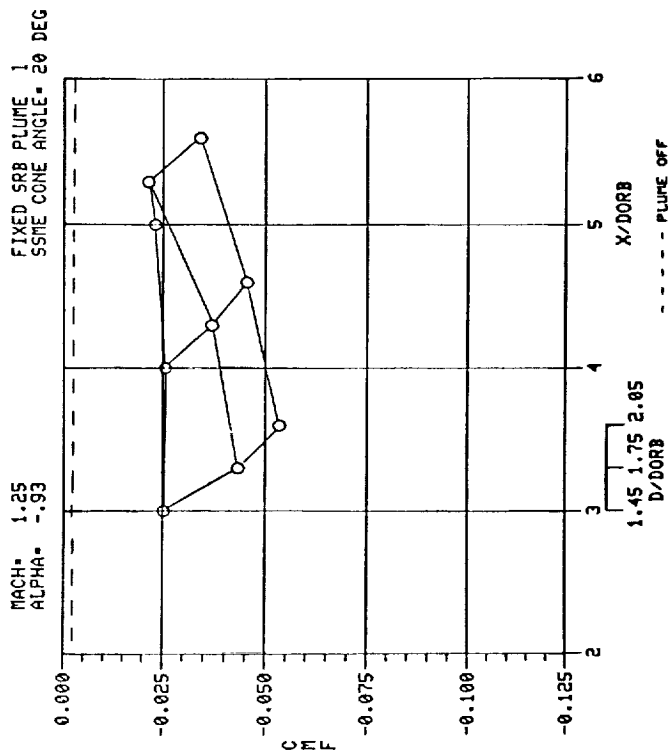
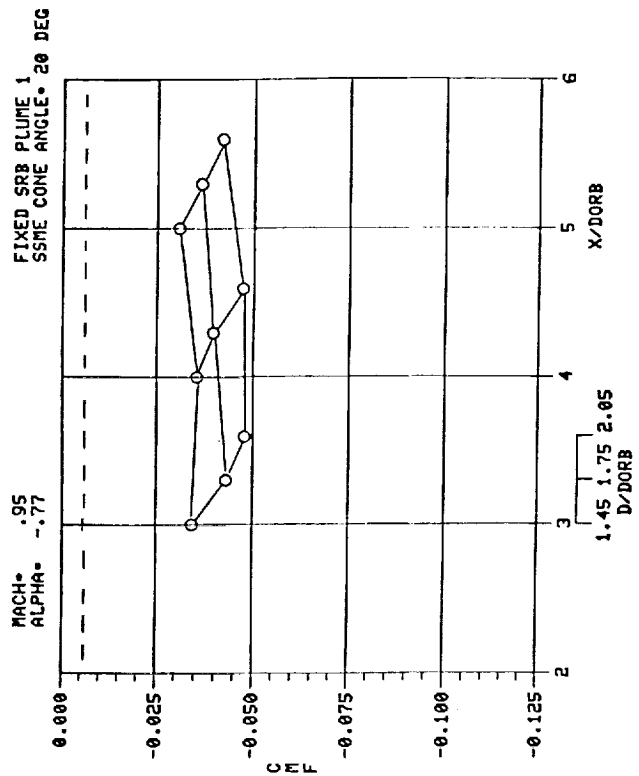


Figure F-7.

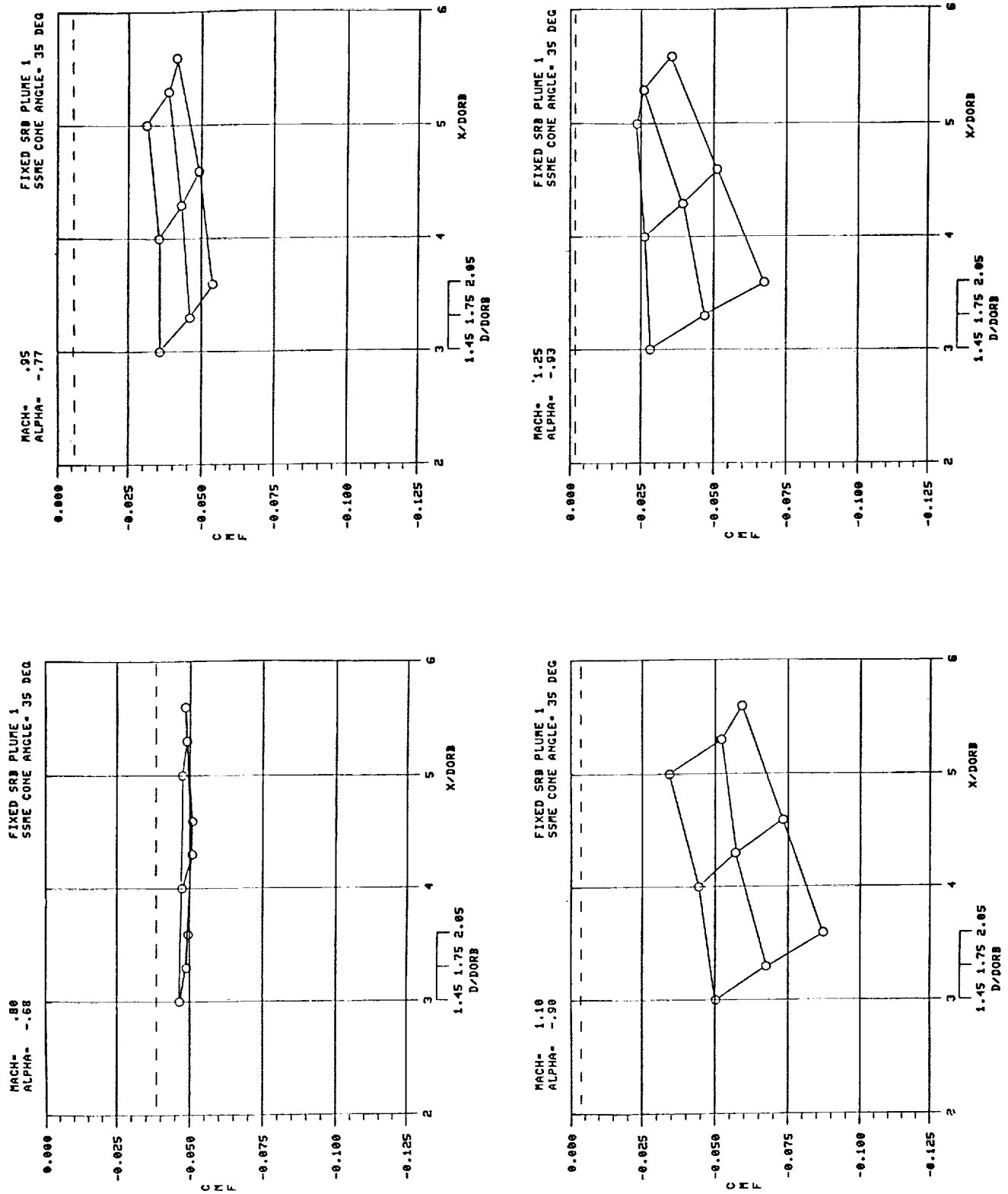


Figure F-8.

ORIGINAL PAGE IS
OF POOR QUALITY

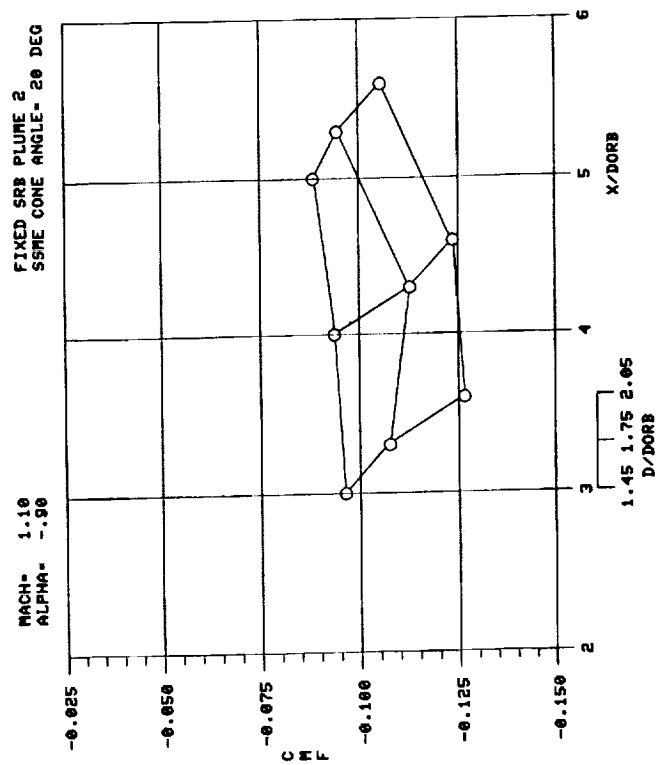
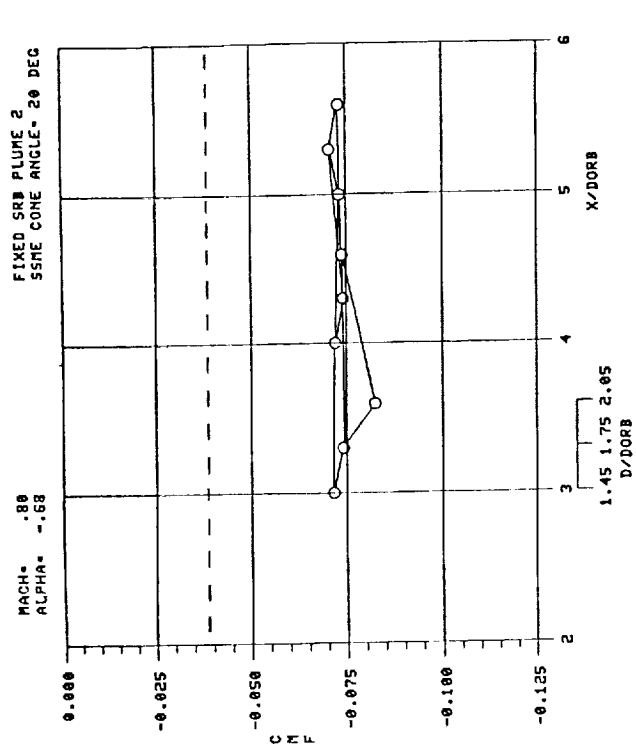
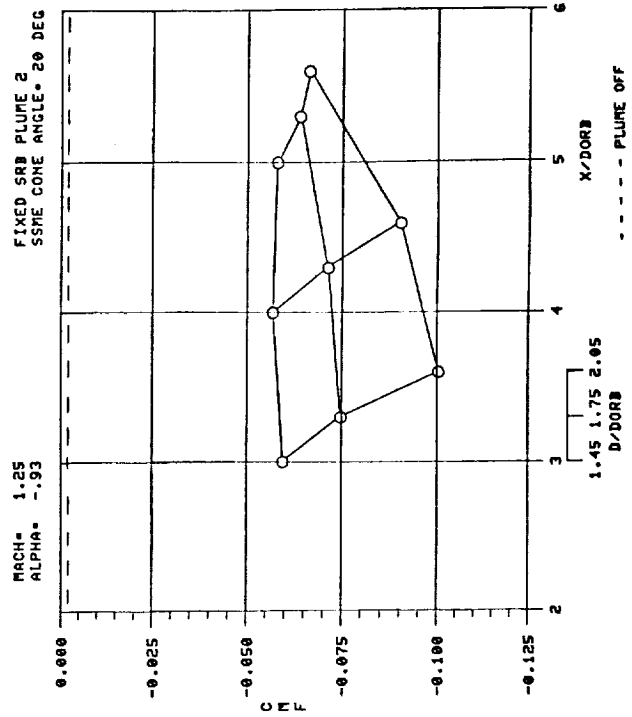
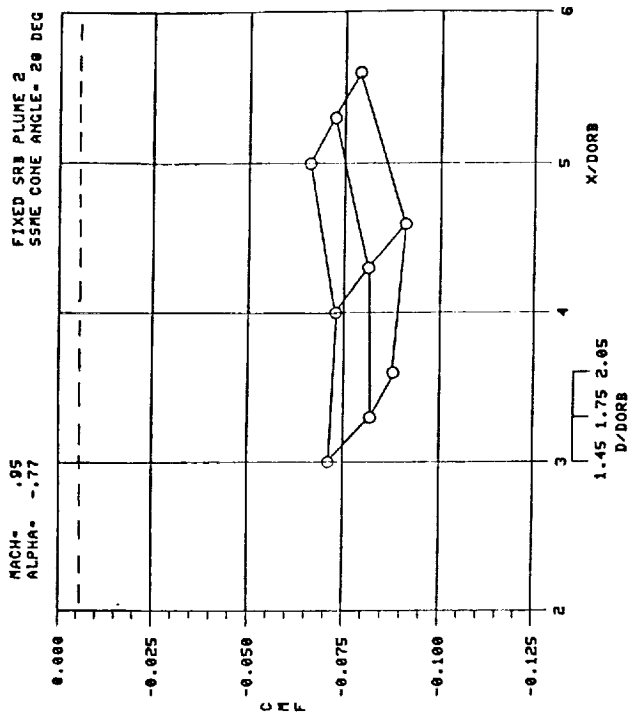


Figure F-9.

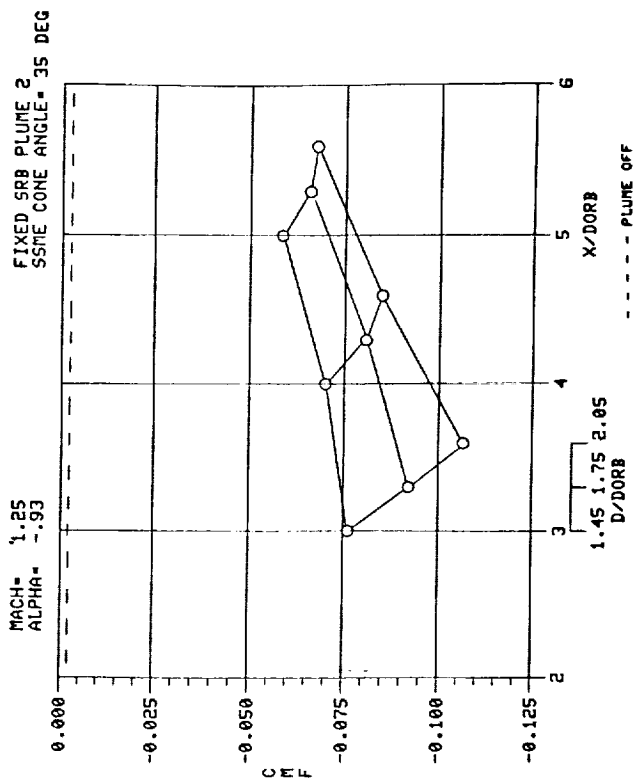
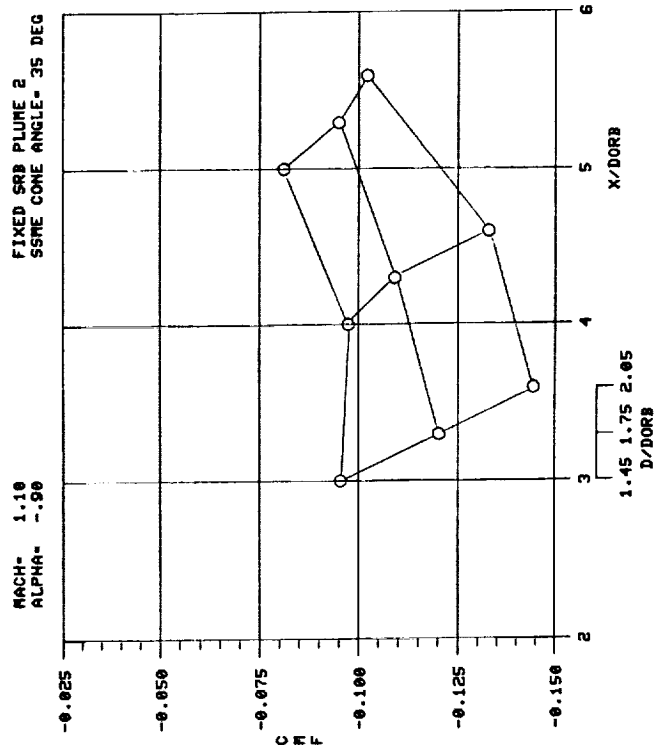
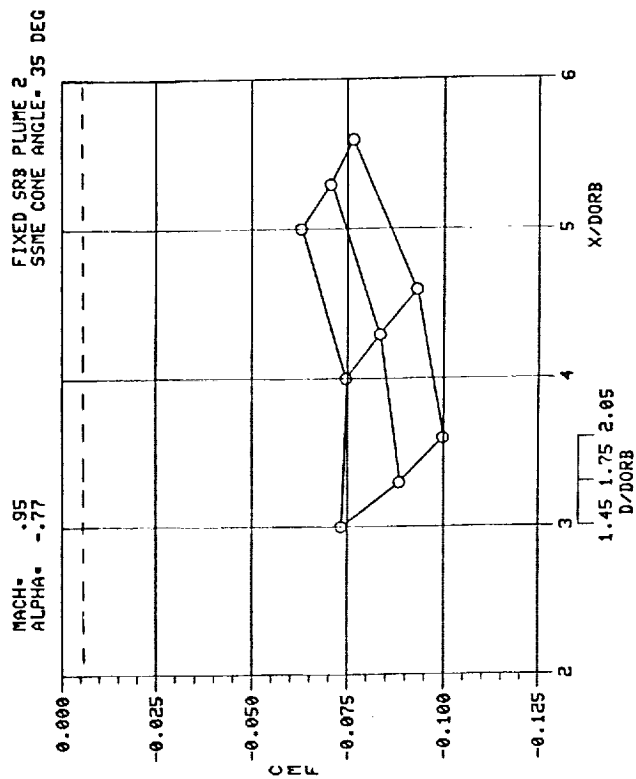
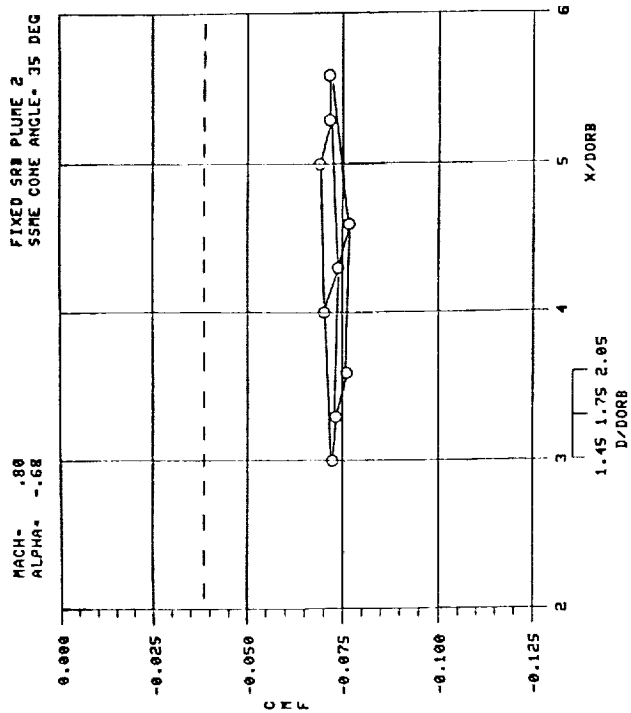


Figure F-10.

APPENDIX G



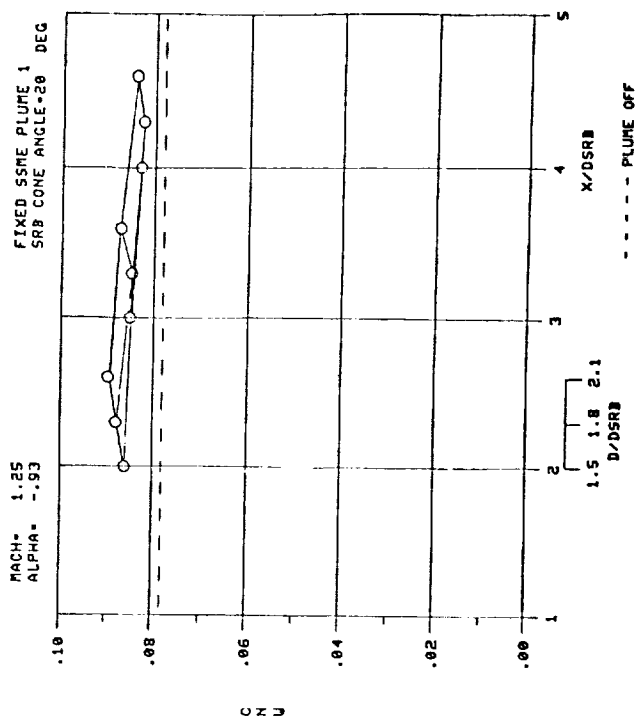
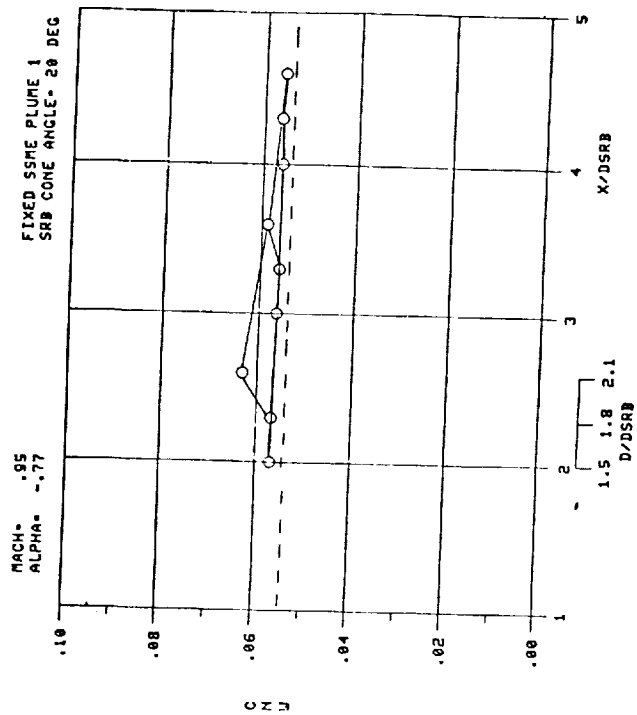
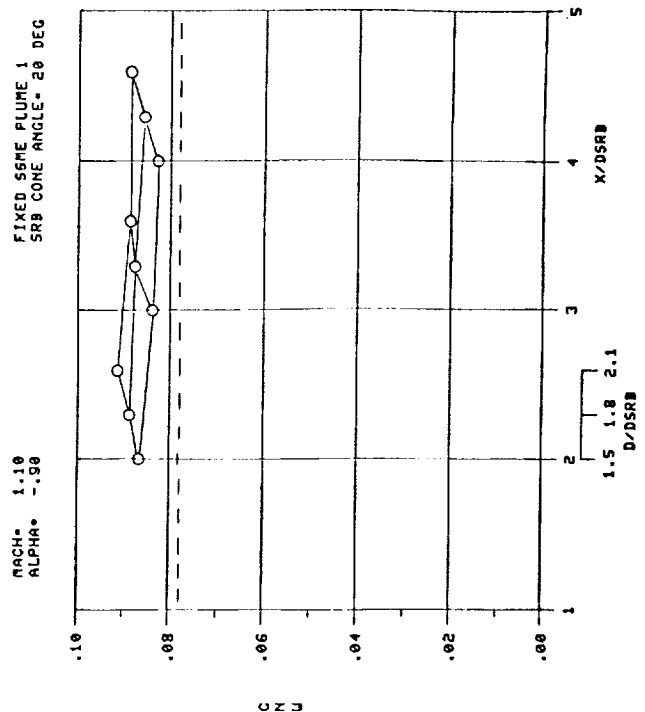
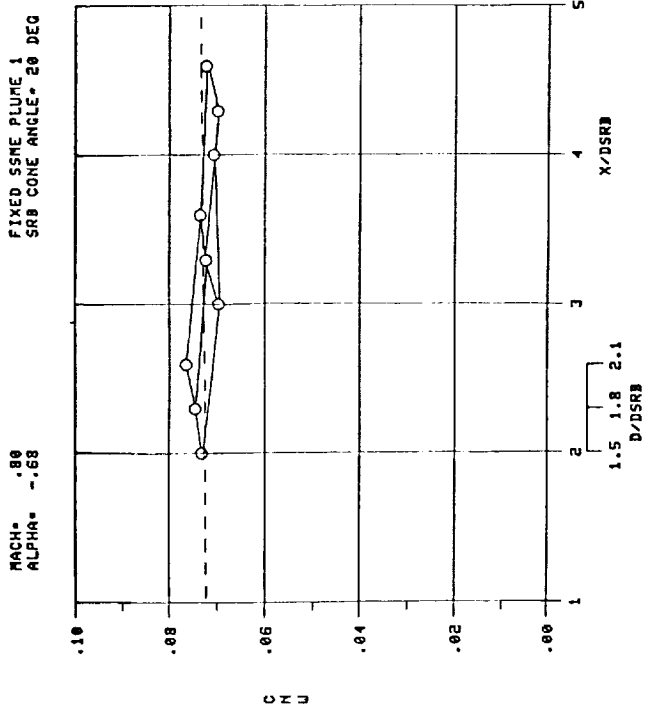


Figure G-1.

PRECEDING PAGE BLANK NOT FILMED

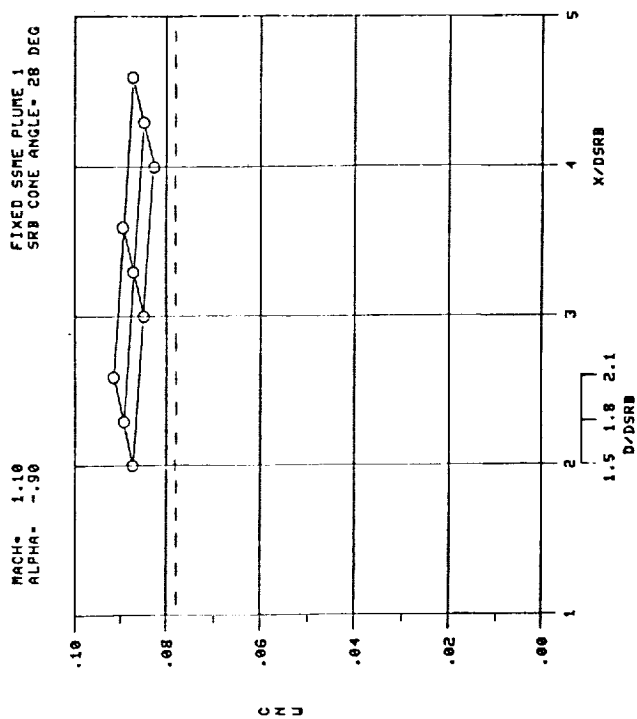
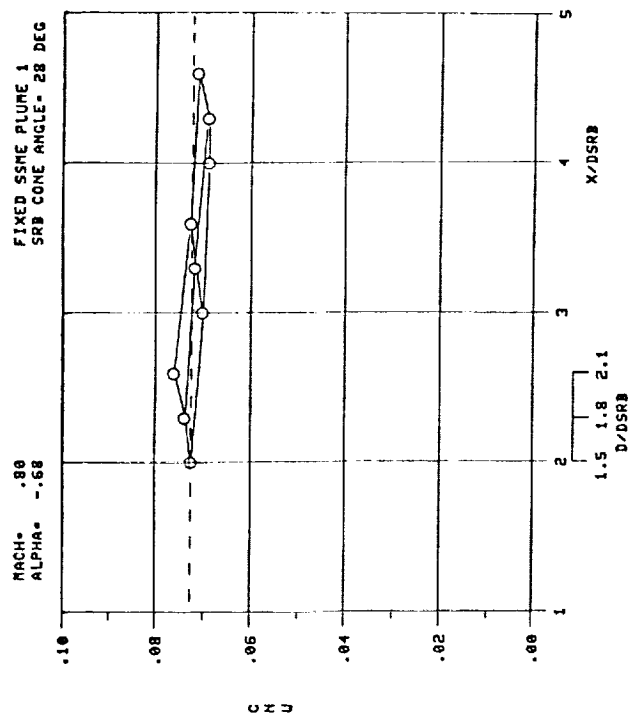
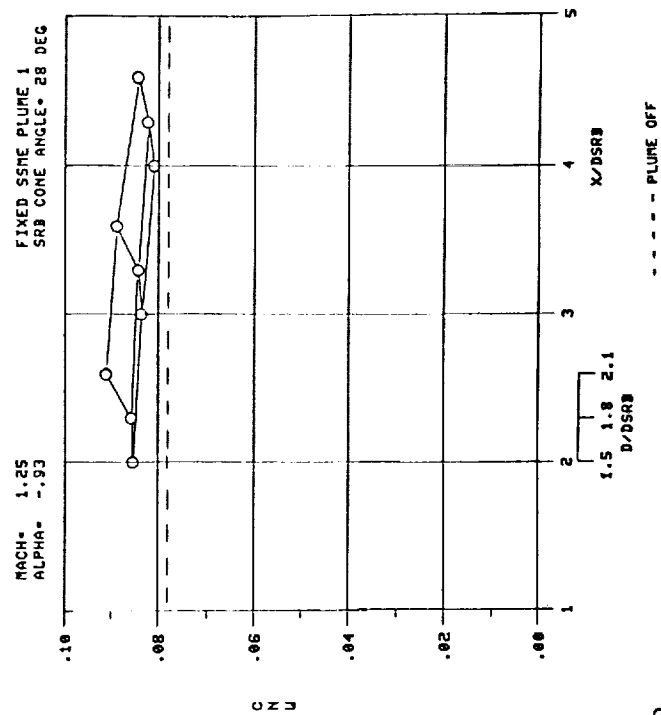
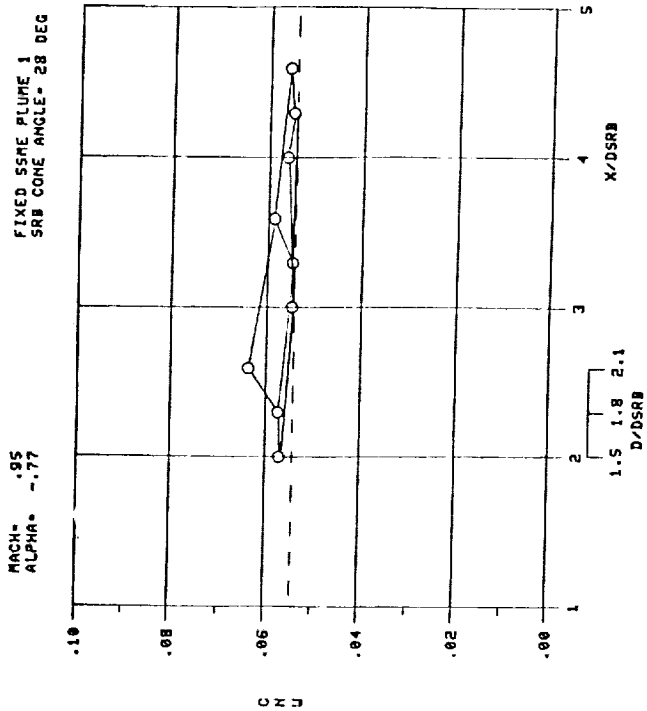


Figure G-2.

ORIGINAL PAGE IS
OF POOR QUALITY

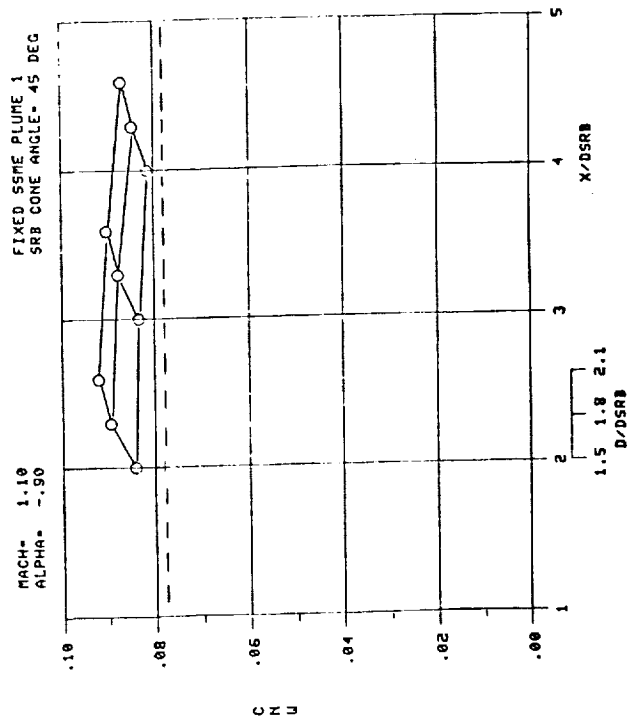
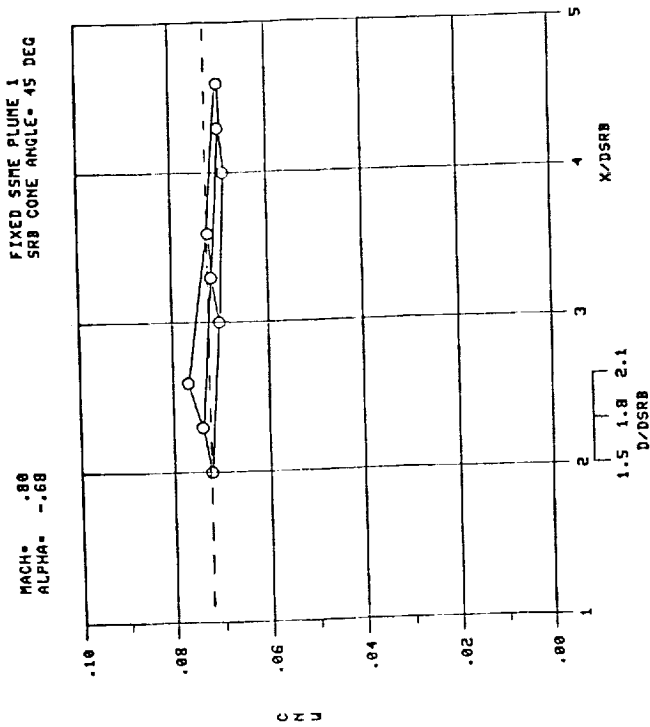
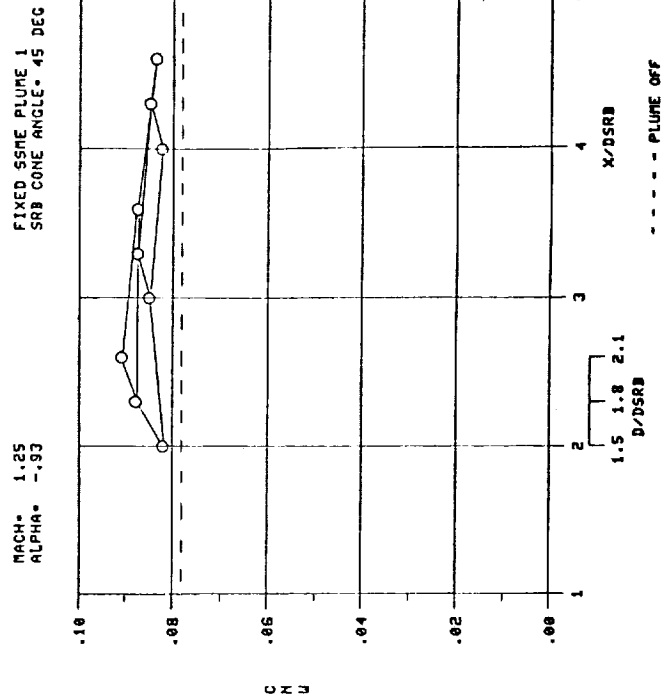
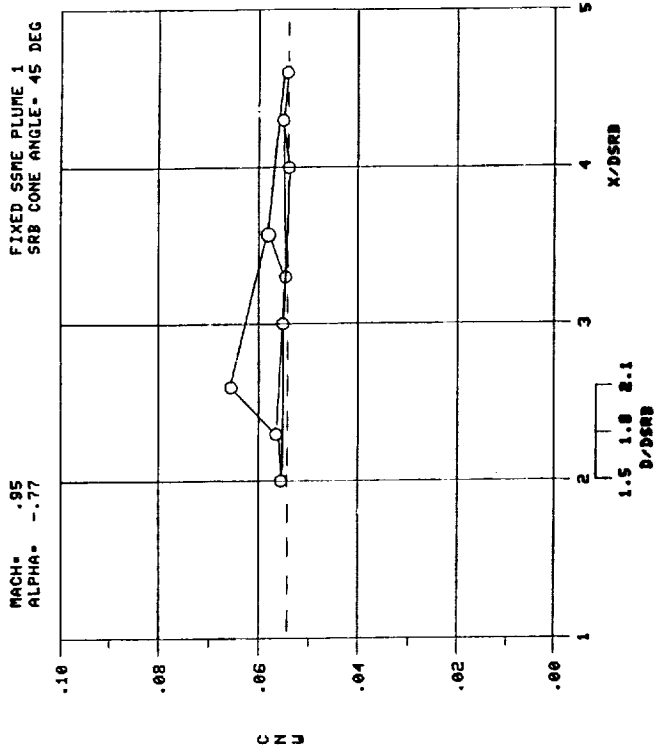


Figure G-3.

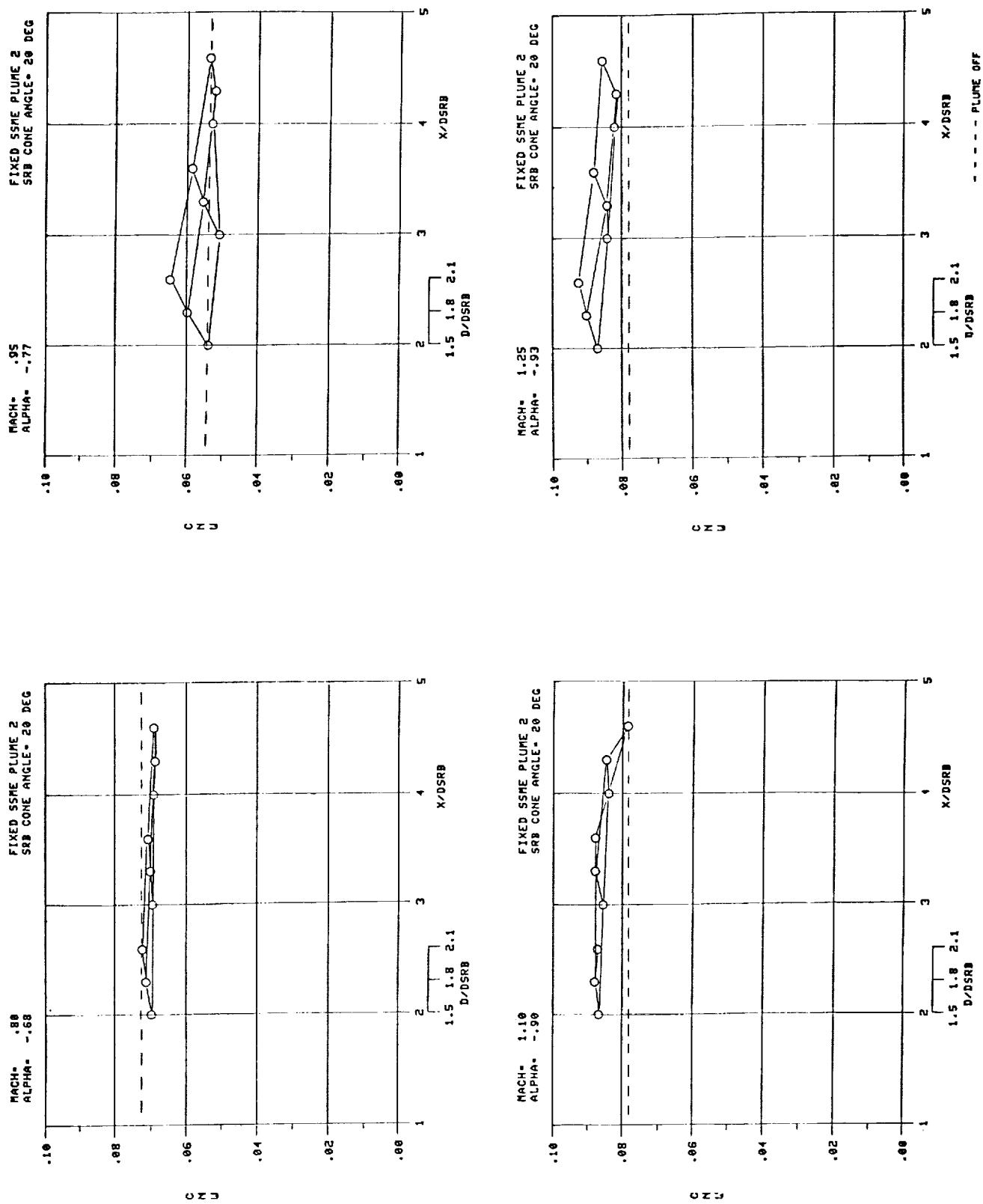


Figure G-4.

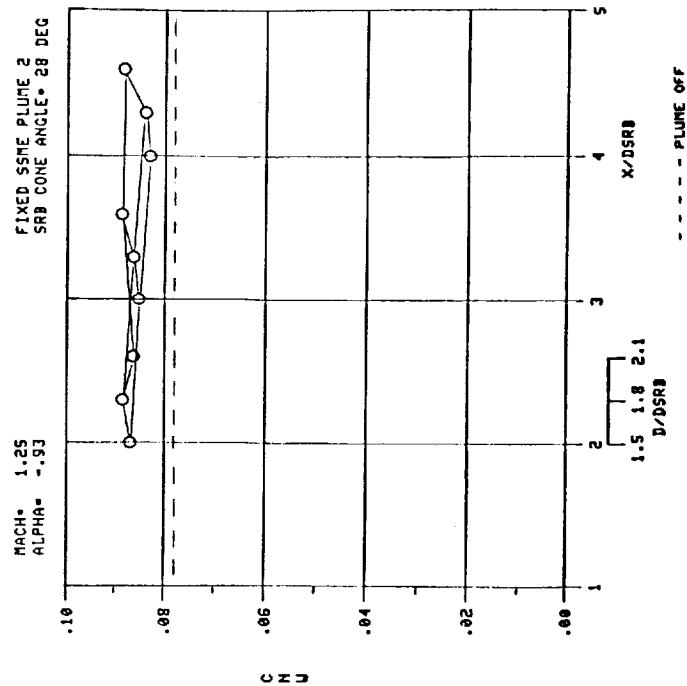
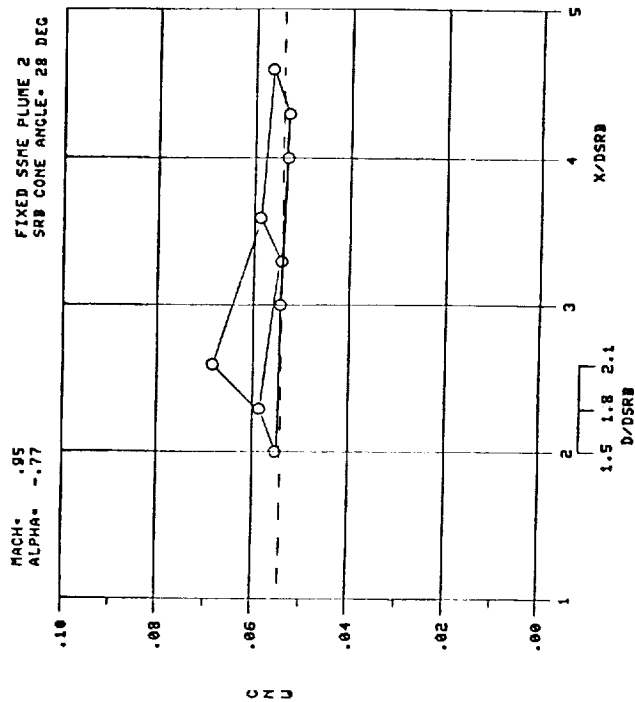
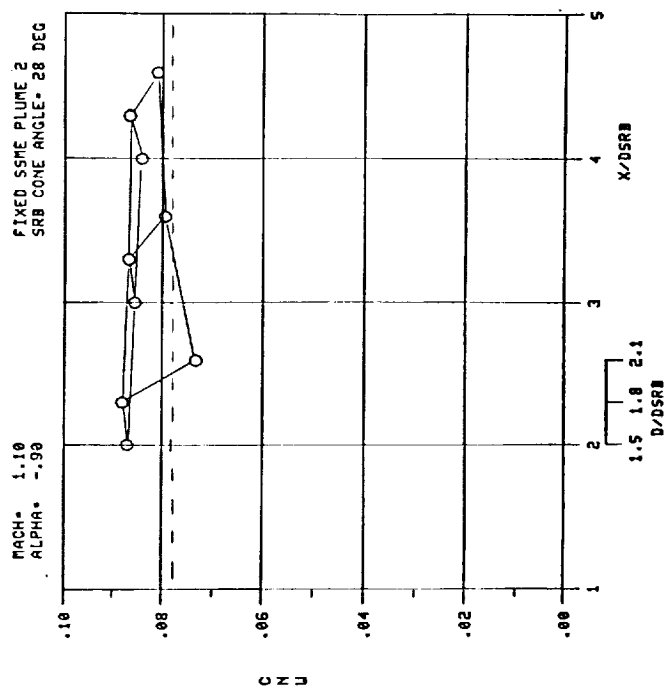
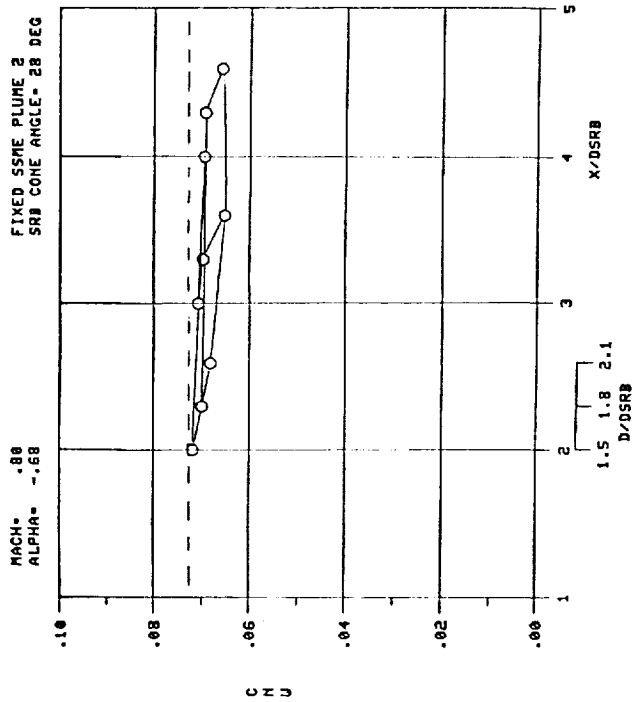


Figure G-5.

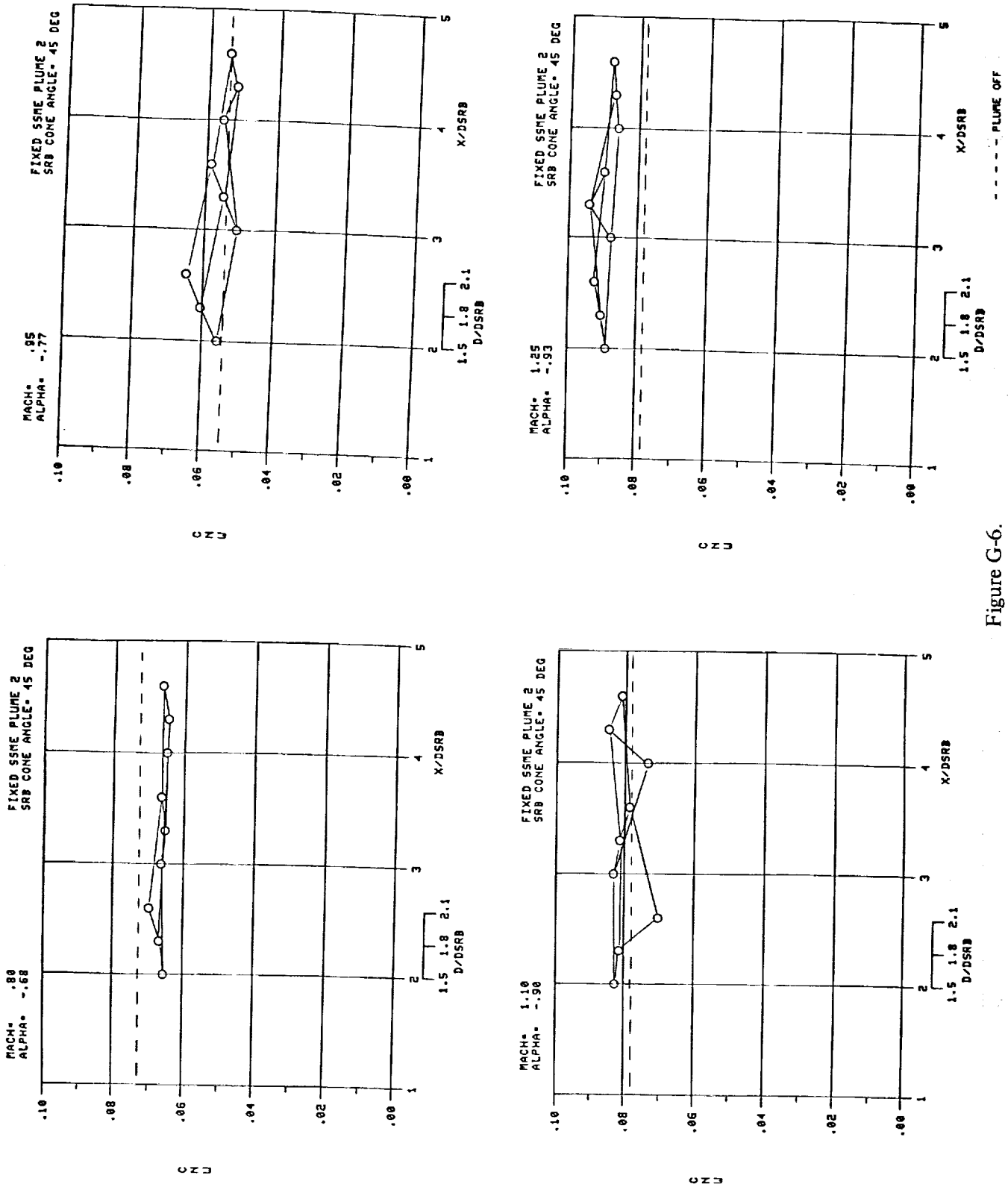


Figure G-6.

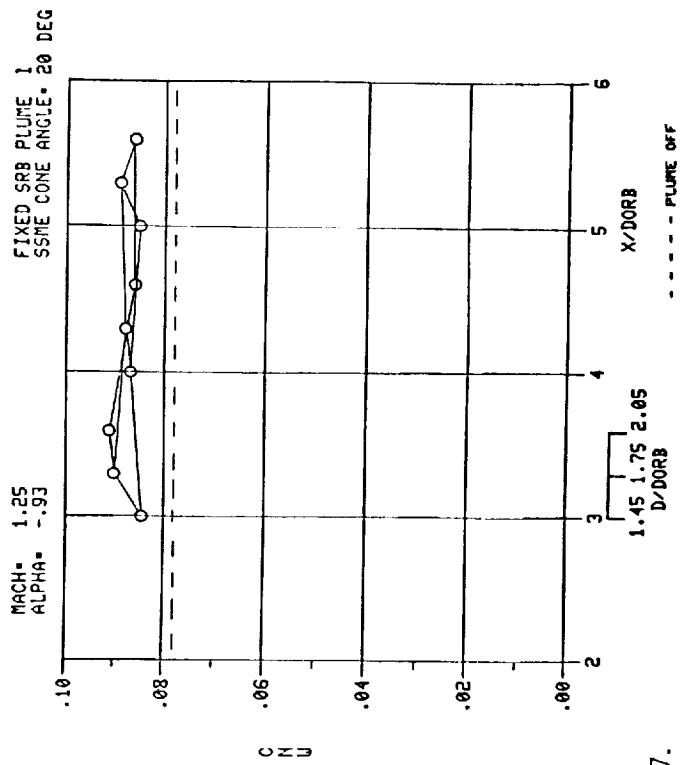
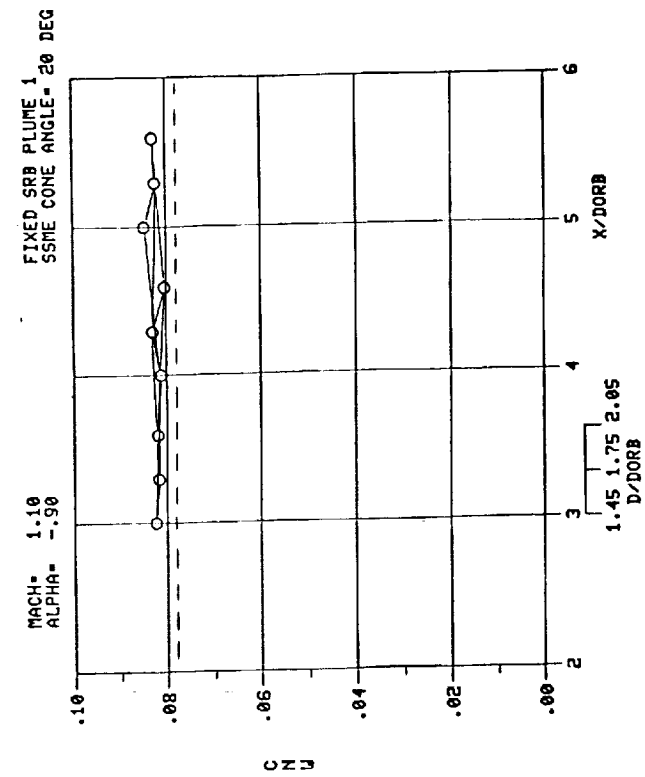
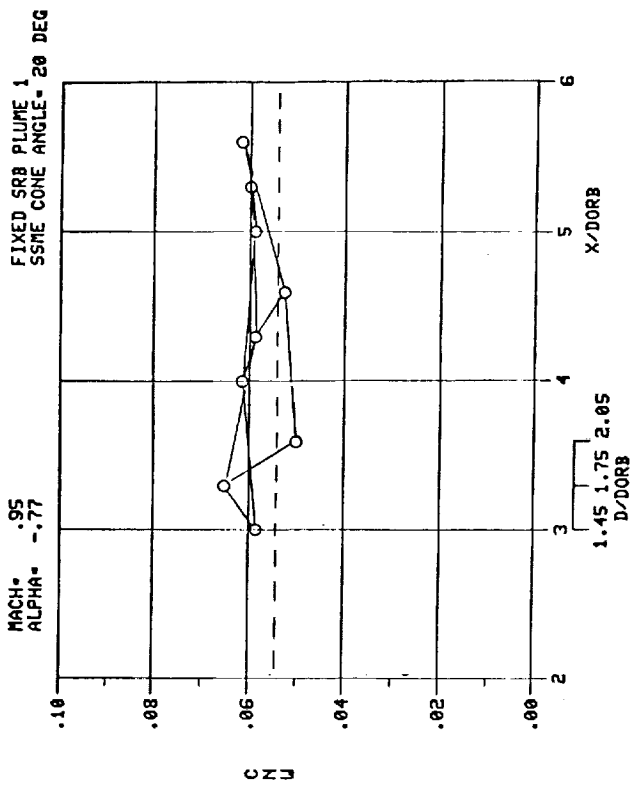
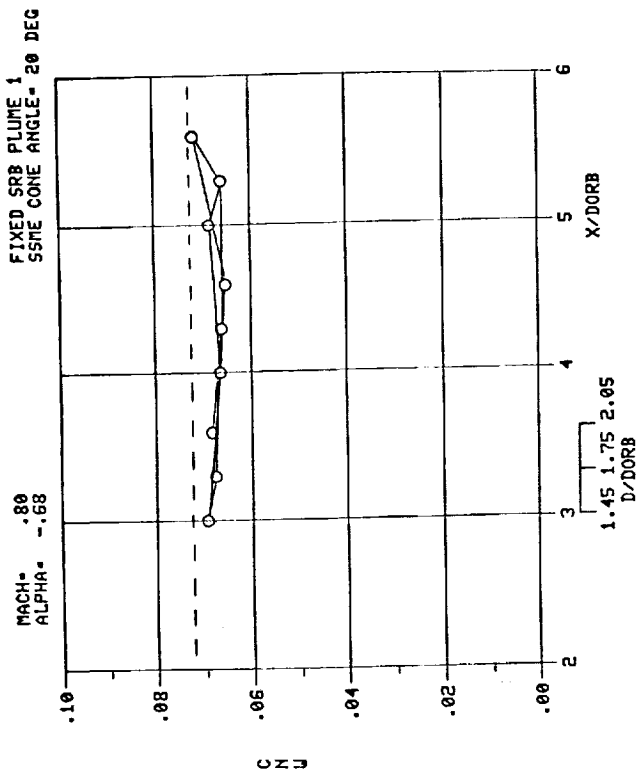


Figure G-7.

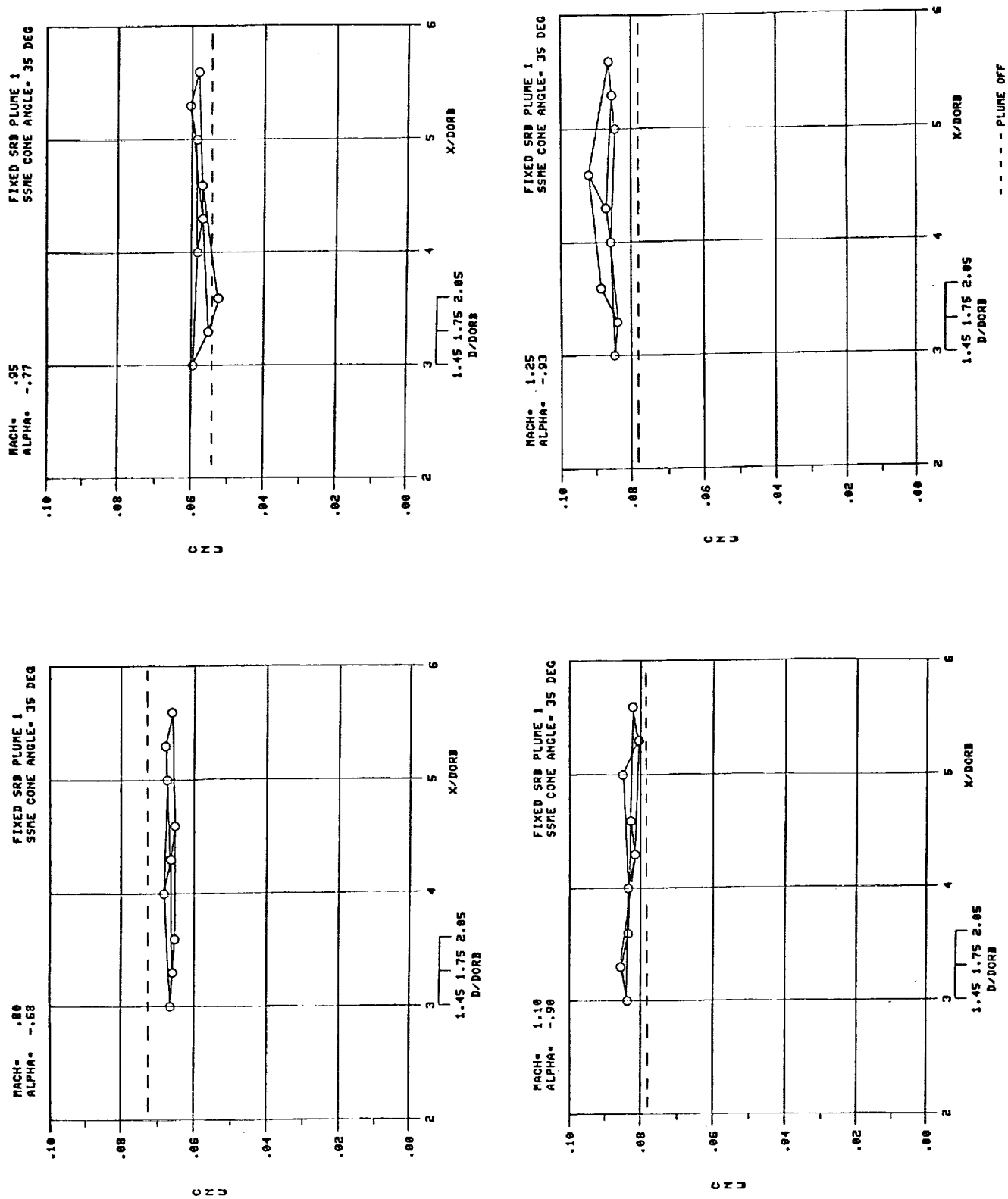


Figure G-8.

ORIGINAL PAGE IS
OF POOR QUALITY

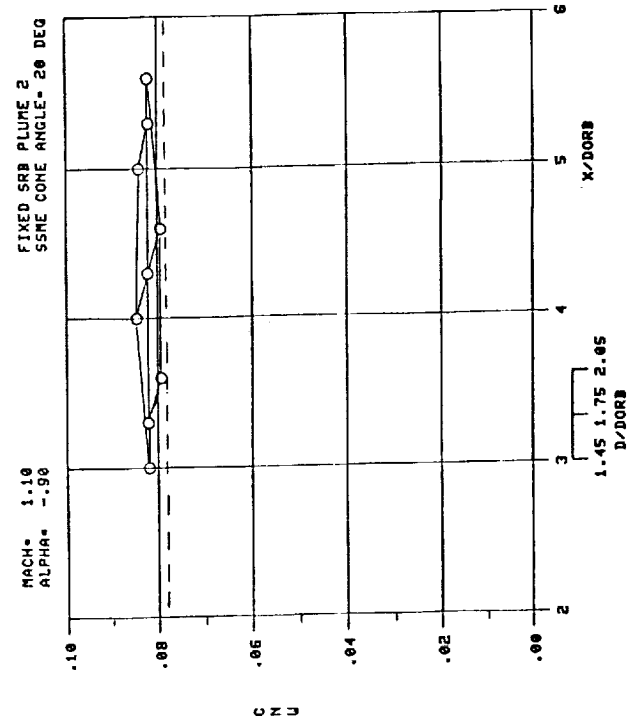
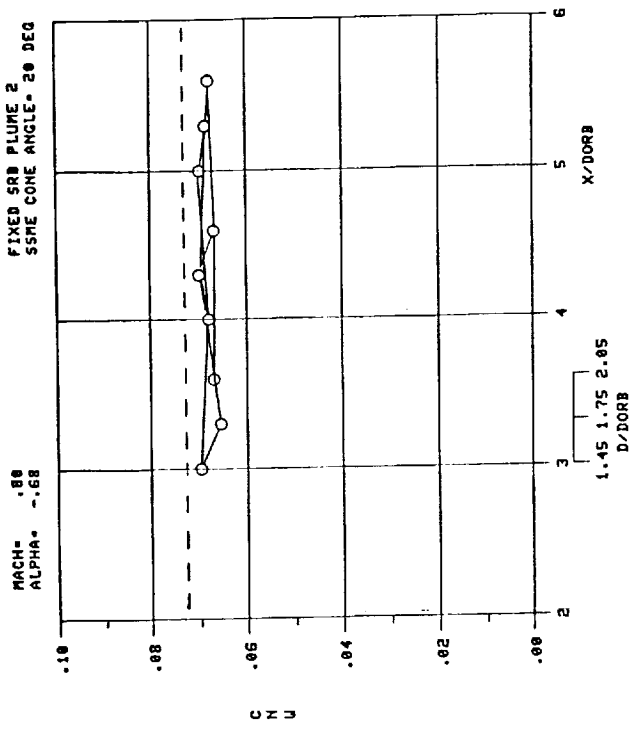
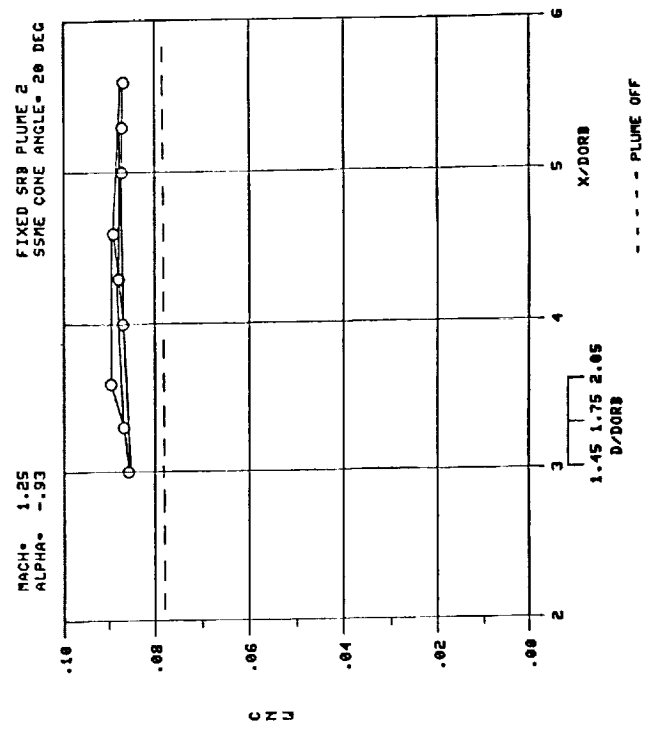
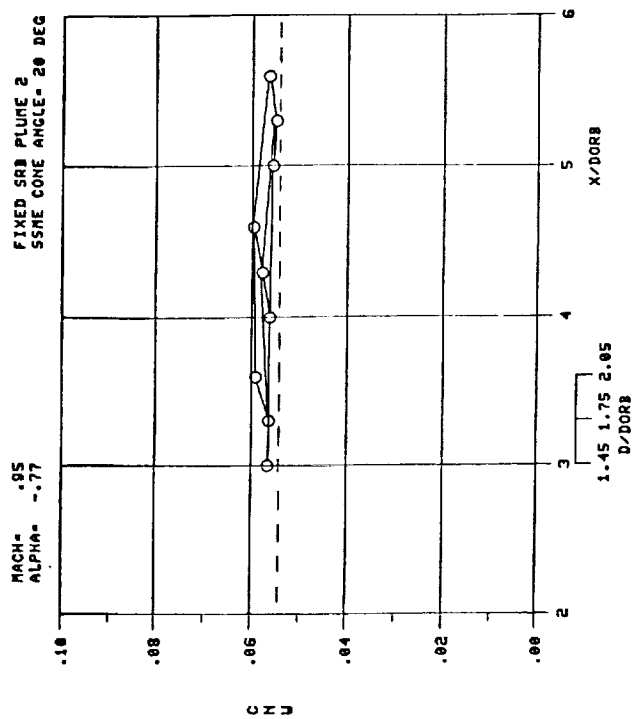


Figure G-9.

C-2

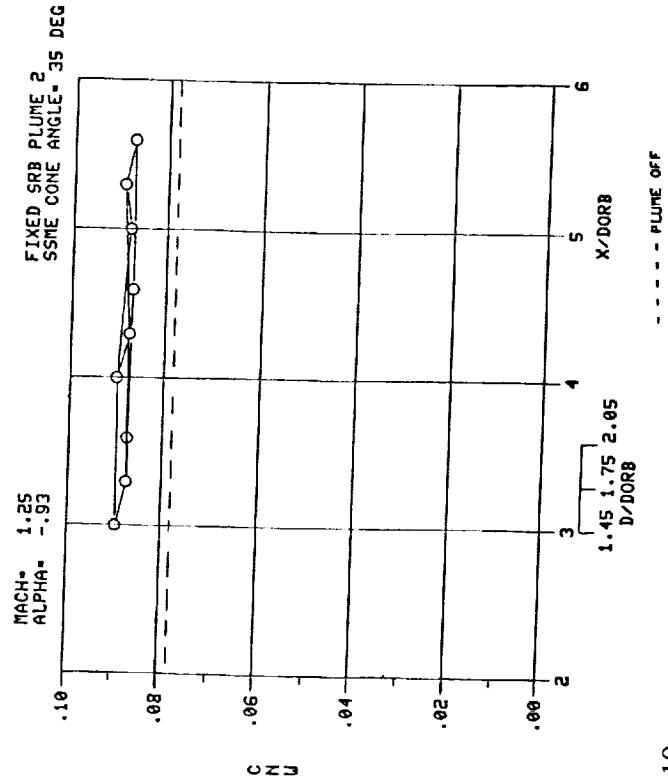
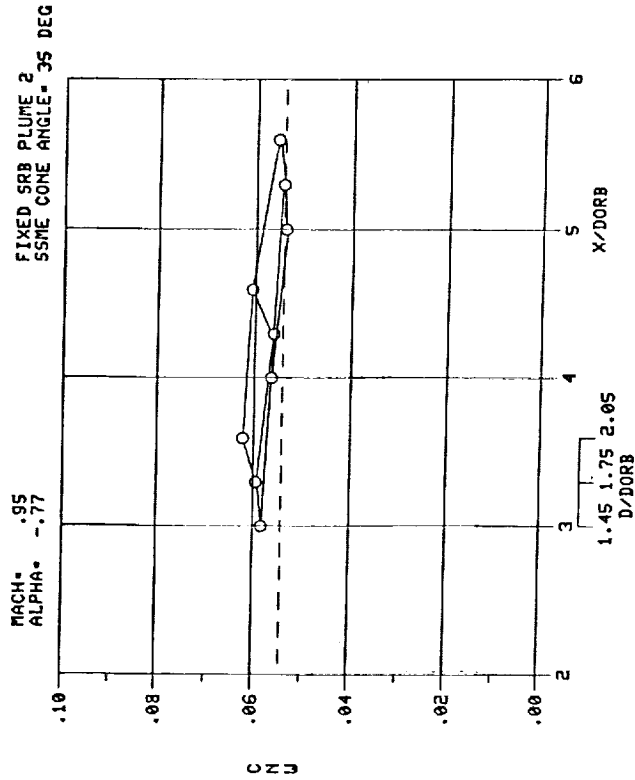
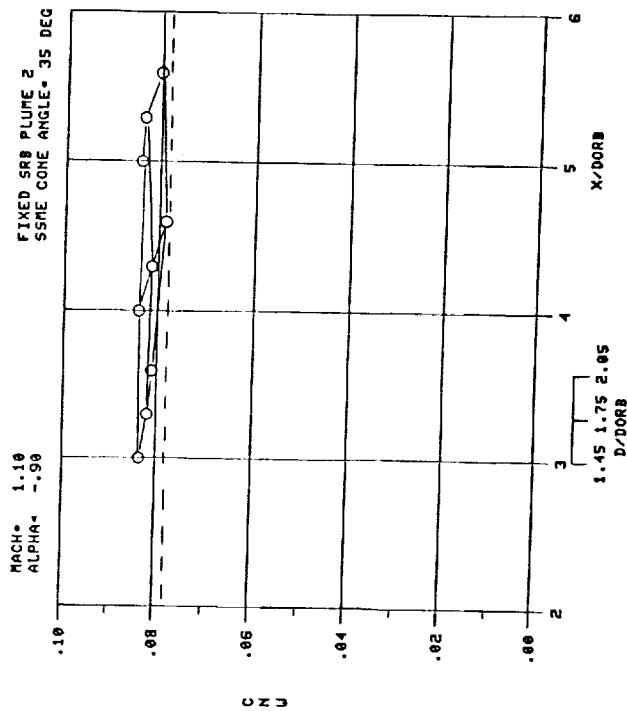
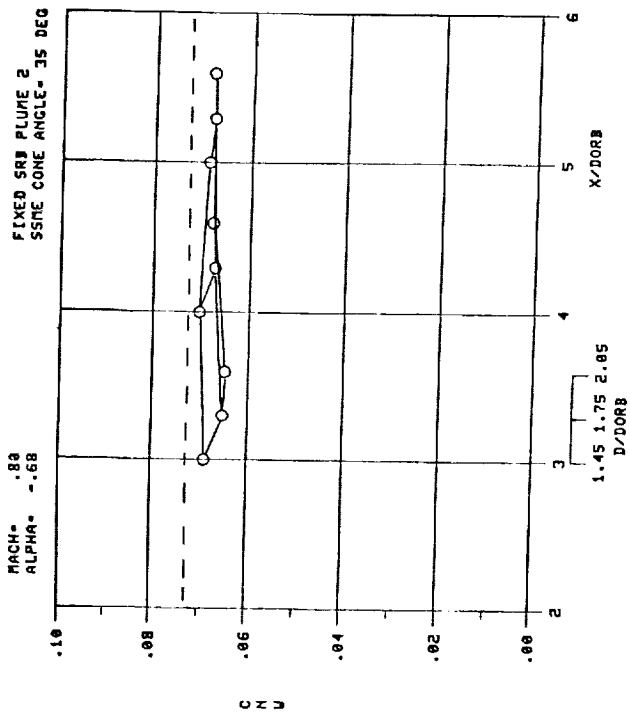


Figure G-10.

APPENDIX H

1-1

1-1

1-1

1-1

1-1

1-1

1-1

1-1

1-1

1-1

1-1

1-1

1-1

1-1

1-1



ORIGINAL PAGE IS
OF POOR QUALITY

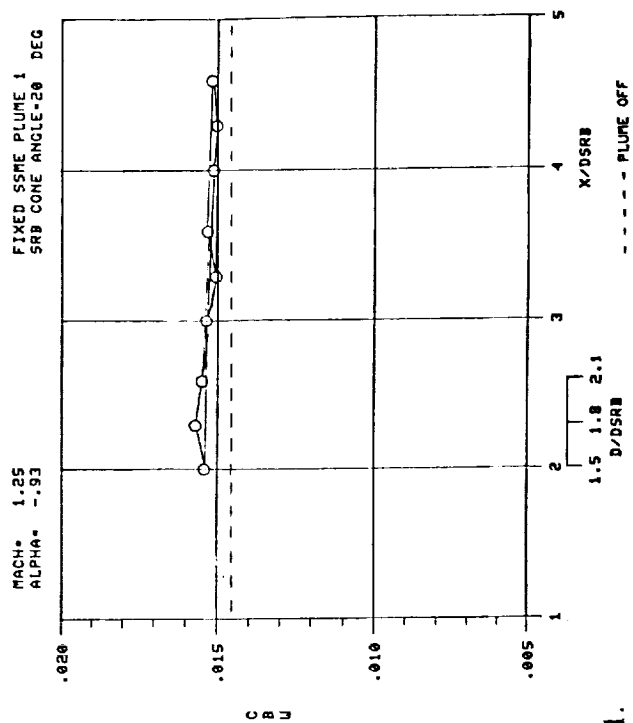
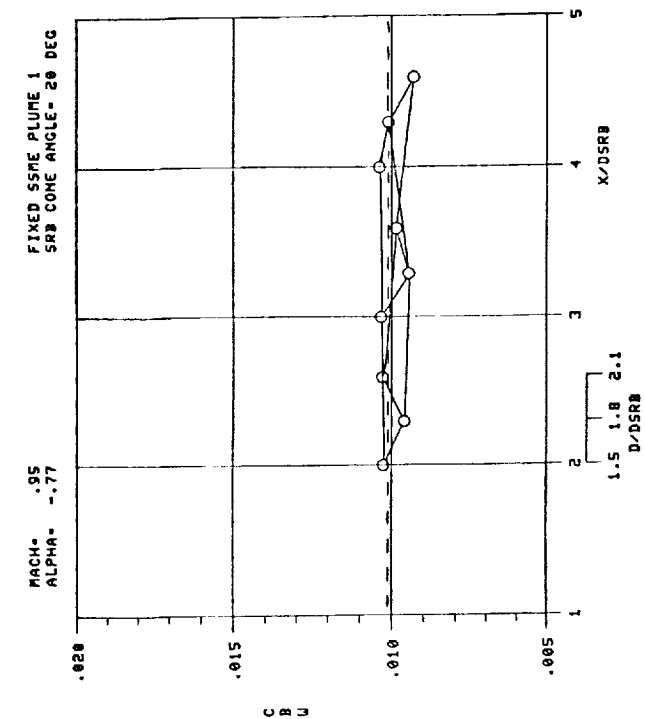
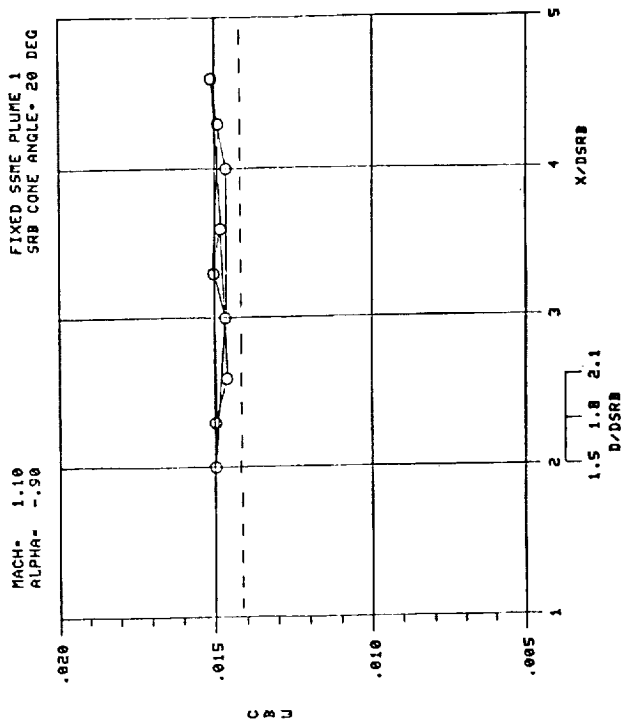
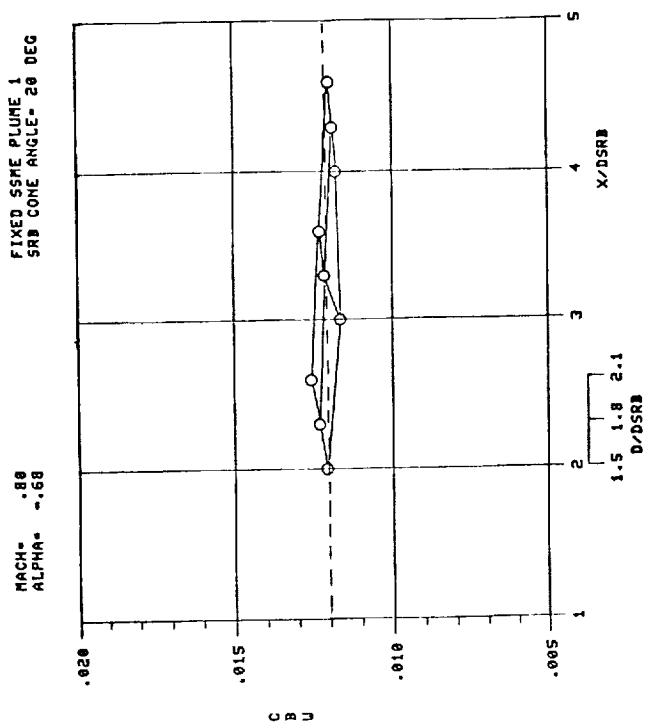


Figure H-1.



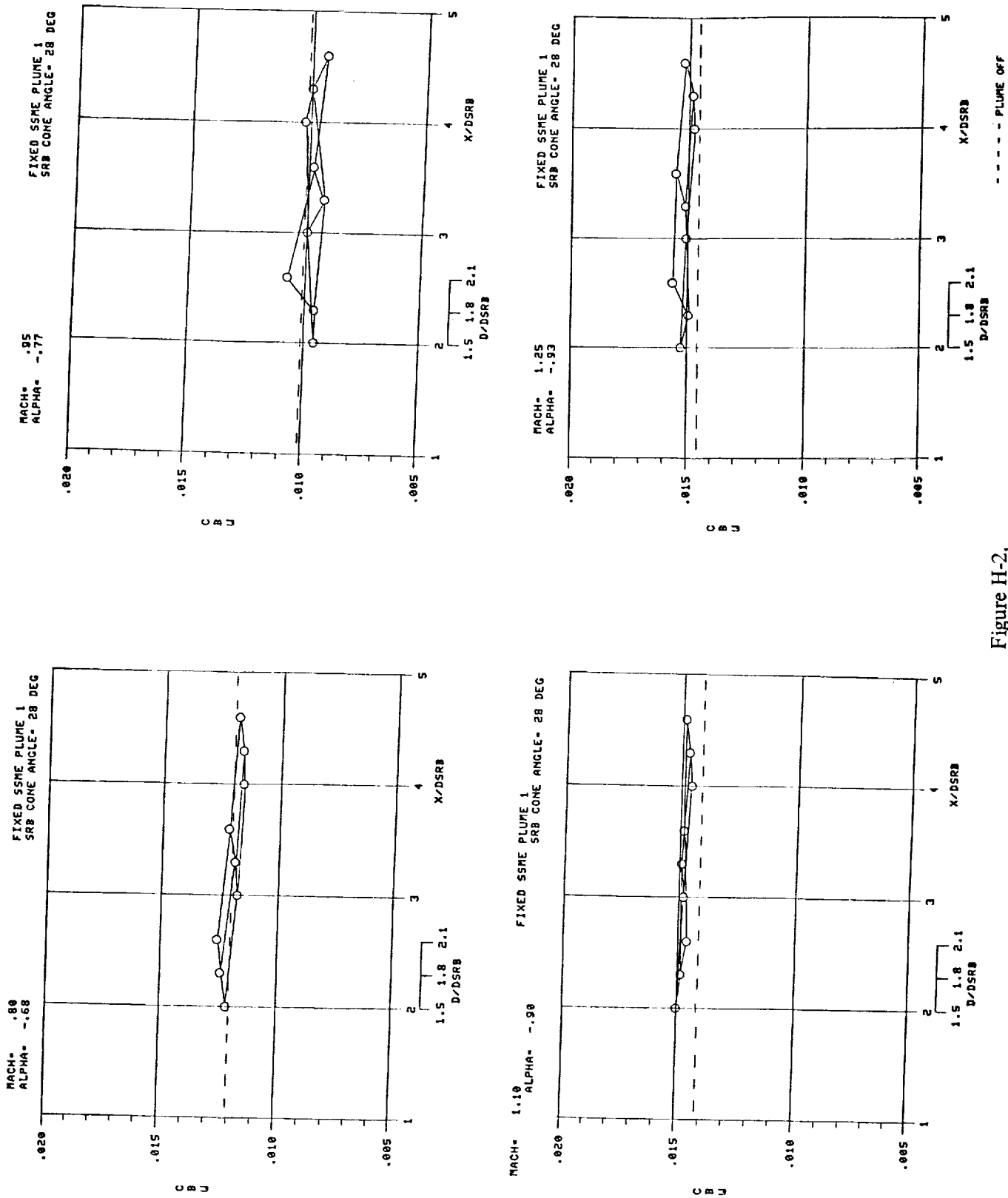


Figure H-2.

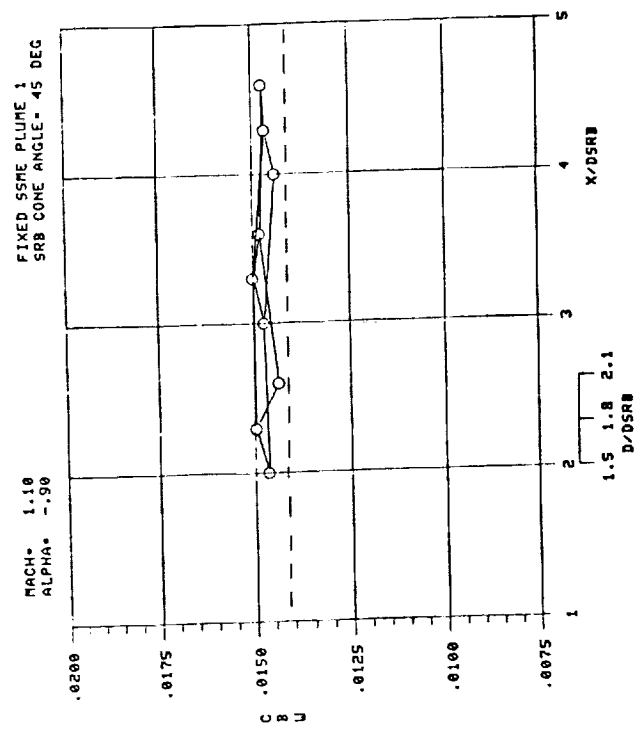
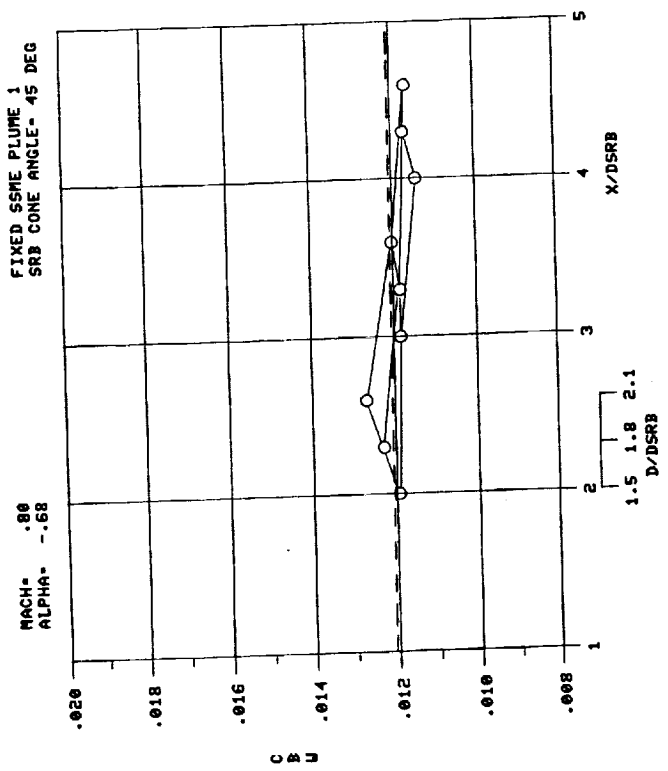
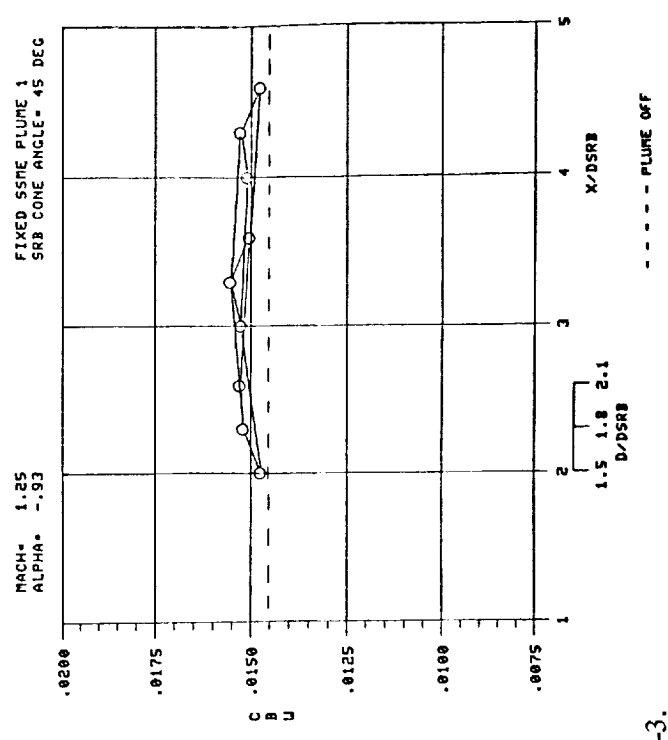
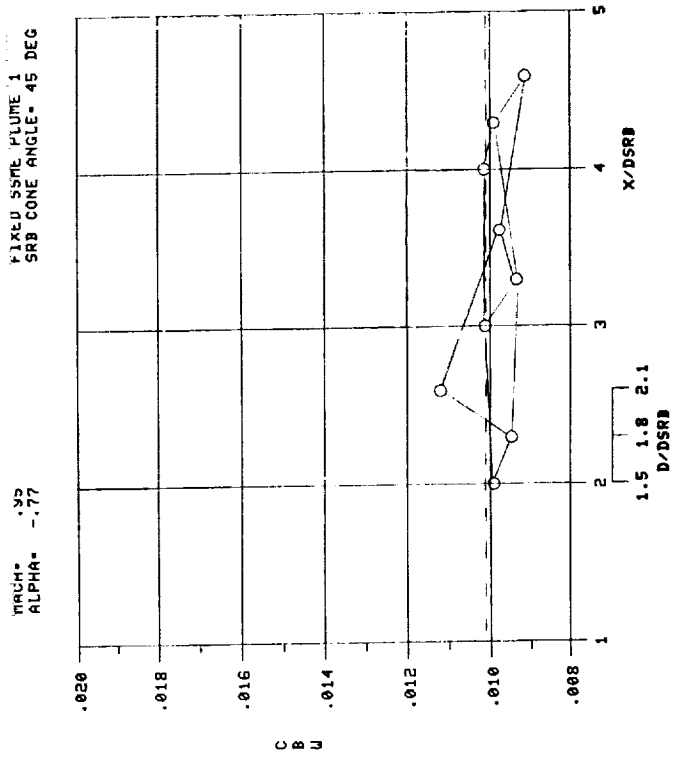


Figure H-3.

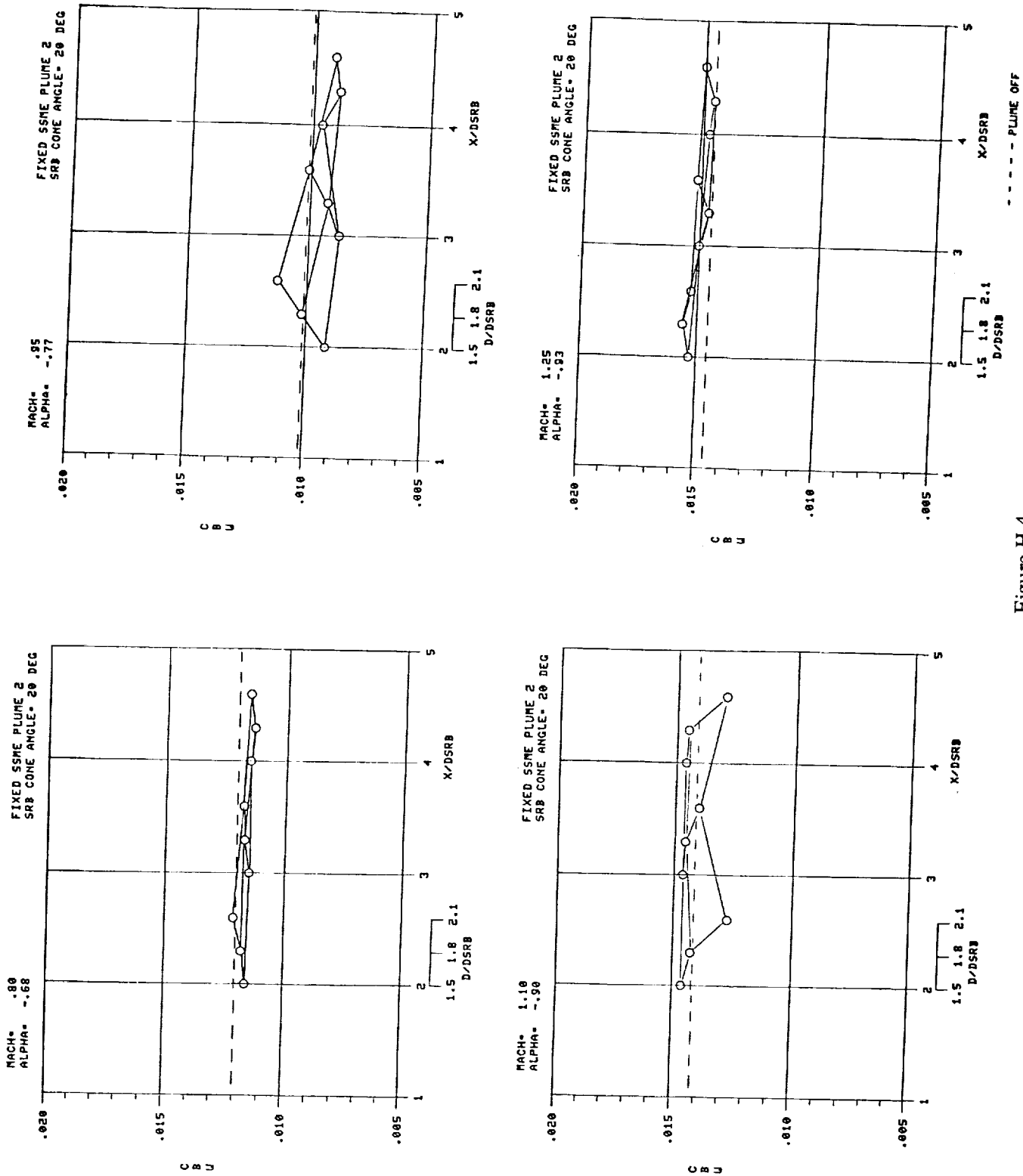


Figure H-4.

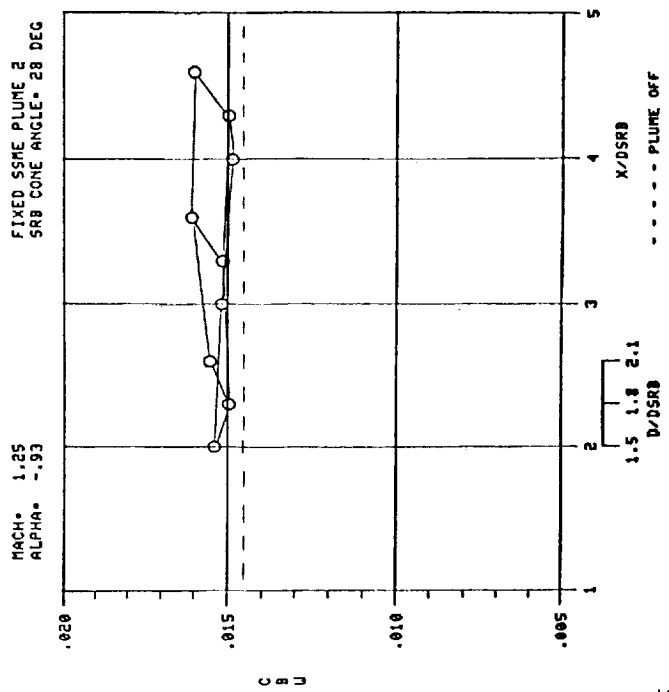
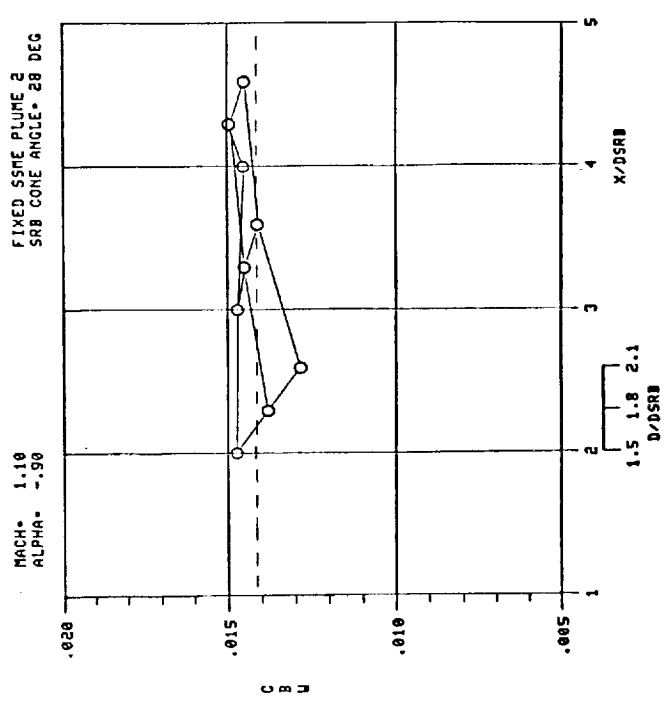
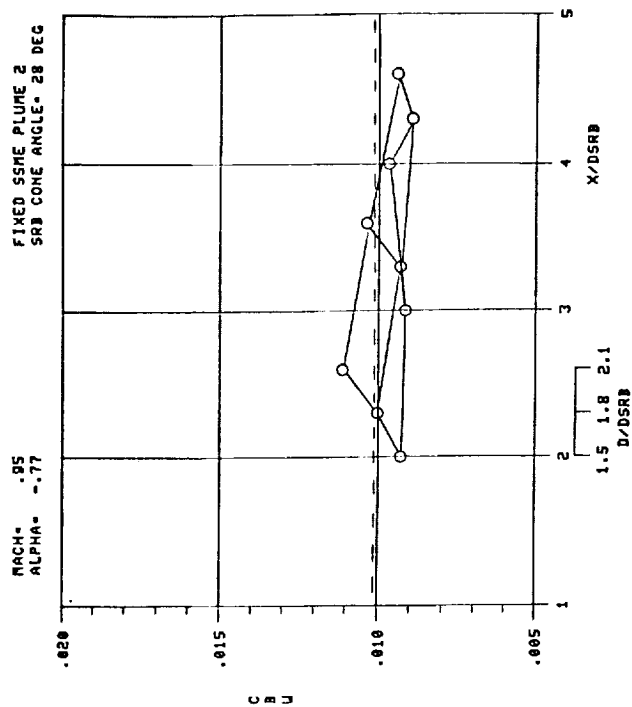
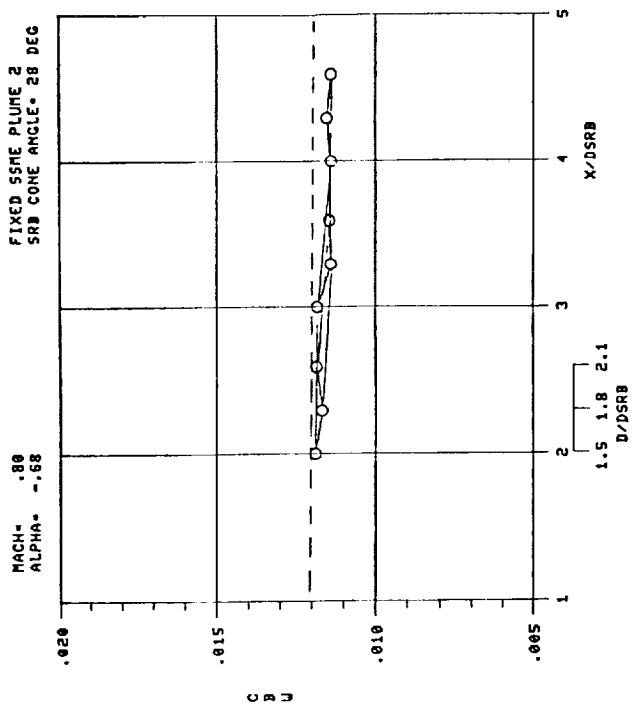


Figure H-5.

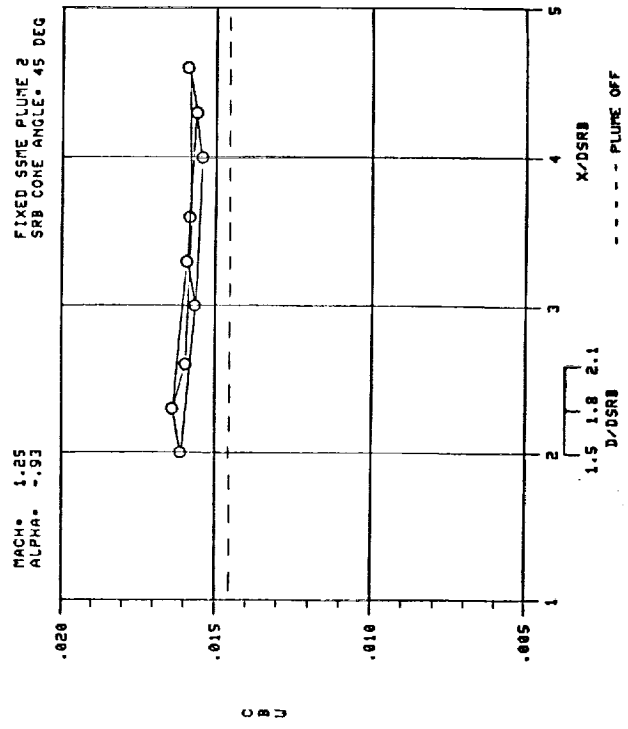
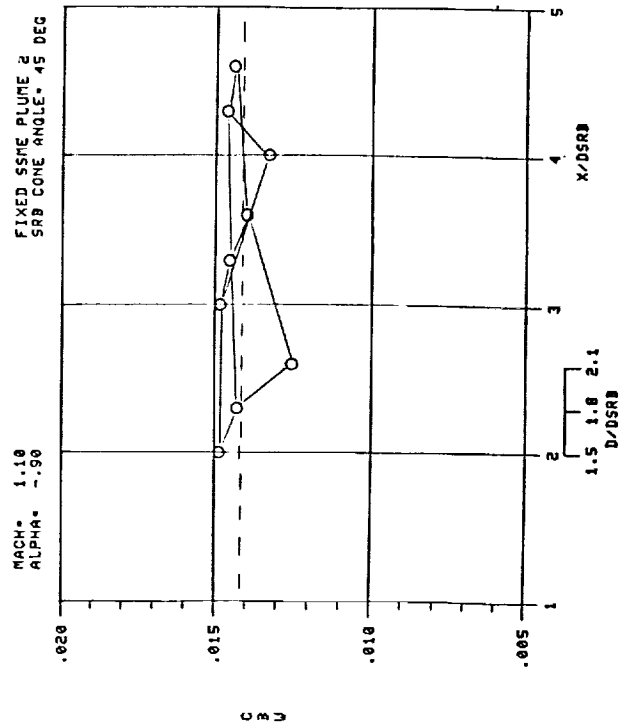
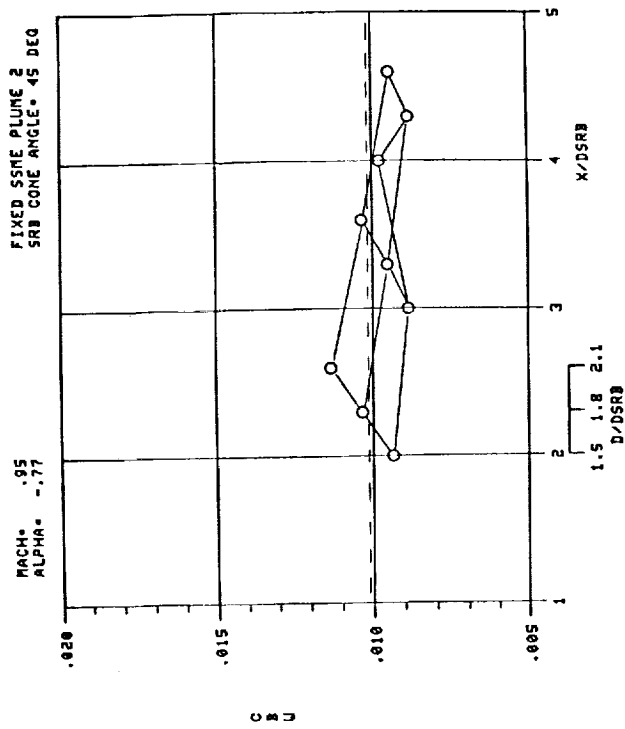
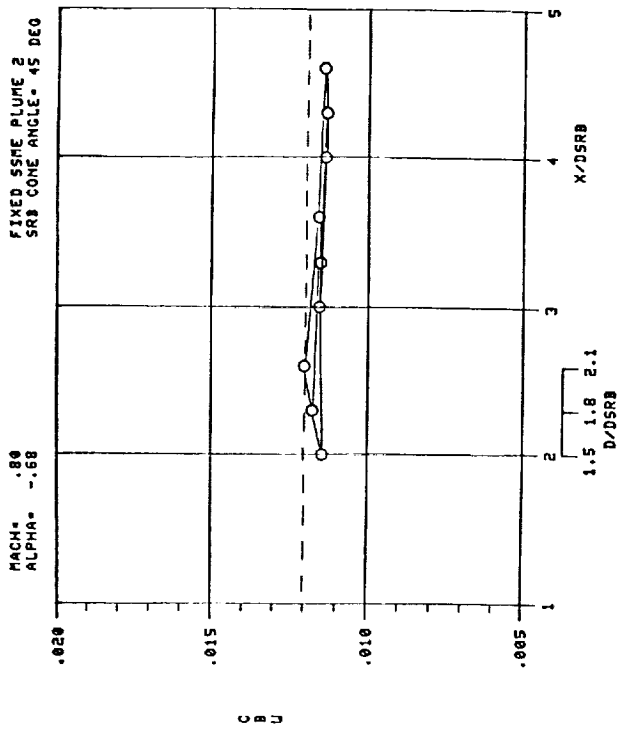


Figure H-6.

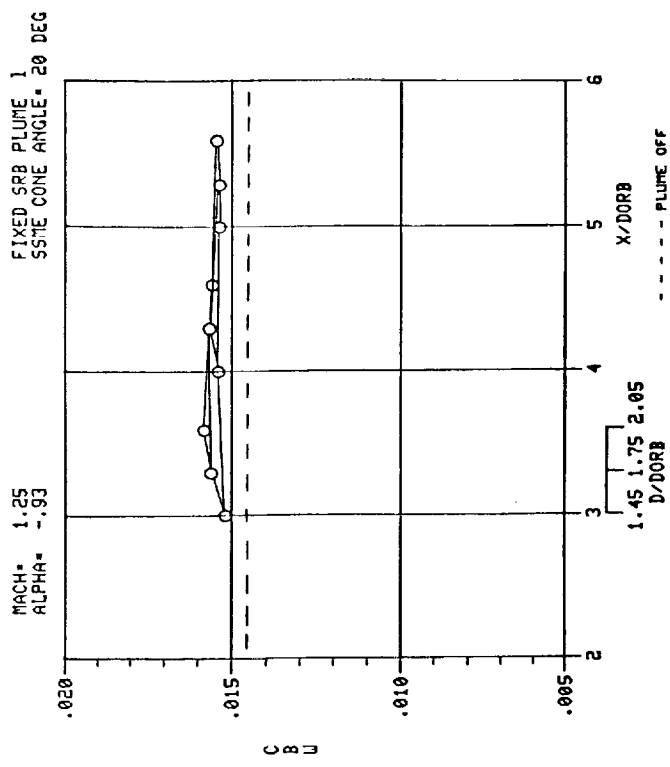
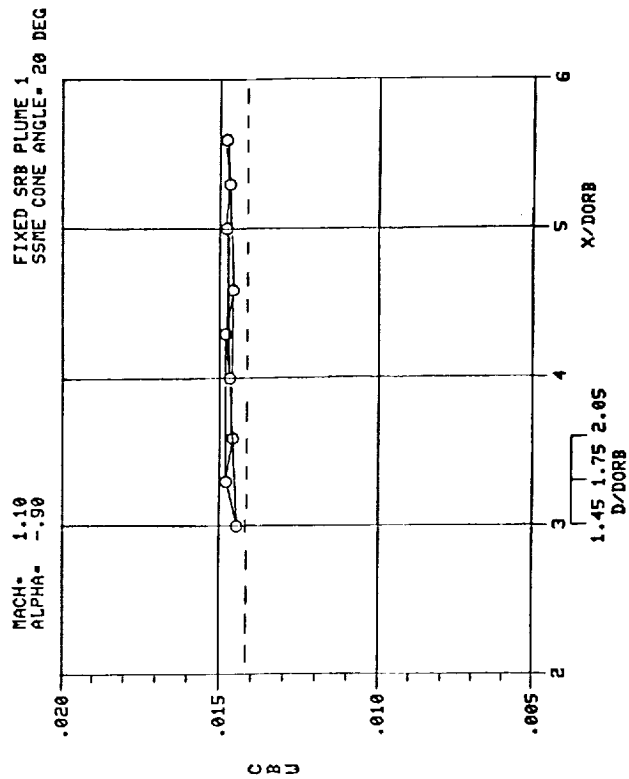
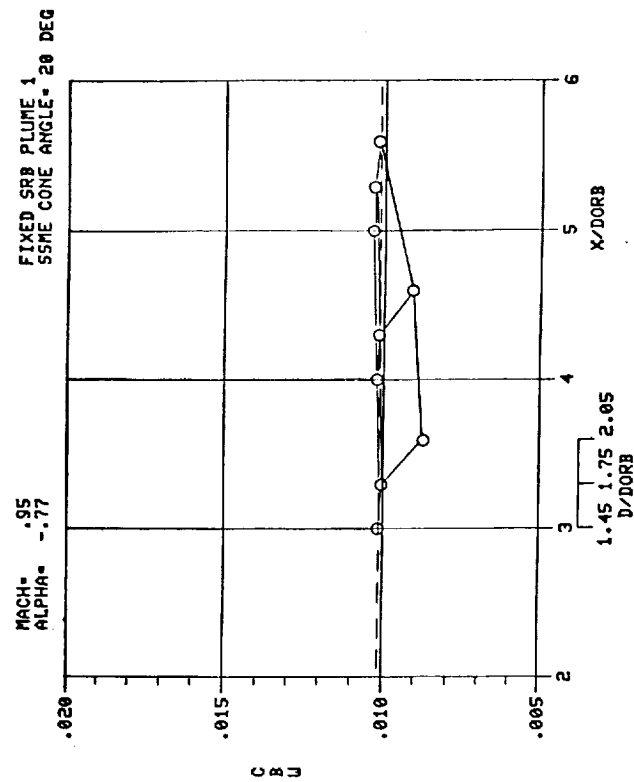
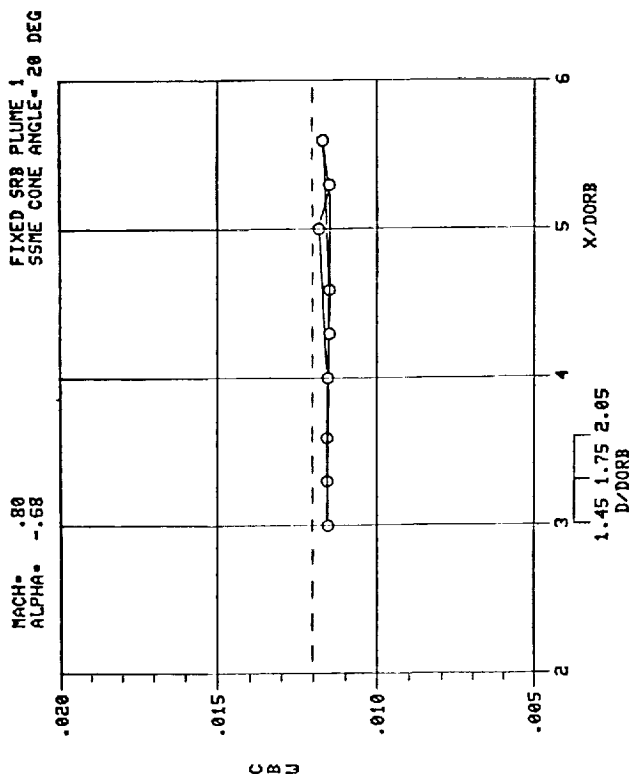


Figure H-7.

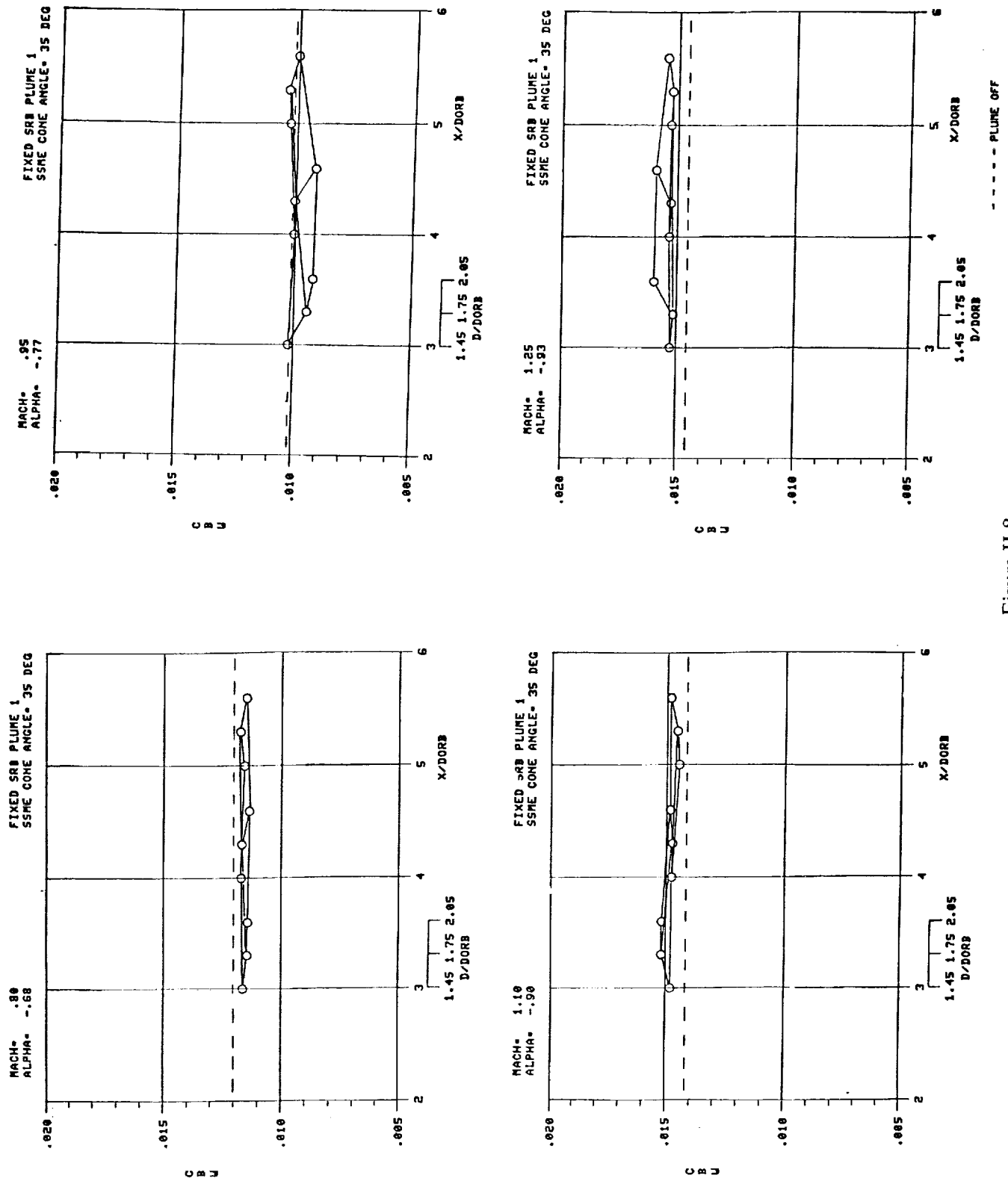


Figure H-8.

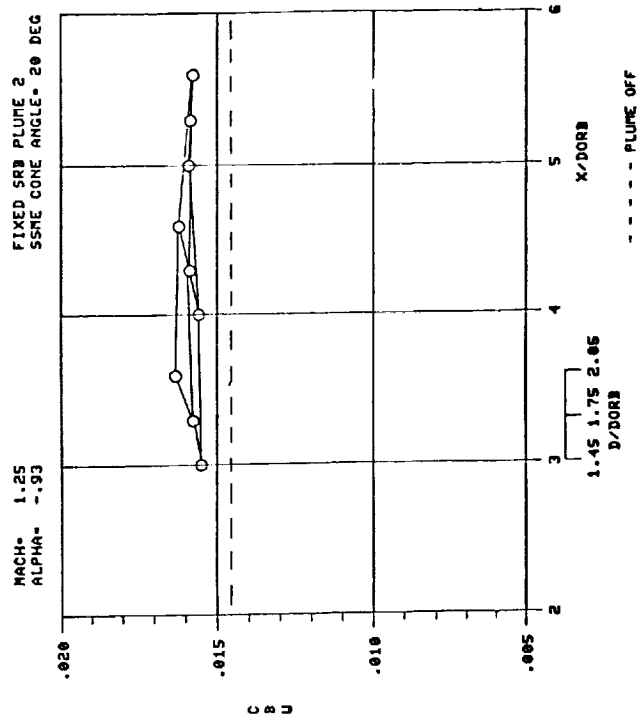
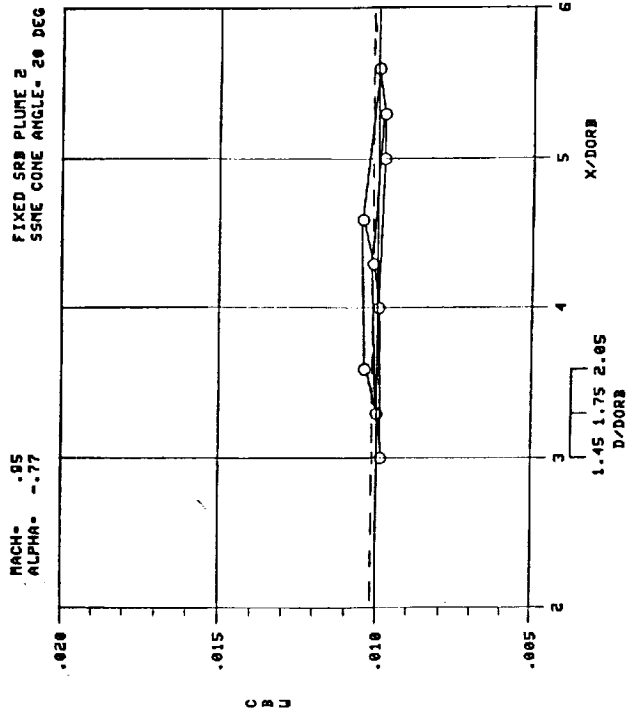
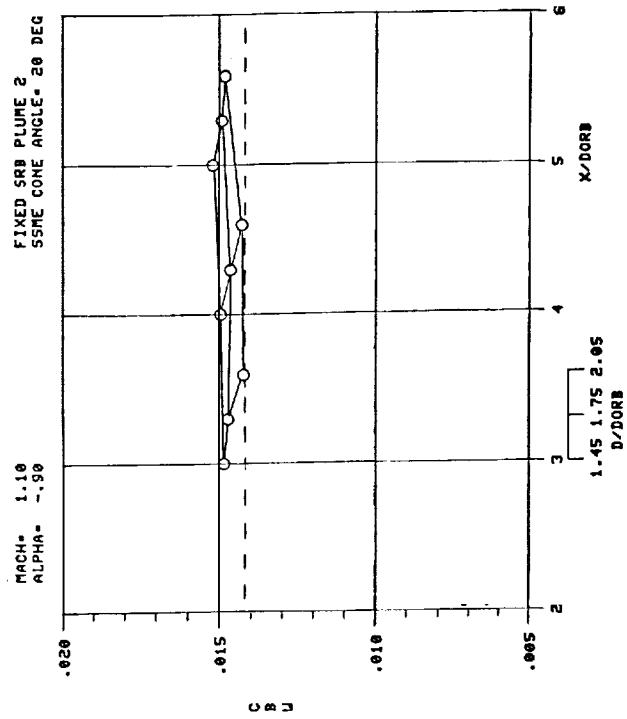
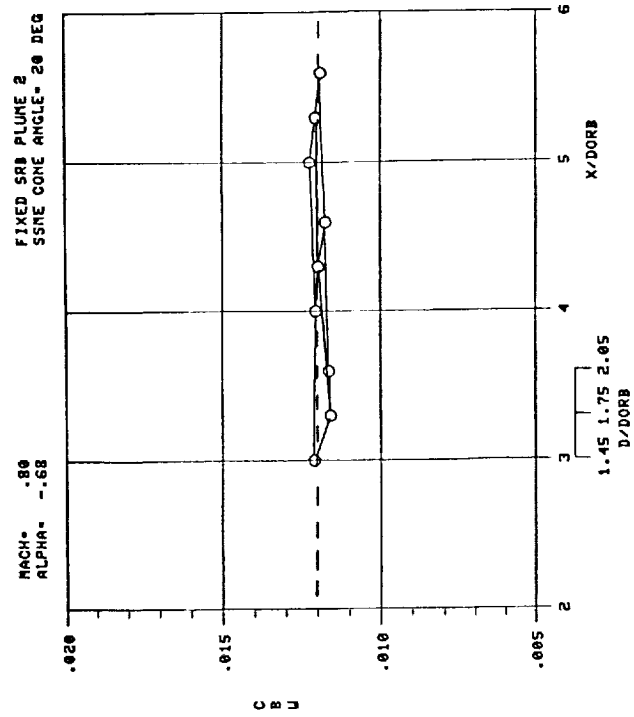
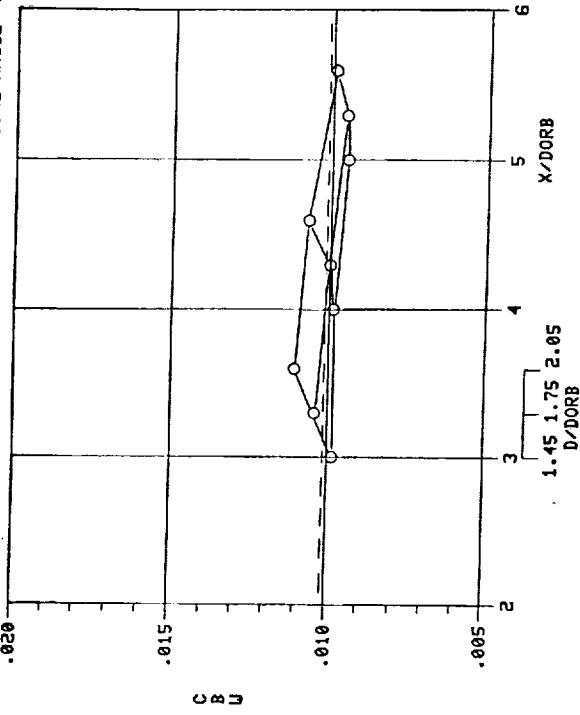


Figure H-9.

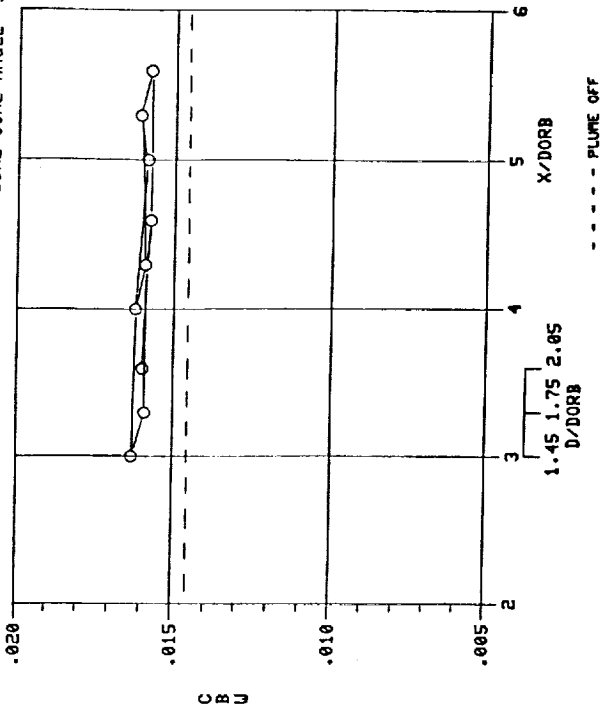
FIXED SRB PLUME 2
SSME CONE ANGLE = 35 DEG

MACH = .95
ALPHA = -.77



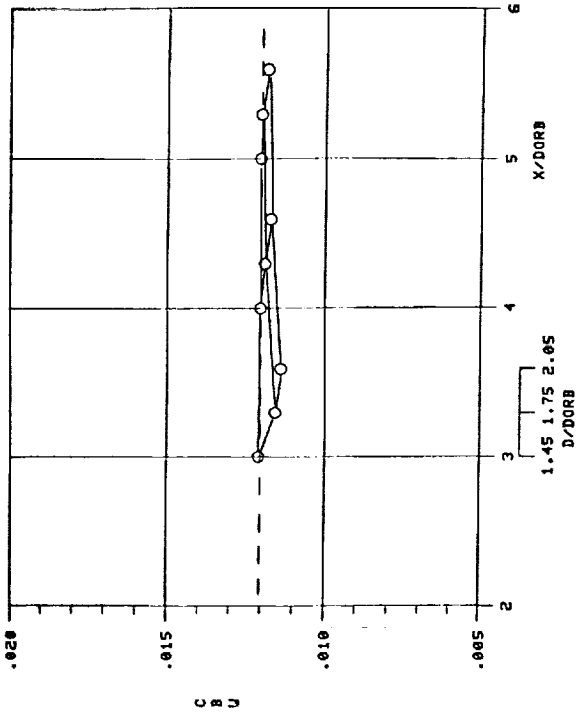
FIXED SRB PLUME 2
SSME CONE ANGLE = 35 DEG

MACH = 1.25
ALPHA = -.93



FIXED SRB PLUME 2
SSME CONE ANGLE = 35 DEG

MACH = .80
ALPHA = -.68



FIXED SRB PLUME 2
SSME CONE ANGLE = 35 DEG

MACH = 1.10
ALPHA = -.90

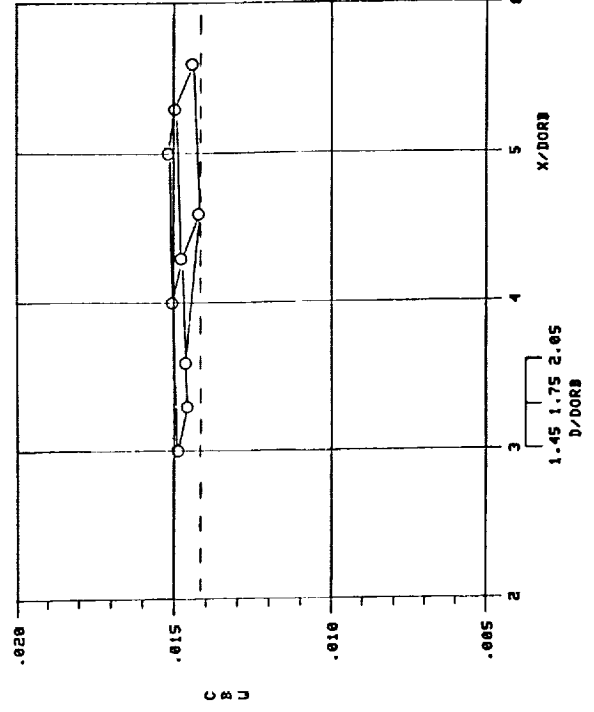


Figure H-10.

APPENDIX I



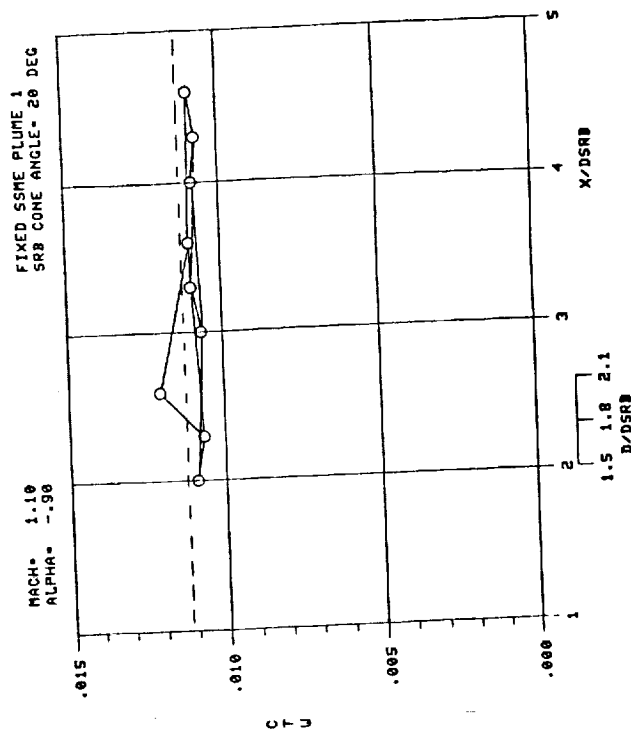
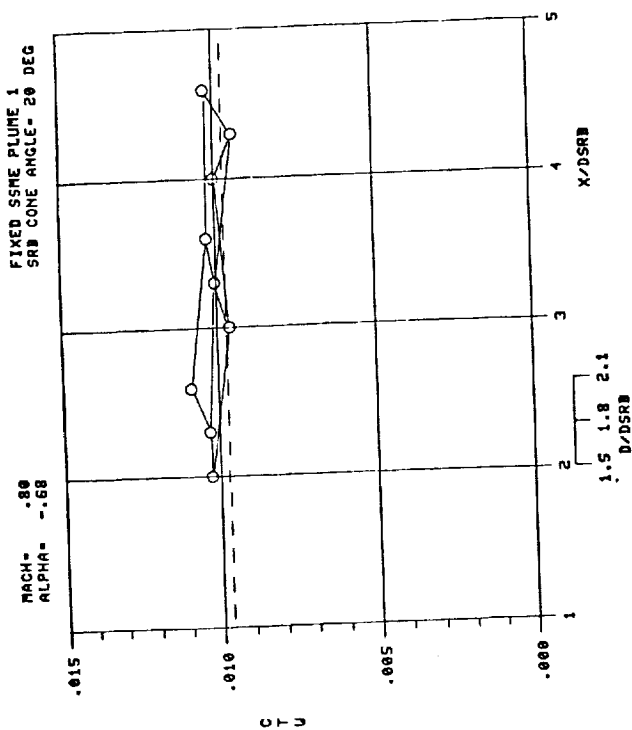
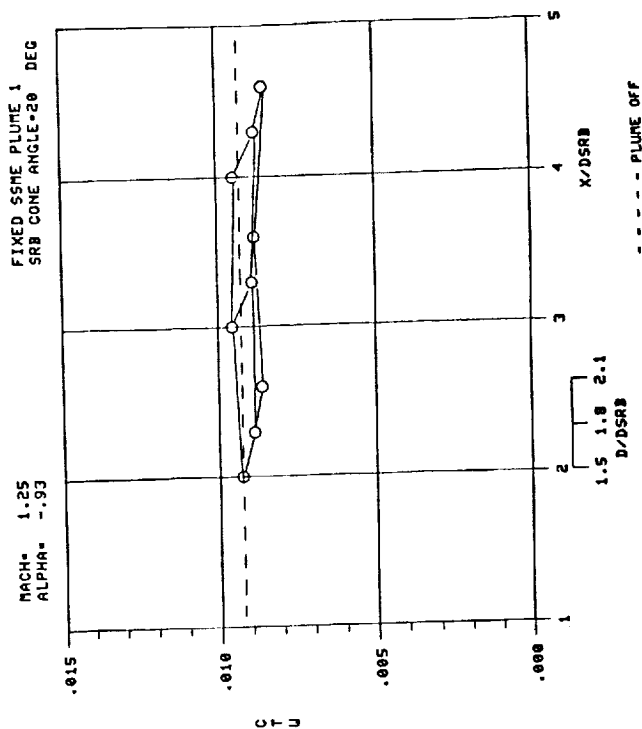
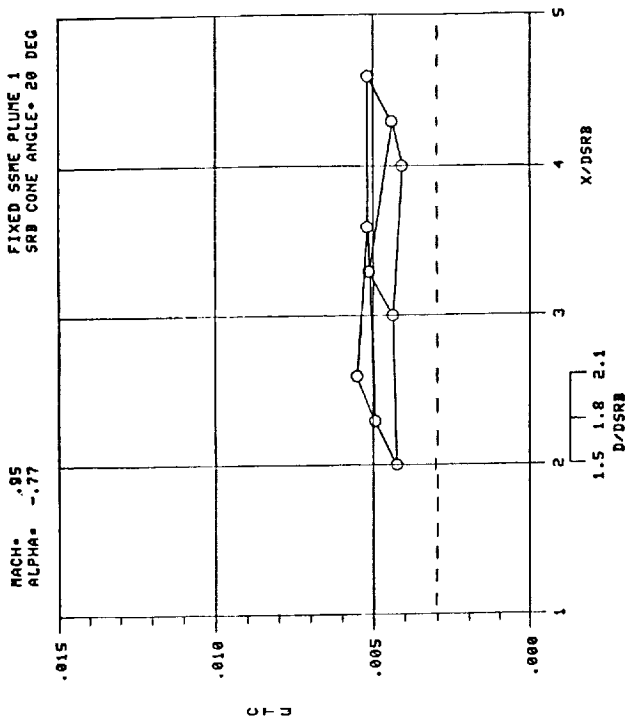


Figure I-1.

PRECEDING PAGE BLANK NOT FILMED

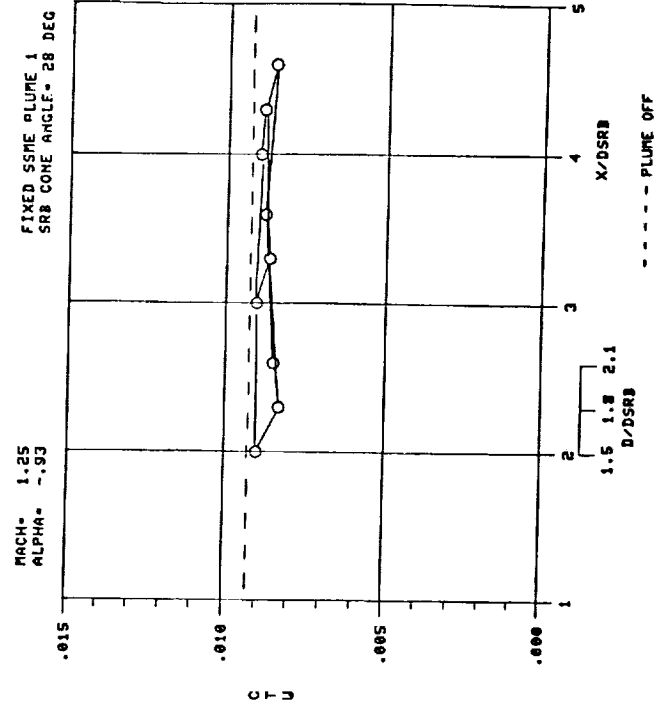
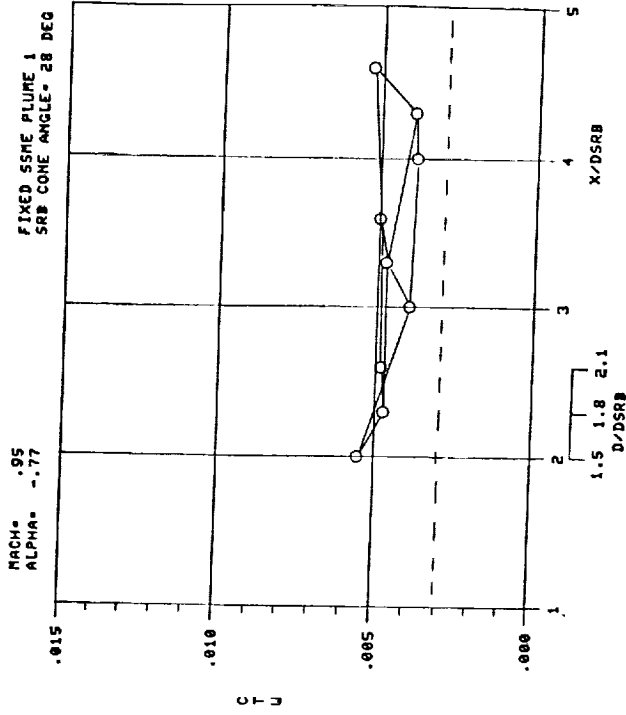
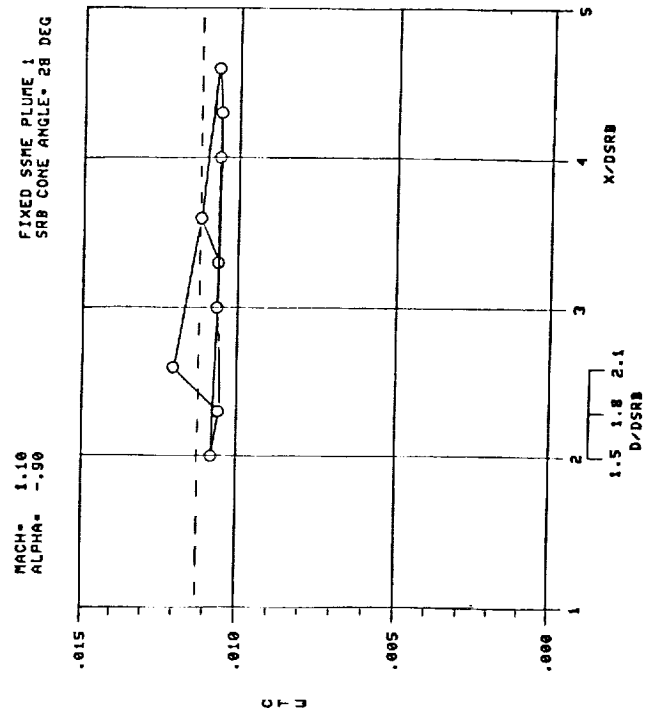
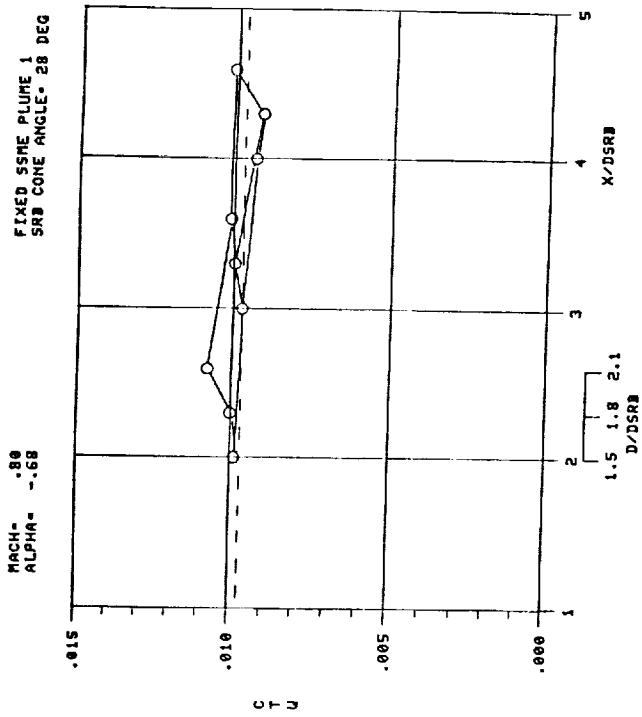


Figure I-2.

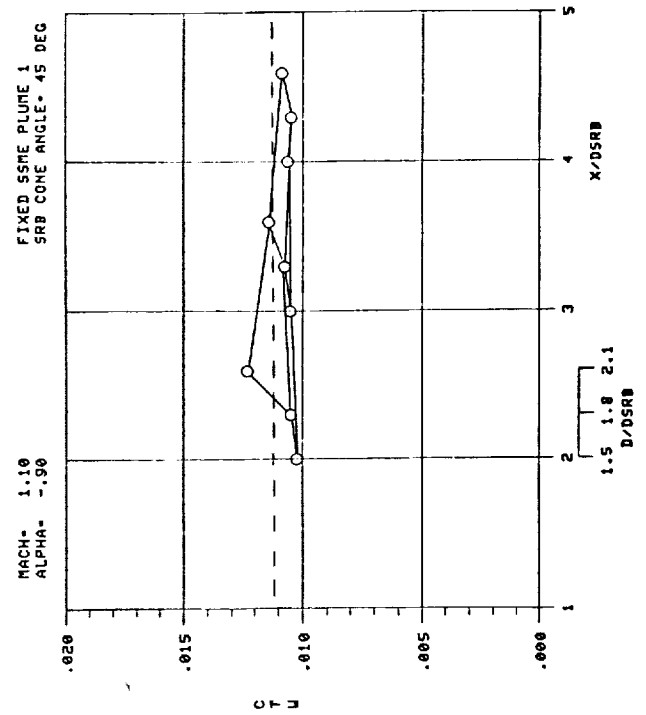
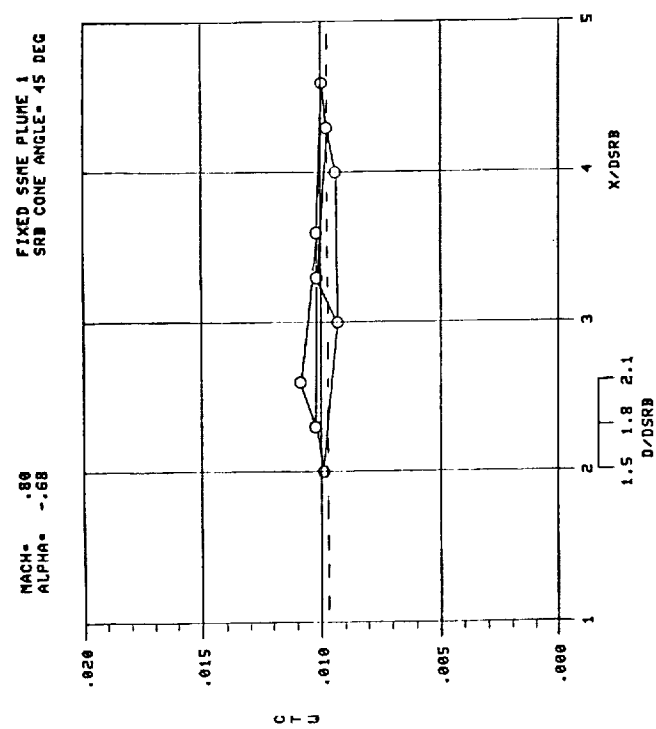
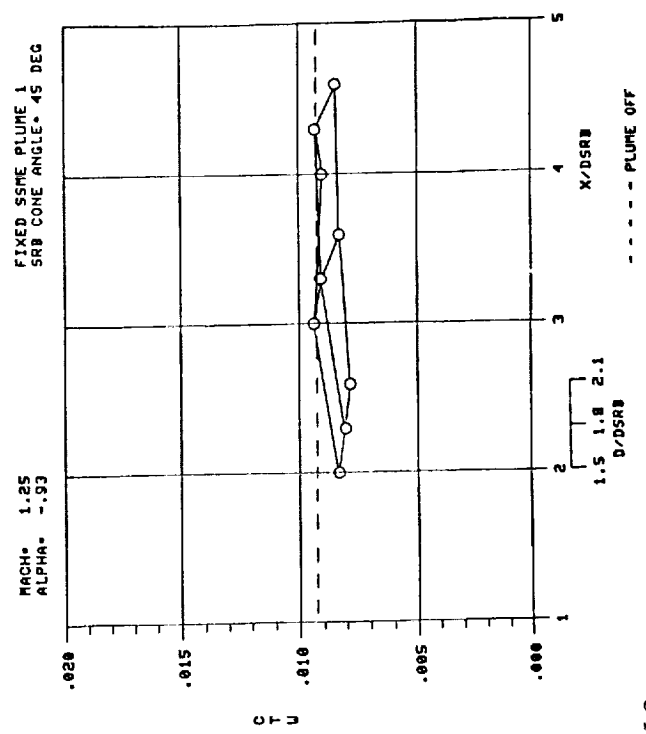
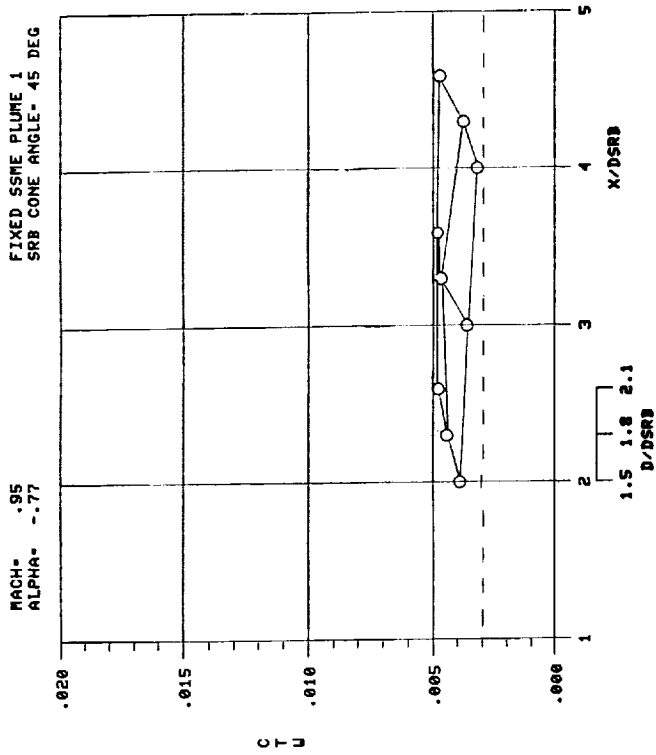


Figure I-3.

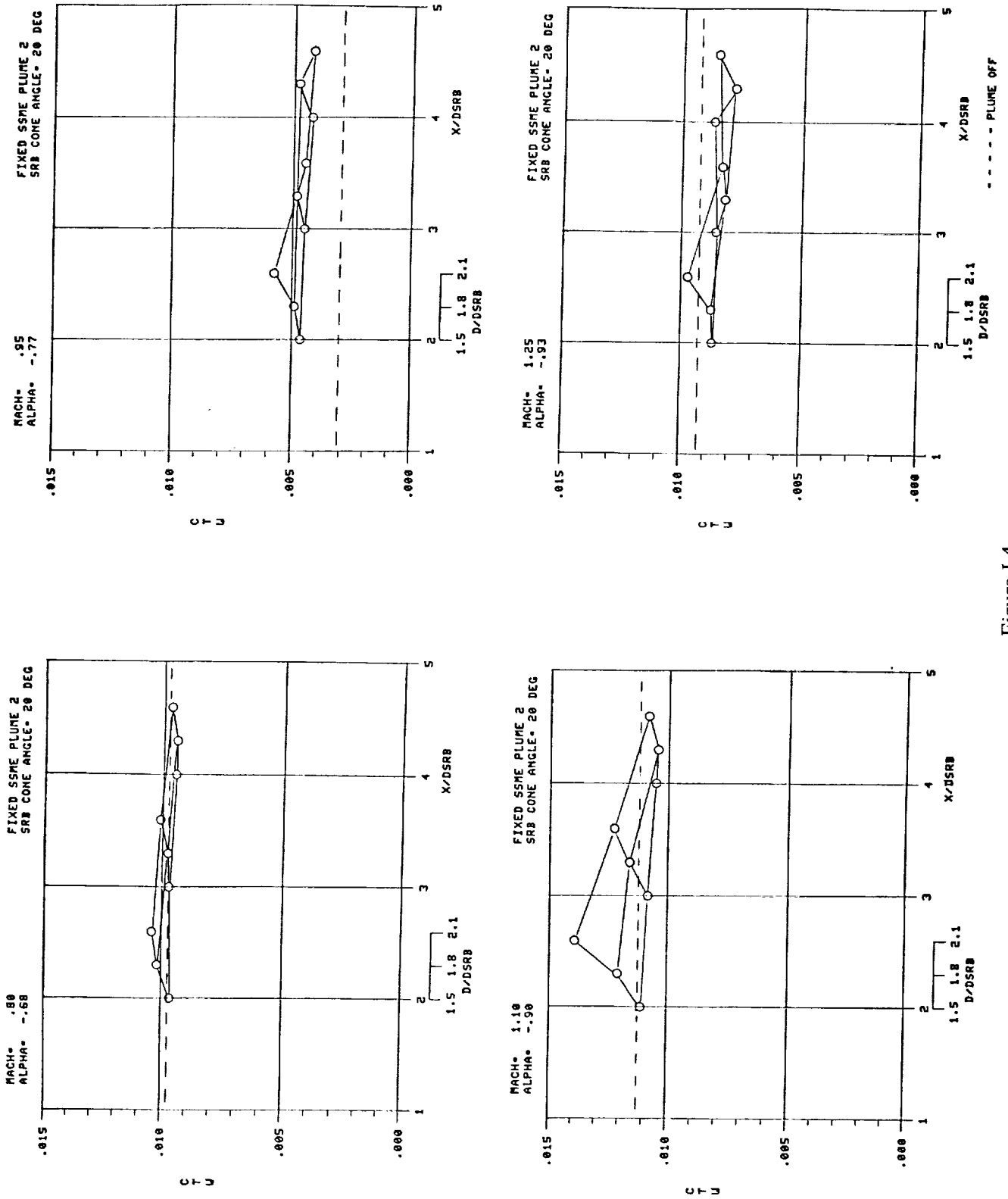


Figure I-4.

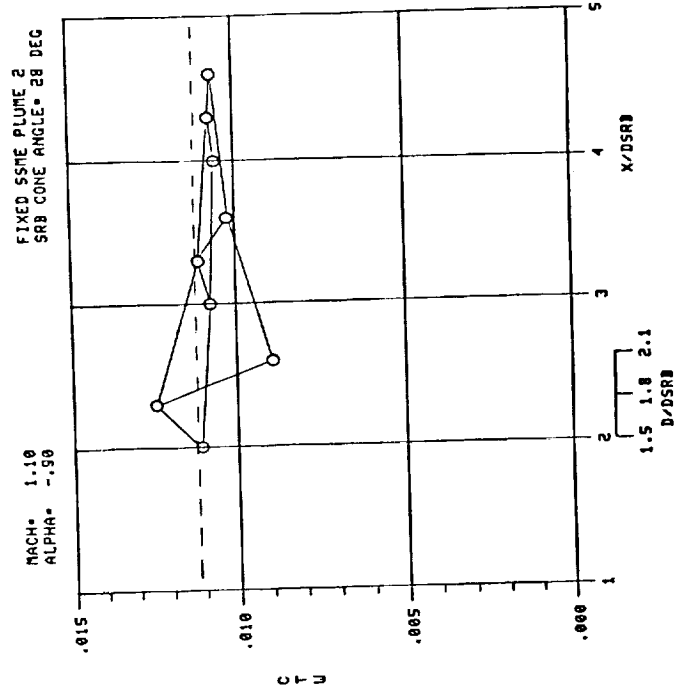
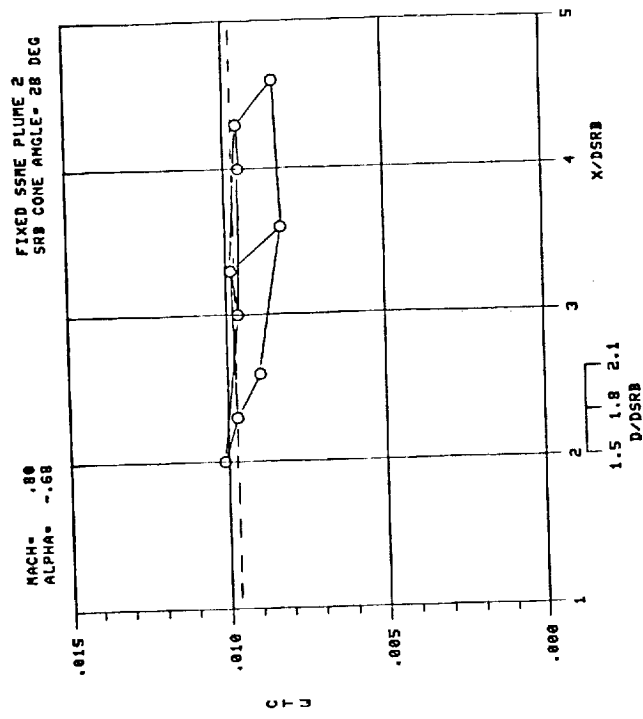
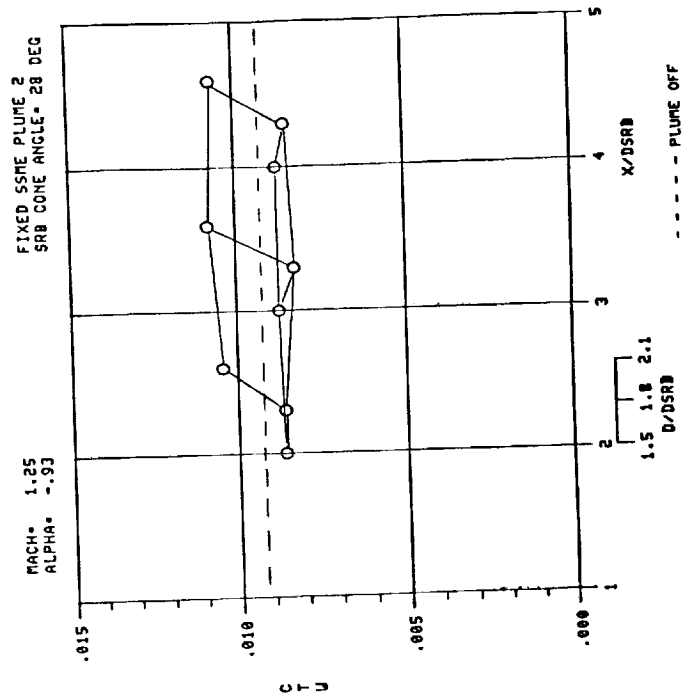
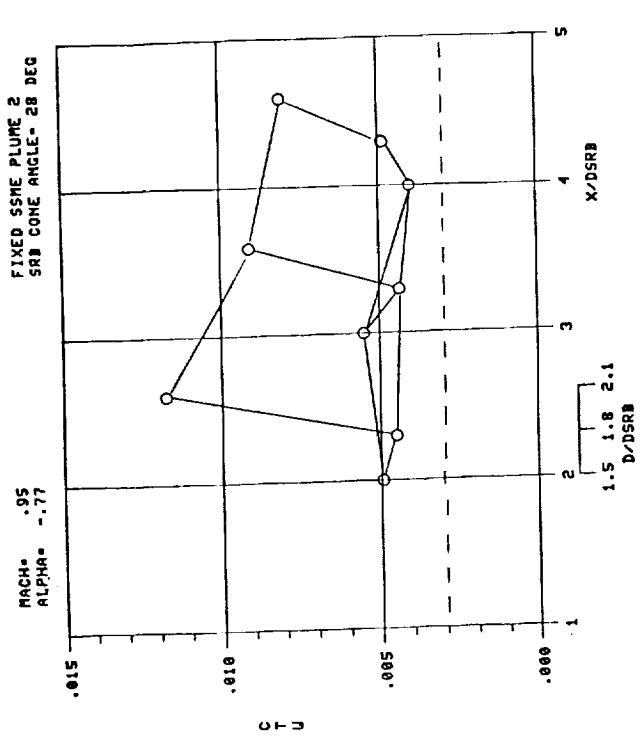


Figure I-5.

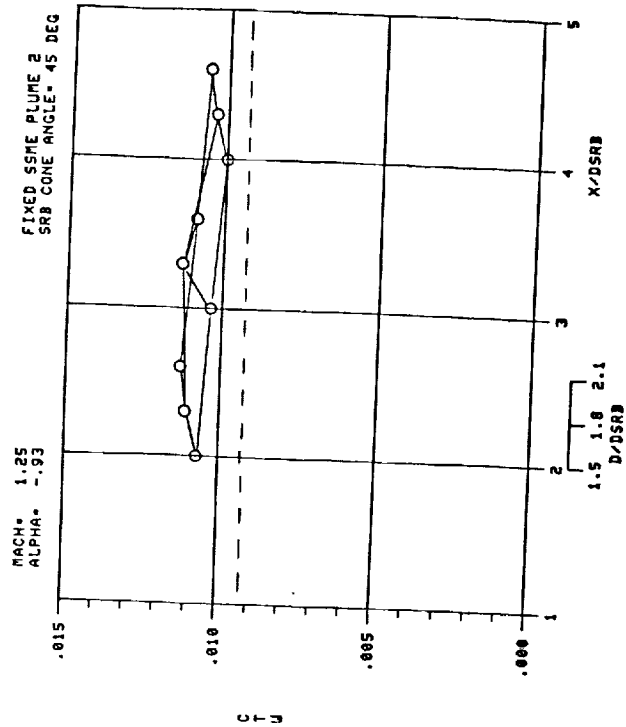
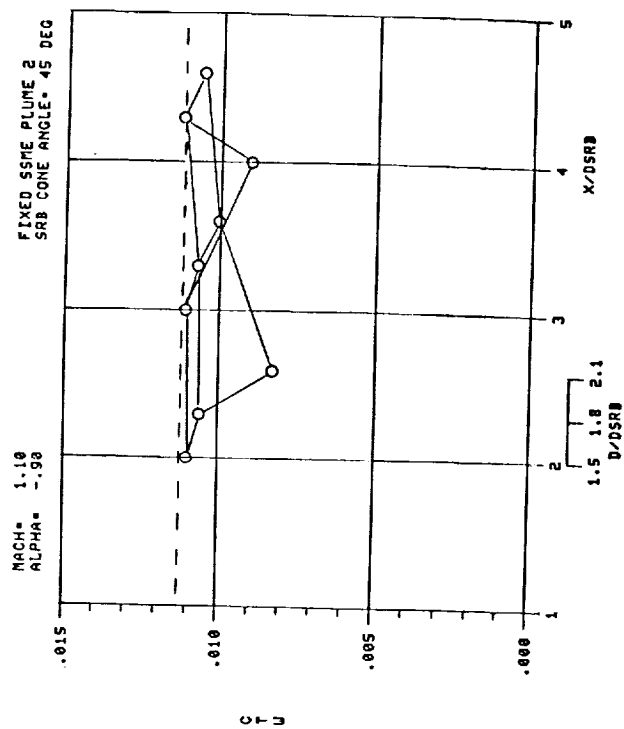
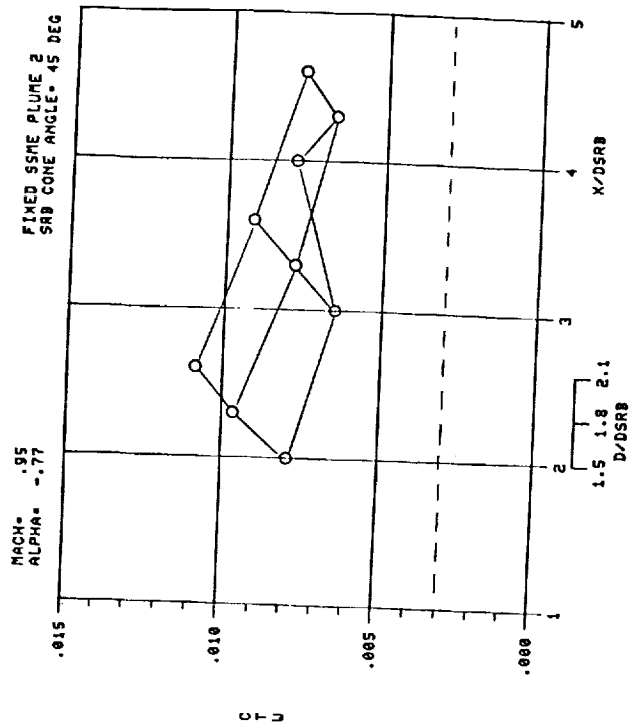
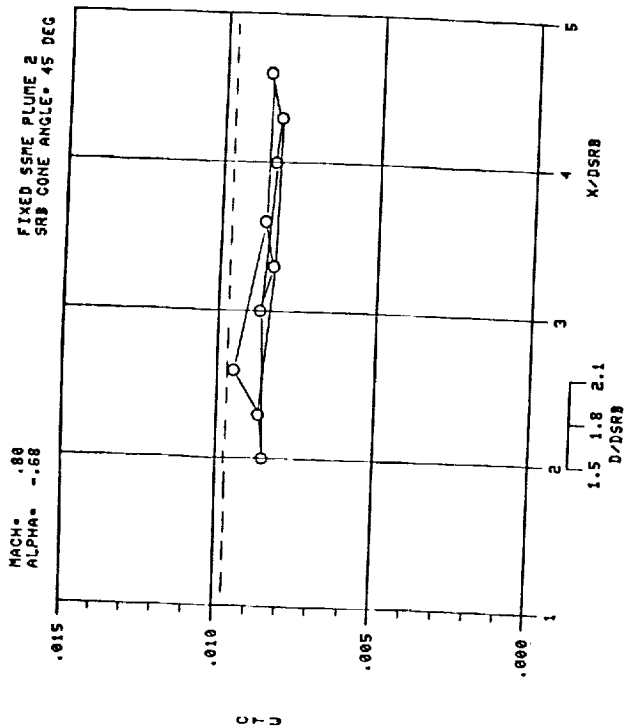


Figure I-6.

----- PLUME OFF

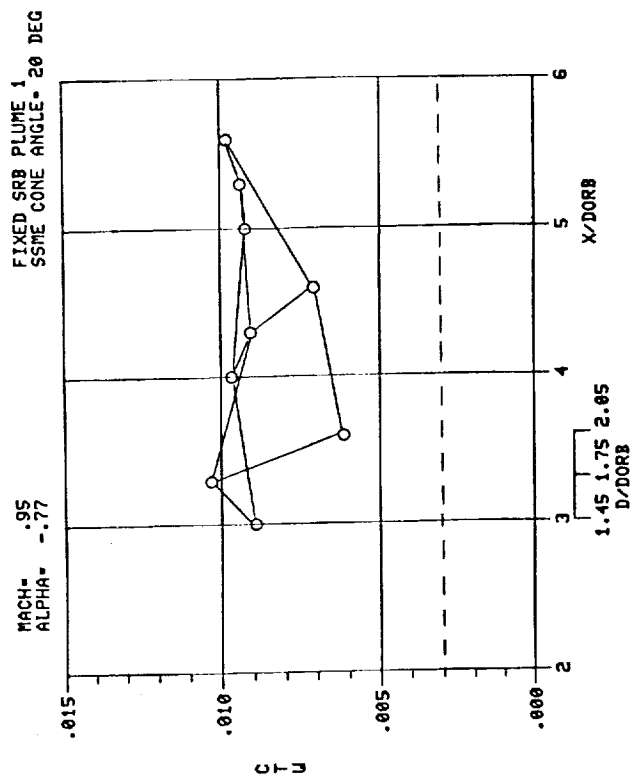
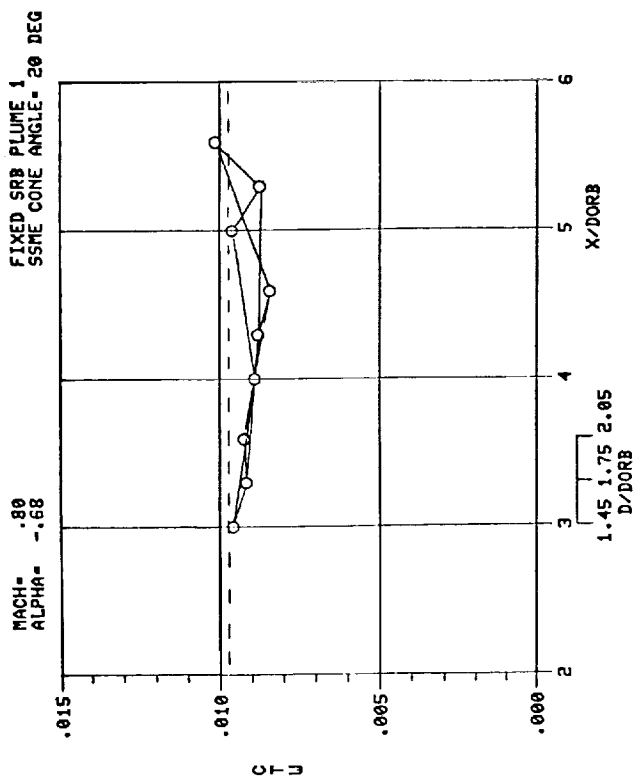
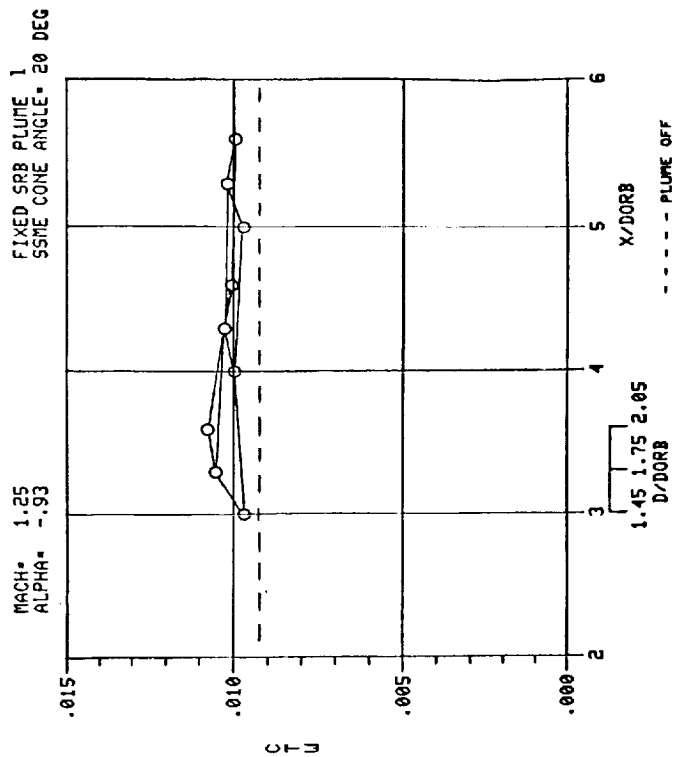
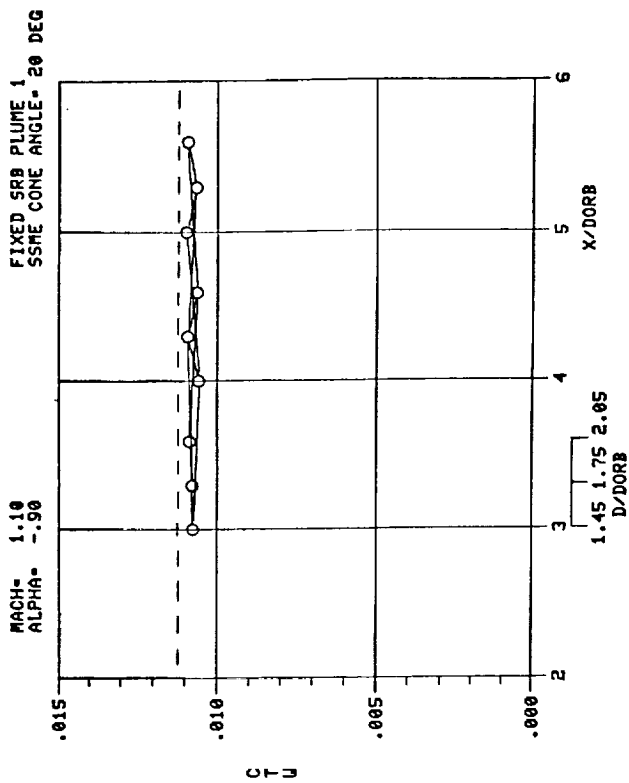


Figure I-7.

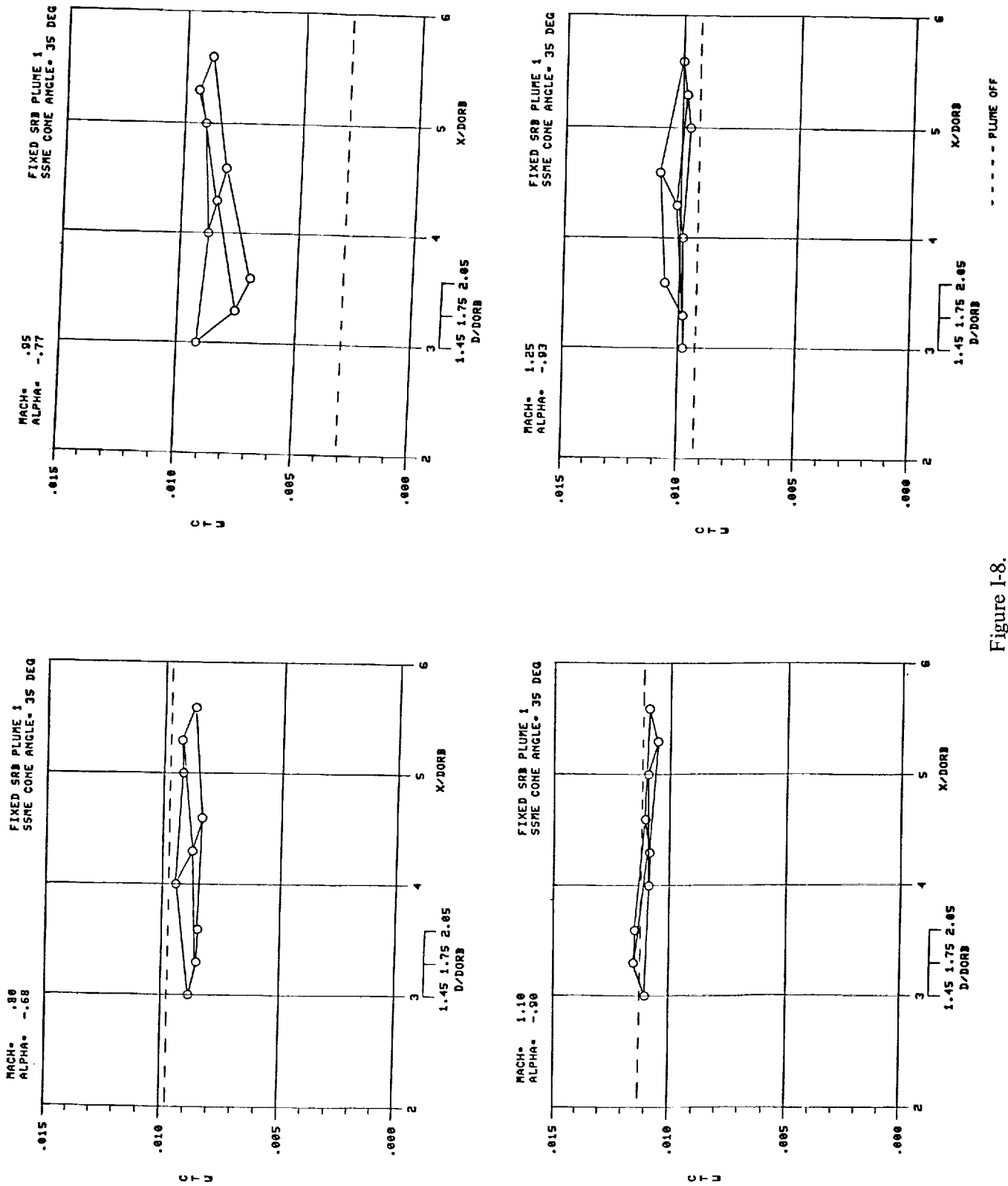


Figure I-8.

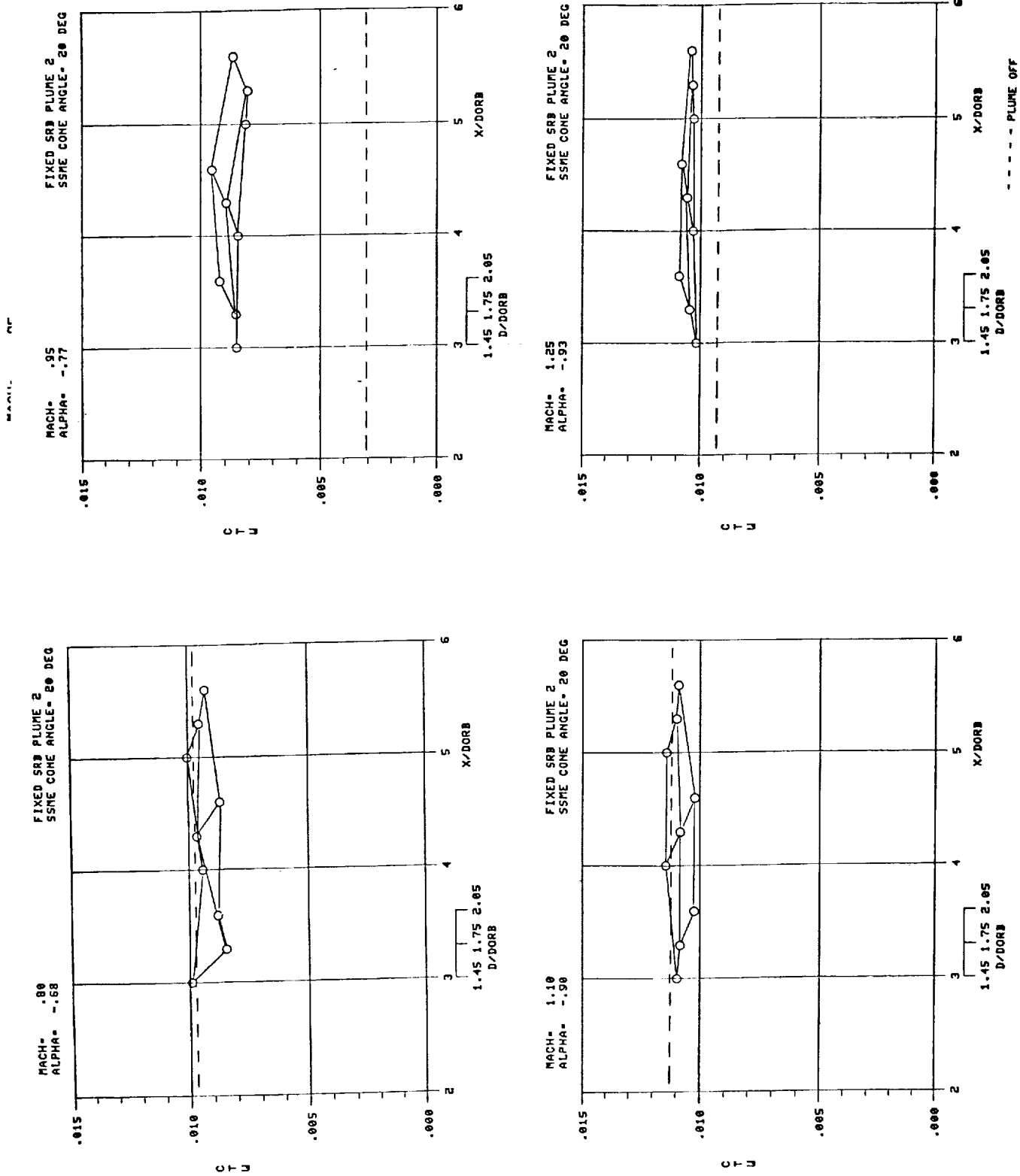


Figure I-9.

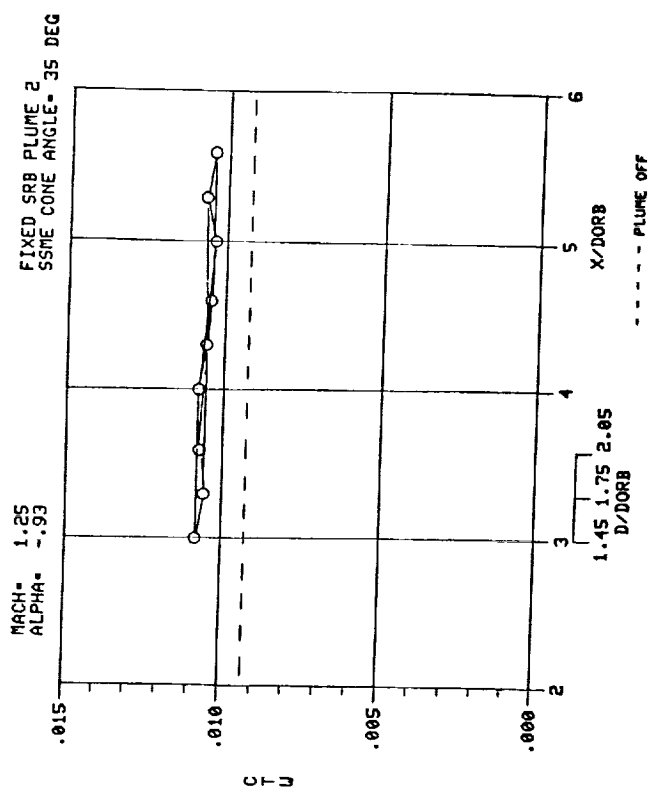
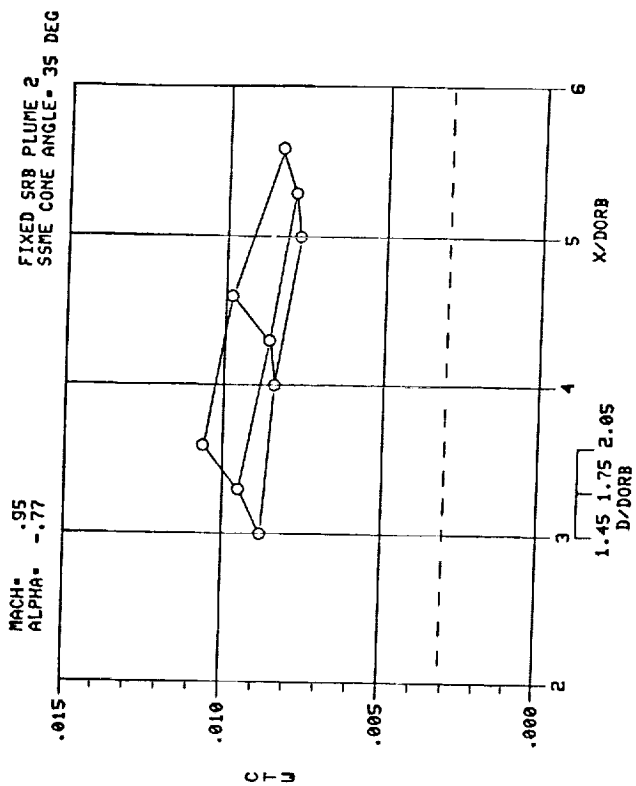
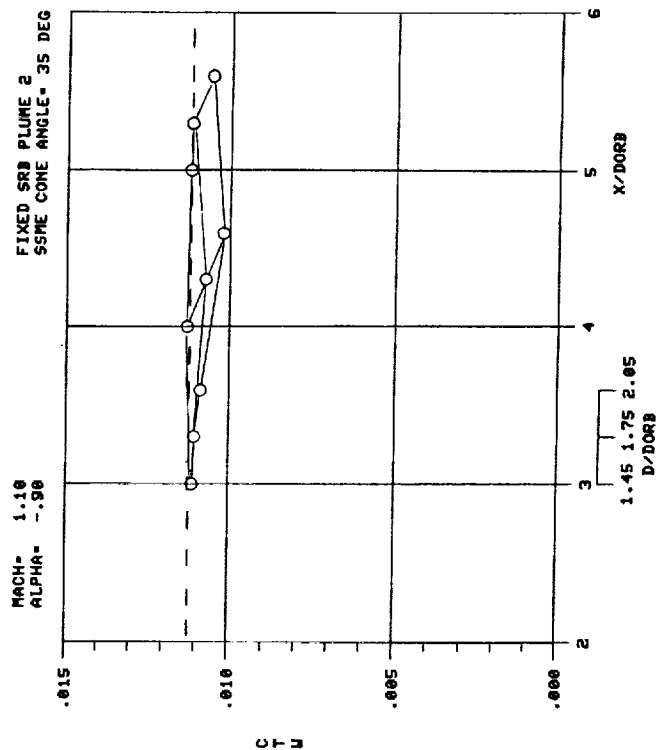
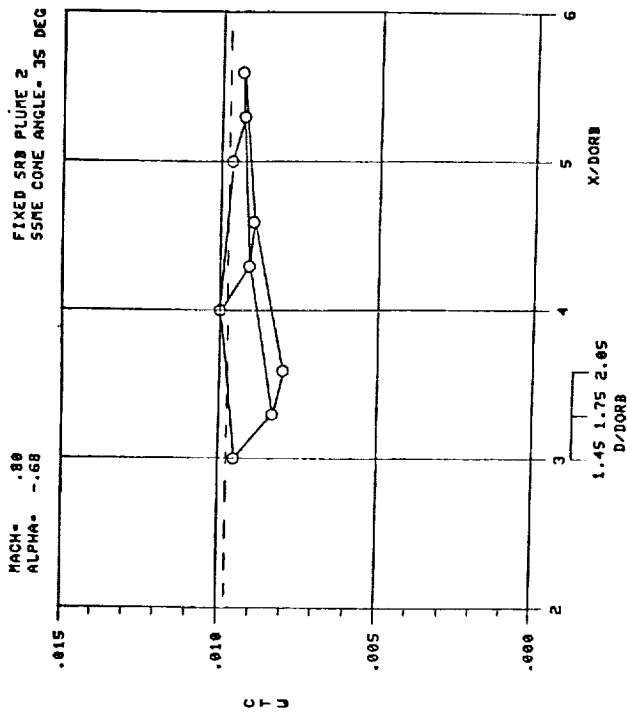
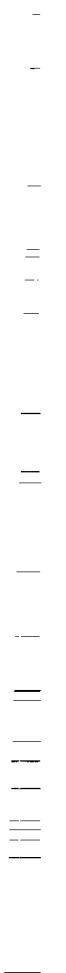


Figure I-10.

APPENDIX J



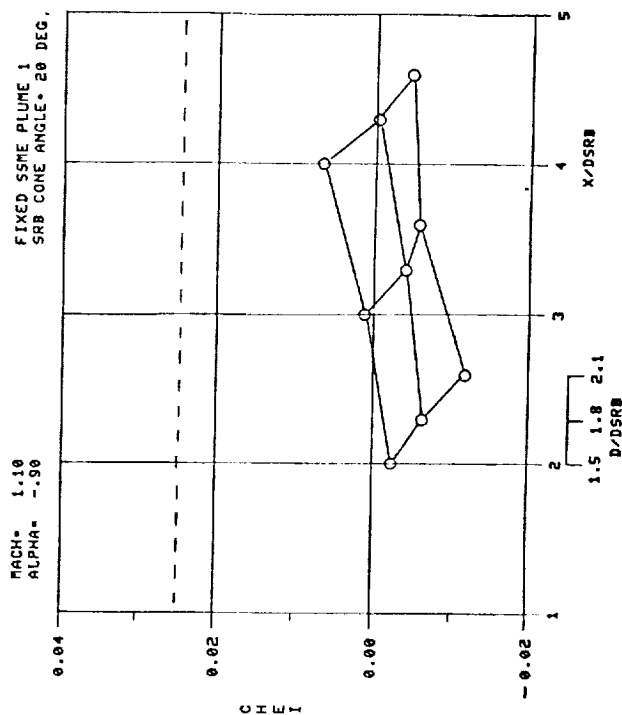
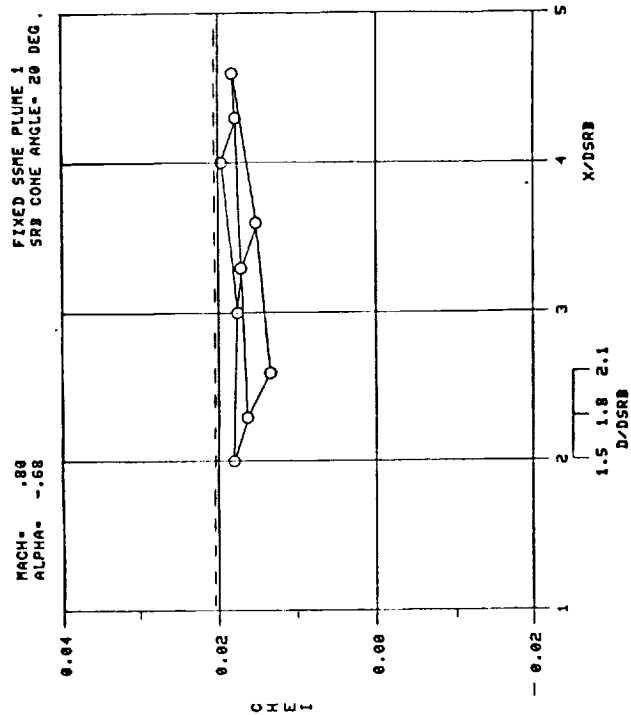
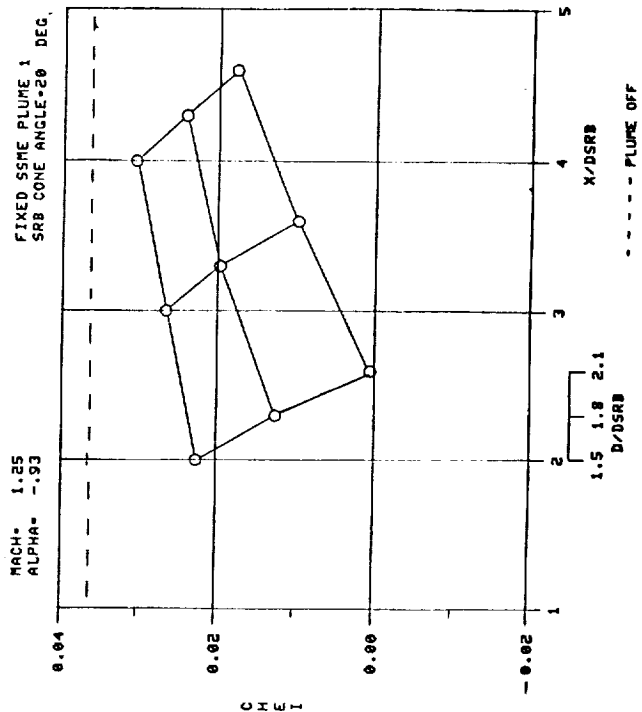
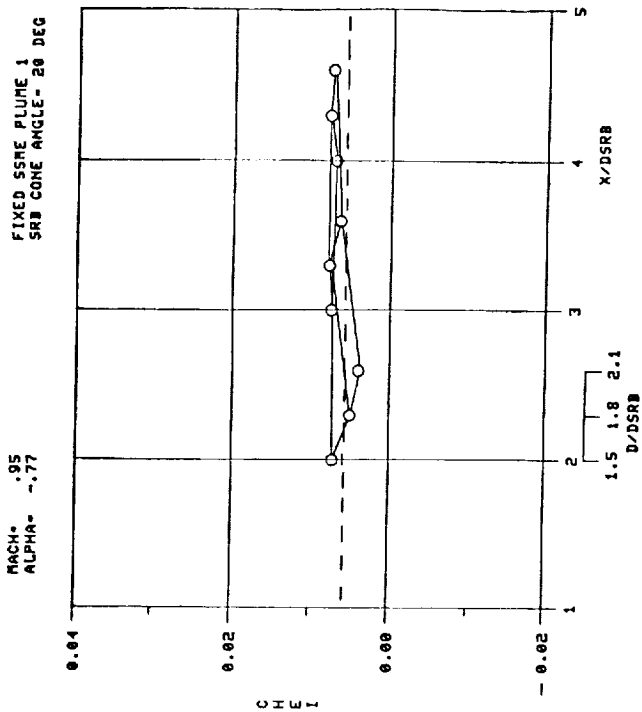


Figure J-1.

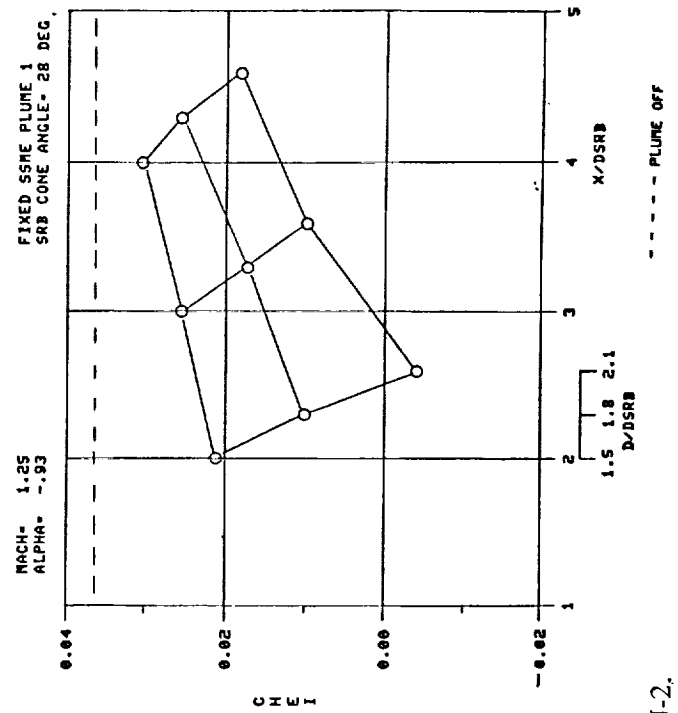
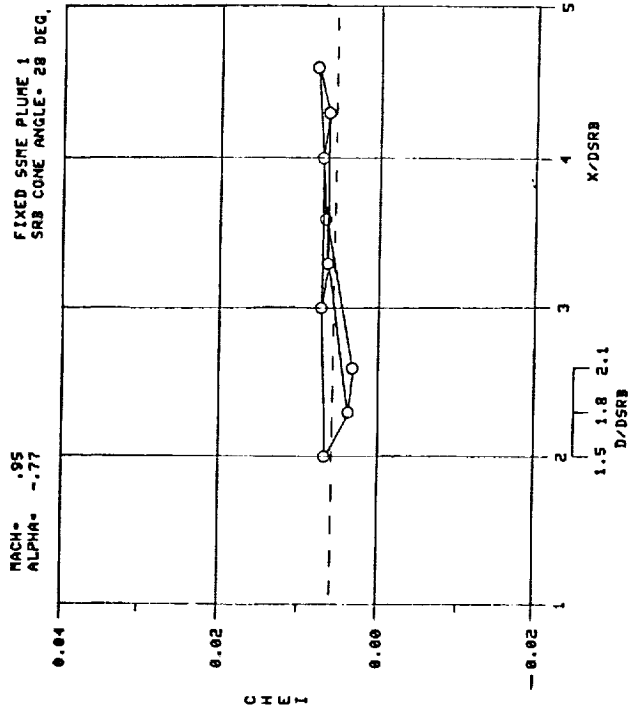
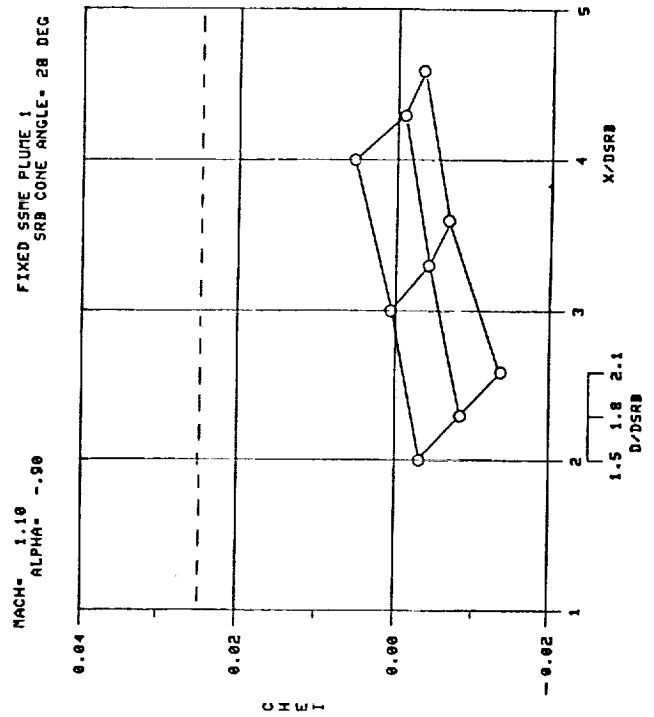
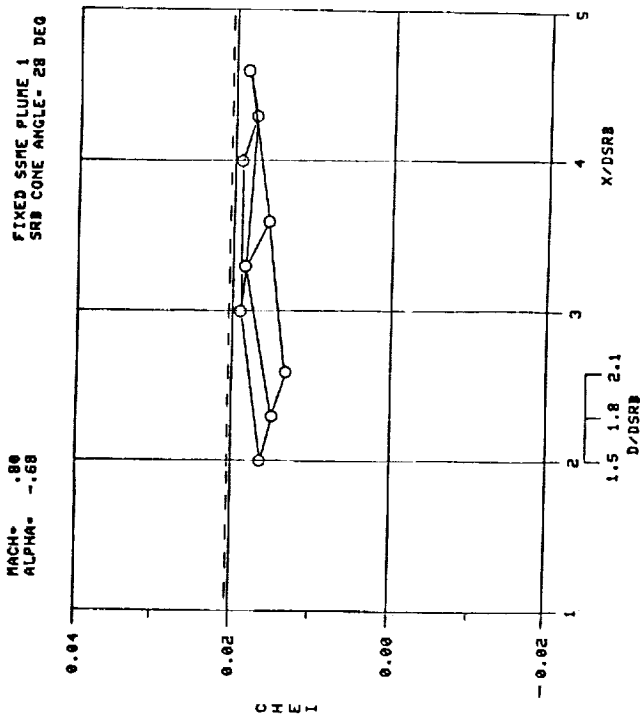


Figure J-2.

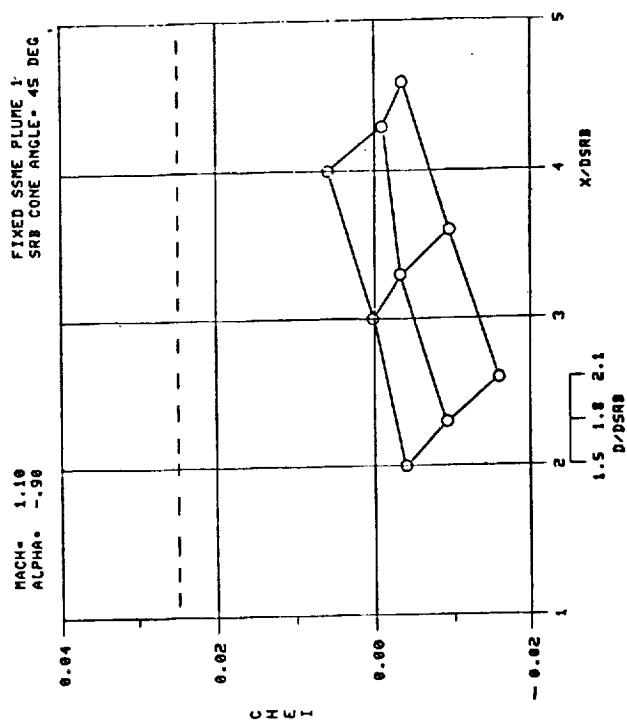
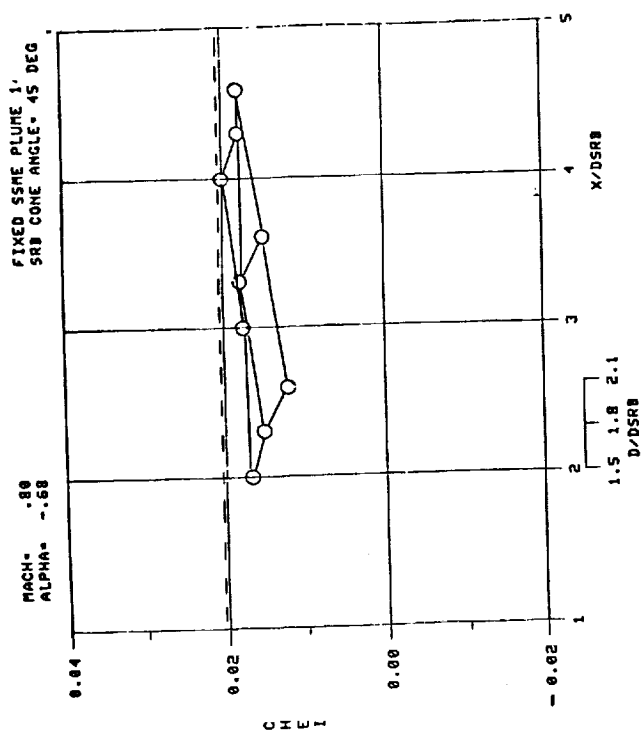
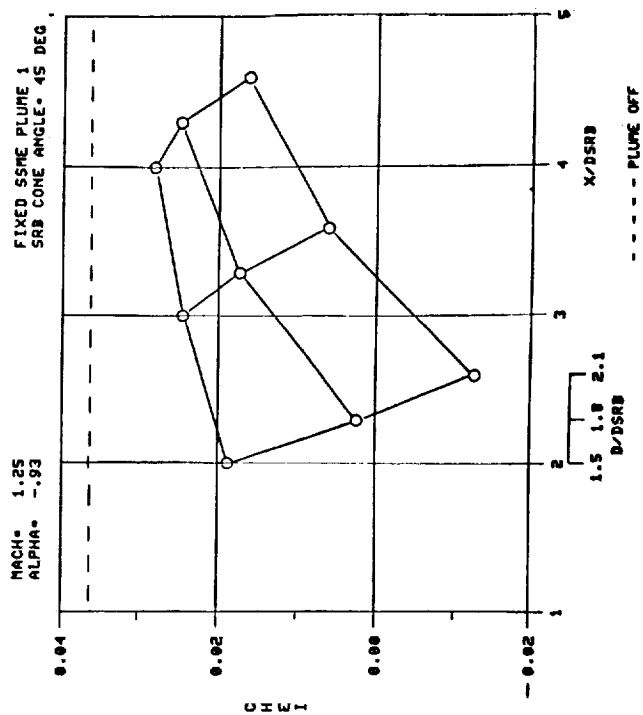
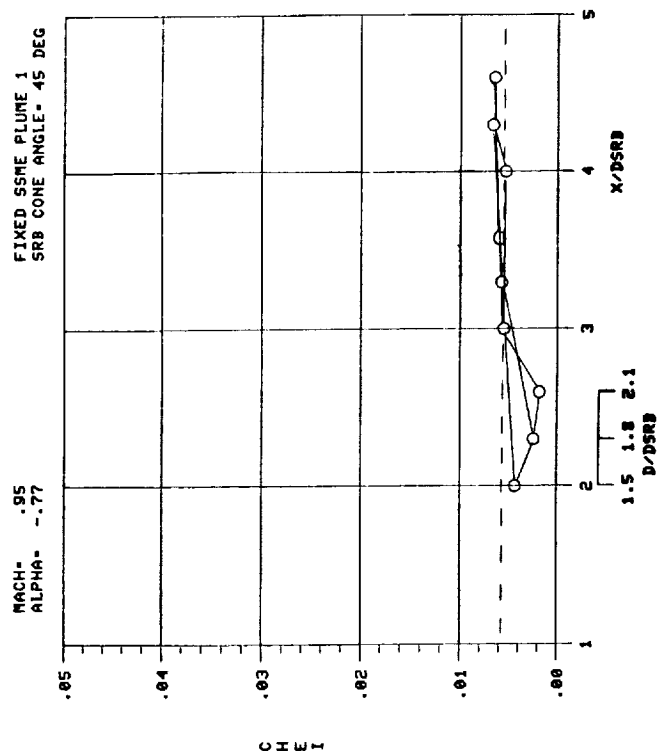


Figure J-3.

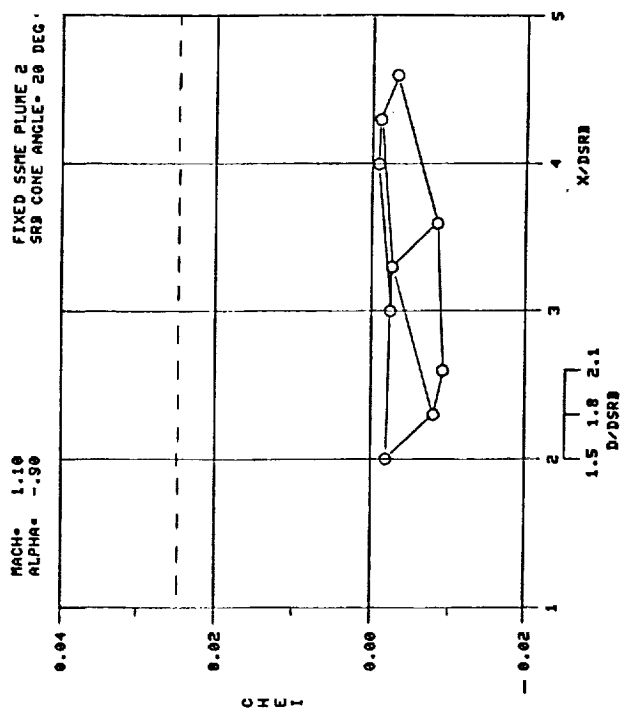
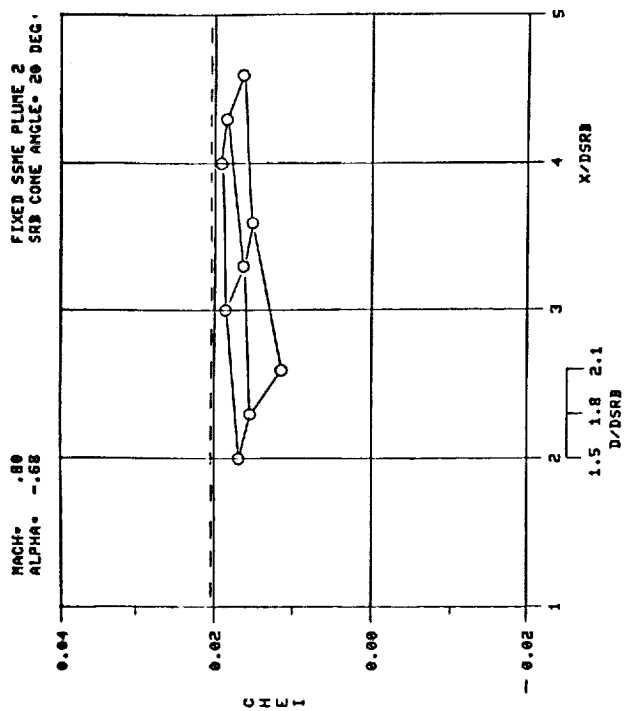
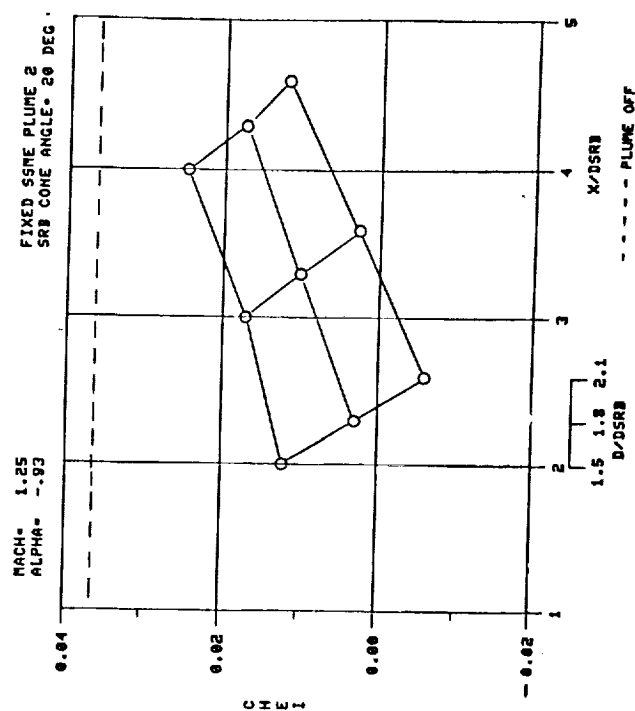
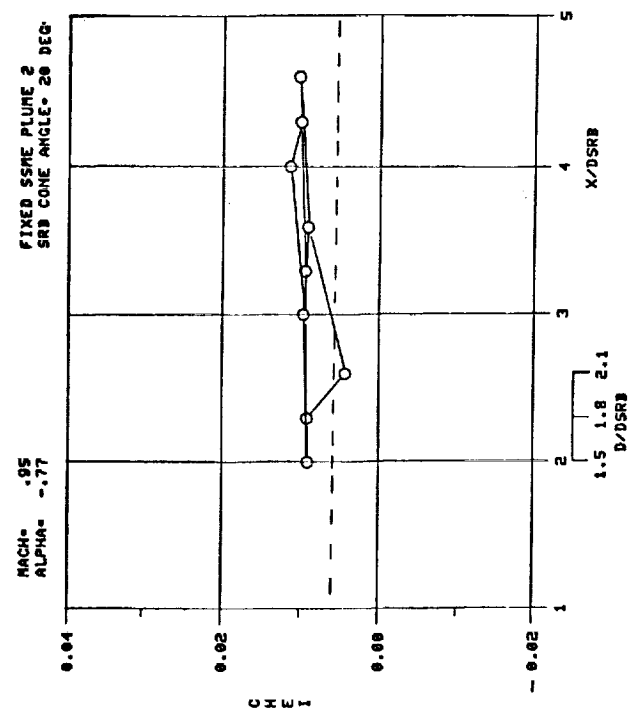


Figure J-4.

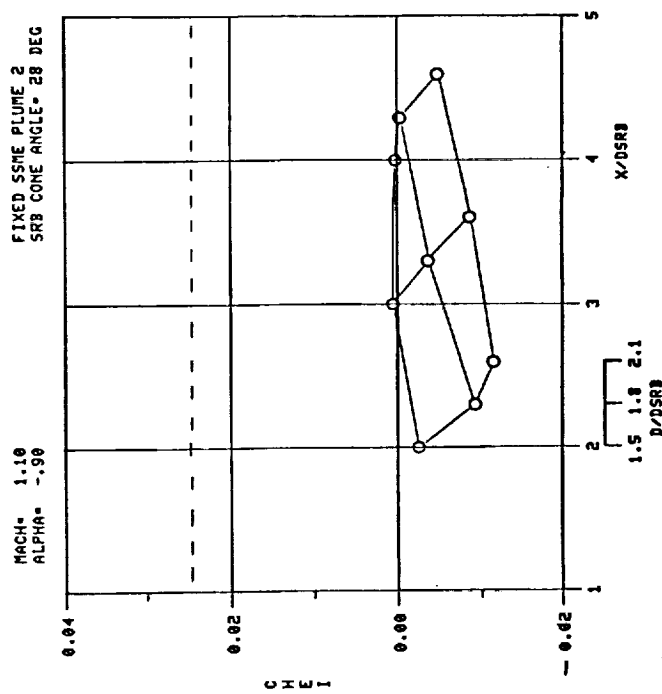
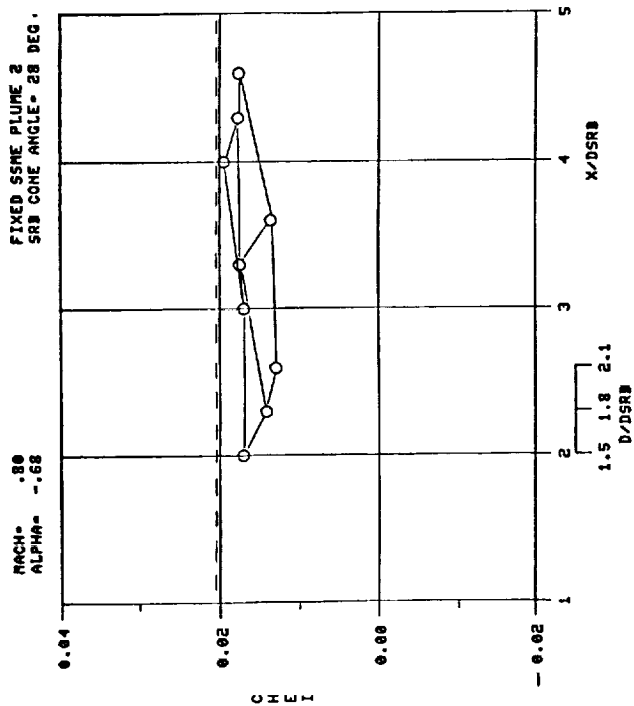
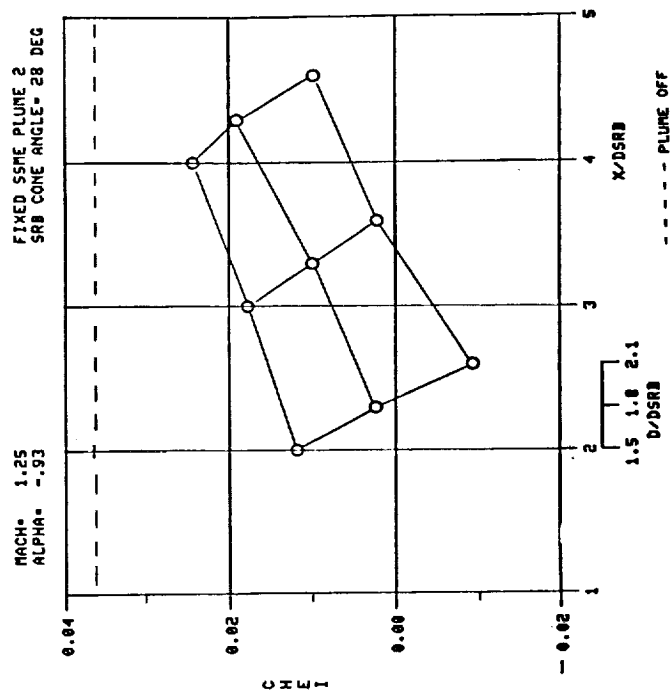
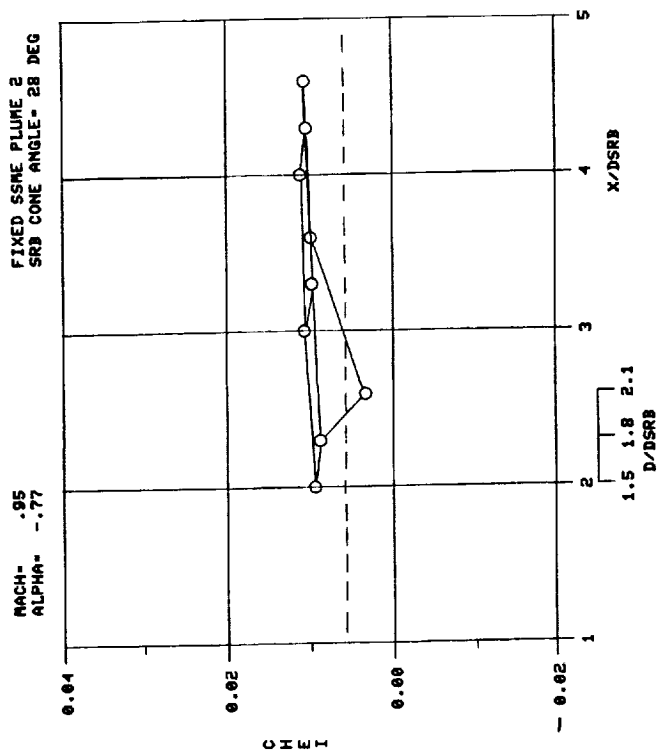


Figure J-5.

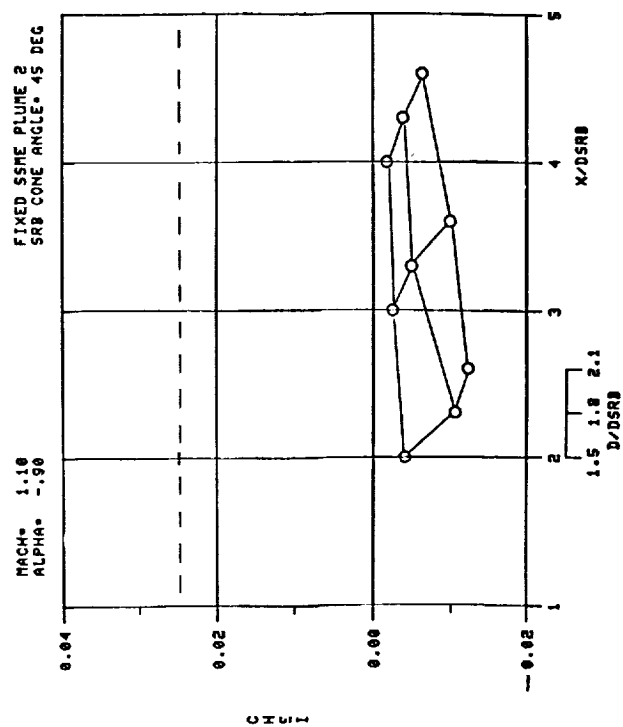
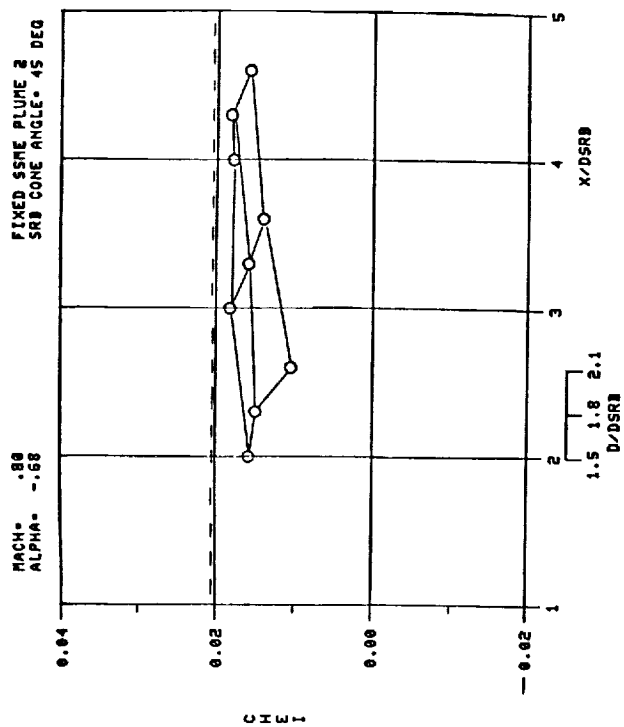
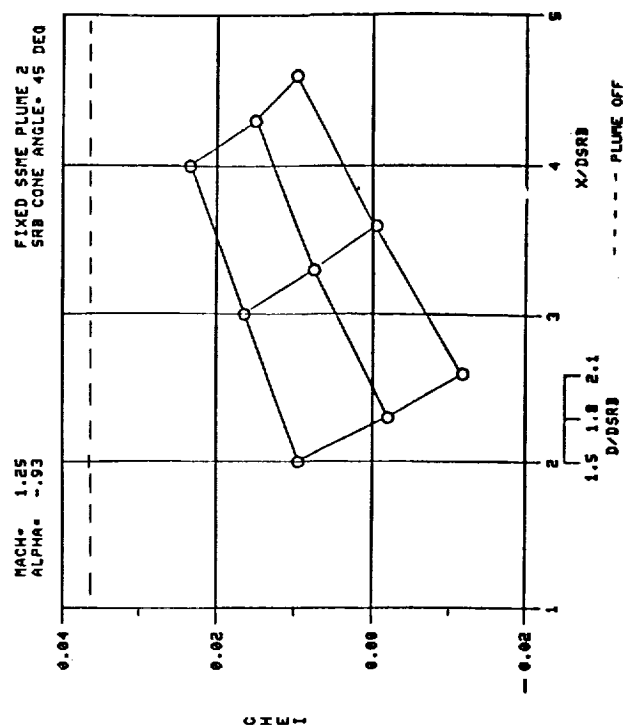
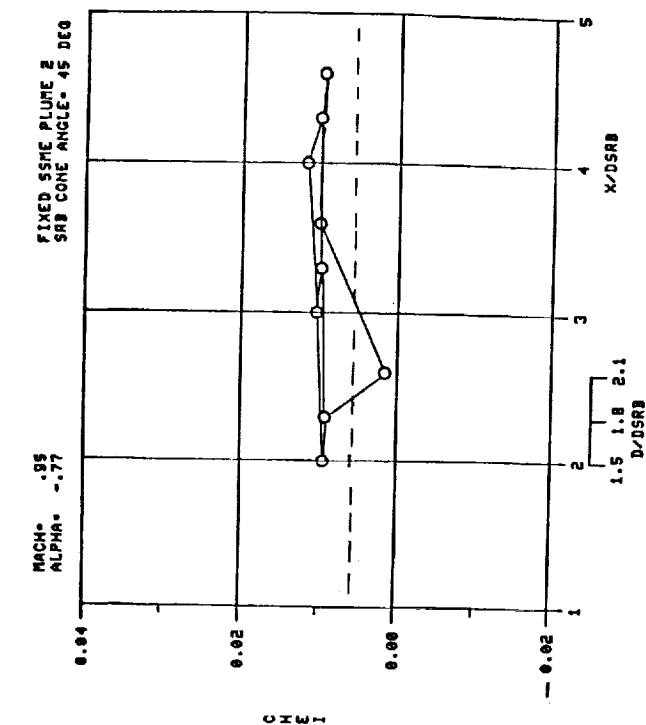
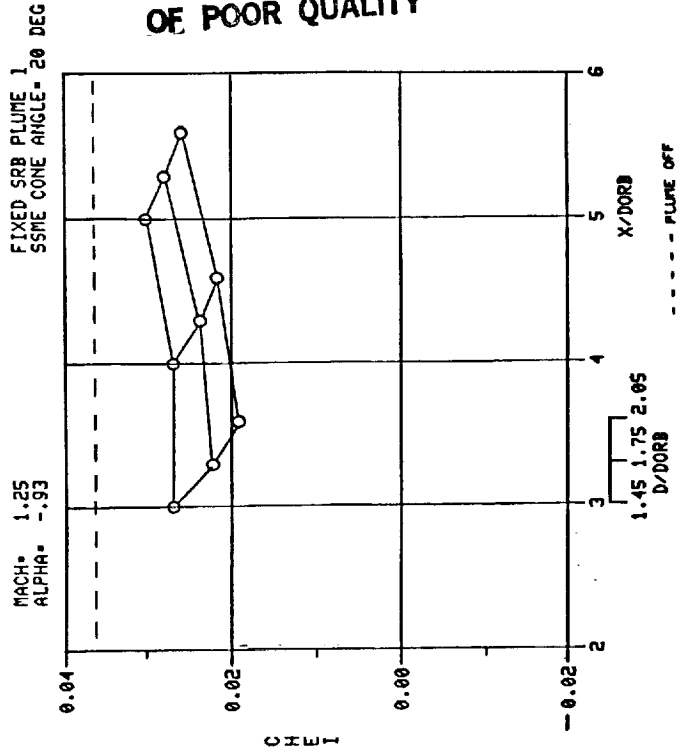
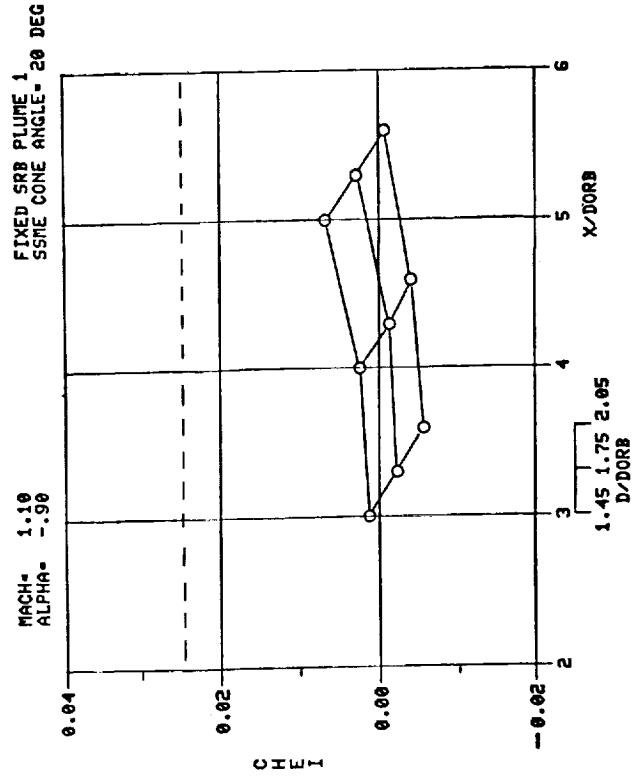
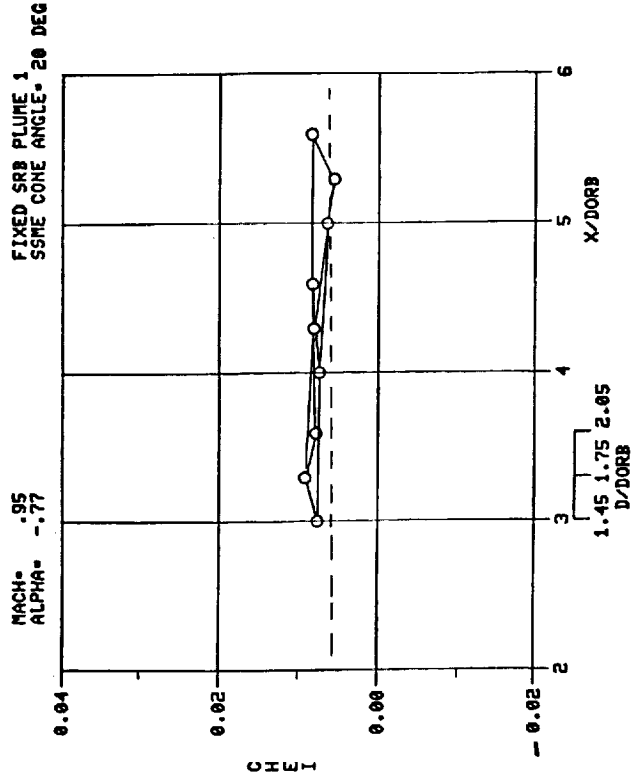
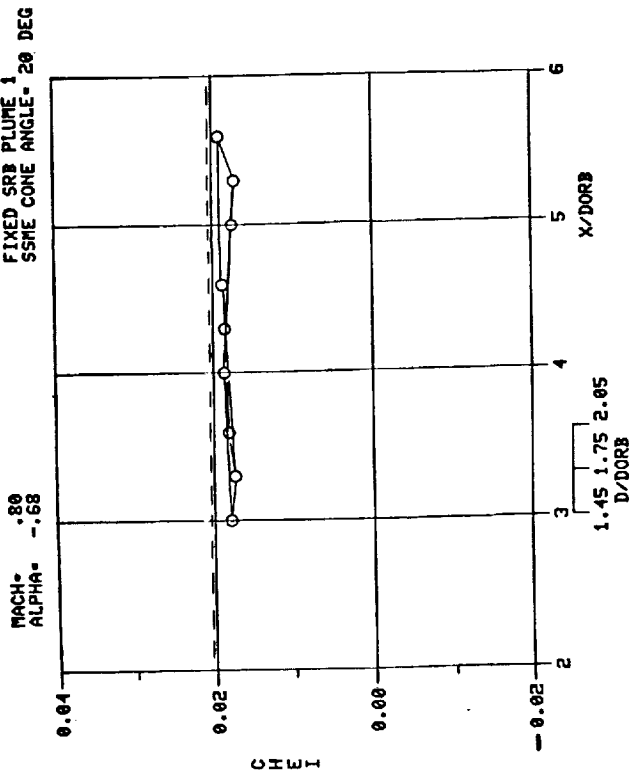


Figure J-6.



ORIGINAL PAGE IS
OF POOR QUALITY

Figure J-7.

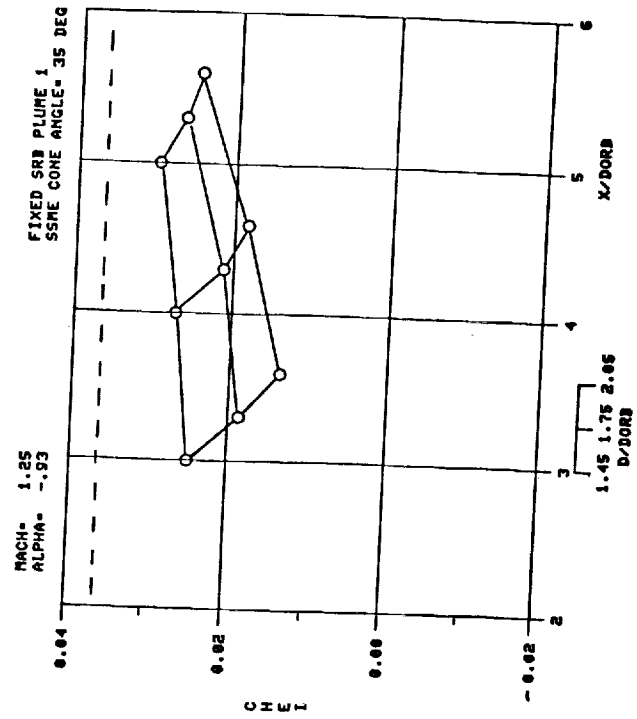
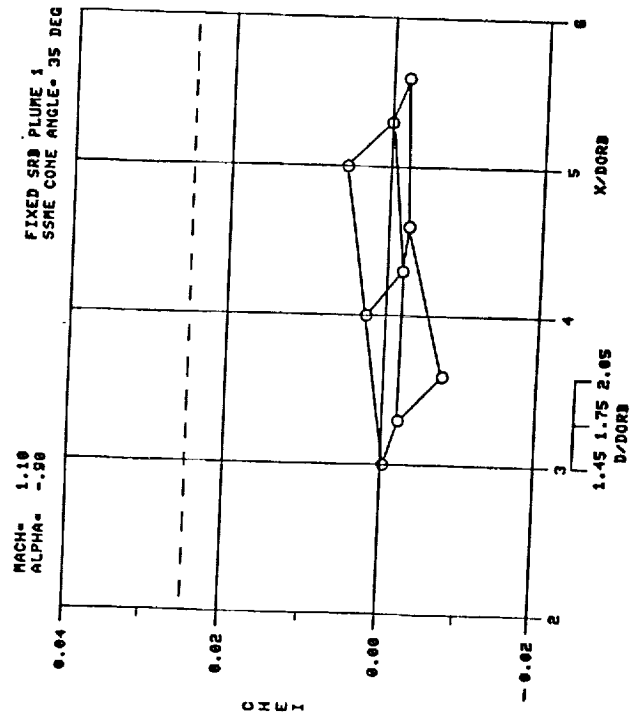
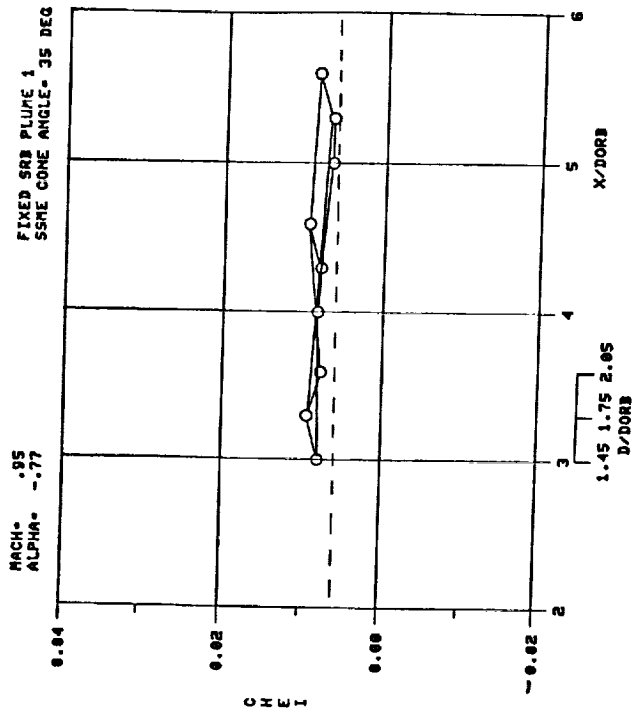
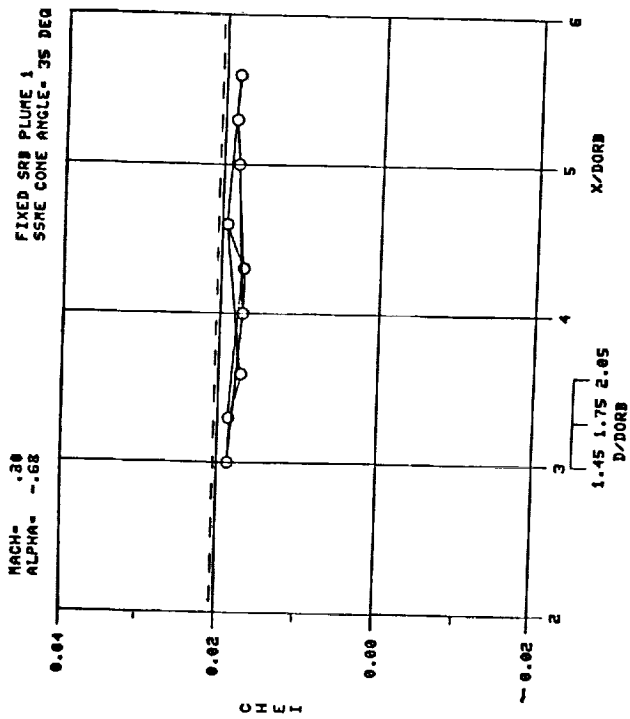


Figure J-8.

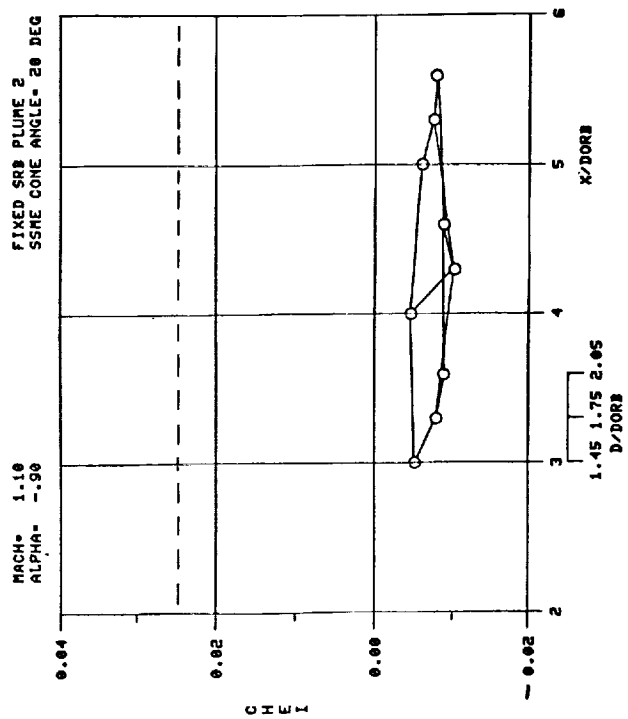
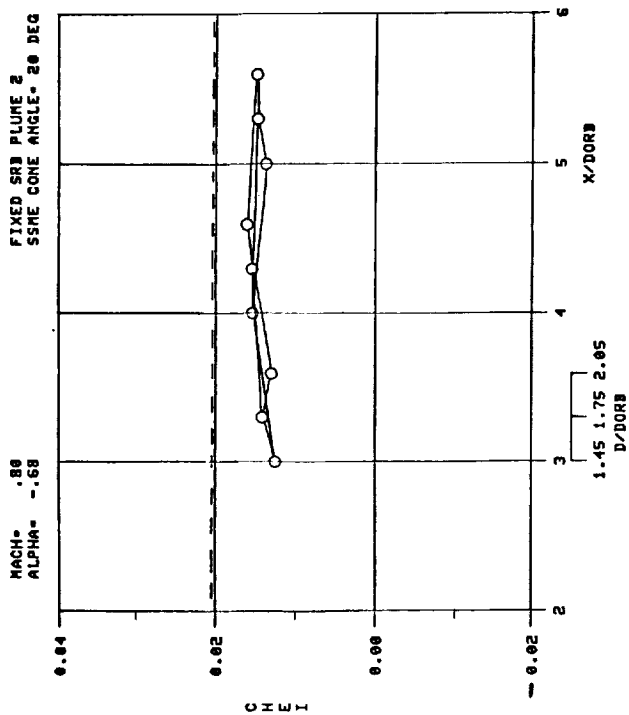
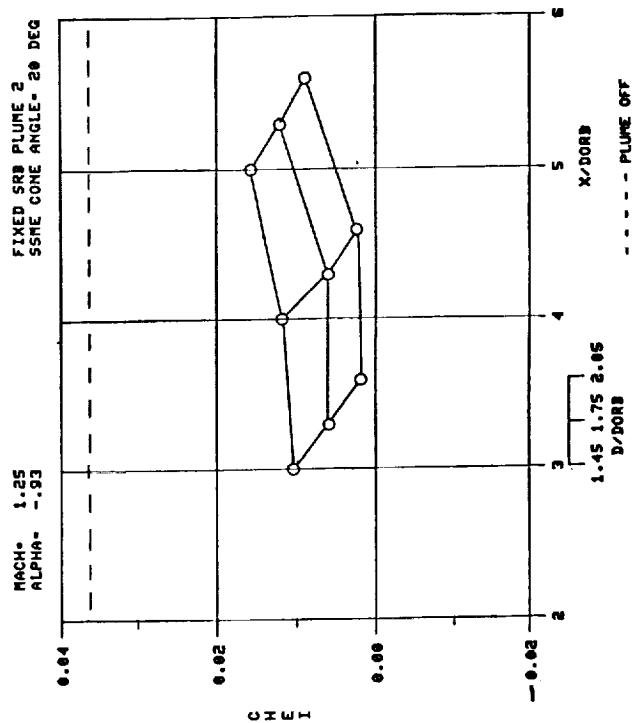
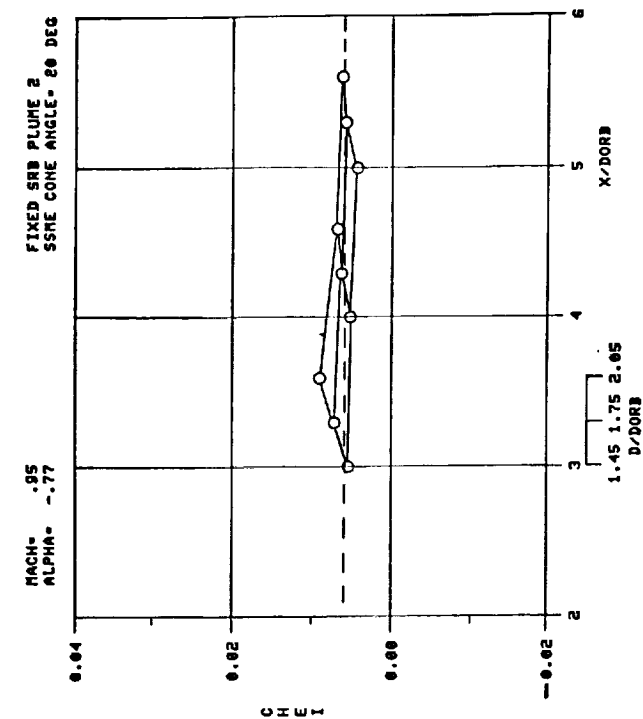


Figure J-9.

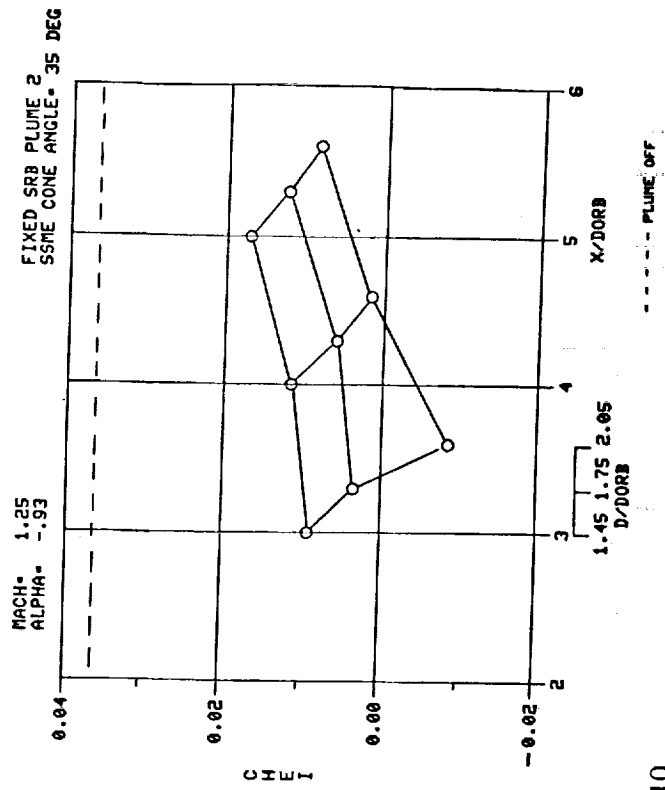
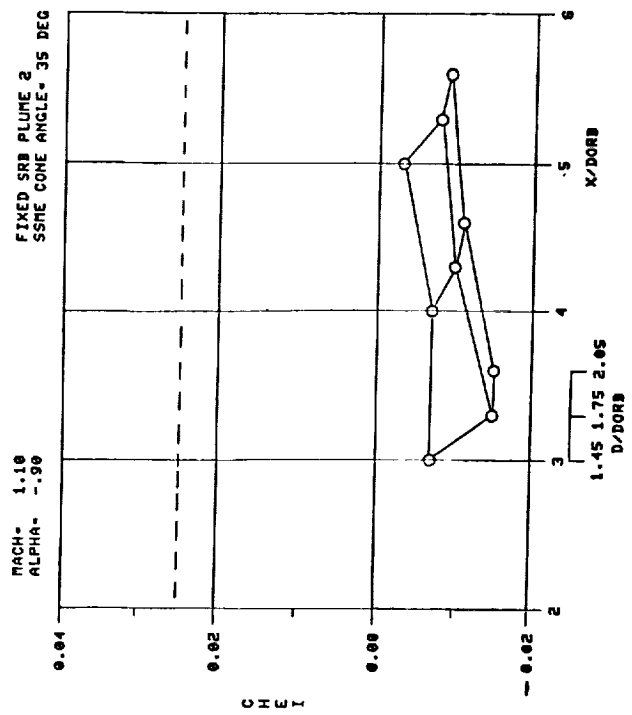
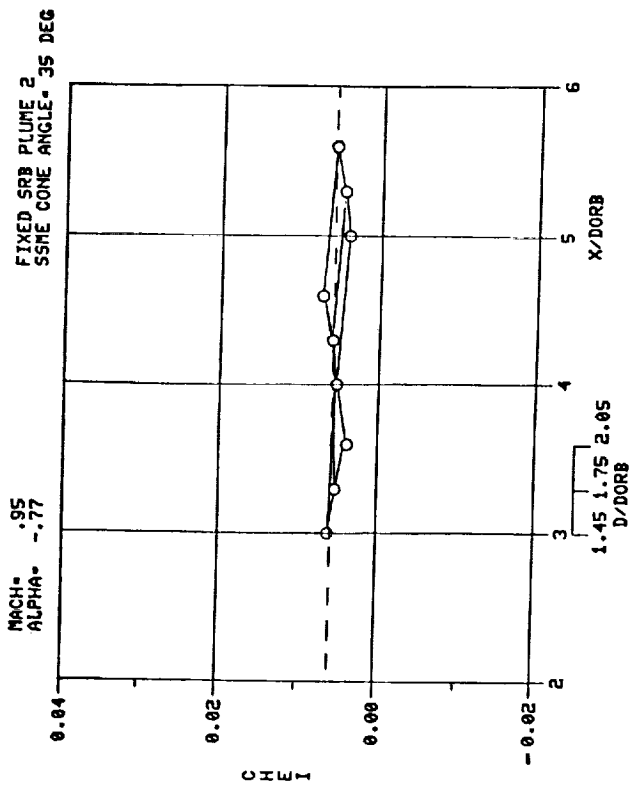
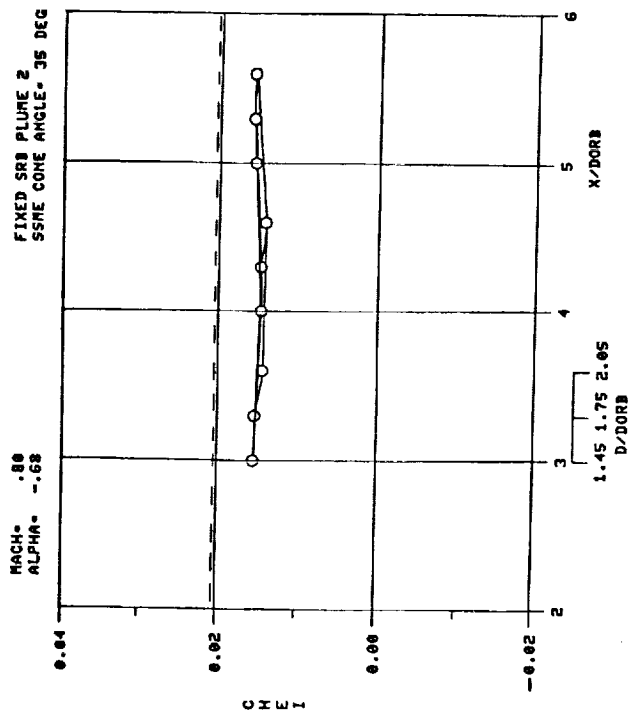


Figure J-10.

APPENDIX K

1000

1000

1000

1000

1000

1000

1000

1000

1000

1000



ORIGINAL PAGE IS
OF POOR QUALITY

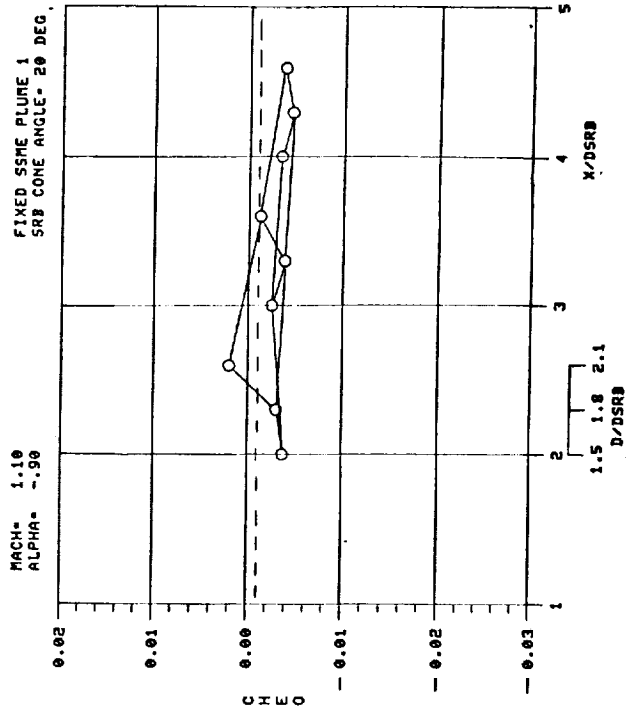
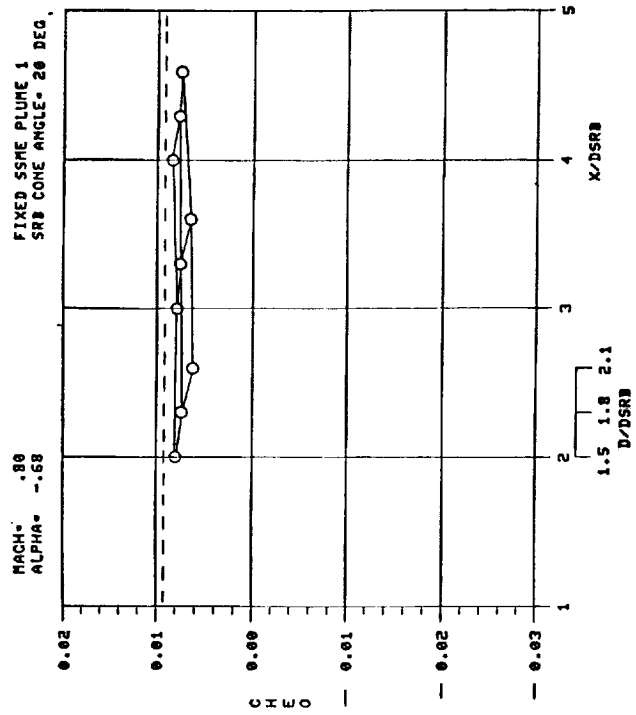
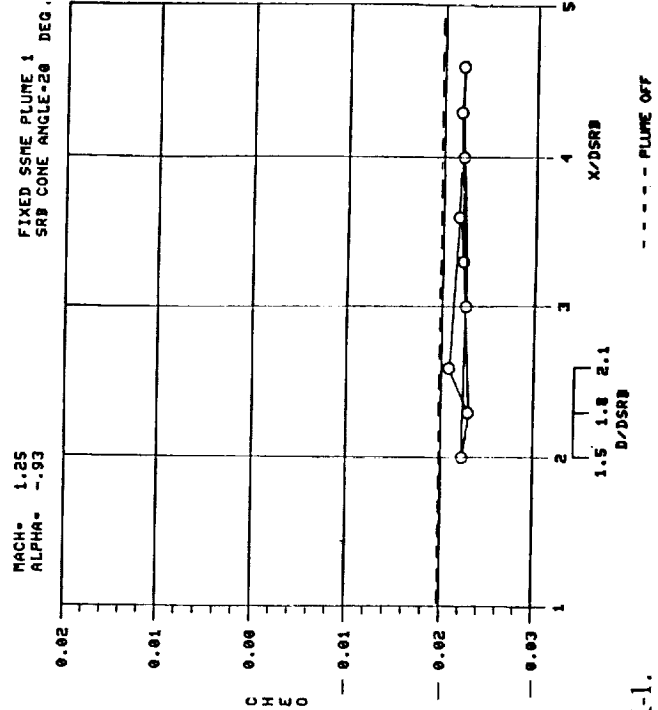
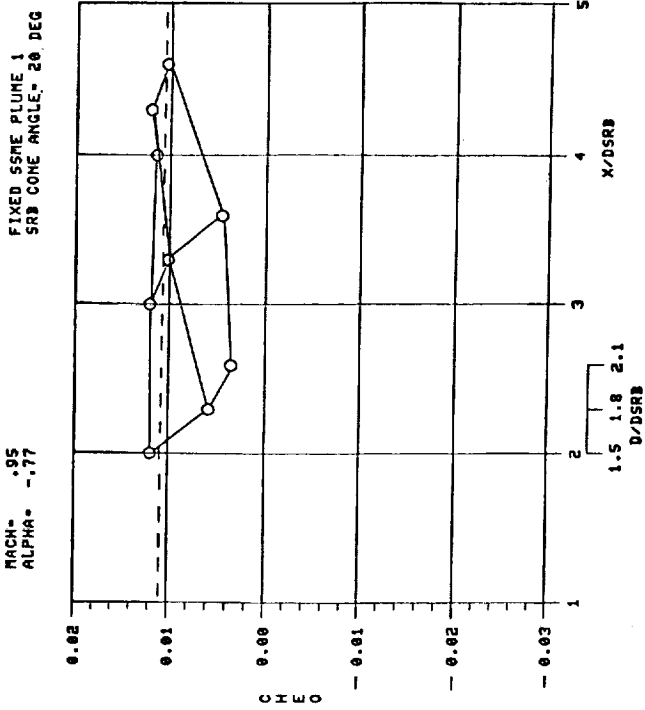


Figure K-1.

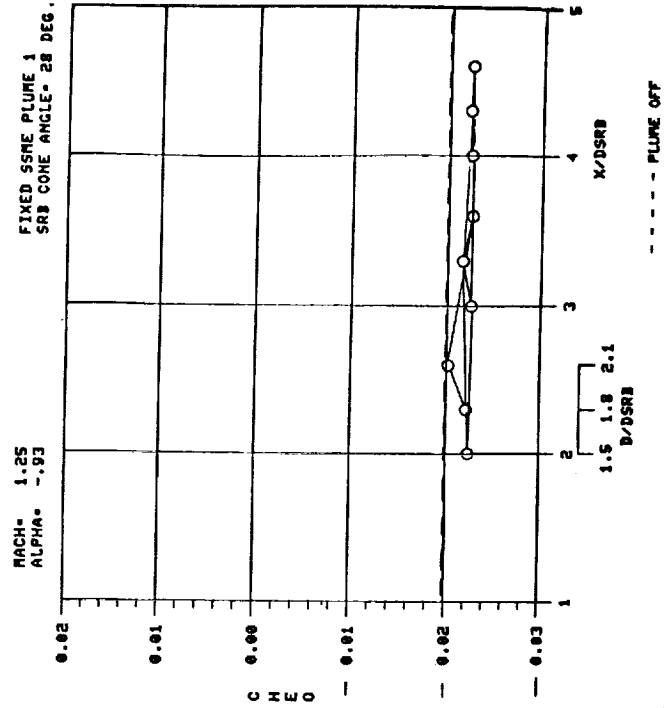
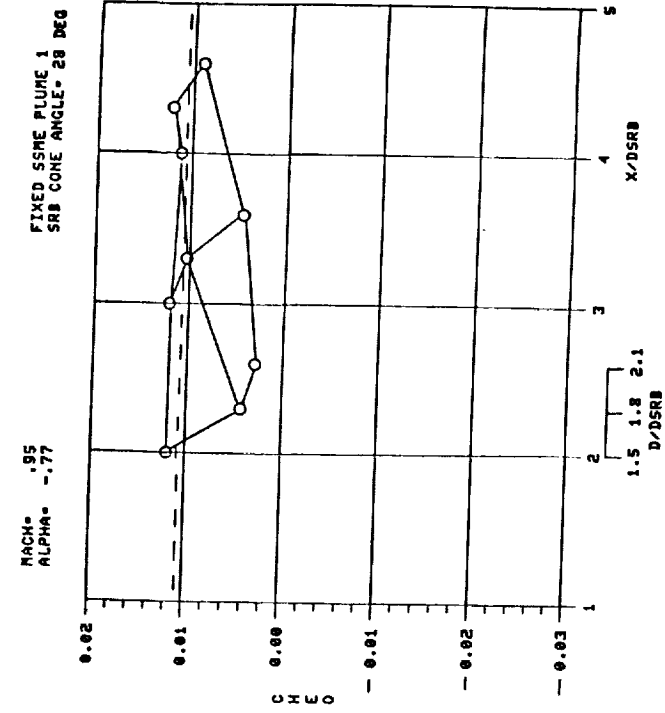
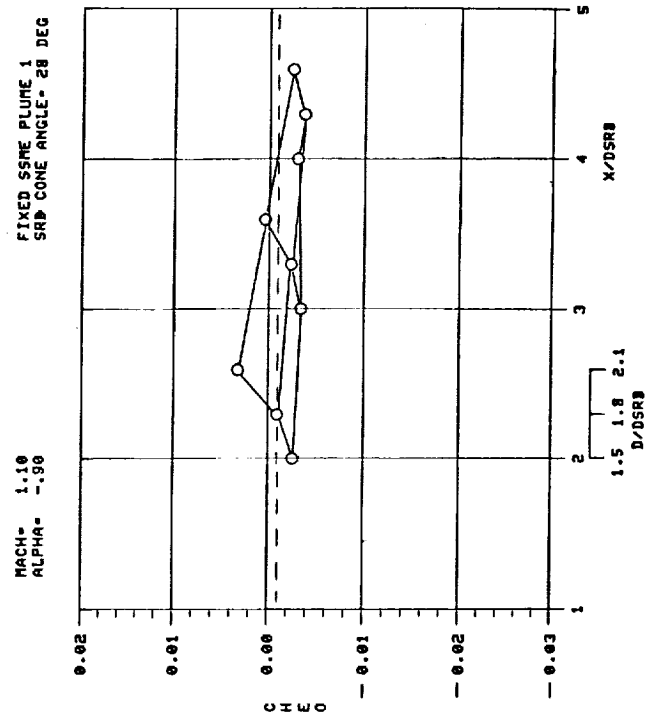
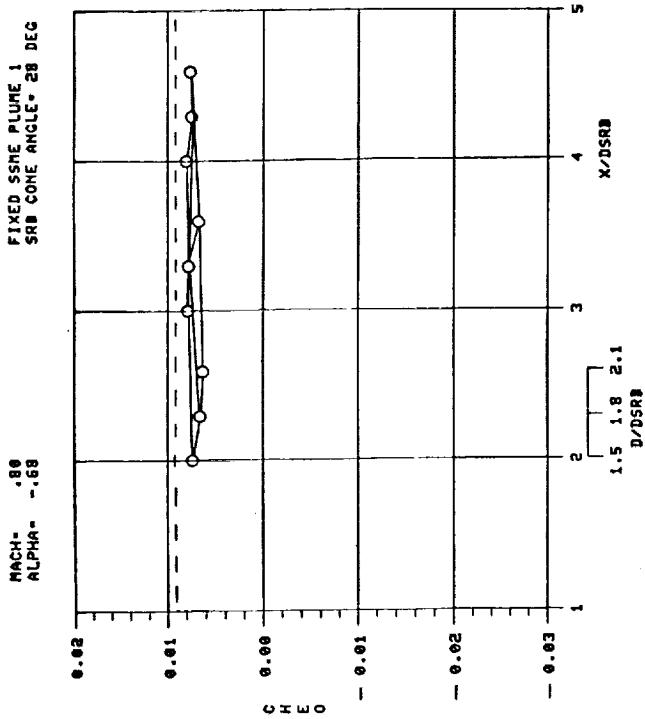


Figure K-2.

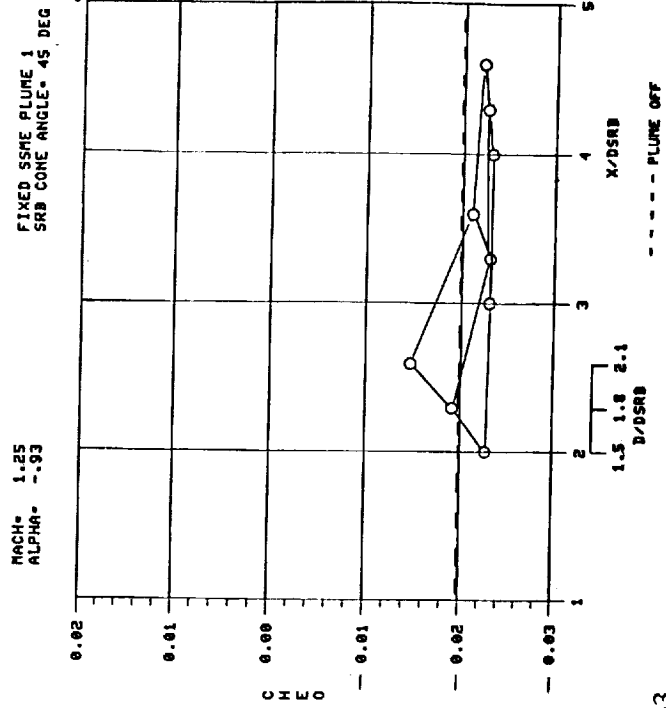
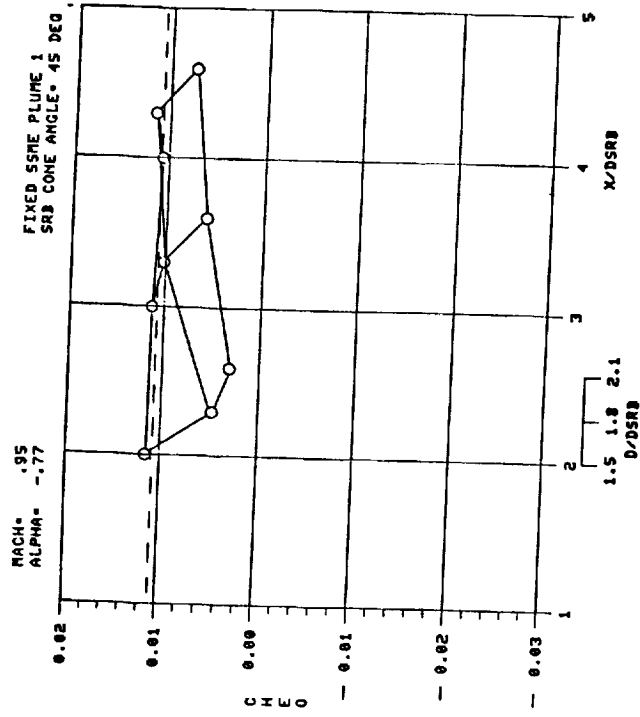
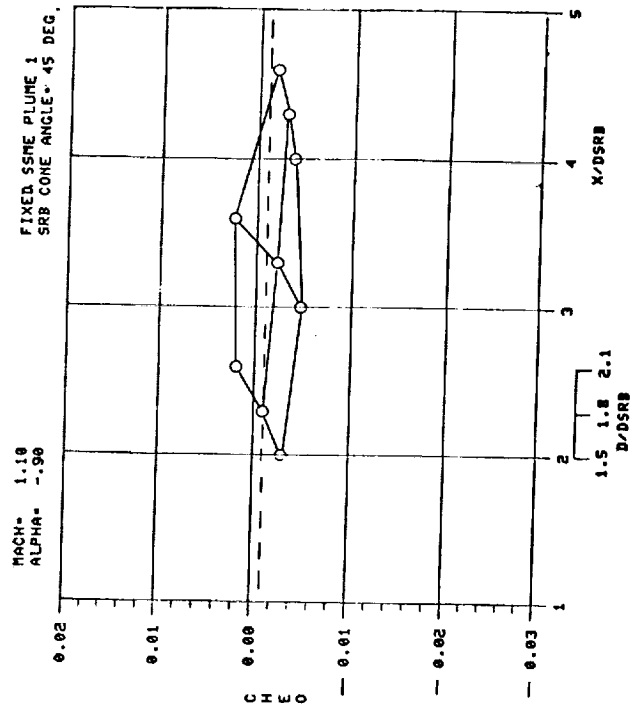
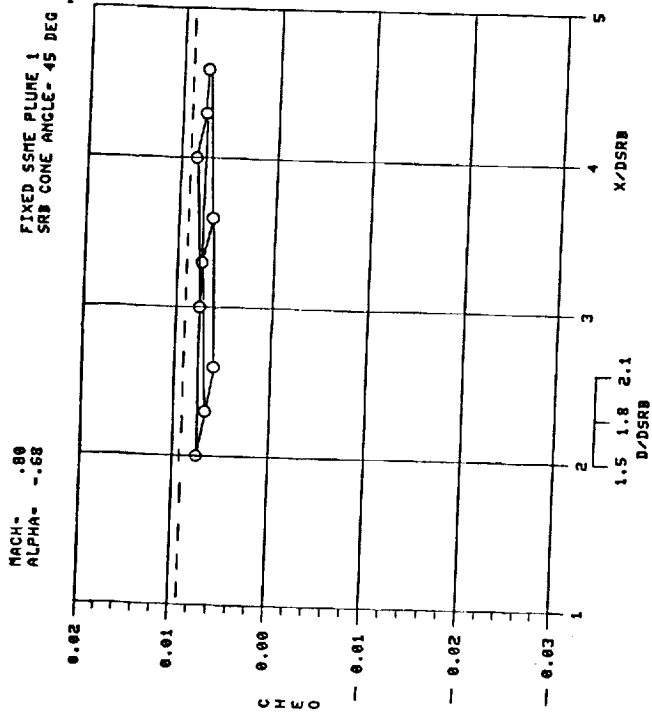


Figure K-3.

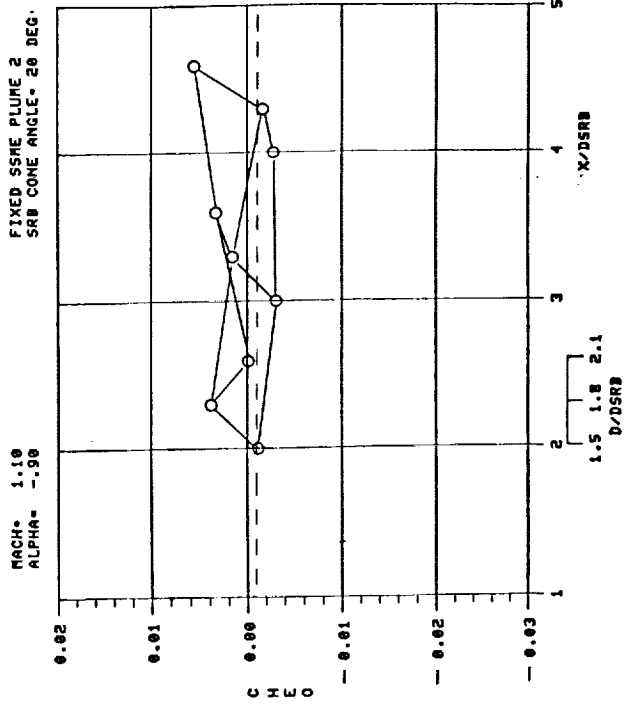
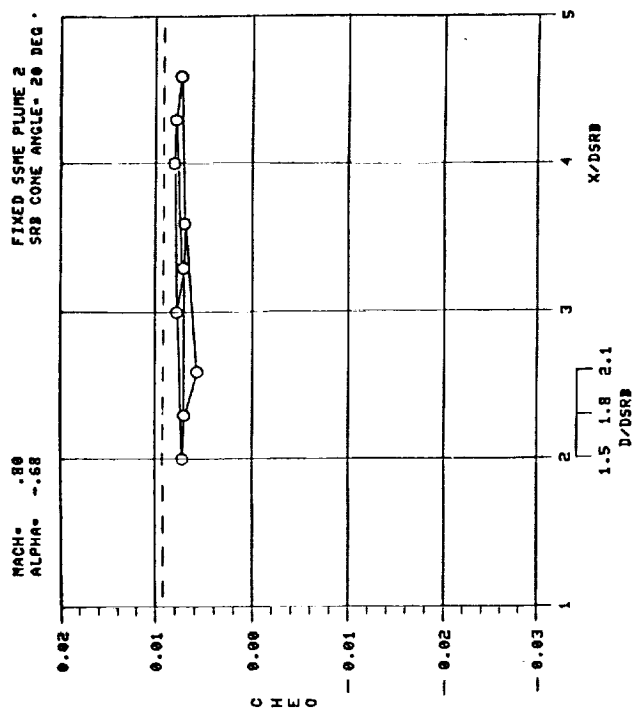
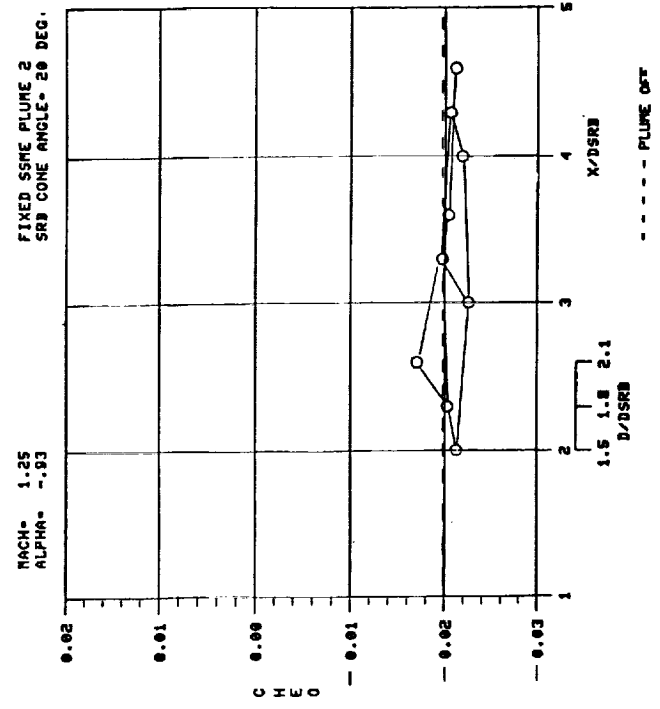
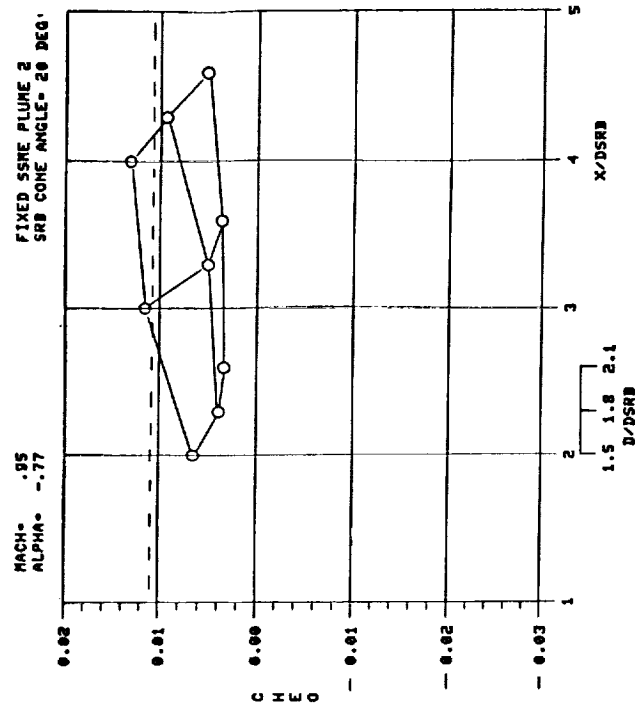


Figure K-4.

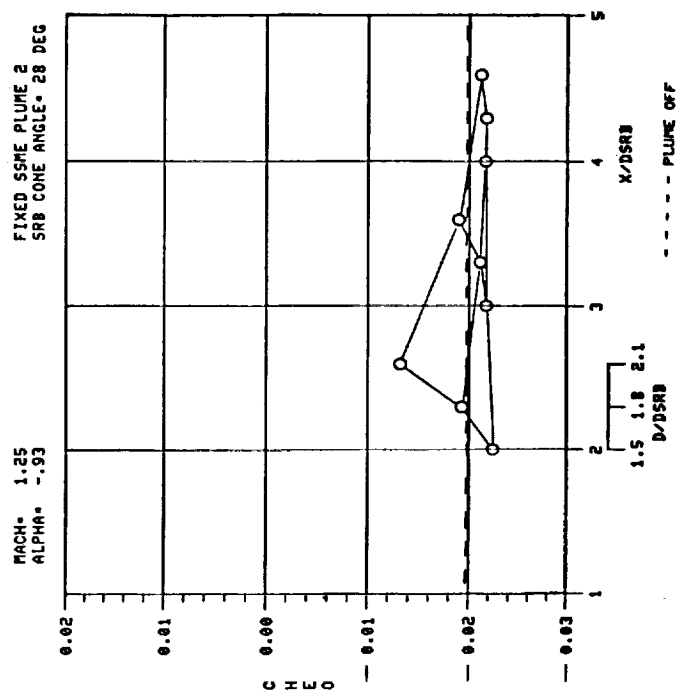
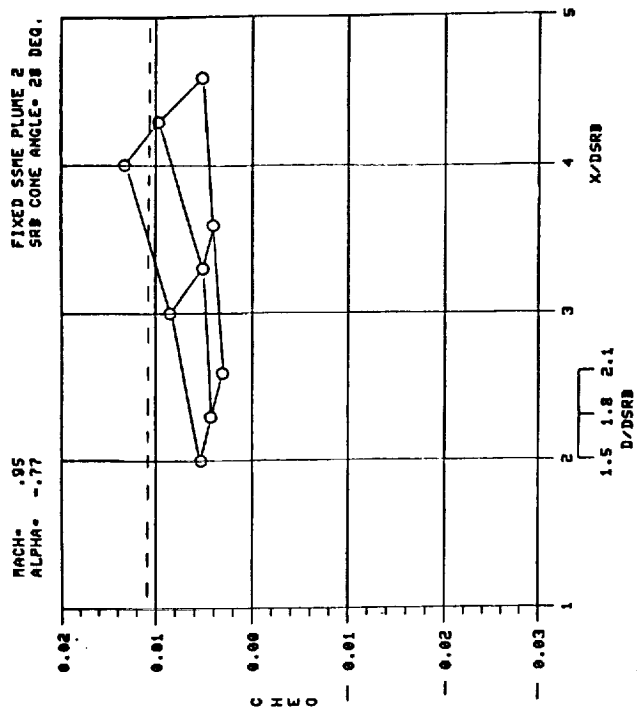
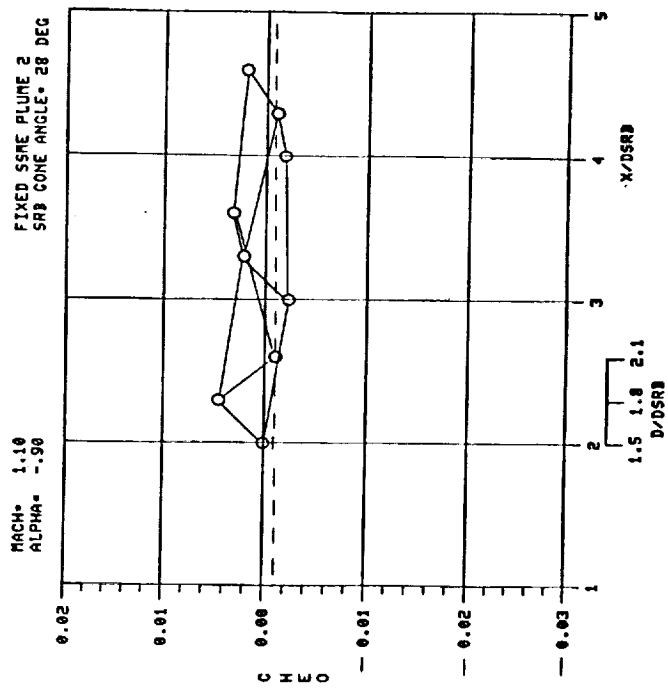
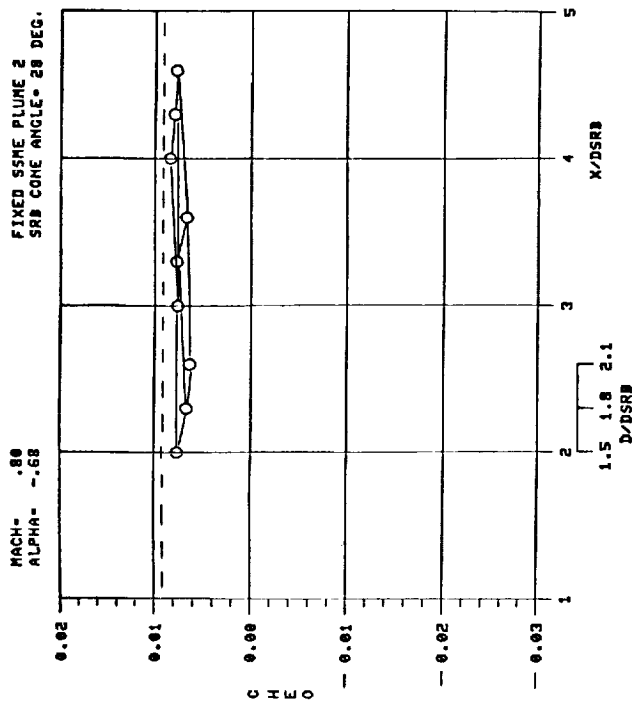


Figure K-5.

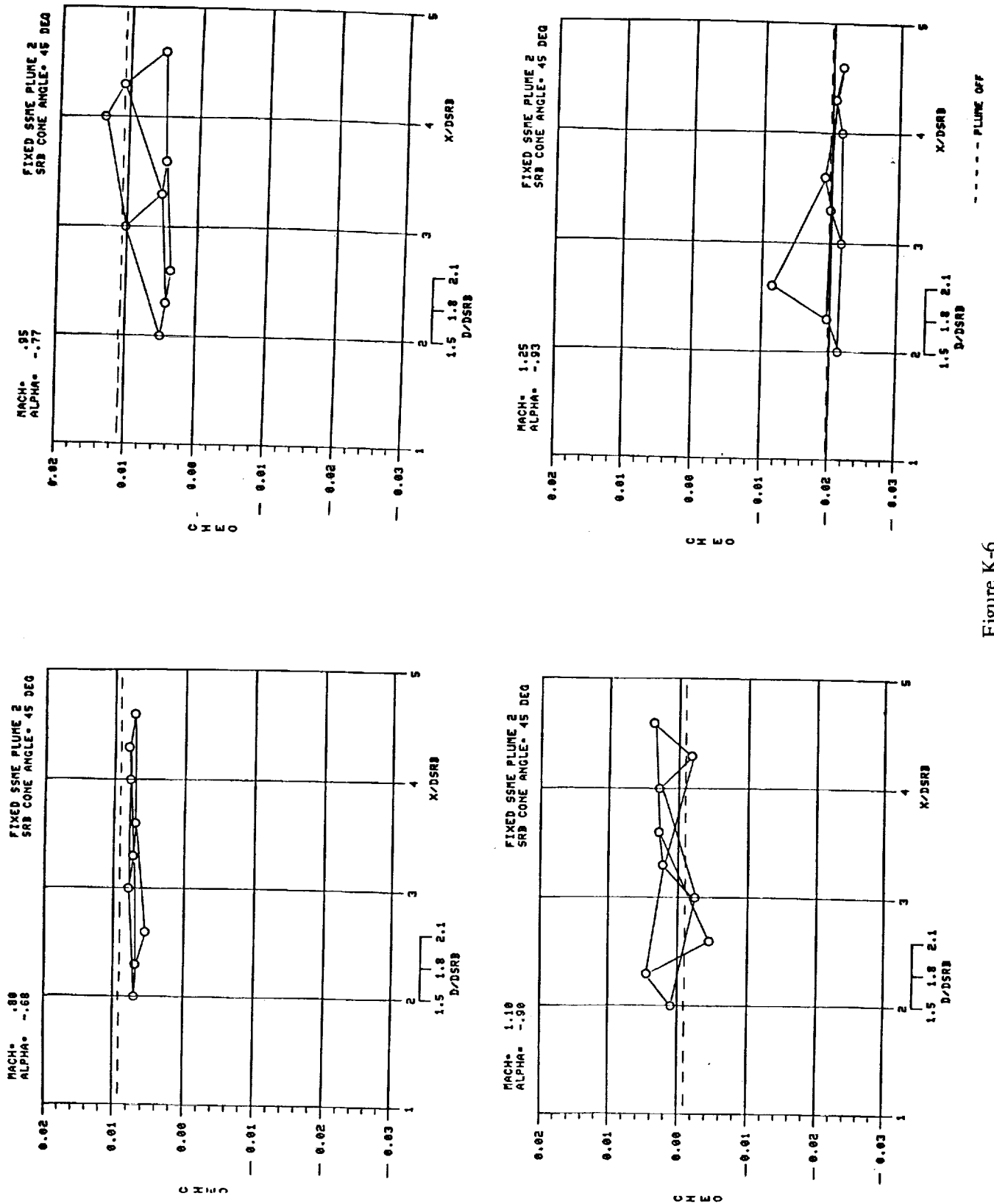


Figure K-6.

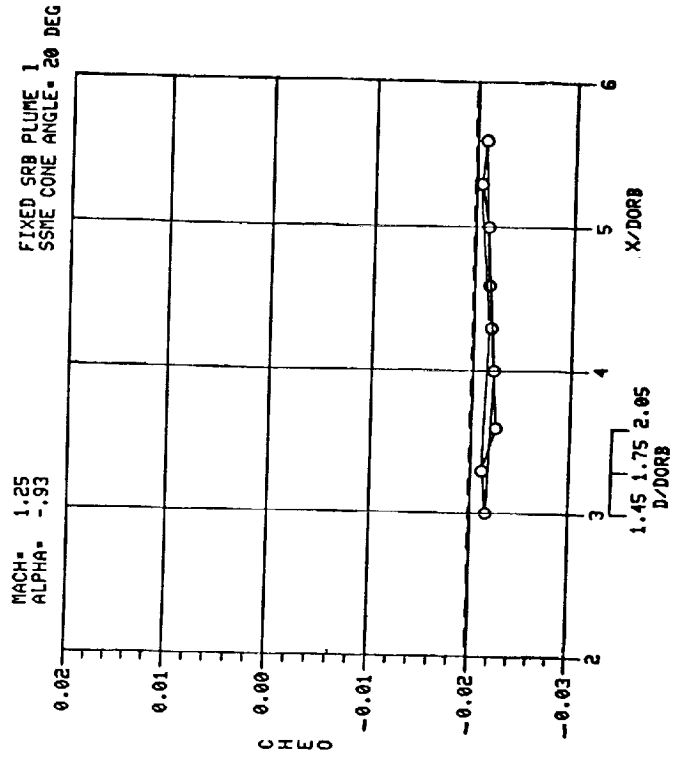
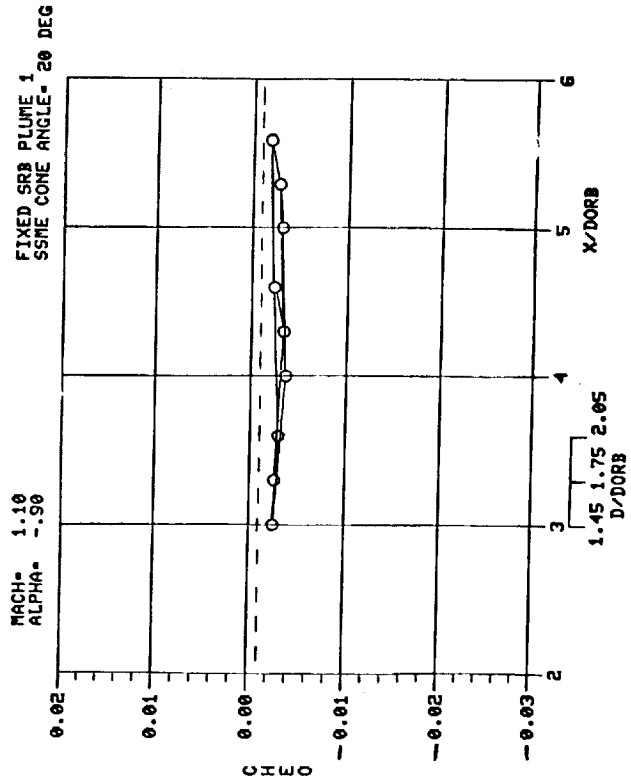
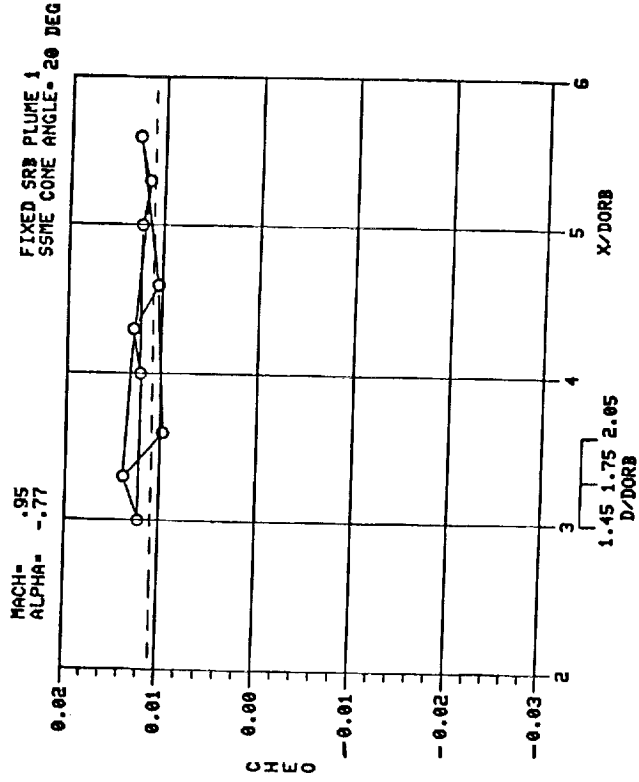
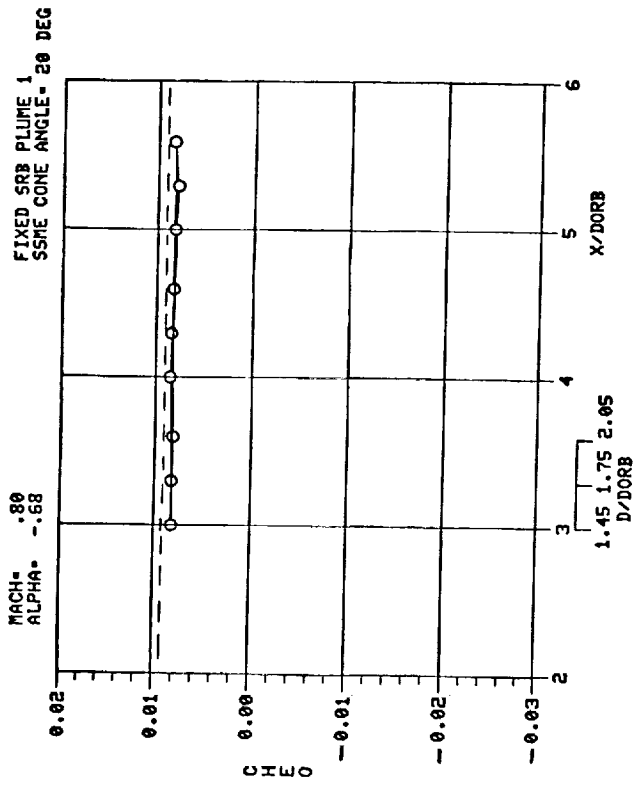


Figure K-7.

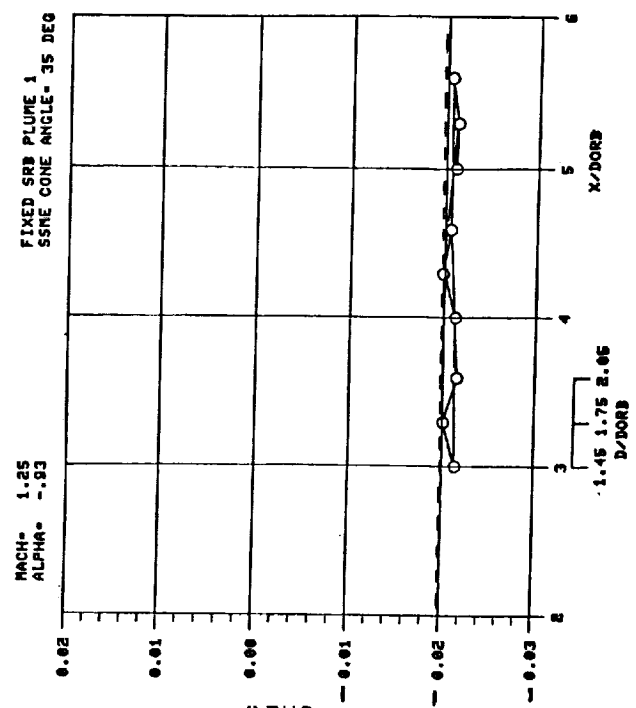
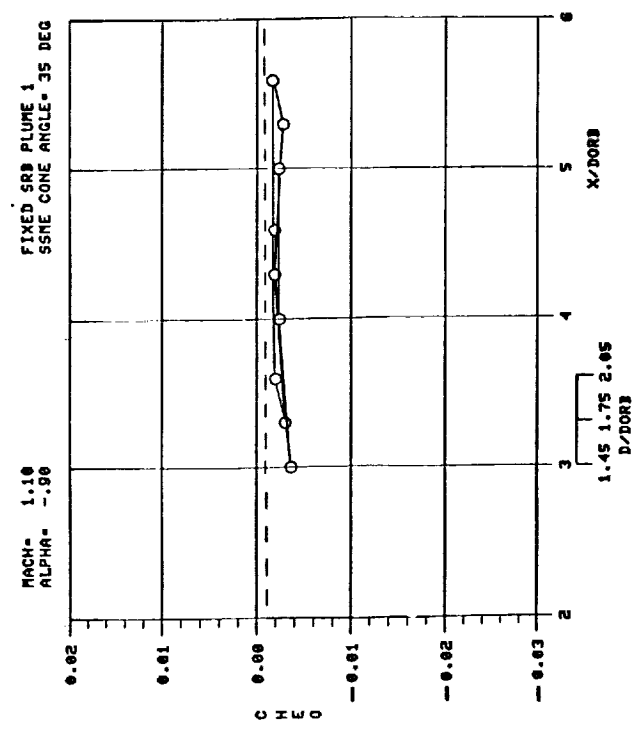
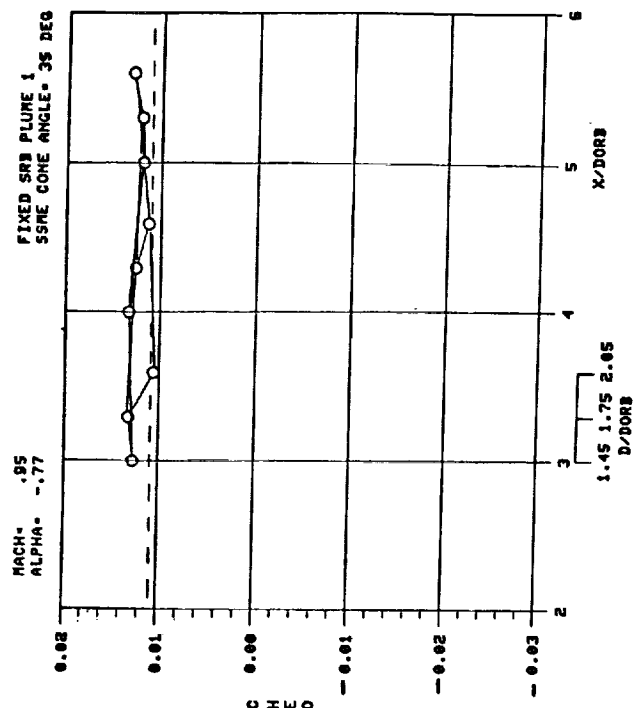
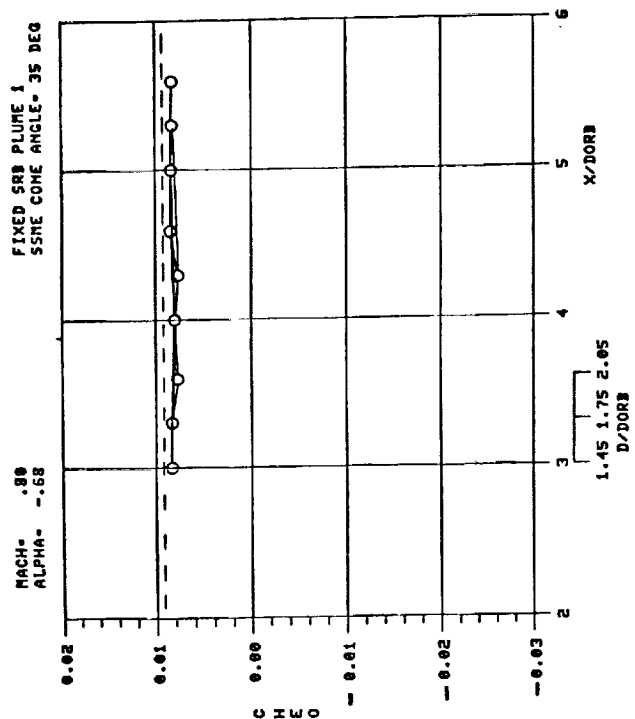


Figure K-8.

ORIGINAL PAGE IS
OF POOR QUALITY

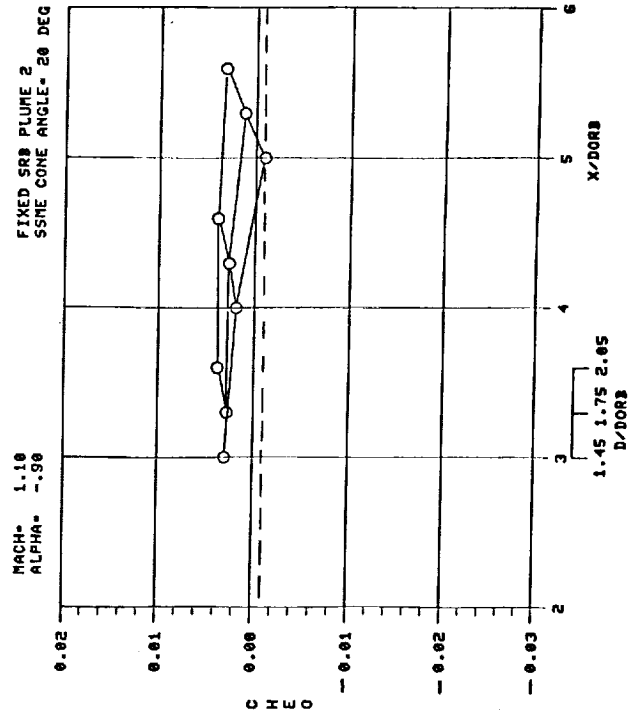
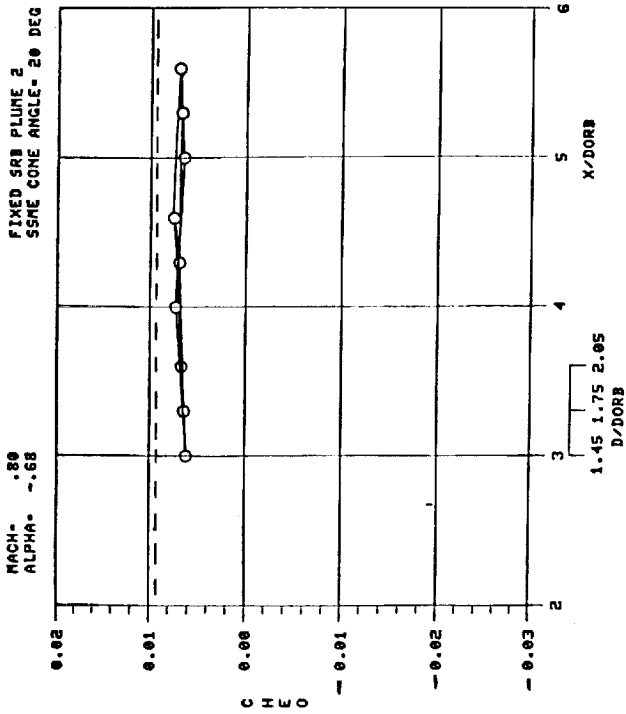
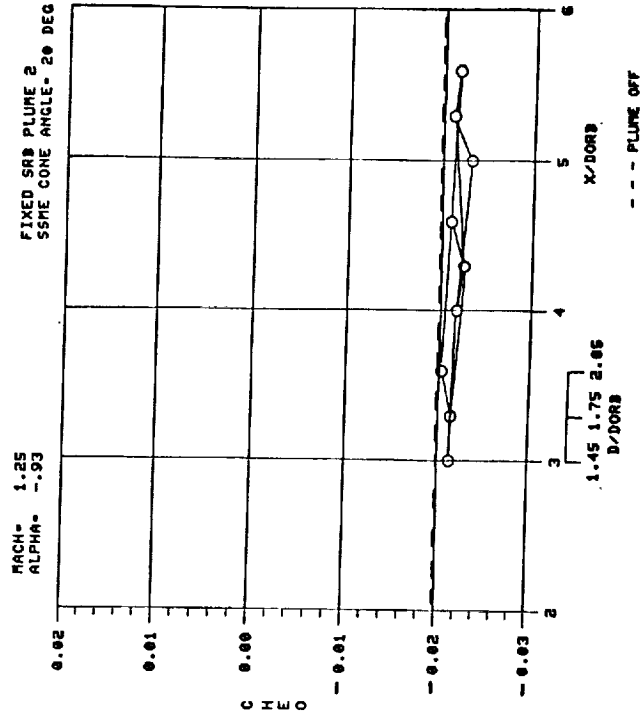
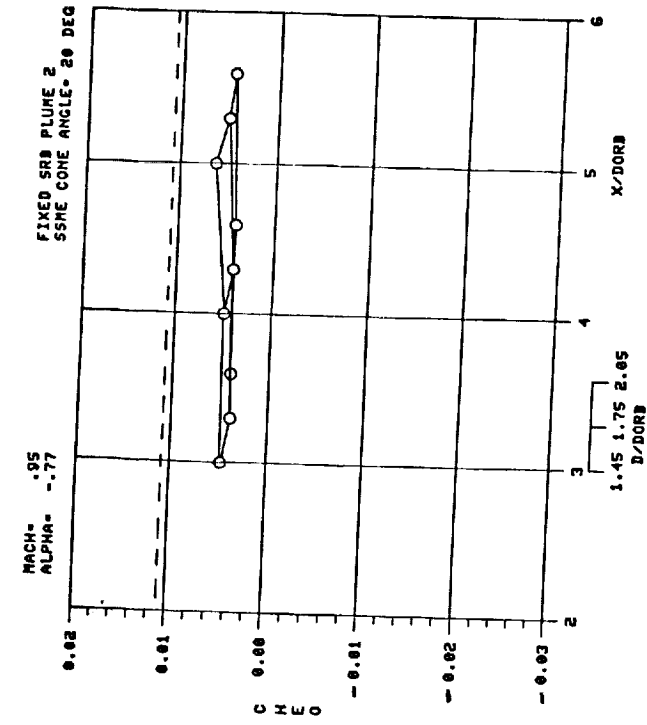


Figure K-9.

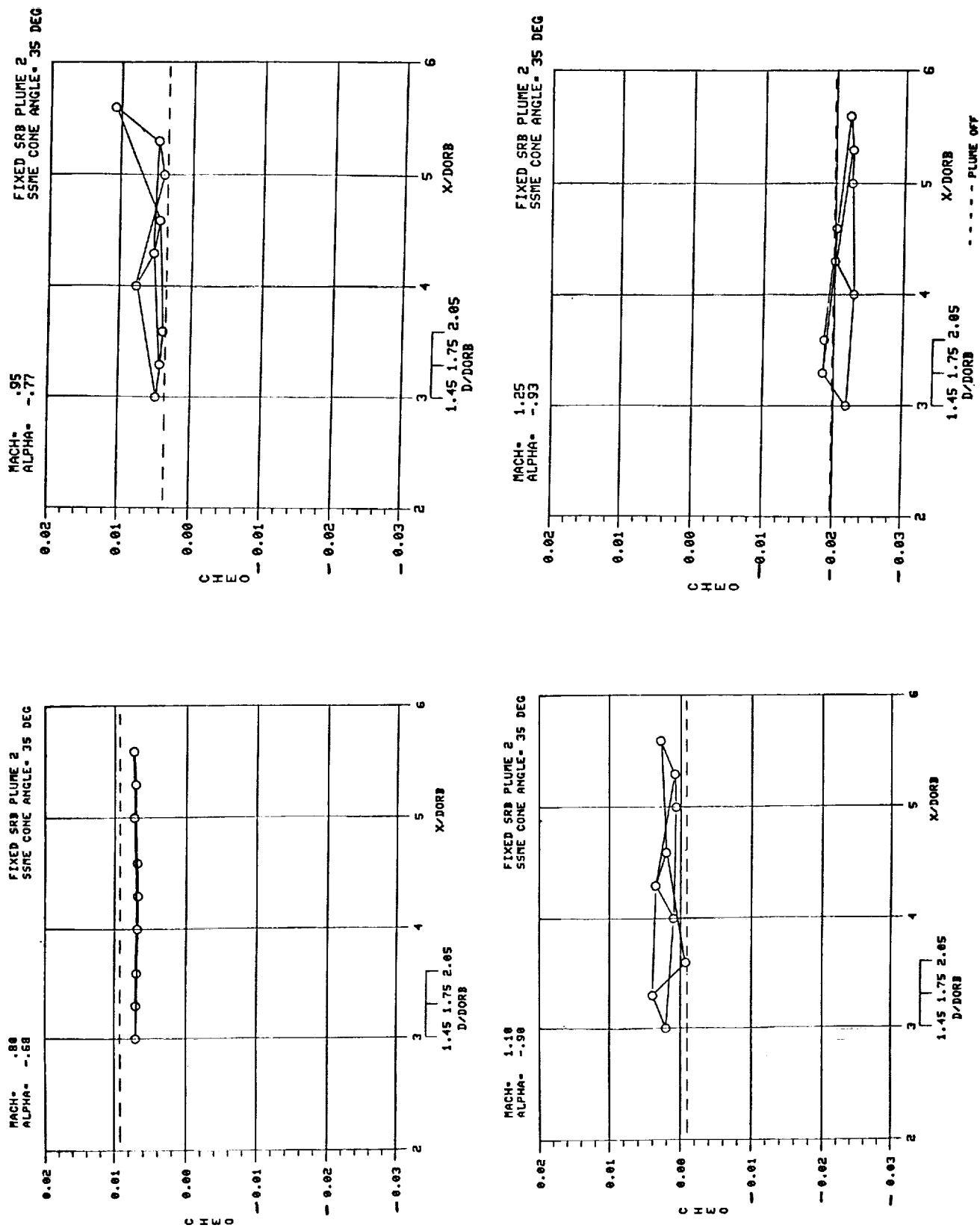


Figure K-10.

APPENDIX L

ORIGINAL PAGE IS
OF POOR QUALITY

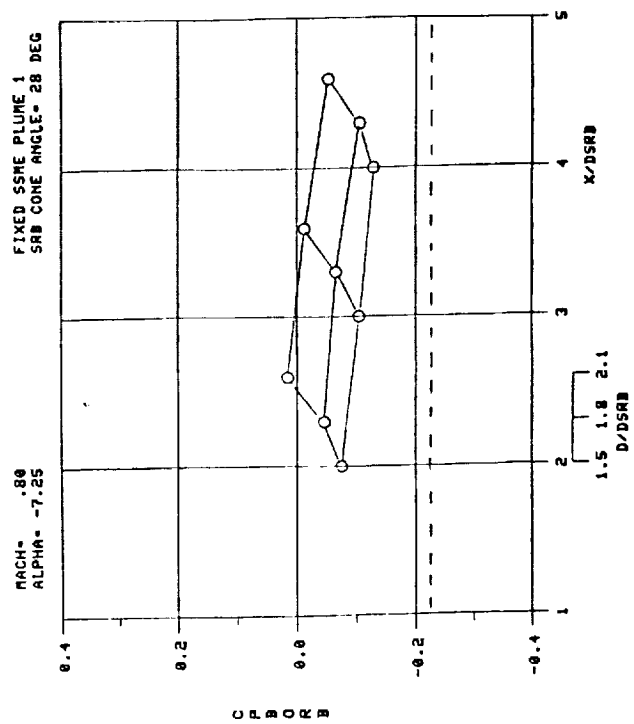
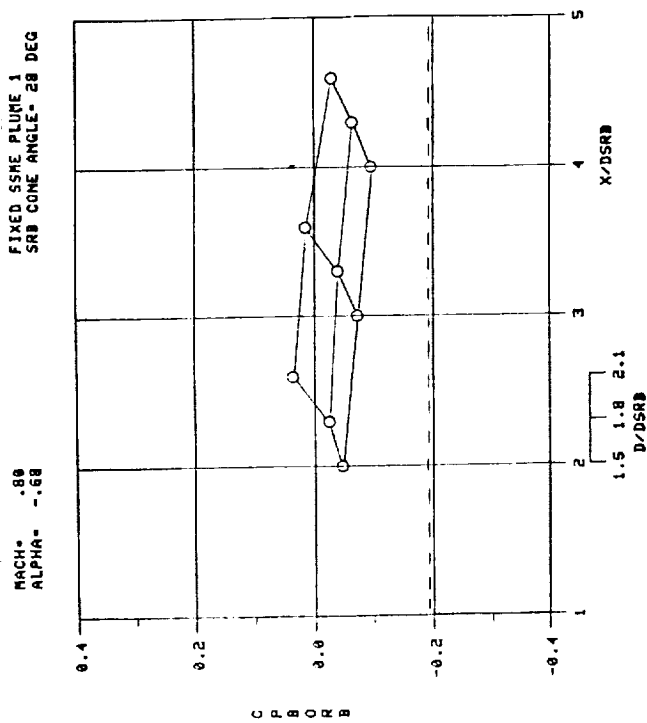
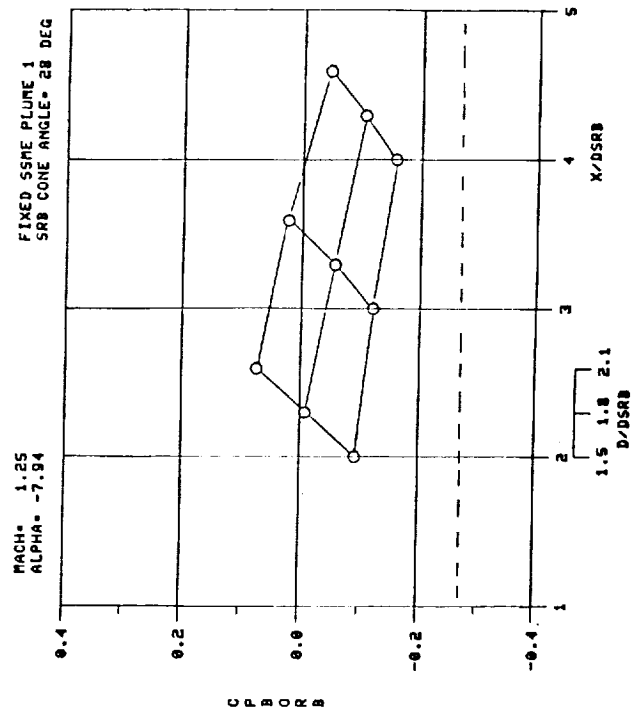
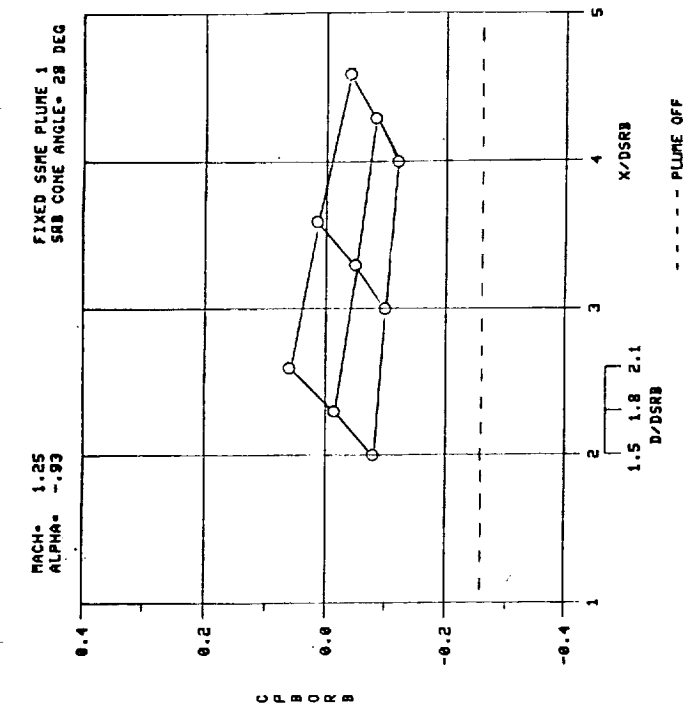


Figure L-1.

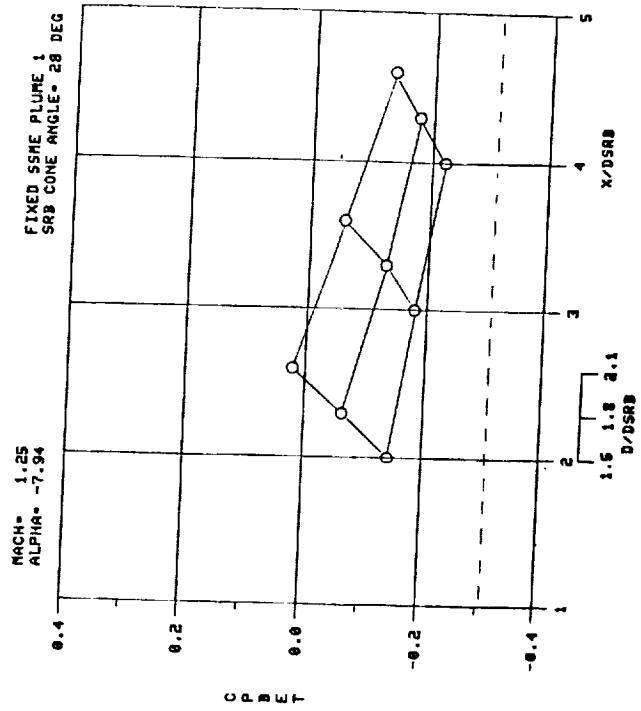
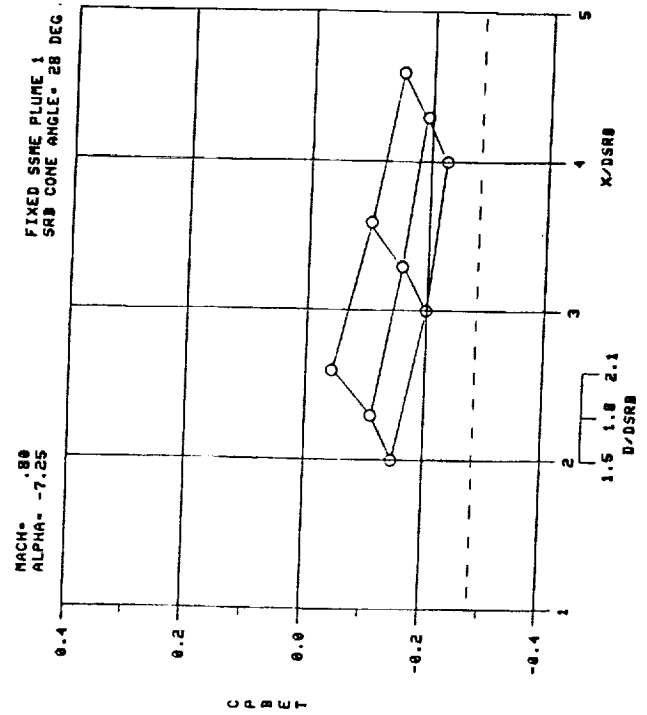
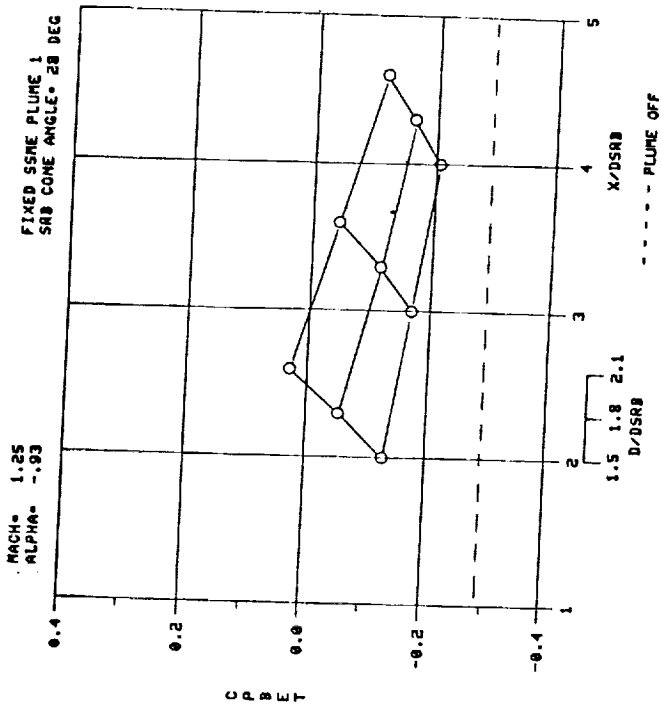
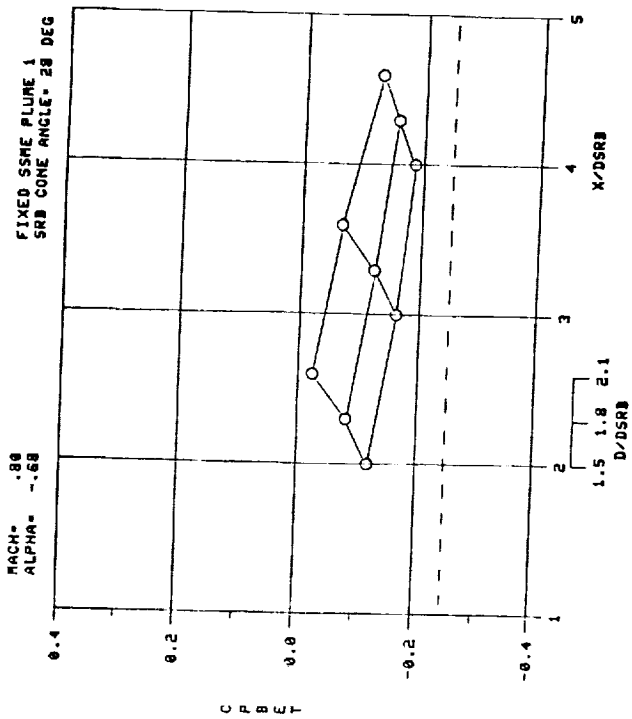


Figure L-2.

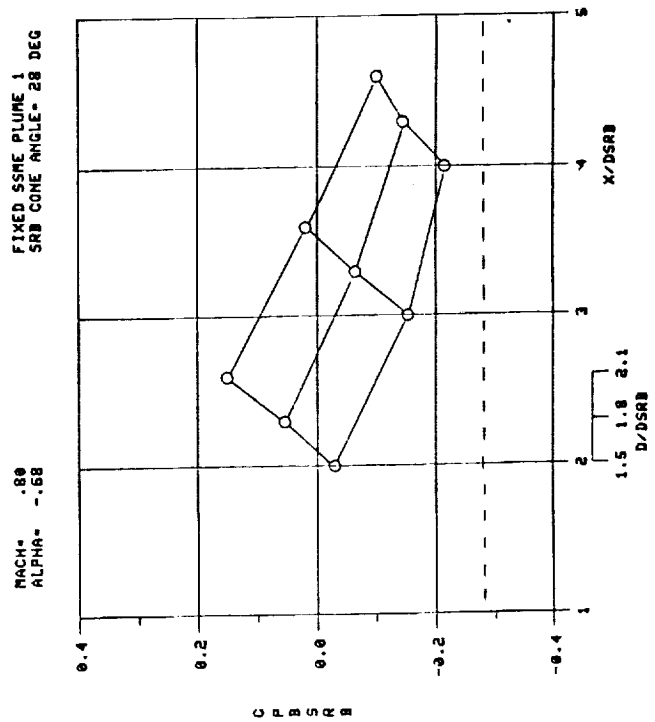
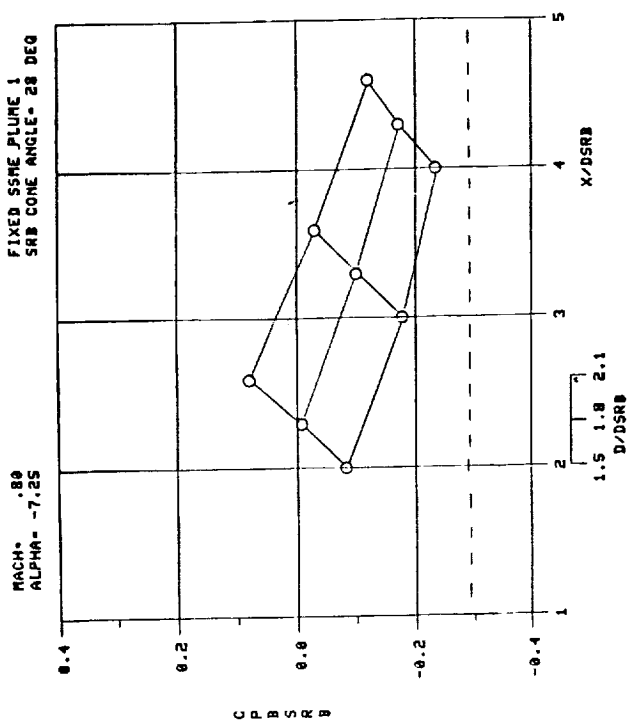
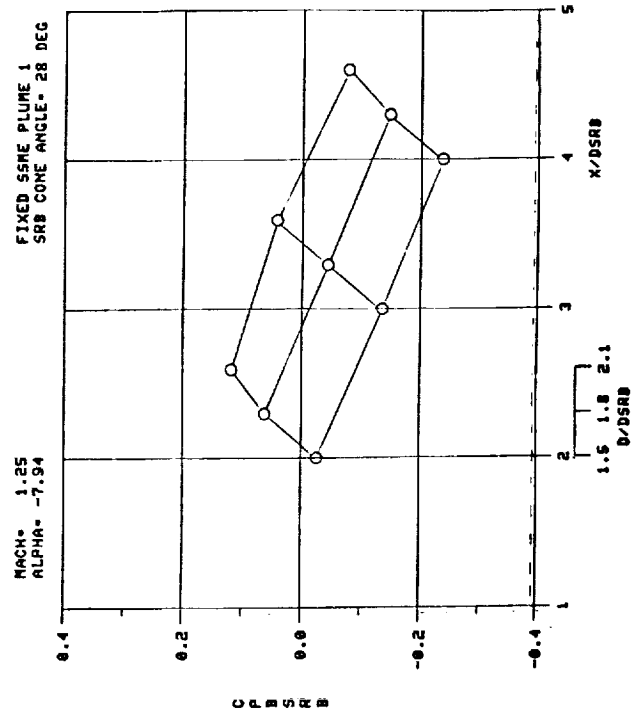
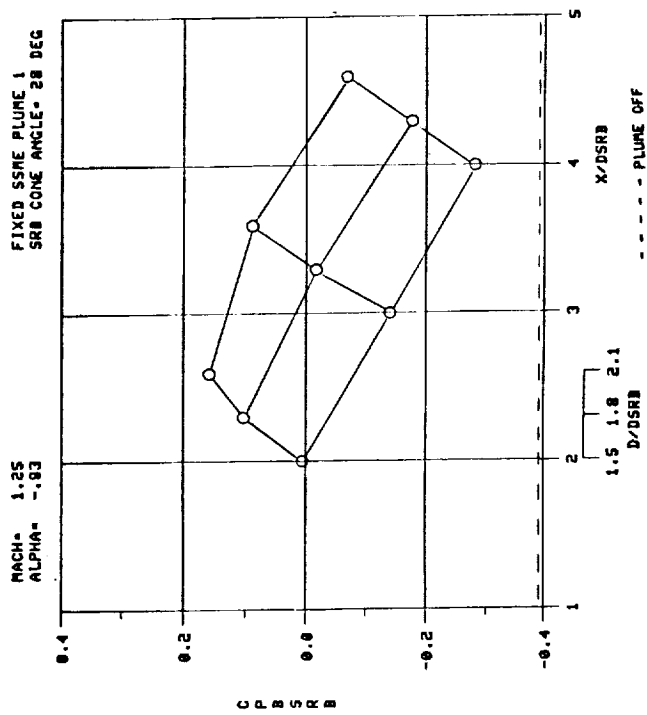


Figure L-3.

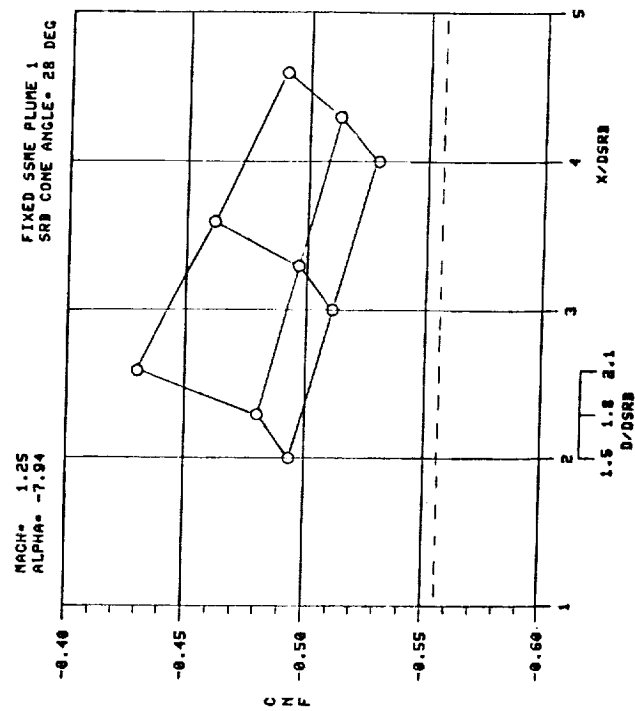
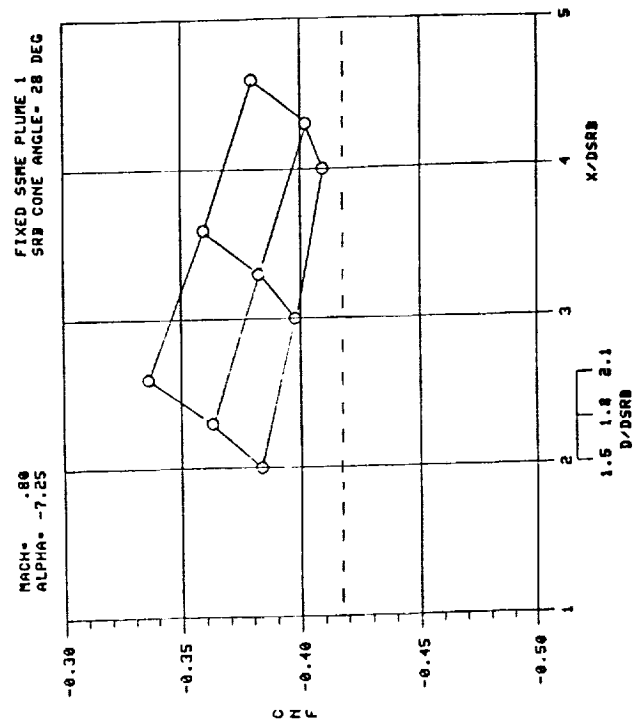
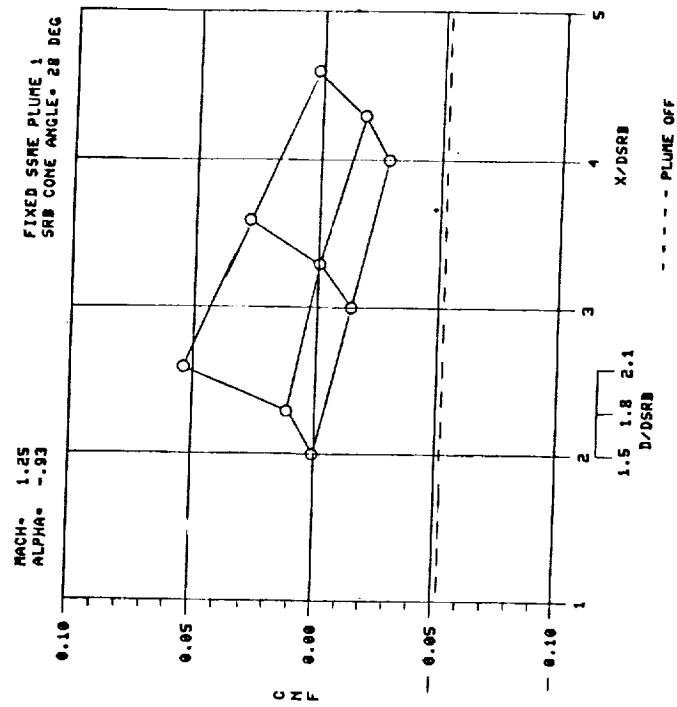
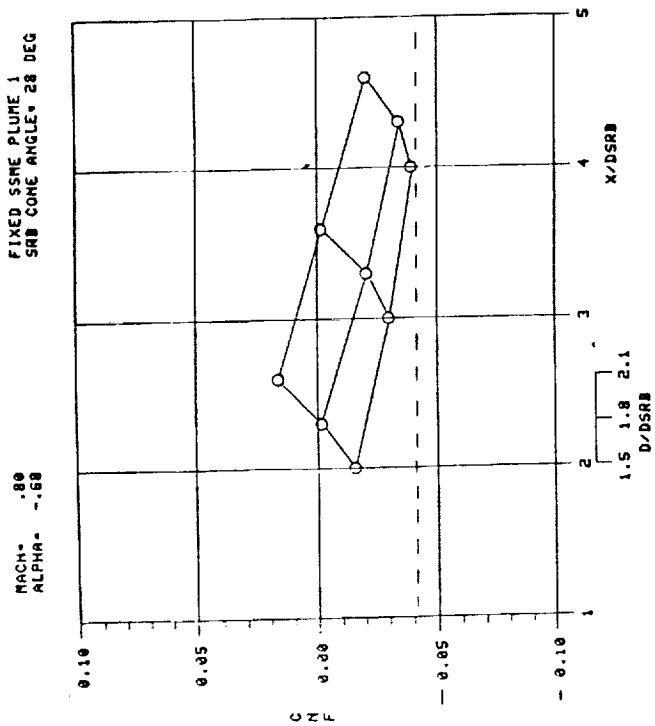


Figure L-4.

ORIGINAL PAGE IS
OF POOR QUALITY

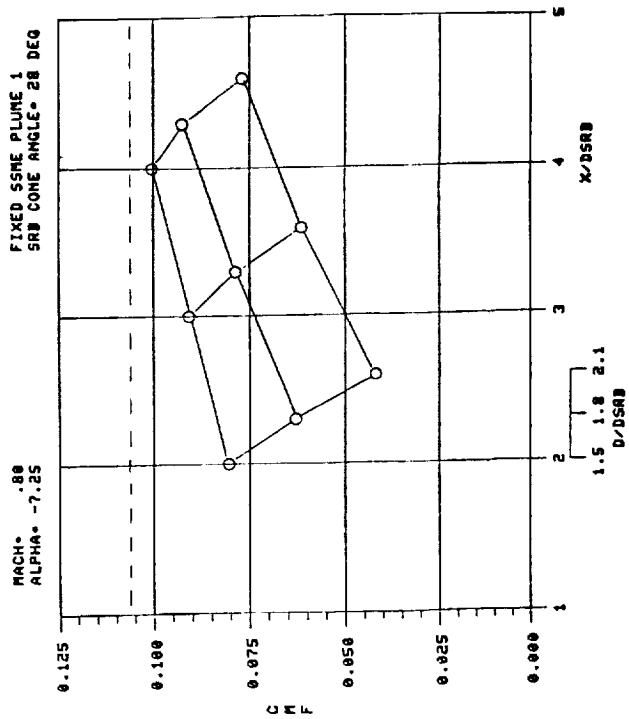
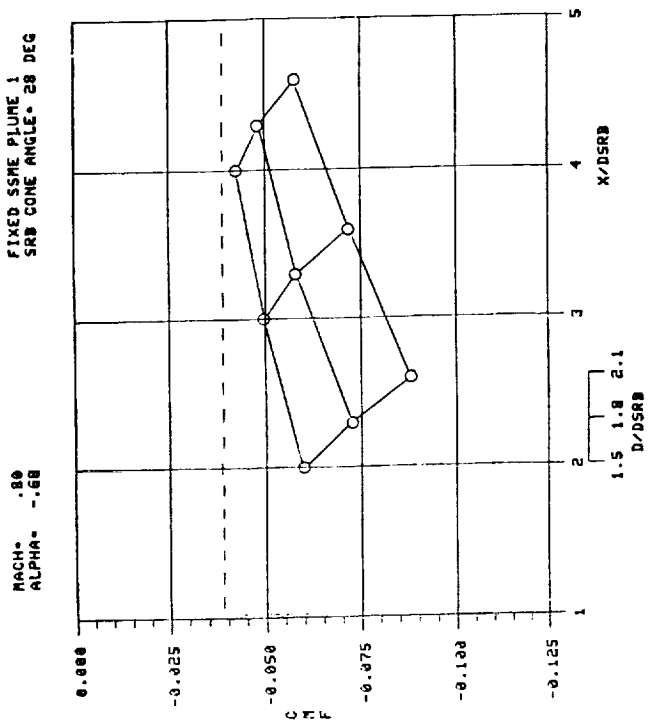
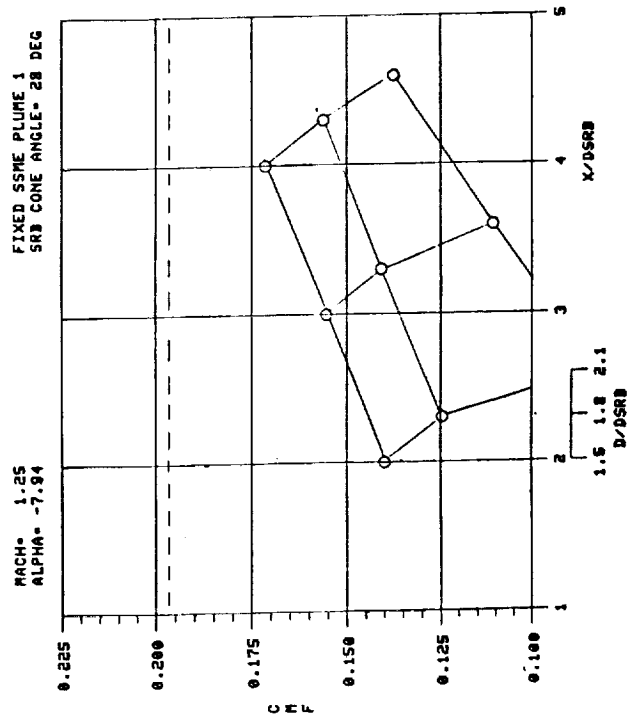
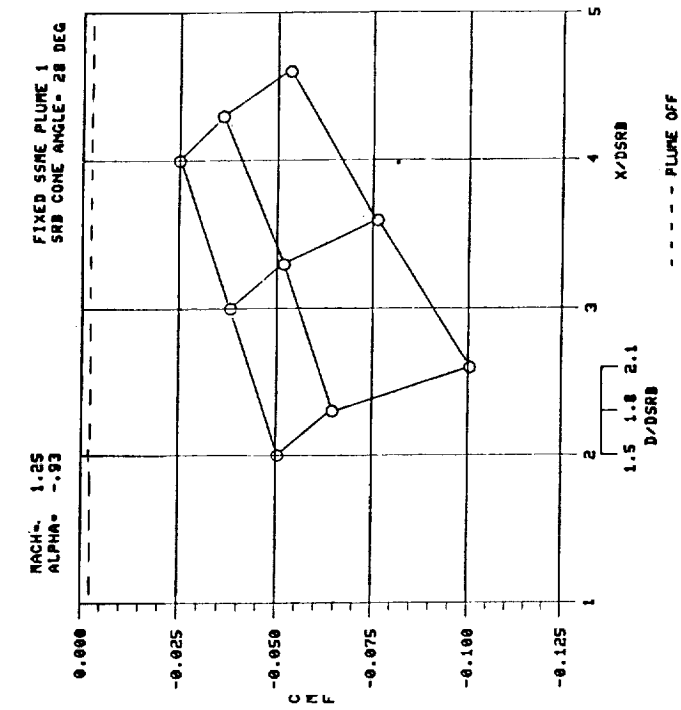


Figure L-5.

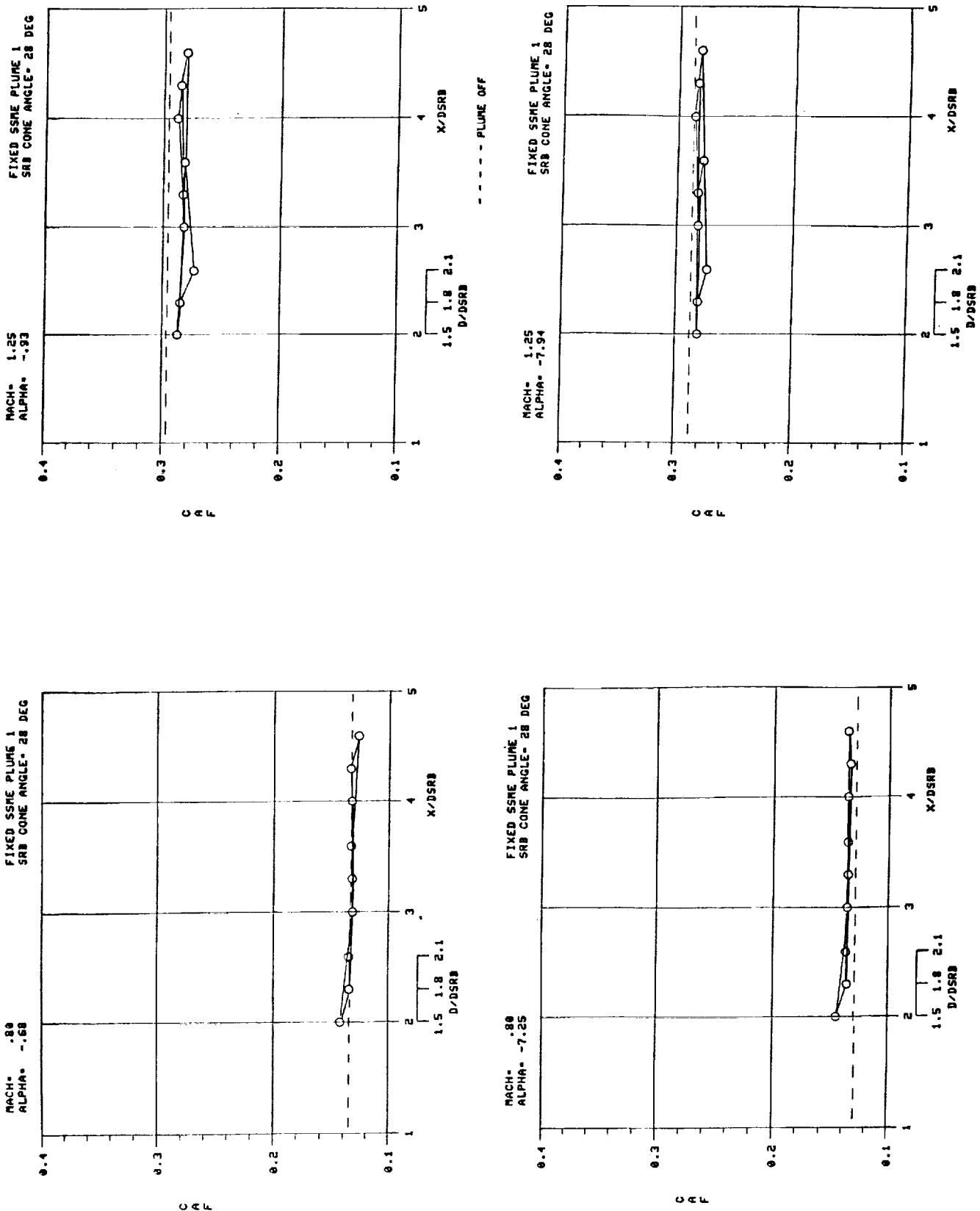


Figure L-6.

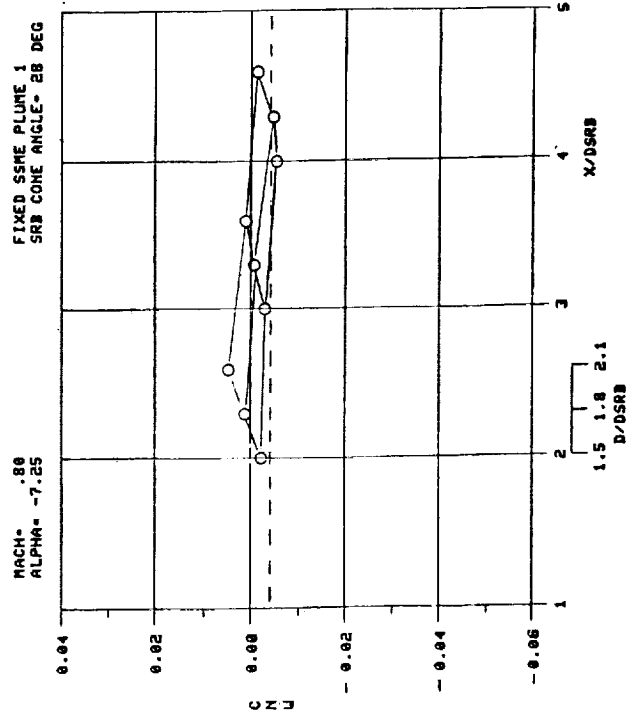
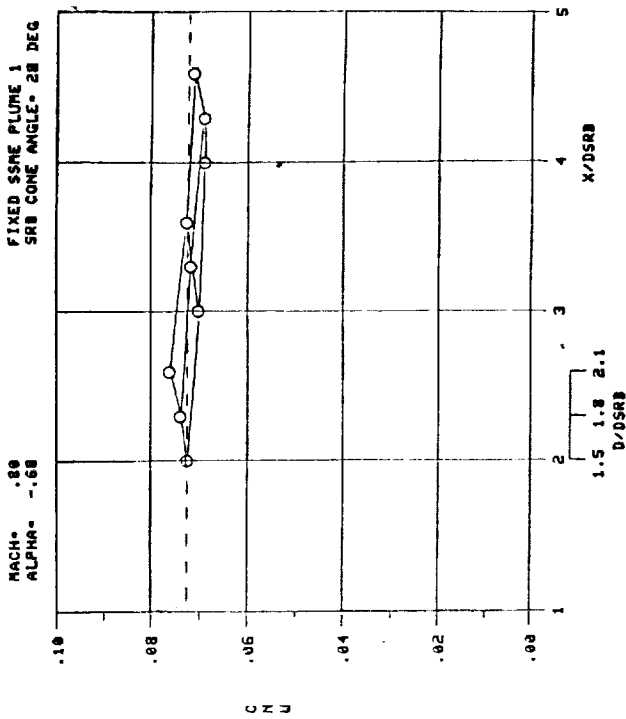
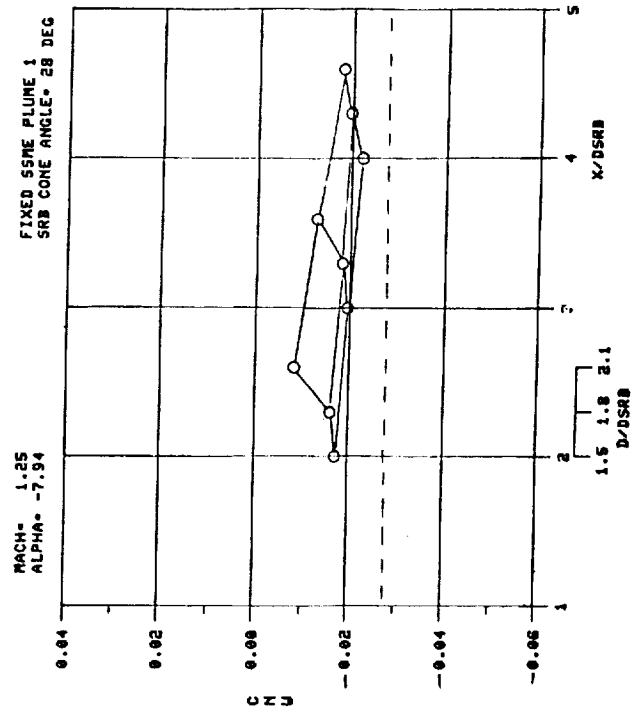
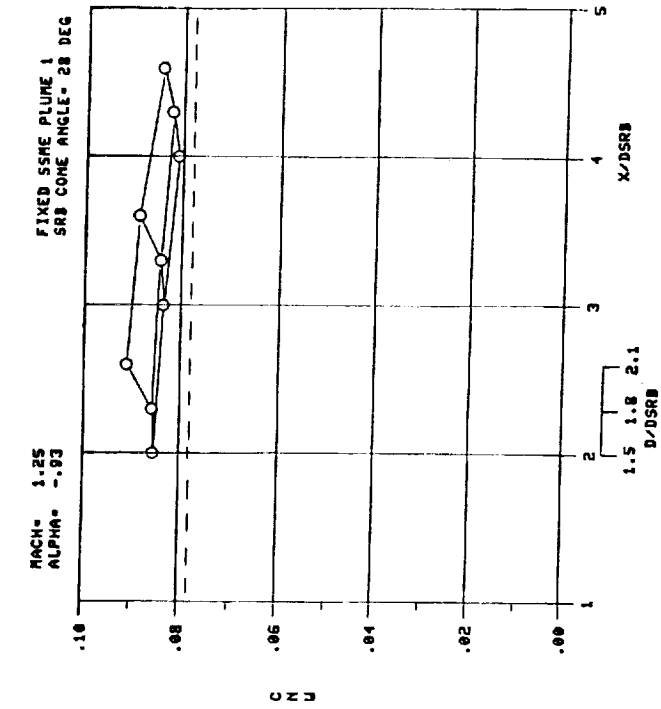


Figure L-7.

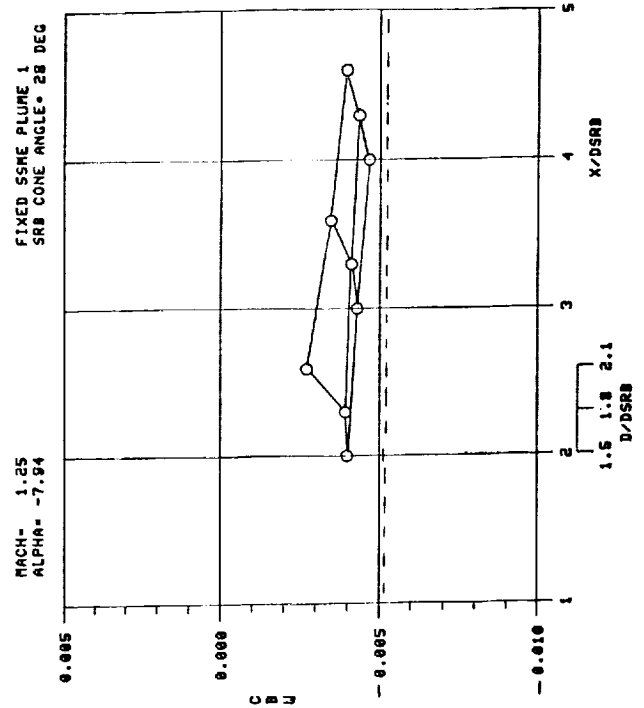
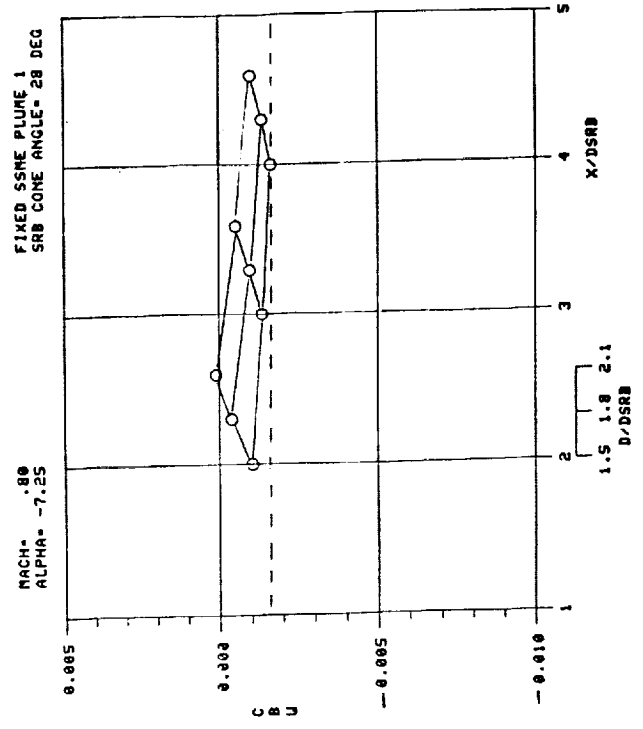
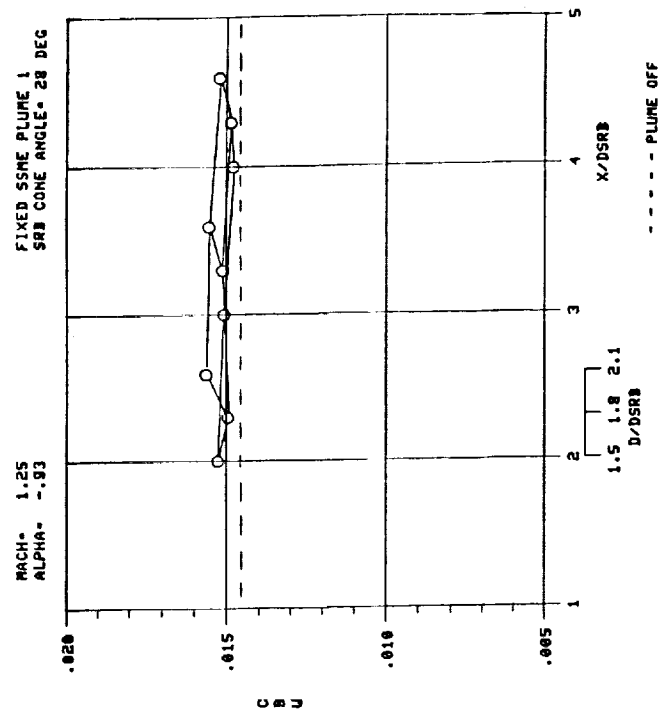
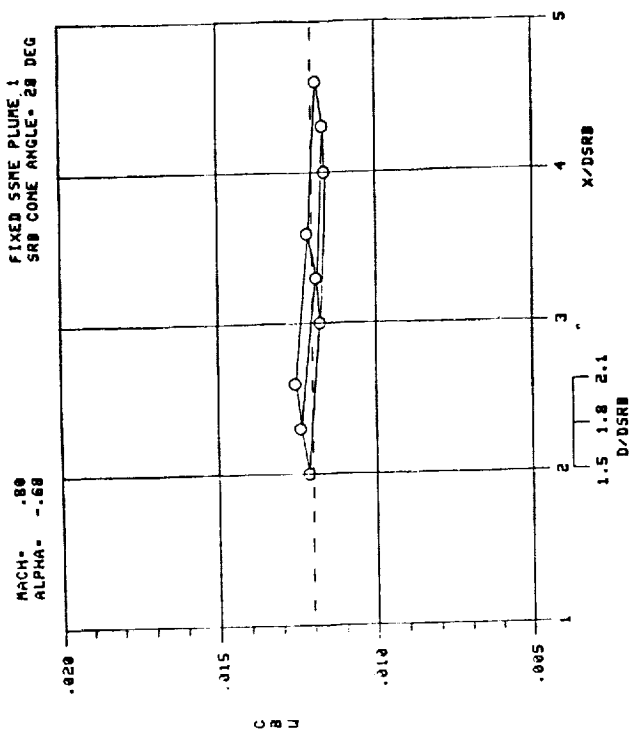


Figure L-8.

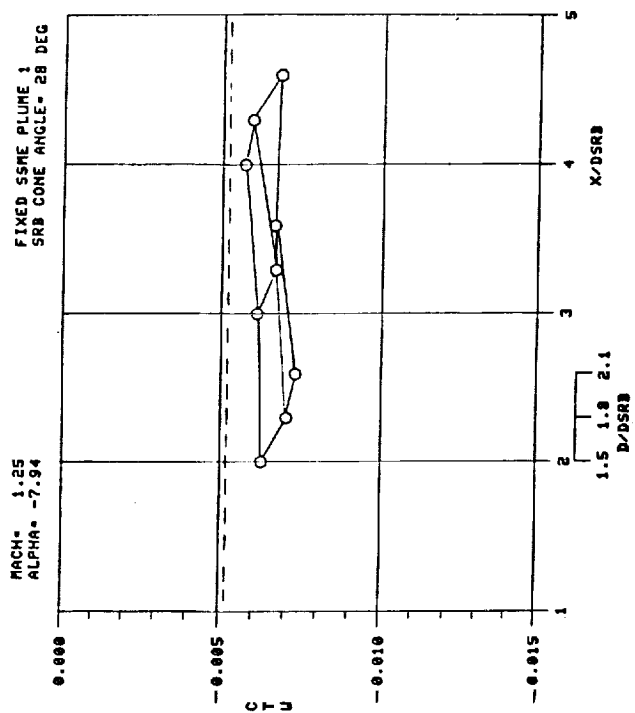
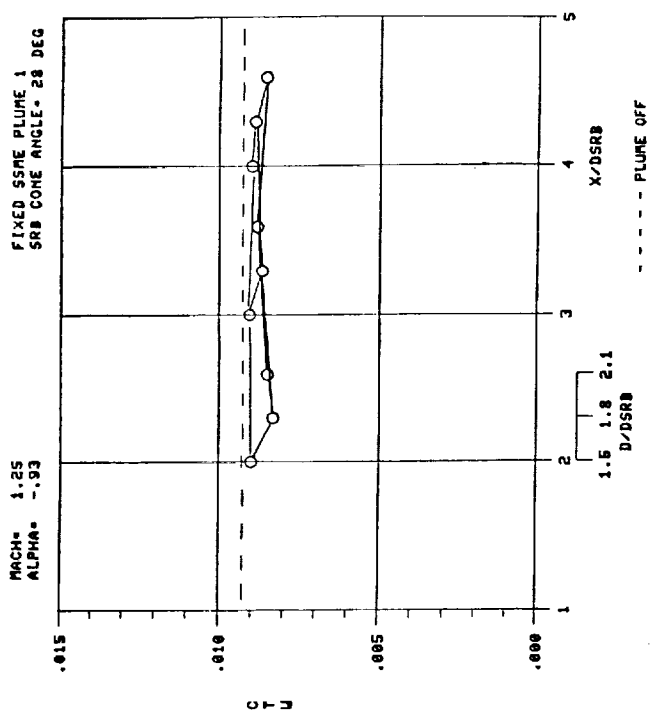
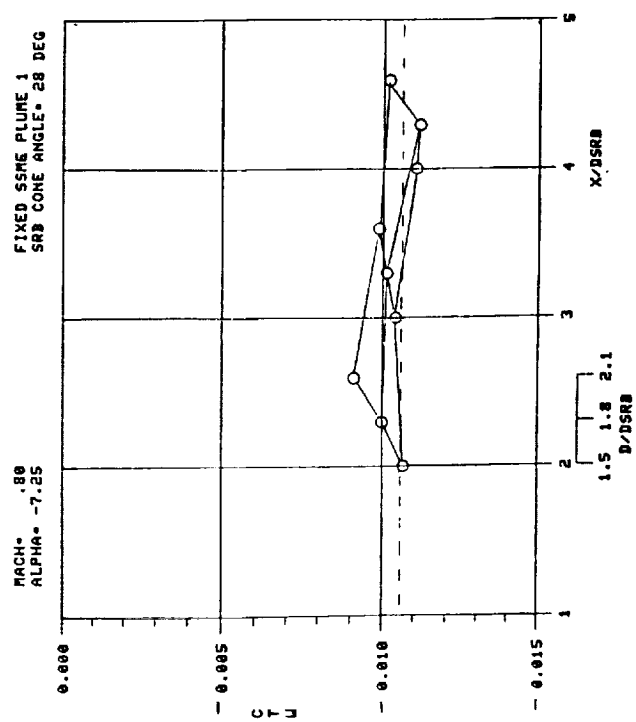
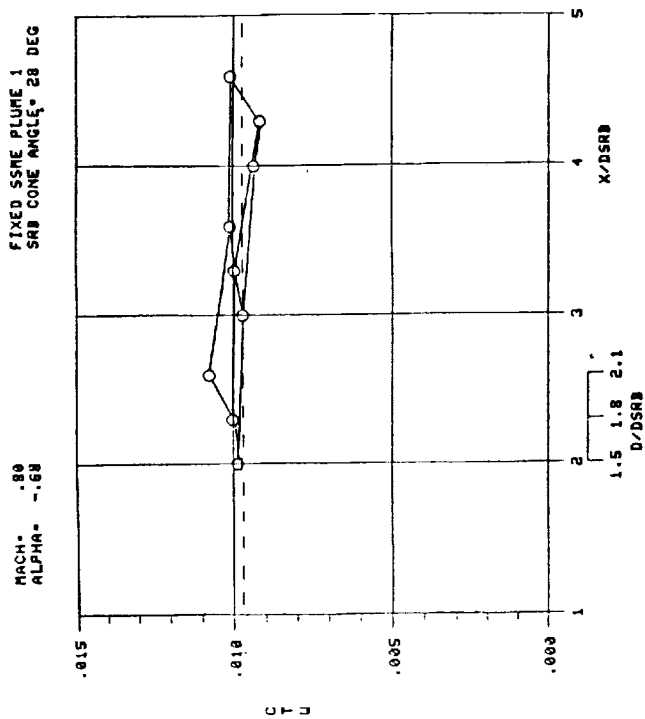


Figure L-9.

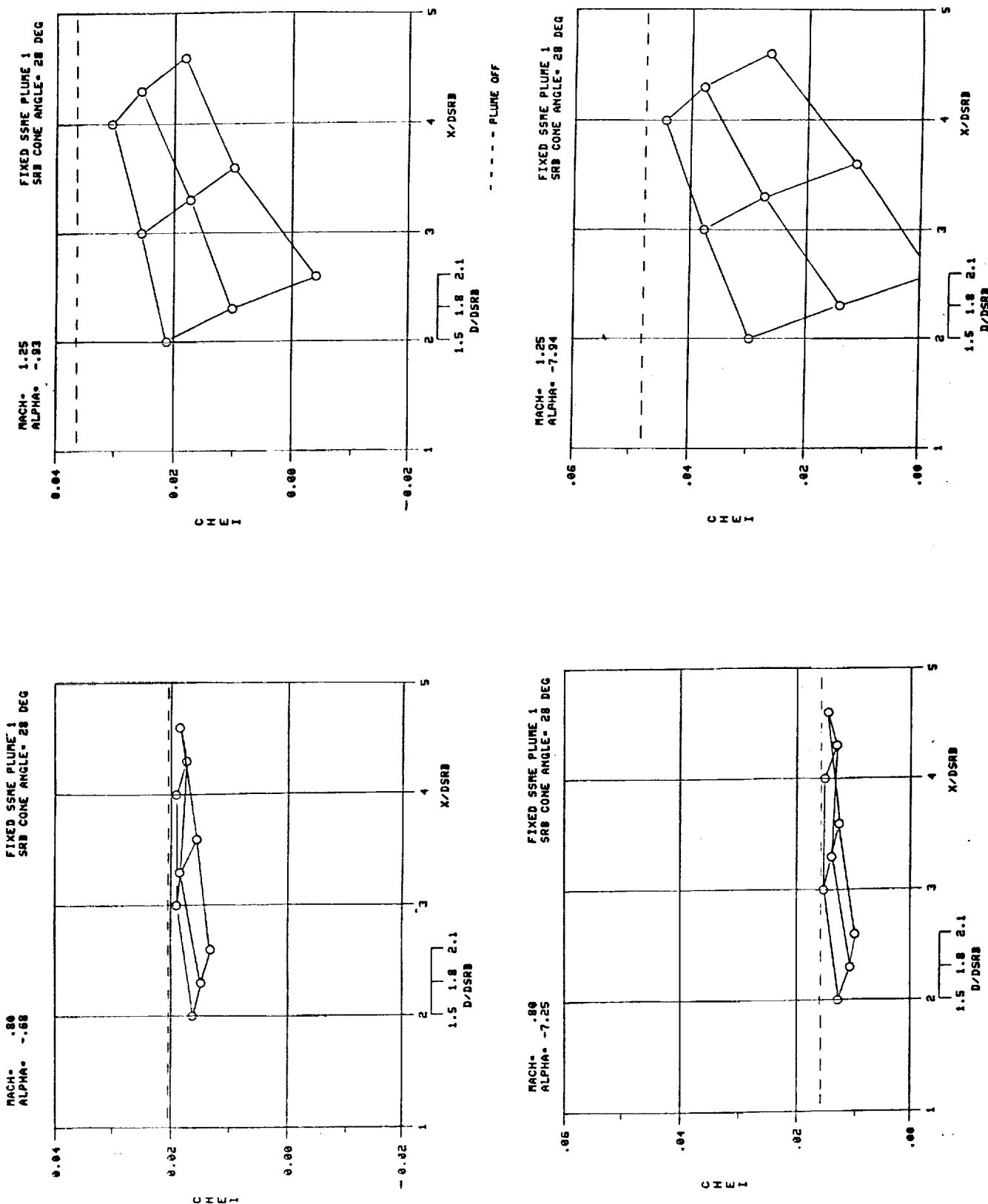
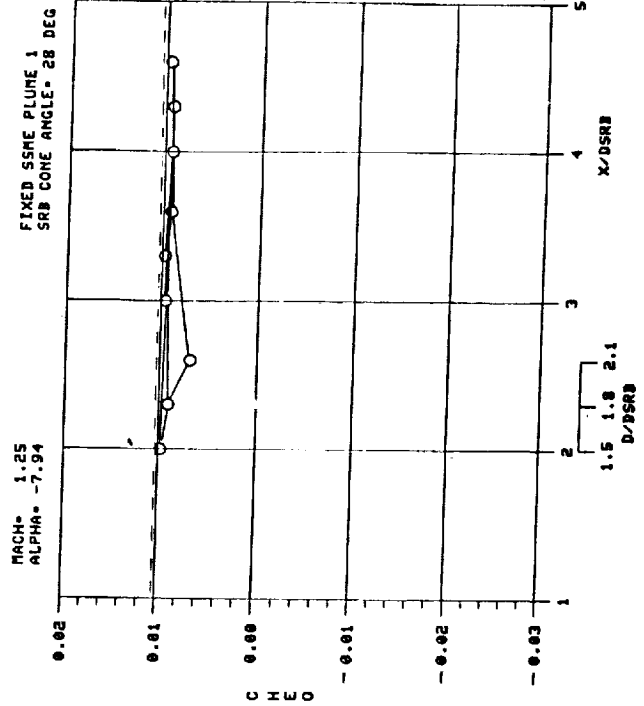
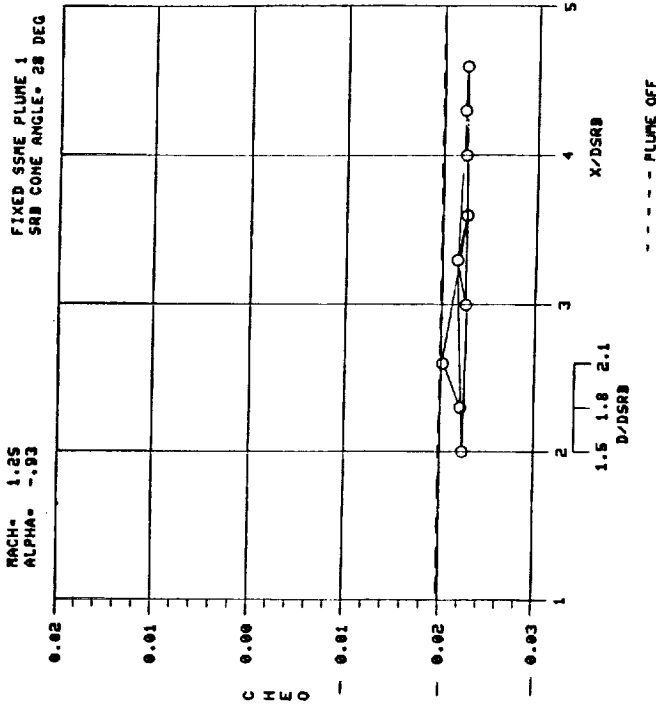
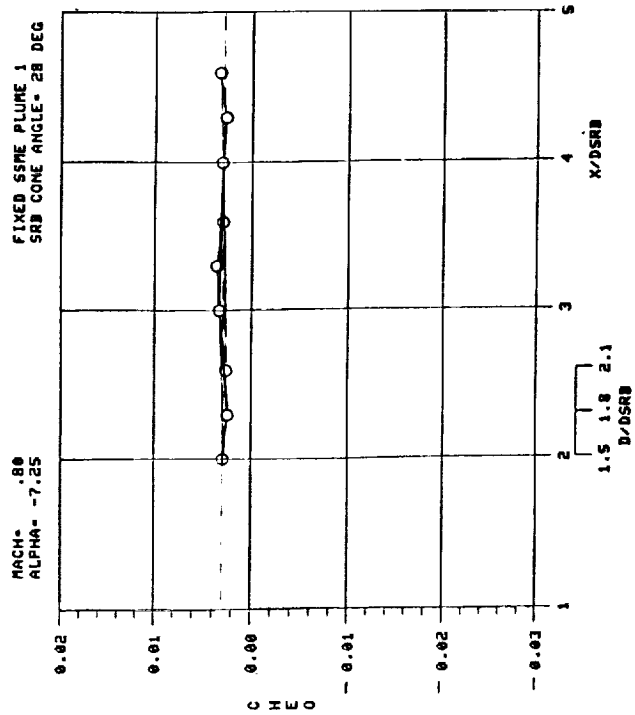
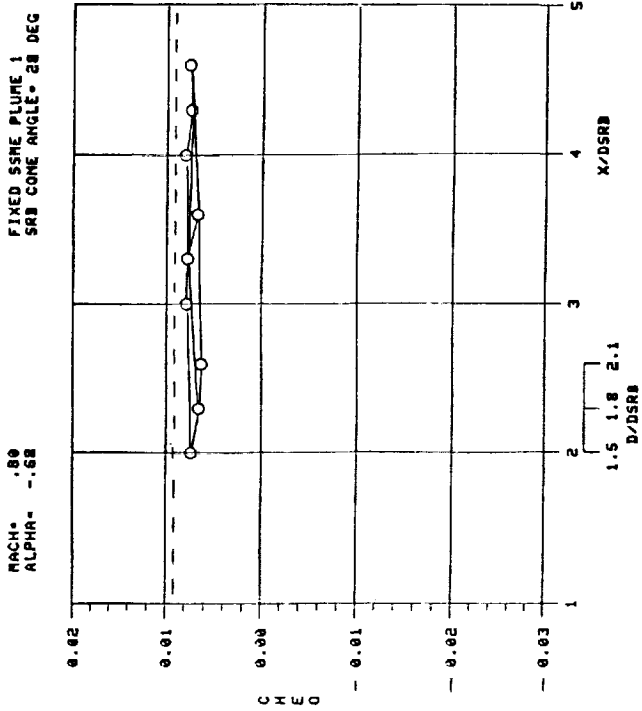


Figure L-10.



ORIGINAL PAGE IS
 OF POOR QUALITY

Figure L-11.

APPENDIX M

PRECEDING PAGE BLANK NOT FILMED

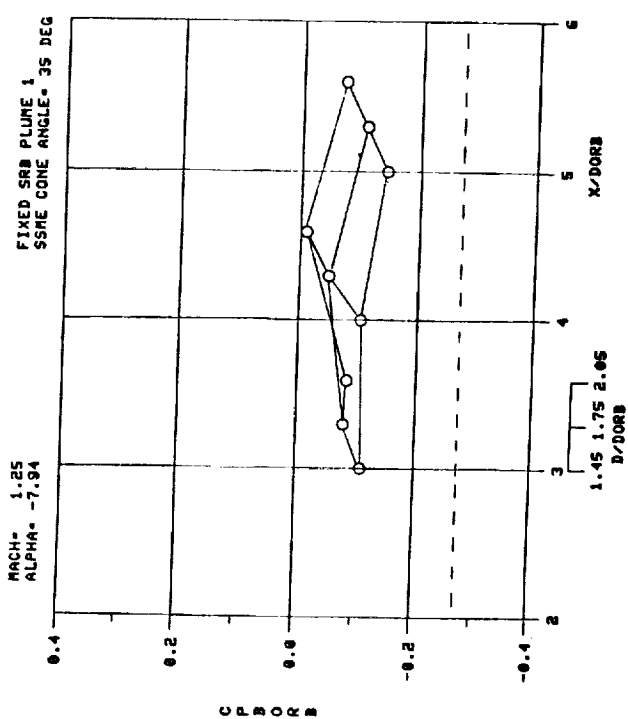
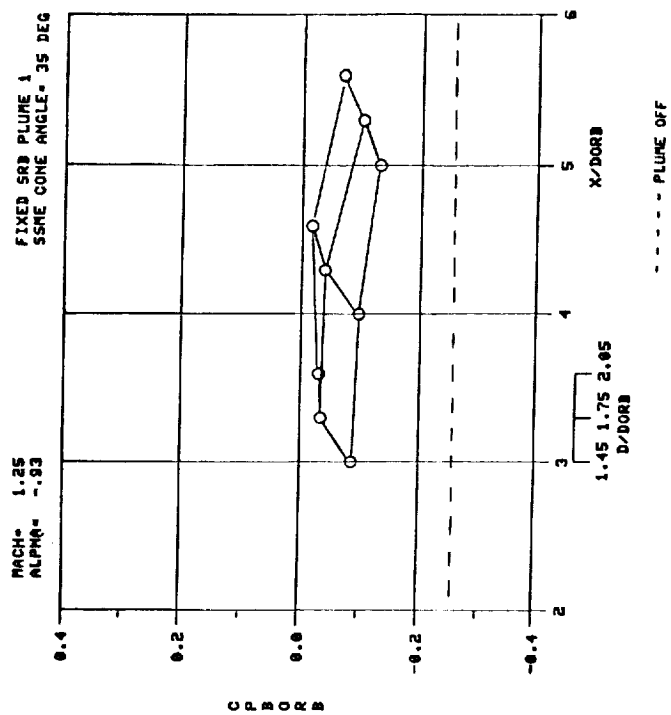
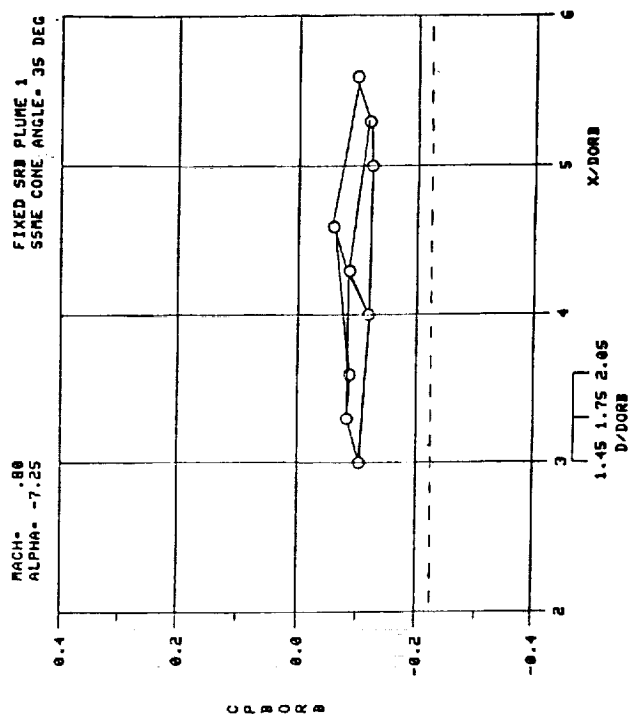
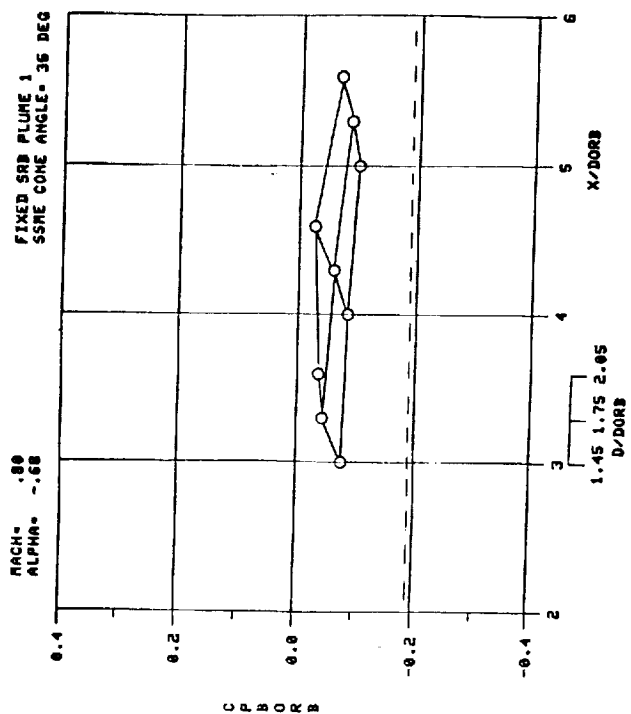


Figure M-1.

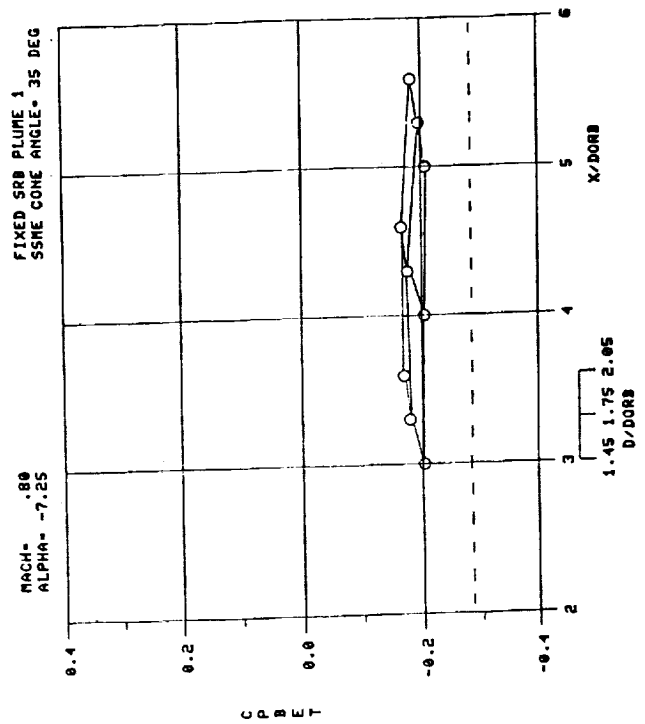
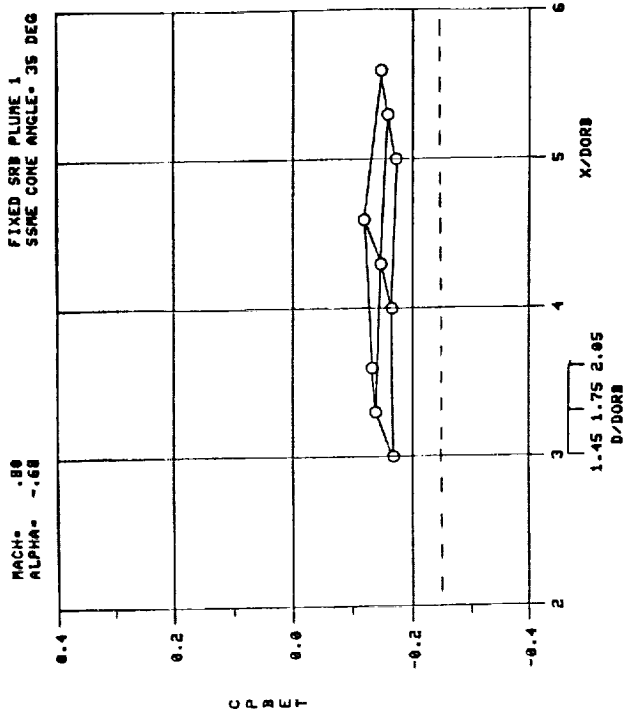
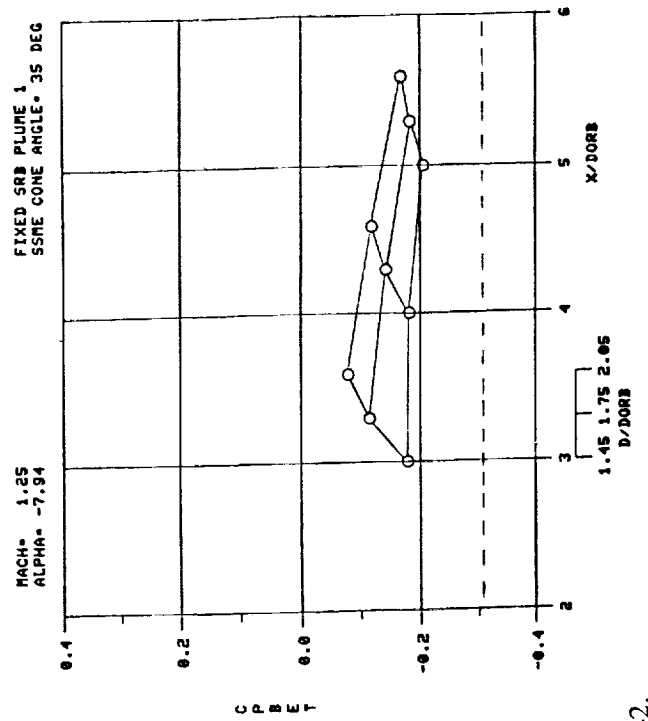
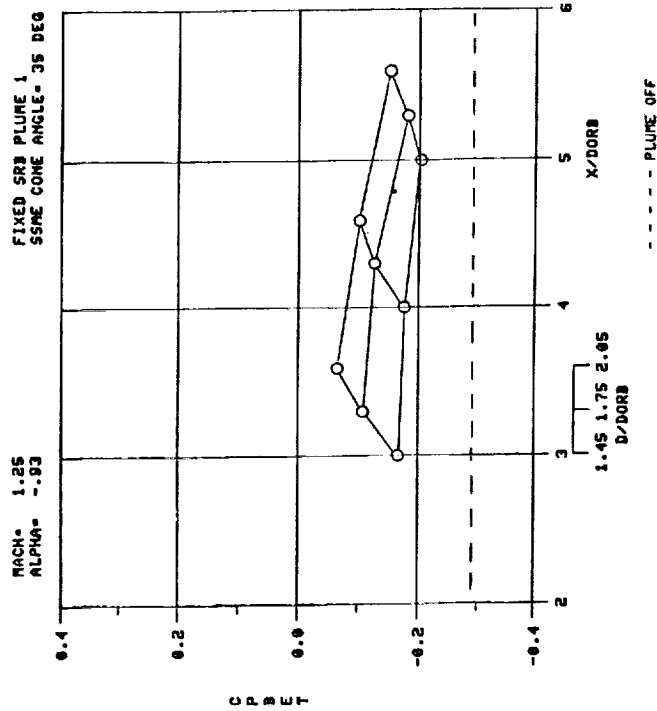


Figure M-2.

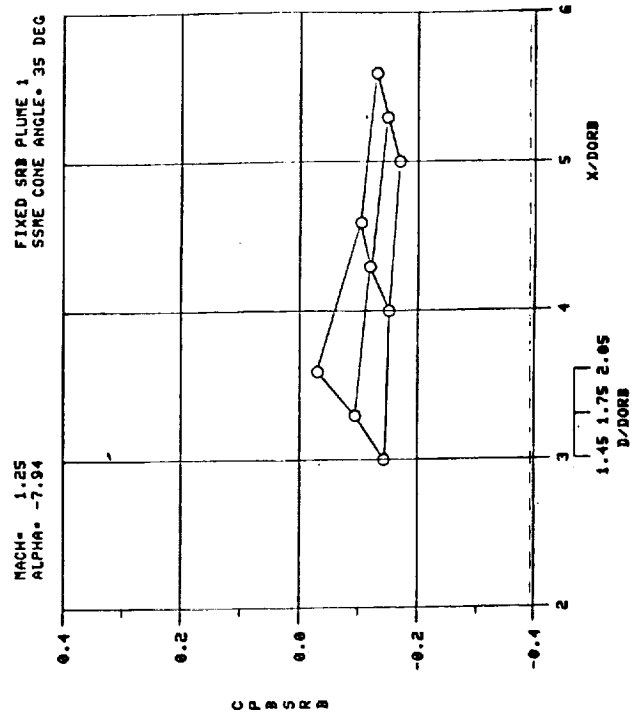
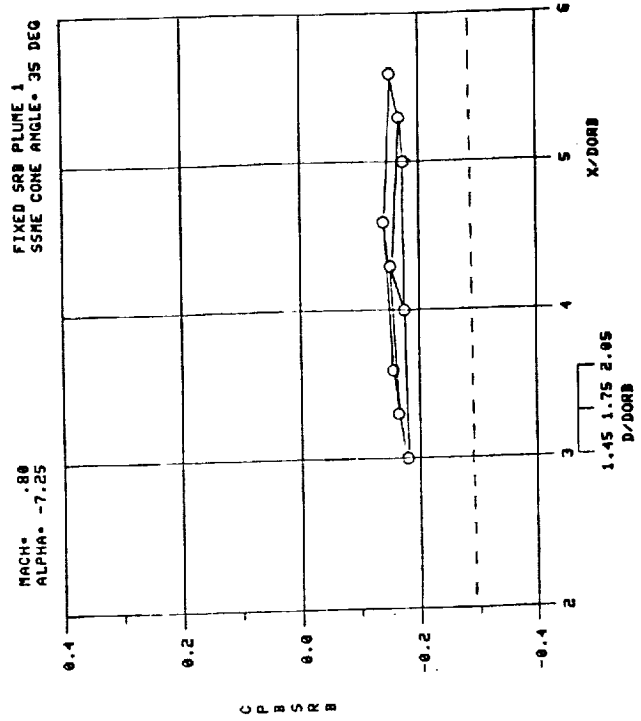
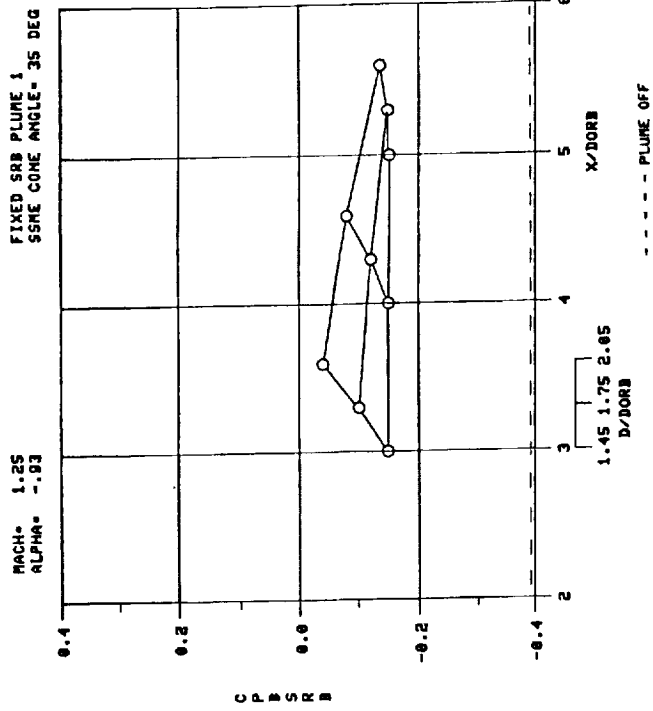
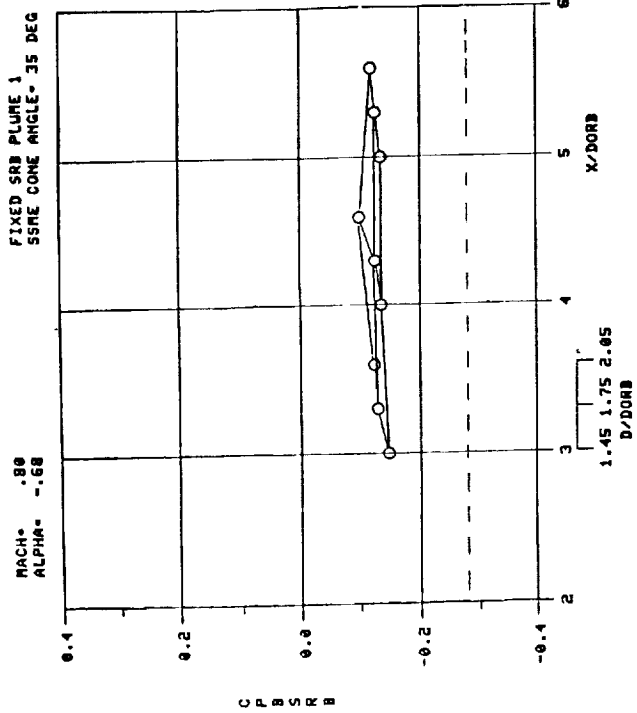


Figure M-3.

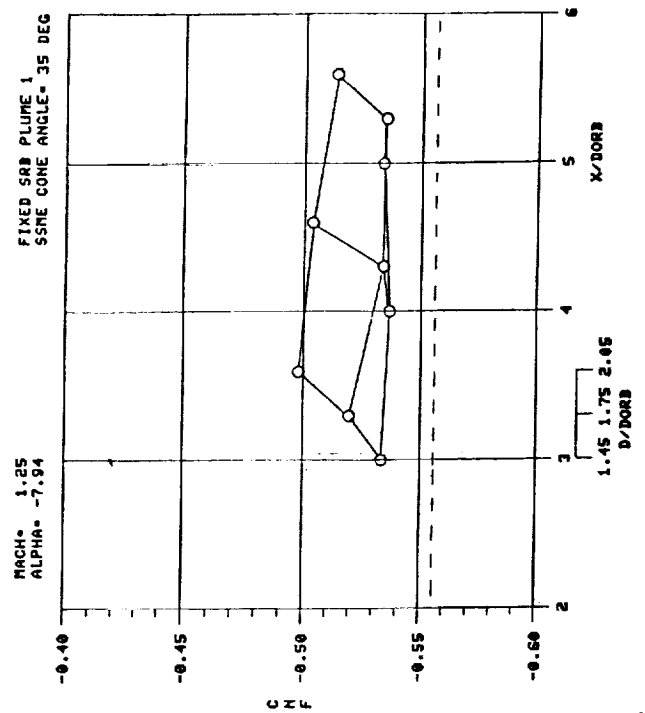
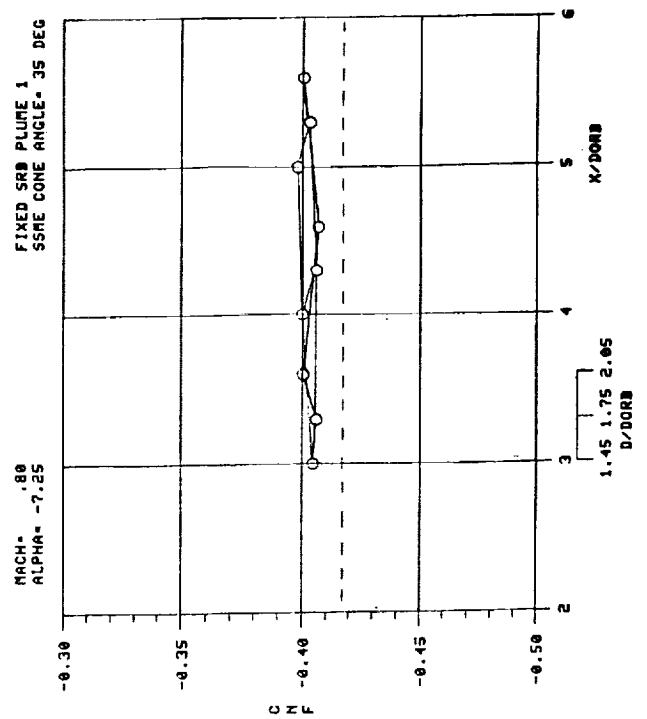
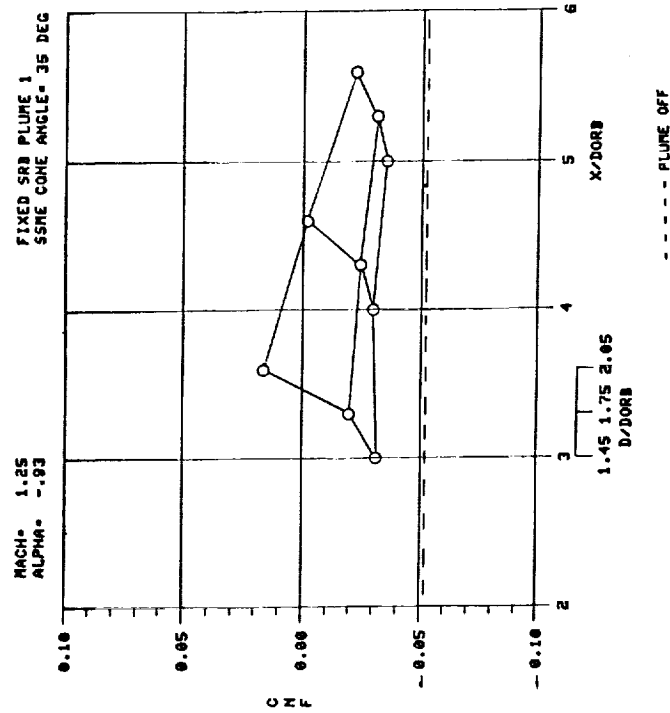
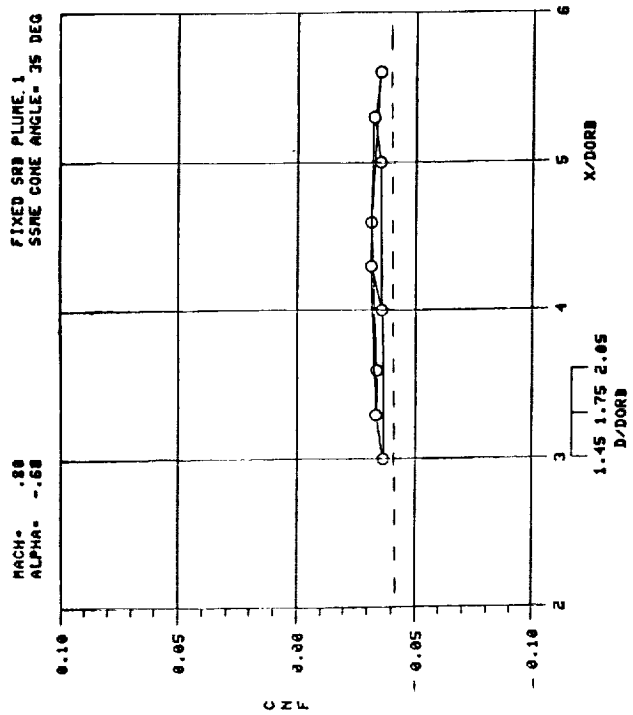


Figure M-4.

ORIGINAL PAGE IS
OF POOR QUALITY

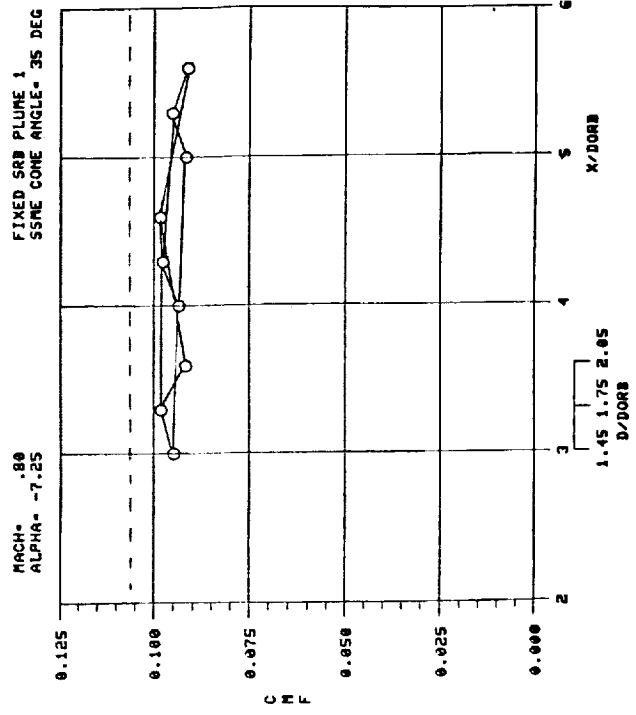
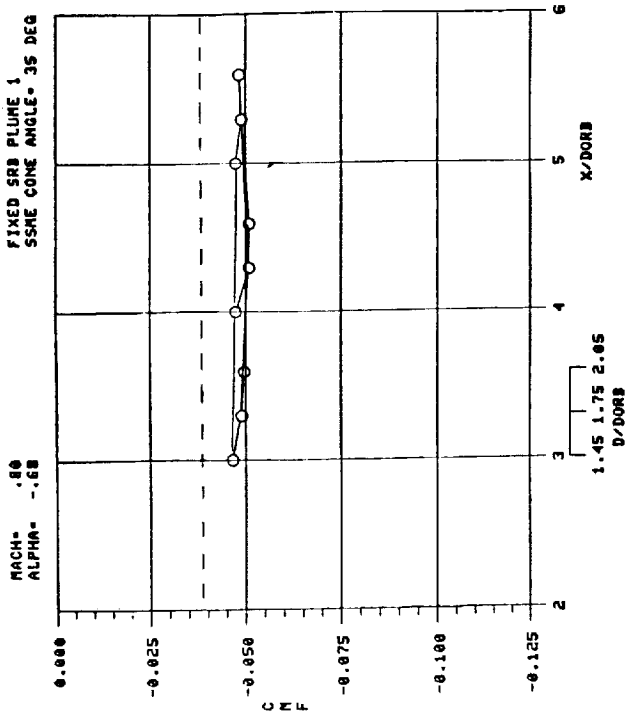
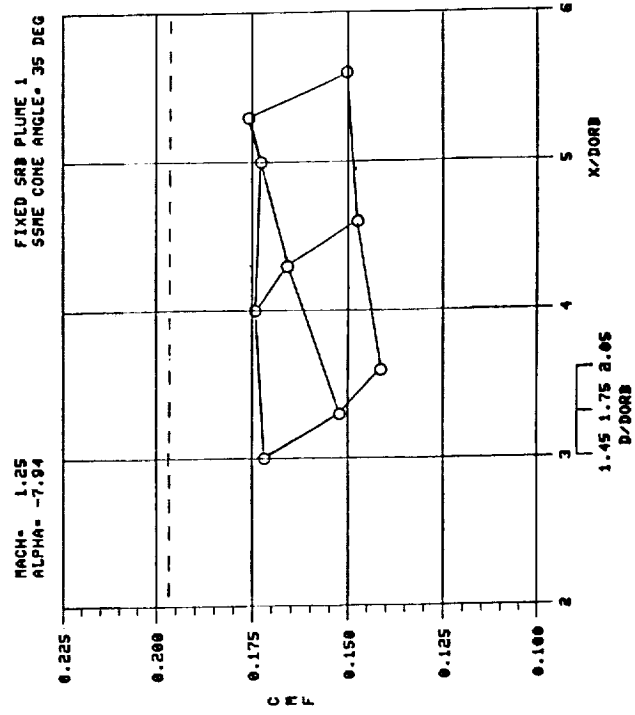
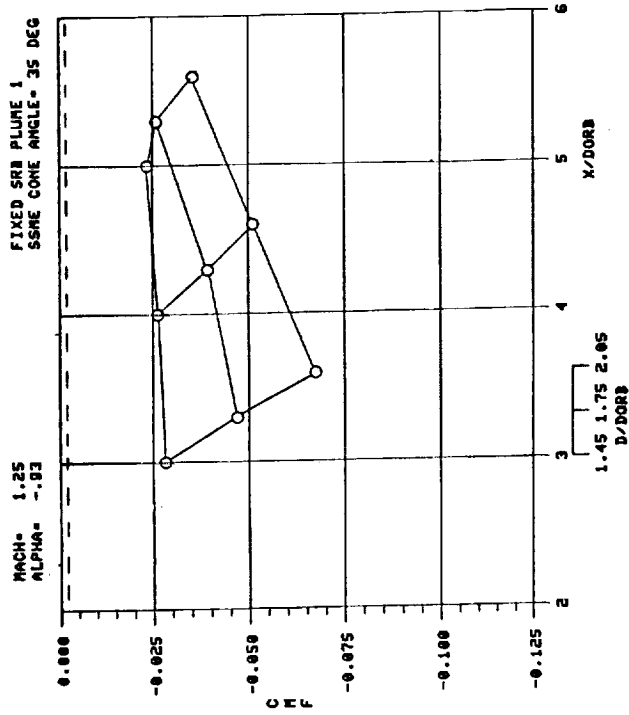


Figure M-5.

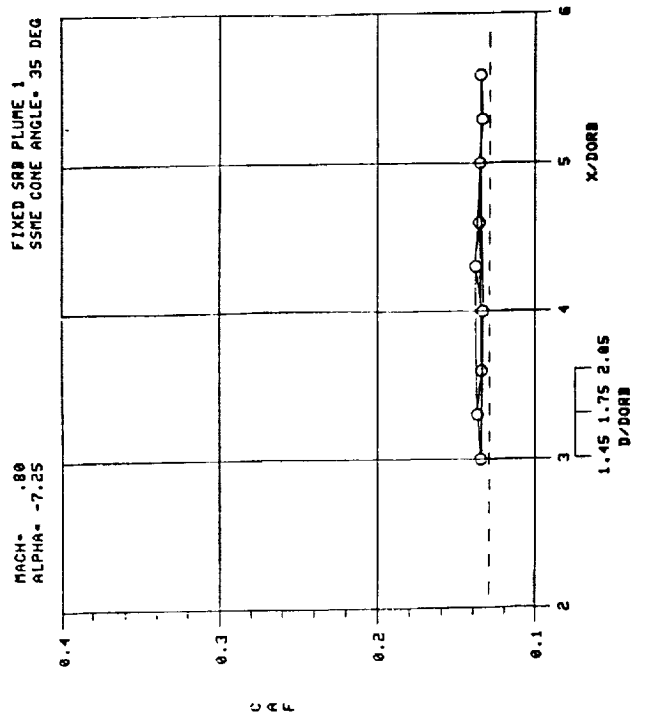
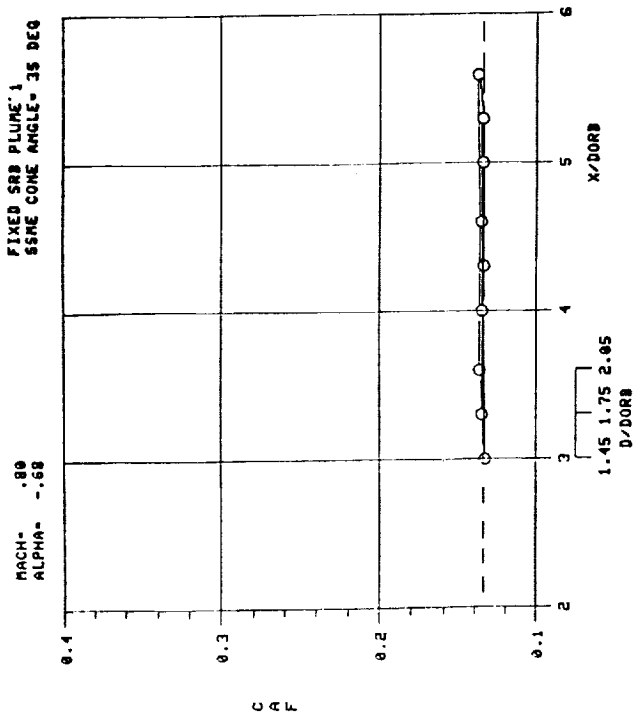
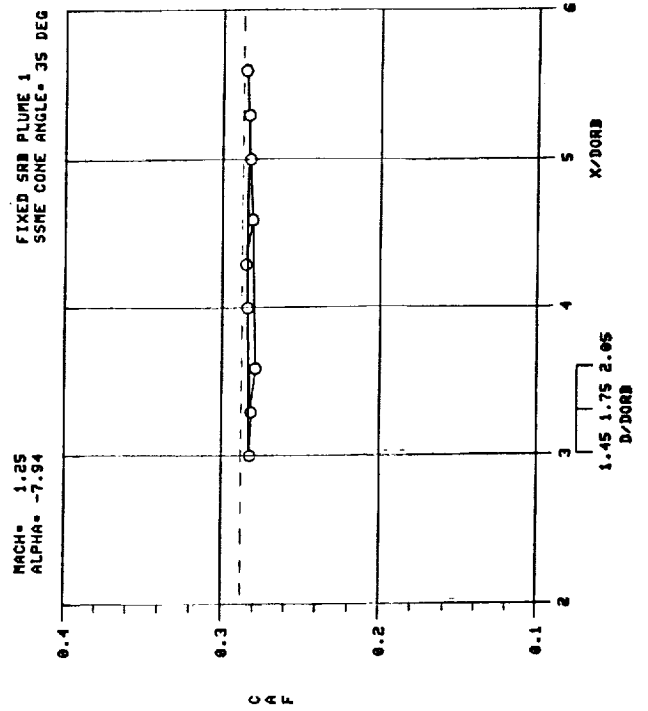
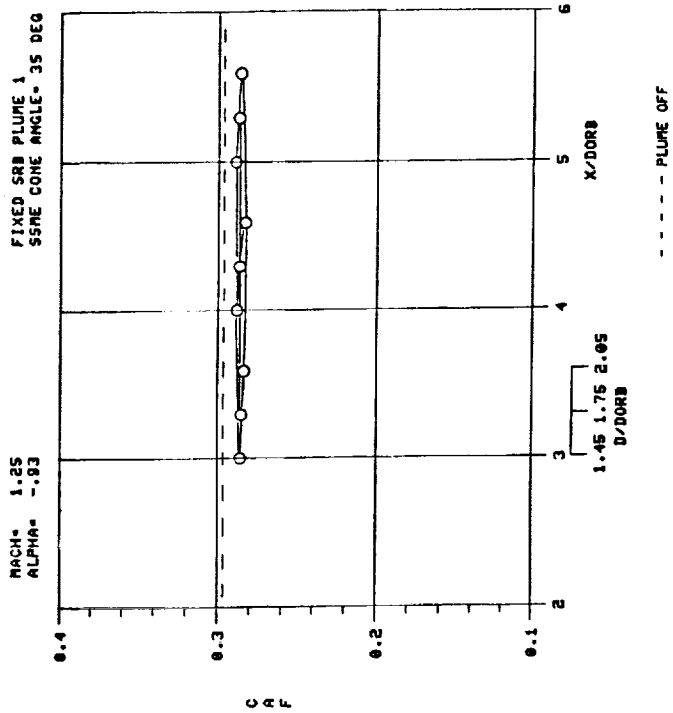


Figure M-6.

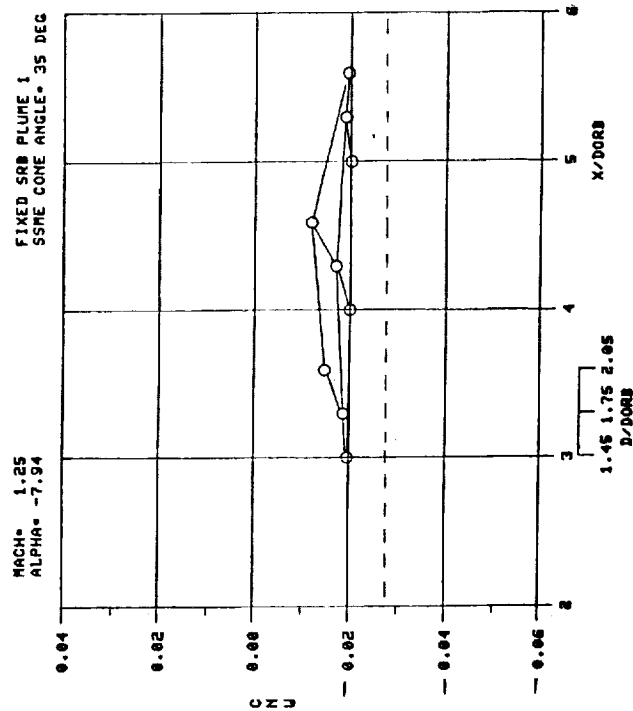
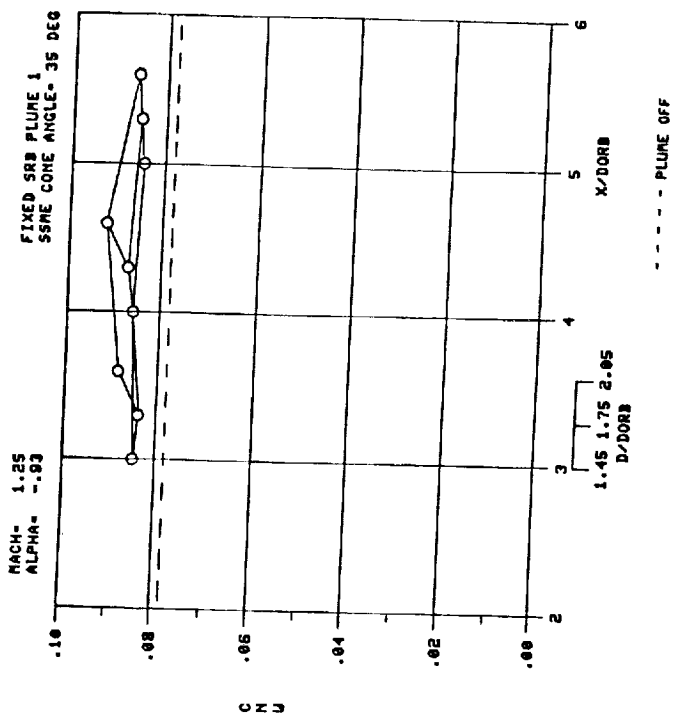
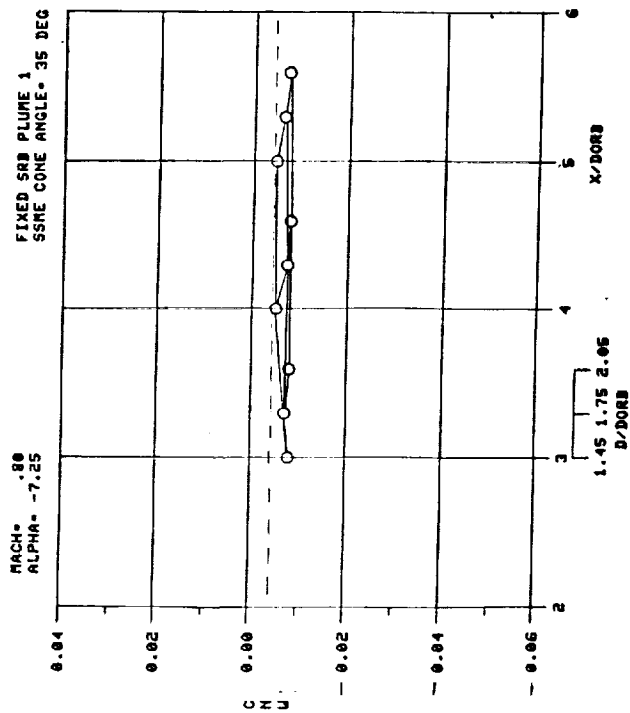
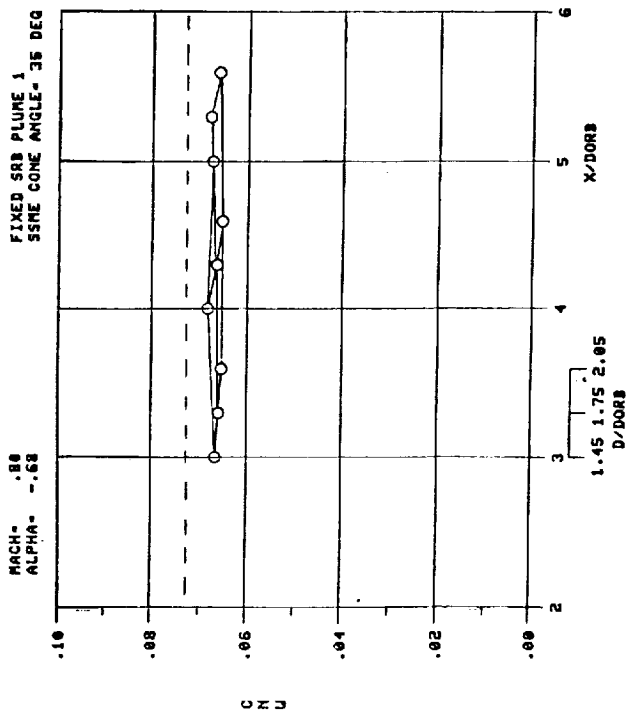


Figure M-7.

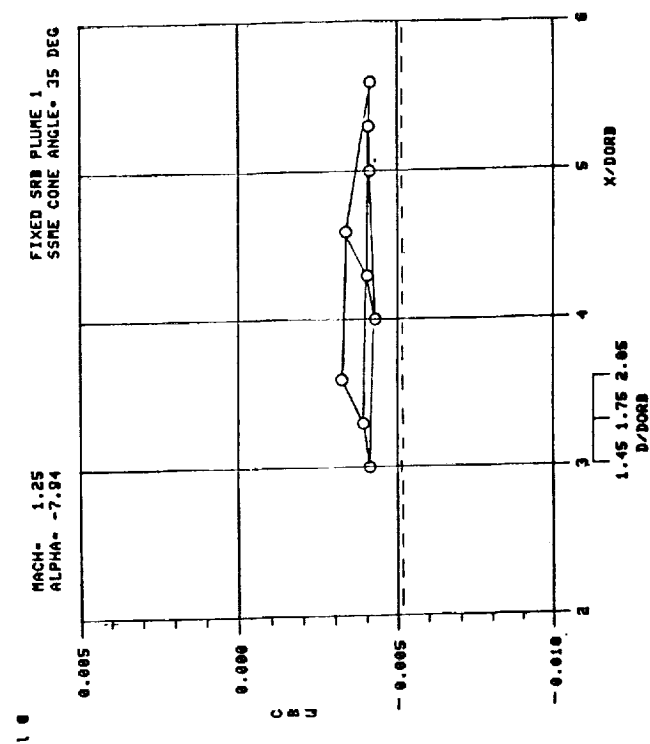
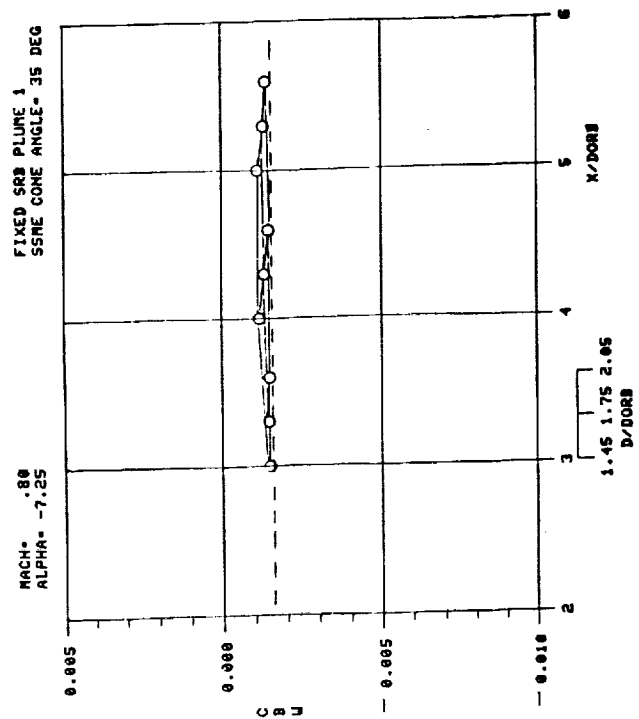
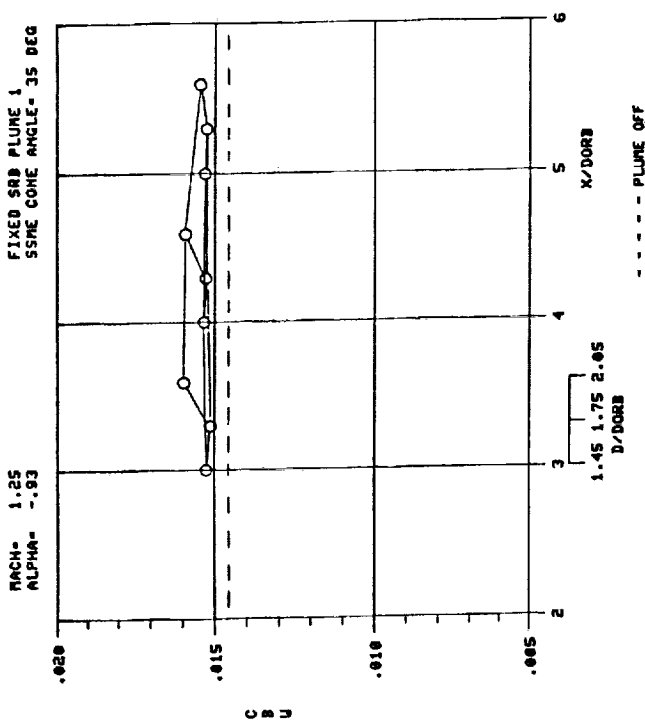
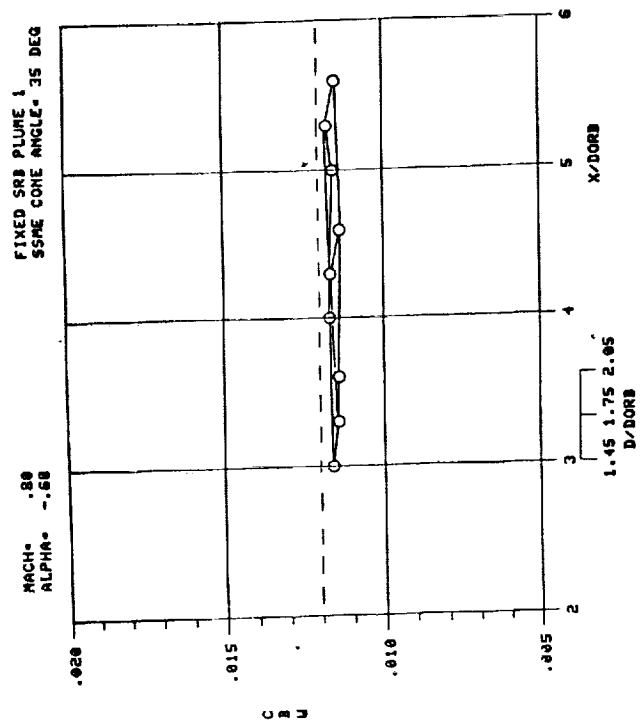


Figure M-8.

ORIGINAL PAGE IS
OF POOR QUALITY

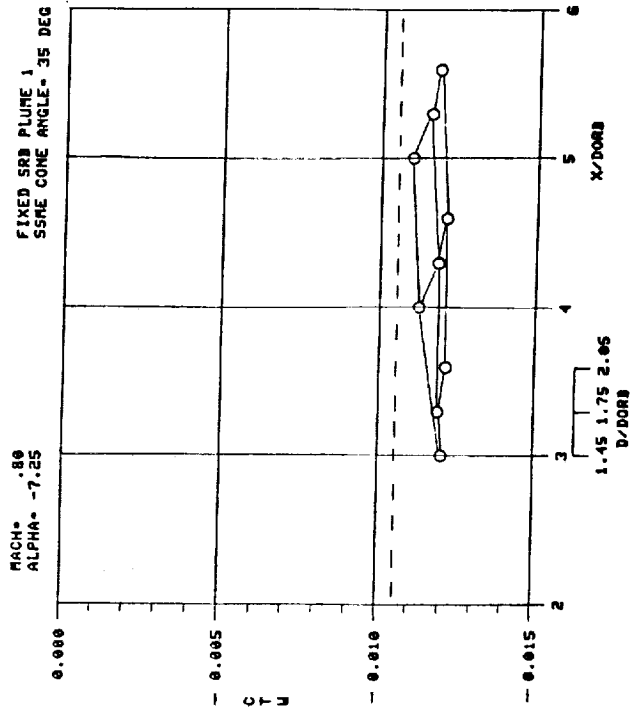
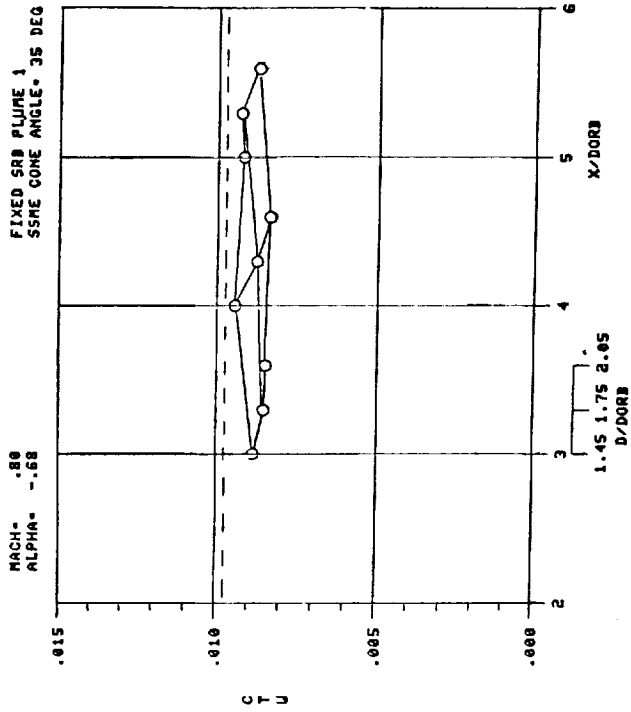
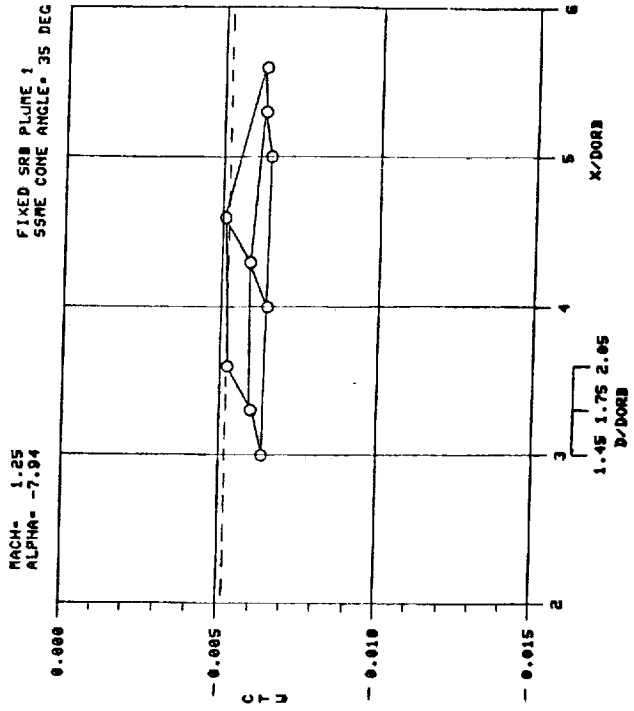
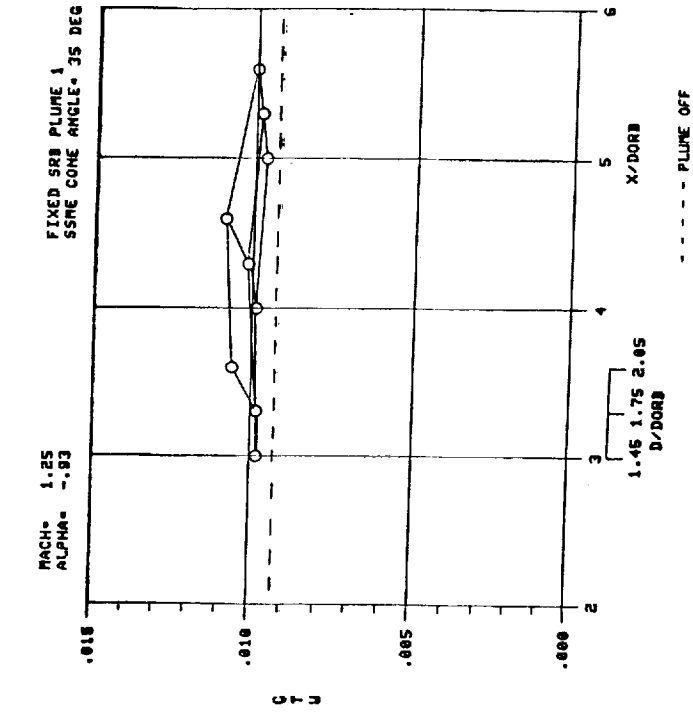


Figure M-9.

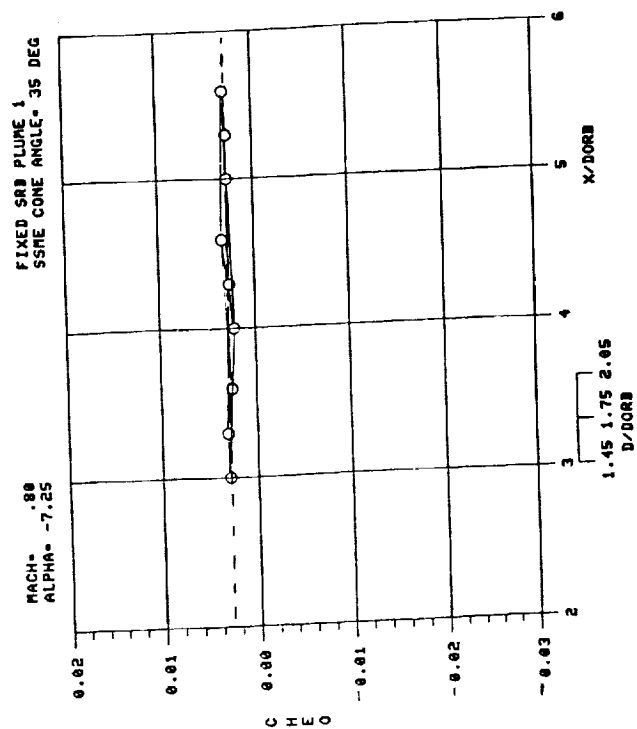
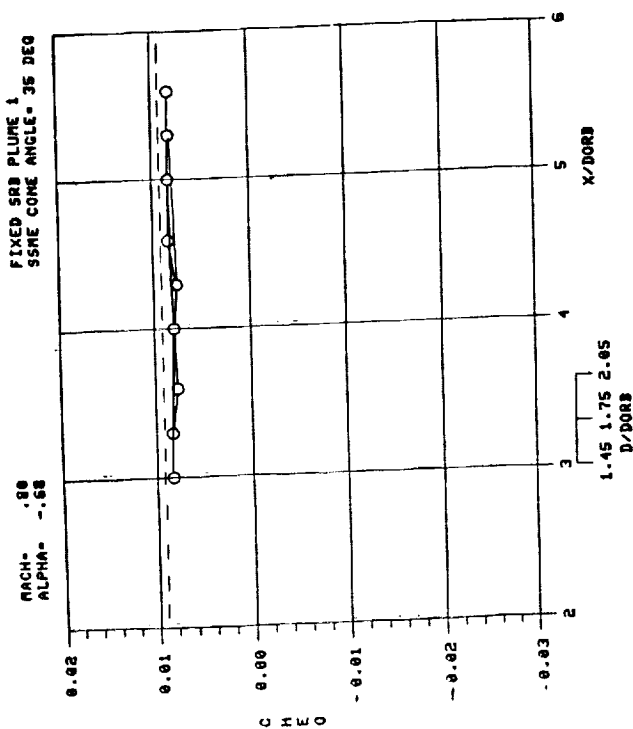
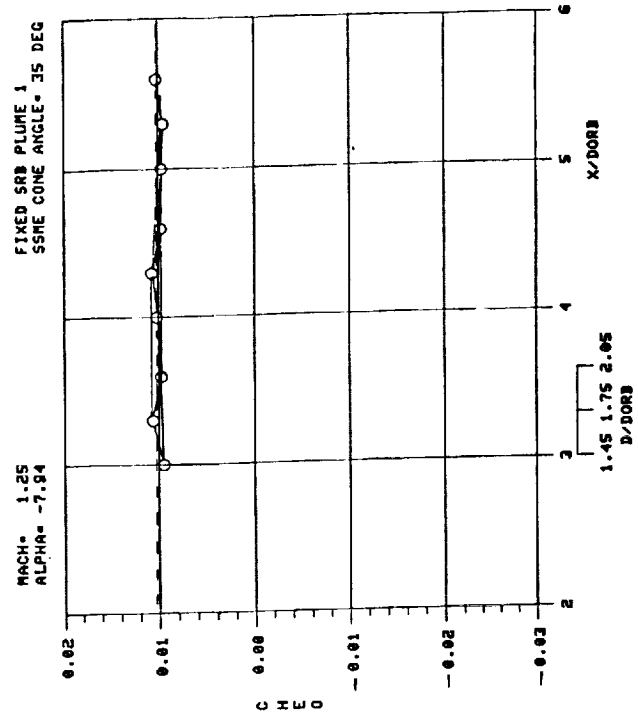
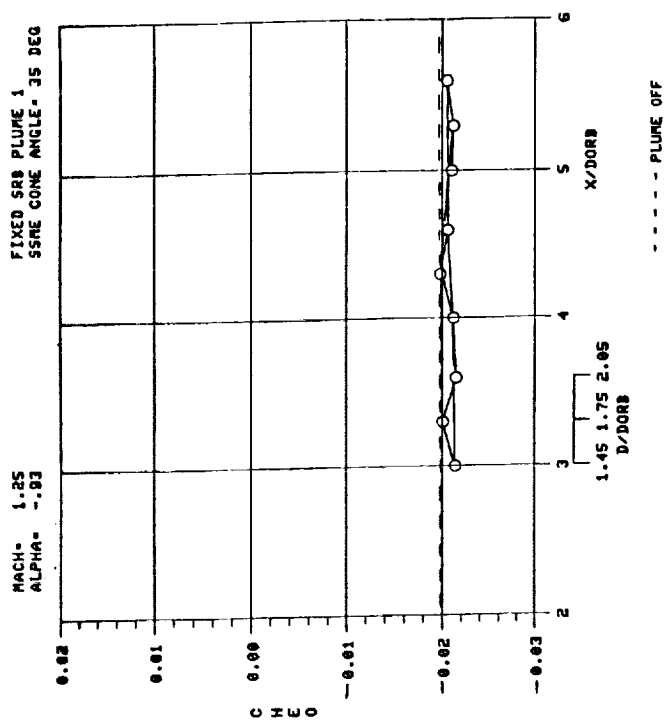


Figure M-10.

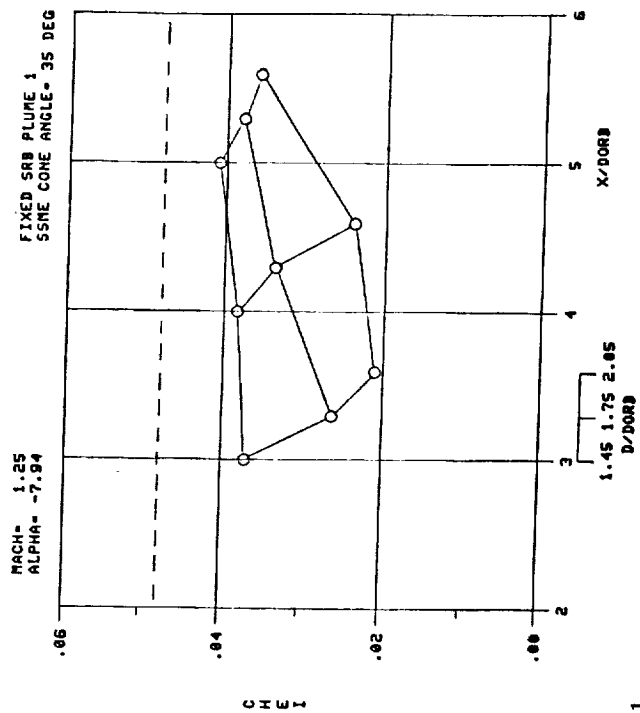
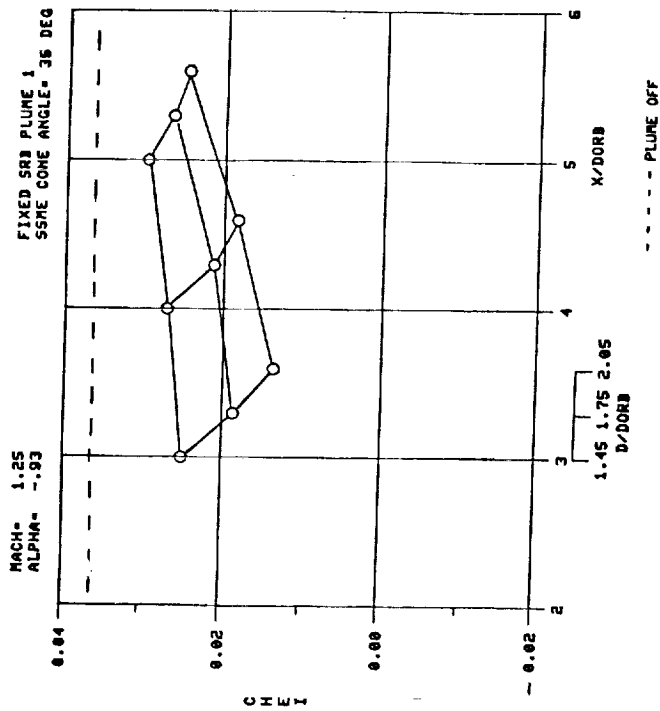
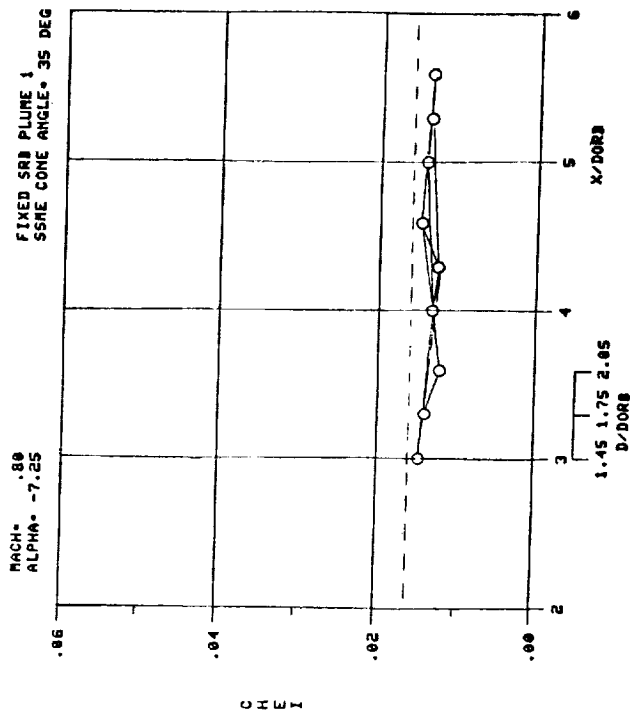
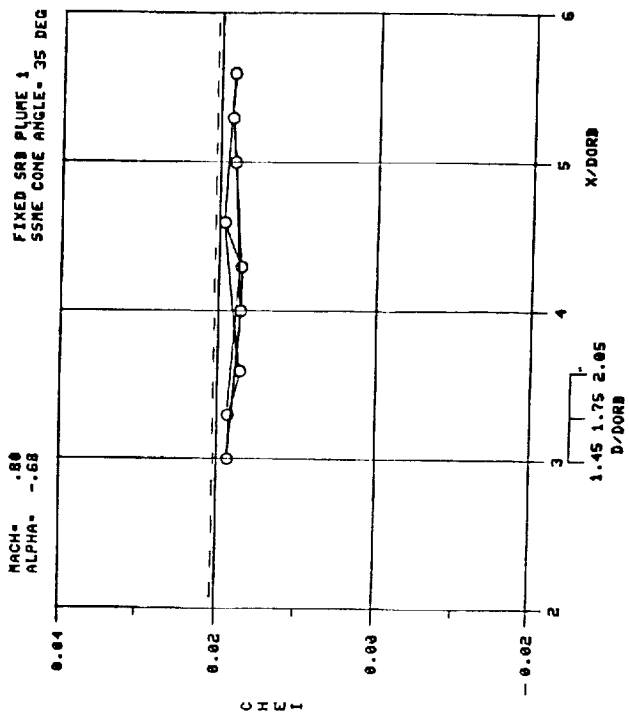


Figure M-11.

7

11

12

13

1. REPORT NO. NASA TP -2569		2. GOVERNMENT ACCESSION NO.		3. RECIPIENT'S CATALOG NO.	
4. TITLE AND SUBTITLE Investigation of Solid Plume Simulation Criteria To Produce Flight Plume Effects on Multibody Configuration in Wind Tunnel Tests				5. REPORT DATE March 1986	
				6. PERFORMING ORGANIZATION CODE ED32	
7. AUTHOR(S) Alonzo L. Frost and Charlie C. Dill				8. PERFORMING ORGANIZATION REPORT #	
9. PERFORMING ORGANIZATION NAME AND ADDRESS George C. Marshall Space Flight Center Marshall Space Flight Center, Alabama 35812				10. WORK UNIT NO. M-514	
				11. CONTRACT OR GRANT NO.	
				13. TYPE OF REPORT & PERIOD COVERED Technical Paper	
12. SPONSORING AGENCY NAME AND ADDRESS National Aeronautics and Space Administration Washington, D.C. 20546				14. SPONSORING AGENCY CODE	
15. SUPPLEMENTARY NOTES Prepared by Aerodynamic Analysis Branch, Aerophysics Division, Systems Dynamics Laboratory, Science and Engineering Directorate.					
16. ABSTRACT An investigation to determine the sensitivity of the Space Shuttle base and forebody aerodynamics to the size and shape of various solid plume simulators was conducted. Families of cones of varying angle and base diameter, at various axial positions behind a Space Shuttle launch vehicle model, were wind tunnel tested. This parametric evaluation yielded base pressure and force coefficient data which indicated that solid plume simulators are an inexpensive, quick method of approximating the effect of engine exhaust plumes on the base and forebody aerodynamics of future, complex multibody launch vehicles.					
17. KEY WORDS Plume Simulation Solid Plume Simulation Wind Tunnel Testing			18. DISTRIBUTION STATEMENT Category: 02 Unclassified - Unlimited		
19. SECURITY CLASSIF. (of this report) Unclassified		20. SECURITY CLASSIF. (of this page) Unclassified		21. NO. OF PAGES 181	
				22. PRICE A09	

